IDENTIFICATION OF AN INDUSTRIAL PROCESS: A MARKOV PARAMETER APPROACH

Proefschrift

Ter verkrijging van de graad van doctor aan de Technische Universiteit Eindhoven, op gezag van de rector magnificus, prof. dr. F.N. Hooge, voor een commissie aangewezen door het college van dekanen in het openbaar te verdedigen op dinsdag 3 november 1987 te 14.00 uur

door

Antonius Cornelius Petrus Maria BACKX

Geboren te Roosendaal

Druk: Dissertatiedrukkerij Wibro, Helmond.

Dit proefschrift is goedgekeurd
door de promotoren

Prof. Dr. Ir. P. Eykhoff

en

Prof. Ir. O. Rademaker

Copromotor Dr. Ir. A.A.H. Damen

Aan

Lianne,
Peter en Nicole

voor hun steun
en
eindeloze geduld

VOORWOORD

Dit proefschrift beschrijft de technieken, die in het kader van het sinds medio 1982 binnen de HTG Glas van Philips lopende onderzoekproject PICOS (Process Identification and Control Systems) zijn ontwikkeld voor het identificeren van industriële processen. De beschreven technieken zijn inmiddels op ruime schaal beproefd en het onderzoekproject bevindt zich in de eindfaze.

In de eerste plaats wil ik de direktie en het management van de HTG Glas bedanken voor de gelegenheid, die zij mij heeft geboden, om een zo omvangrijk project als "PICOS" in nauwe samenwerking met onder andere het Philips Research Laboratorium Brussel, de Technische Universiteit Eindhoven, de Technische Universiteit Delft en de Katholieke Universiteit Leuven op te zetten en uit te voeren, en voor de toestemming, die ik heb gekregen, om de resultaten van de door mij in het kader van het project ontwikkelde en beproefde identificatie technieken mede te gebruiken voor het realizeren van dit proefschrift.

Aangezien het PICOS project veel te omvangrijk was voor de kleine groep van 4 mensen, die het onderzoek binnen de HTG Glas van Philips hebben verricht, zijn de samenwerkingen met diverse groepen van onderzoekinstituten binnen en buiten Philips van wezenlijk belang geweest voor het succes van het PICOS project. Deze gezamenlijke ontwikkeling zou nooit tot stand gekomen zijn zonder de medewerking van prof. Eykhoff, prof. Genin, prof. Hautus, prof. Rademaker, prof. Vandewalle en prof. Verbruggen.

Als groot stimulator en beschermheer van het PICOS project binnen Glas wil ik Bert van den Braak bedanken voor zijn steun en initiatieven in moeilijke tijden.

In de afgelopen jaren zijn heel wat mensen betrokken geweest bij de ontwikkeling en de praktische beproeving van de nieuwe technieken. Diegenen, die een bijdrage hebben geleverd, zijn Jos Vaessen, Yao Ting Ting, Han van der Weijden, John van Diepen, Paul Carriere, Jan van Straaten, Pablo Silberfisch, Ton van der Vorst, Leo van der Wegen, Alexander Loontjens, Peter Berben, Roel Oudbier, Jobert Ludlage, Geert van Vucht, Gert Jan van der Hurk en Owen Burg. De resultaten van de deelonderzoeken en ontwikkelingen, die in samenwerking met deze afstudeerders en stagiairs zijn verricht vormen de ruggegraat van de ontwikkelde technieken, die nu met succes worden toegepast voor het analyseren, modelleren en besturen van industriële produktie processen.

Zoals gezegd, is het onderzoek verricht in nauwe samenwerkingen met diverse groepen. Met plezier denk ik terug aan de vele inspirerende discussies, die ik heb gevoerd met onder andere Ad Damen, Andrzej Hajdasinski, Ad van den Boom, Paul van den Hof, Peter Janssen, Paul van Dooren, Bart de Moor en Sabine van Huffel.

Een essentieel onderdeel bij het ontwikkelen van nieuwe technieken is de praktische beproeving. Zoals altijd met een eerste praktische test verliepen

ook onze eerste praktijkproeven niet altijd even soepel. Robert Engelen, Jan van de Einden, Gonard Jaspers, Paulus Boorsma, Ruud van Leersum, Theo Boonen en Woud Kusters bedank ik voor de vele, tengevolge van tegenslagen ook vaak nachtelijke, maar altijd plezierige uren, die wij in het stralend bereik van de ovens en het warme glas hebben doorgebracht.

In onze eigen projectgroep PICOS hebben wij, vaak onder niet geringe tijdsdruk, plotseling opdoemende problemen moeten oplossen. Met ons team zijn we er, door onze goede onderlinge samenwerking, onze verschillende achtergronden en zienswijzen en onze volharding, steeds in geslaagd op tijd passende oplossingen te bedenken. Op deze plaats wil ik Pieter van Santen, Anton Koenraads, Theo Beelen en Andre Boot danken voor deze prettige samenwerking.

De vele, soms heftige, maar altijd boeiende discussies met mijn kamergenoot Pieter van Santen hebben steeds de rode draad geleverd, waarlangs het PICOS project binnen Glas is uitgevoerd, en zijn voor mij mede de drijfveren geweest om dit werk op deze wijze af te ronden.

Het maken van mooie illustraties is niet mijn sterkste kant. Ton Emmen en Kees Korsmit ben ik dan ook dankbaar voor hun bijdragen.

Met bedanken ben je nooit in staat iedereen op passende wijze te vernoemen. De lange lijst van namen is nooit compleet. Naast al diegenen, die ik met name heb genoemd, dank ik ook alle anderen, die op enigerlei wijze bij het onderzoek betrokken zijn geweest en die niet persoonlijk zijn vermeld.

Zeker niet op de laatste plaats dank ik Lianne, Peter en Nicole voor de zovele uren, die zij samen met mij hadden willen doorbrengen, maar die zij mij hebben gegeven om dit werk te voltooien. Heel leuk was dan ook het laatste deel van het werk, waarbij we met het hele gezin de uiteindelijke versie van het proefschrift al knippend en plakkend hebben samengesteld.

Tenslotte moet ik bekennen, dat het mij oprecht spijt, dat het mij reglementair niet is toegestaan mijn beide promotoren, de overige leden van de commissie en, in het bijzonder, mijn co-promotor te danken voor de vele opbouwende discussies, die wij hebben gevoerd en die hebben geleid tot het voor u liggende resultaat.

Veldhoven, Augustus 1987

Ton Backx

IDENTIFICATION OF AN INDUSTRIAL PROCESS: A MARKOV PARAMETER APPROACH

IDENTIFICATION OF AN INDUSTRIAL PROCESS: A MARKOV PARAMETER APPROACH

Summary

This study describes a method that has been developed for the identification of multi-input, multi-output (MIMO) industrial processes. The method can be used for modelling the dynamic input output behaviour of a large class of industrial processes in the vicinity of a working point.
Tests of the developed method on industrial processes have shown that a straightforward application of the method results in models that give good insight in the dynamics of the modelled processes. Furthermore it has been shown that the obtained models can be successfully applied for the design of industrially applicable MIMO control systems for such processes.
Validation tests of the obtained models show differences between the simulated model outputs and the measured process outputs that are close to the observed output noise level of the processes.

The motive for this study is given by the growing need in industry for a thorough understanding of the dynamic behaviour of processes in order to enable a high flexibility with respect to changeovers and to increase the quality of the control of the processes.

Essentially, the developed identification method consists of three identification steps:

- The first step is directed to the determination of a Finite Impulse Response (FIR) model of the process. The set of the finite impulse response models is the largest possible modelset of linear, causal, time invariant, stable, discrete time models. Estimation of a FIR model only requires a-priori information with respect to the length of the impulse responses of the process. This information can be obtained from recorded step responses of the process.
  In general, the FIR model obtained from the estimation in general gives a good representation of the process input output behaviour. However, the FIR model is quite complex. Therefore it is not very well suited for simulation of the process input output behaviour and for control system design.

- The second identification step is directed to the determination of a Minimal Polynomial Start Sequence of Markov parameter (MPSSM) model on the basis of the FIR model obtained from the first identification step. In general, the MPSSM model has much less parameters than the FIR model. The MPSSM model can easily be translated into a relative low order state space model. For the determination of an MPSSM model it is necessary to estimate an appropriate value for the degree of the minimal polynomial.

An MPSSM model of degree r (the degree of the minimal polynomial) generically has a corresponding state space model of the order $r \cdot \min(p,q)$ with p the number of inputs of the process and q the number of outputs of the process.
As opposed to (pseudo) canonical models the MPSSM model does not require the determination of an appropriate structure. This is an attractive property of the MPSSM model especially in cases where the process to be modelled does not have a clear structure. In general it can be stated that the MPSSM model does not favour nor suppresses specific input output transfers during the modelling.
The model obtained from this second step generally gives a less accurate description of the input output behaviour of the process than the earlier estimated FIR model does. Still it is attractive to do this second identification step, as the resulting model is much better suited for the analysis and simulation of the input output behaviour of the process. Furthermore, the one to one relation of MPSSM models with relative low order state space models gives immediate access to the extensive set of analysis tools and control system design tools that are available for state space models.

- The third identication step is used to refine the MPSSM model. In this step the MPSSM model parameters are estimated on the basis of the input output data that have also been used for the estimation of the FIR model parameters in the first step. The MPSSM model parameters obtained in the second step are used as initial values for the iterative minimization process that is used for the direct estimation of the MPSSM model parameters. Finally, on the basis of the obtained MPSSM model an approximate realization is computed to get rid of inherently present irrelevant modes for the input output behaviour of the model.
  A nice property of the MPSSM model compared to (pseudo) canonical models is observed in the direct estimation of the MPSSM model parameters on the basis of an output error criterion: The numerical minimization method has to minimize a function of the minimal polynomial coefficients only. The number of minimal polynomial coefficients (r for a MPSSM model of degree r) in general is much smaller than the number of parameters that has to be manipulated by the numerical algorithm in case of a (pseudo) canonical model ($\approx n \cdot \min(p,q)$ with n the order of the state space model).
  Norwithstanding the large difference in number of degrees of freedom tests have shown that the MPSSM model obtained from the direct estimation on input output data has the simulation qualities of the FIR model obtained in the first step.

The first part of this thesis describes the three identification steps. Various alternatives for the estimation of model parameters and for the determination of required a-priori knowledge are investigated for each of the three steps. To test each of the alternatives simulations have been performed with four different systems. The simulation results have been

evaluated with respect to the fit of the resulting models to the simulated processes and with respect to the average processor time required for an estimation. For each step that method is retained that performs best. Furthermore techniques are described that have to be used to prepare data collected in a real industrial environment for process identification.

The second part of the thesis describes the results obtained with the developed identification method for two different industrial processes.
The first identified process is the shaping part of a Vello tube glass production process. The model reflects the transfer of two process inputs (mandril pressure and drawing speed) to the tube dimensions (wall thickness and diameter).
The second process that has been identified is a feeder. A feeder is the part of a process installation for melting glass that has to condition the glass for further processing. The model of the feeder depicts the transfer of three energy inputs of the feeder to six temperatures measured at different positions in a cross section of the feeder close to the outlet for the glass (the "spout").
To validate the models obtained from the identification special validation experiments have been done with both processes. During the validation experiments the processes have been excited over their full dynamic range in the vicinity of the working point. The same inputs applied to the process have also been applied to the models. Comparison of the outputs simulated by the models with the outputs measured from the true processes gives a measure for the qualities of the models with respect to the simulation of the process input output behaviour.

The model obtained for the shaping part of the tube glass production process has been used to design a MIMO control system for that process. With this control system the accuracy of the tube dimensions has been significantly improved. Furthermore changeover times can be largely reduced with this MIMO control system.

The results, obtained with the developed identification method on the processes used to test the method, allow the conclusion that straightforward application of the method results in a model that gives detailed information on the dynamic properties of the input output behaviour of the process and that is very well suited for the design of industrially applicable MIMO control systems for the process.
The developed method may serve as a basis for the design of fully automated process control systems (cf. introduction, section 1.2). However, further research will be required to be able to actually realise fully automatically controlled processes.

1. INTRODUCTION

1.1 General introduction

In industry many different processes are used. All these processes require some type of control to finally get products that meet the specifications. In general, the direct control actions required for manufacturing a product can be split into two types:

- sequence control of the various production steps required
- control of process dynamics of a sub-process used for a production step.

In this thesis, a method is developed for the analysis and modelling of the dynamics of a (sub)process that satisfies certain conditions with respect to linearity, stationarity, causality and stability (see: chapter 2). Aim of the method is to enable the control of the accuracy and of the dynamics of this (sub)process.

Control of the dynamics of a (sub)process requires some knowledge of the dynamic behaviour of that specific (sub)process. The knowledge needed for the control of the process highly depends on the demands put on the controlled process, on the process characteristics and on the specific type of control applied (e.g. Single Input Single Output PID control, Multi Input Multi Output Model Reference control, ...). The more accurately one wants to control certain process outputs, the more detailed one needs to know the dynamic relations between the process inputs and outputs. Dependent on the accuracies required for the controlled process also the characteristics of the disturbances influencing the process need to be known more or less accurately. The knowledge of the process behaviour is stored in models (see paragraph 2.2); these are compact representations of a part of the available knowledge. They are used for the control of the process either directly, if a model reference type of control is applied or, in an indirect way, if the model is used for the design of the control system.

1.2 Evolution of the control of industrial processes

Looking at the evolution in the control of industrial processes several phases may be discerned (cf. [Aström, 1985]). In each of the phases discerned specific demands are put on the process control installation and a specific type of model or a specific set of models is used for control of the process. Phases that may be discerned are:

First phase: **Full manual process control**

- The process is completely controlled manually by process operators. The operators know roughly the influence of the process inputs on the process outputs. In general, they have very simple models of the process behaviour in mind. These models are used for the prediction of the dynamic behaviour of the process in response to the adjustment

of a process variable. Most of the time operators just use the insight in the static behaviour of the process for controlling the process. The quality of control is dominated by the human abilities to discern changes in the characteristics of the measured process signals, to predict time responses of the process and to generate input signals on the basis of a mental process and on the basis of changes observed in the measured process variables.
Some characteristics of this phase are:

- o Only disturbances with dynamic properties in the time span of seconds to a few hours can be controlled; all other disturbances remain unchanged in the process.
- o Only very limited interactions between the various process parameters and the process outputs can be coped with.
- o Changes of working points of the process are accomplished in an iterative way where only a very restricted number of process variables, which determine the working point, is adjusted in each iteration cycle.
- o Changeovers are very time consuming compared to the physical properties of the process.

Second phase: **Automatic control of primary process parameters**

- Part of the process -the lowest level- is controlled by single input single output (SISO) P[+I[+D]]-controllers. Adjustment of the proportional, integral and derivative action of the controllers requires just a simple model of the dynamic behaviour of the process [Ziegler and Nichols, 1943; Aström, 1984]. Due to the limited number of degrees of freedom of a P[+I[+D]] controller (1-3), in general a second order model with time delay derived from a step response of the process (fig. 1.1) is sufficient to reach a satisfying behaviour of the controlled process. Typical applications of P[+I[+D]] controllers are found in the control of primary functions (e.g. pressures, flows, velocities, positions, temperatures, forces) at many places in a process. On a higher level operators still have to control the process by manipulating the setpoints of the P[+I[+D]] controllers and by manual adjustment of not automatically controlled process parameters on the basis of observed behaviour of measured process variables. Especially interactions between the various process variables are taken care of by the process operators.
  Some general characteristics of this phase are:
  - o Primary process parameters are adequately controlled with P[+I[+D]] controllers.
  - o Disturbances observed at the process outputs that have short delay times compared to the process dynamics and that can be manipulated via one process parameter without having too much influence on other important process outputs can be controlled automatically.
  - o Only very limited interactions between the various process parameters and the process outputs can be coped with.
  - o Also in this phase changes of working points of the process are accomplished in an iterative way where only a very restricted

number of process variables is adjusted at a time in each iteration cycle.

- o Changeovers are again very time-consuming compared to the physical properties of the process due to the limited knowledge on the responses of the process to combined changes of many process parameters as a function of time.

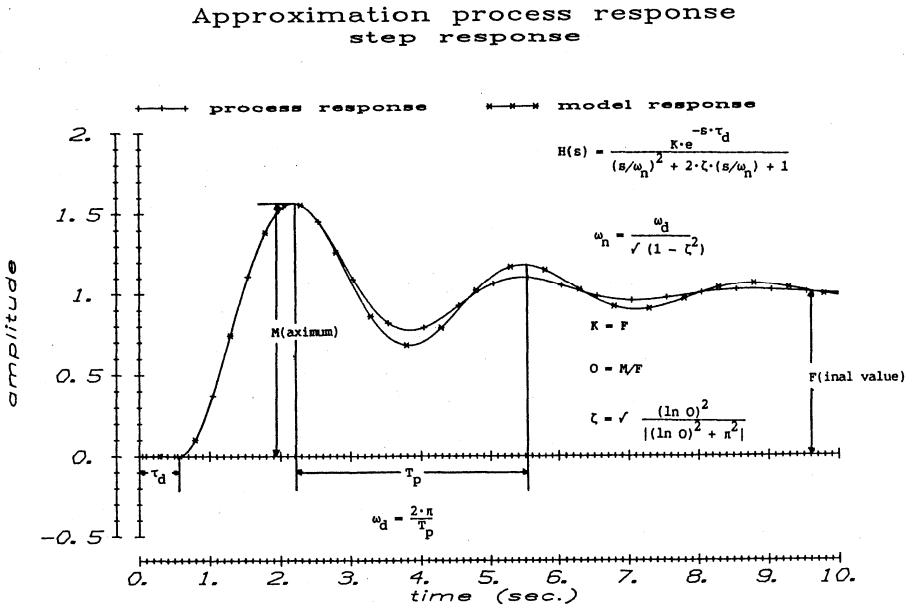

Fig. 1.1 Second order plus delay-time approximation of the step response of a system

Third phase: **Automatic control of multi-input multi-output (MIMO) sub-processes**

- Further demands on the behaviour of the controlled process require control systems that take into account dynamic interactions between process variables. Also quick changeovers between the production of one product to another product need further (supervisory) control. For the design of such control systems sufficiently accurate knowledge of the dynamic behaviour of the complete sub-process in its

various working points is needed. Simple second order SISO models with delay-times are no longer sufficient. For the design of the MIMO control systems the knowledge of the process dynamics has to be available in mathematical models [cf. Foias, 1986; Kalman, 1960; Kuo, 1980; Landau, 1979; MacFarlane, 1979; Owens, 1978; Richalet, 1978; Rosenbrock, 1970; Smith, 1957; Watanabe, 1981; Zames, 1981, 1983]. By means of the mathematical model the multi input, multi output (MIMO) control system can be designed. In general, operators still control the plant by manipulation of the set points of the supervisory controllers. The operator control focusses on changes of working points. Some general characteristics of this phase are:

- o Set points of controllers of primary process parameters are adjusted by MIMO (supervisory) control systems.
- o Operators have process inputs that are related one to one to the process outputs to be controlled.
- o Dynamic interactions between the various inputs and outputs of a sub-process are taken care of by the MIMO control system.
- o The dynamic behaviour of a sub-process can be optimized with respect to criteria based on items like variances of the process outputs, responses of the outputs to changes of the process inputs, dynamic interactions between the various inputs and outputs.
- o Changes of working points of the process can be partly handled by the MIMO control systems; operator action is still required to modify the characteristics of the control system during changeover and to adjust the process equipment.
- o Changeover times are mainly dominated by the physics of the process and the dynamic characteristics of the information obtained on the actual state of the process.

Fourth phase: **Total automatic control of a factory**

- Besides control of the dynamics of subprocesses, stock control and control of the transport of raw materials, semi-manufactured products and products to and from the subprocesses are important items. These items are strongly interrelated. To enable total automatic control of a factory several production centres are discerned in the factory. A production centre is assumed to consist of one or more processes or production lines. A process or production line is thought to be constituted of one or more process modules or work stations. Finally, each process module is assumed to be built up out of one or more sub-processes [CFT report, 1985]. In this context a sub-process is defined as a part of the process that consists of a set of highly interacting inputs and outputs that cannot be subdivided any more without neglecting important interactions. The total factory is

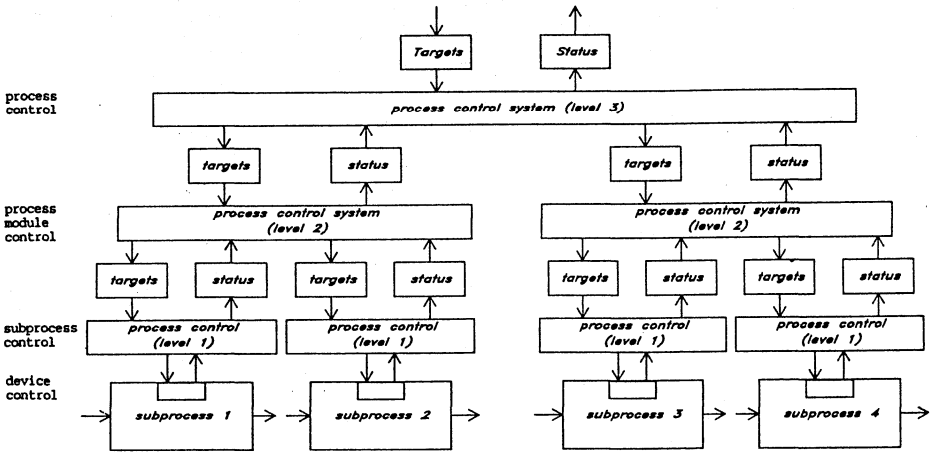

Fig. 1.2 Layered control of industrial processes

controlled at several levels. Levels that may be discerned are (cf. fig. 1.2):

- **primary function or device control level** (level 0)
  At this level control of primary process variables such as flows, speeds, pressures, forces, temperatures, energies, etc. is achieved.
- **sub-process or automation module control level** (level 1)
  This level covers MIMO control of subprocesses according to demands put on the behaviour of the subprocesses with respect to settings of process variables and with respect to dynamic properties of the controlled subprocesses (e.g. response characteristics, accuracies, disturbance rejection, ...).
- **process module or workstation control level** (level 2)
  At this level a process module, consisting of one or more subprocesses, is controlled. Main activities are:
  - .determination of desired characteristics of the sub-processes that constitute the process module on the basis of the demands put on the process module.
  - .control of stocks between subprocesses.
  - .control of material and product flows within the process module.
- **process or workcell control level** (level 3)
  At this level a process, consisting of one or more process modules, is controlled. Typically, the characteristics of the

various process modules are controlled such a way that the demands put on the process as a whole are reached as closely as possible. Main activities are:

.optimization of characteristics of process modules.
.control of flow of materials and products between various process modules.
.control of stocks in the process.
.control of changeovers in the process.

- o **production or shop control level** (level 4)
  At this level the manufacturing of products or semi-manufactured products is controlled. The production to be made is distributed over the available production lines or processes that constitute the production centre or shop on the basis of the available information on the present status of the various production lines or processes and according to given optimization criteria. For each production line or process the desired characteristics are defined and controlled at this level. Control of the flows of raw materials, semi-manufactured products and products to and from the processes is also covered at this level.
- o **Factory control level** (level 5)
  At this level a complete factory, consisting of one or more production centres or shops, is controlled. Typical actions covered at this level are optimizations between the various production centres of the factory, optimizations of the flow of raw materials and optimizations of product and semi-manufactured product flows, optimization of stocks of products and raw materials, order processing, generation of management information, ...

This is called layered control of a factory. At each layer a supervisor is active in coordinating the layers below it. The task of the supervisor at each layer is to generate the setpoints for the controllers at the layer below it, so that the behaviour of the complete part of the factory supervised is in correspondance with the requirements received from a higher layer. For this layered control approach detailed knowledge is desired of the dynamic behaviour of subprocesses in their different working points. Knowledge available in mathematical models enables MIMO control of the subprocesses (cf. chapter 8)
The layered control approach may be an entry towards complete automation of a factory. It may serve as a basis for flexible automation of production processes and opens the way to flexible production (cf. [Gershwin, 1986]).
Operators only need to take over control when an emergency occurs and, e.g. due to a malfunctioning of the equipment, automatic control becomes impossible. Furthermore operators are needed for maintenance and repair of the control equipment and the process installation.

Some general characteristics of this phase are:

- o Process installations and equipment have to be designed for complete automatic control and testing; also automatic changeover between working points needs to be possible.
- o Operators are required for monitoring, repair and maintenance of the processes and process equipment.
- o Changes of working points of the processes are automatically handled by the supervisory control systems that generate the setpoints and parameters for the MIMO subprocess controllers.
- o Changeover times are purely dominated by the physics of the process and process equipment and by the characteristics of the information obtained on the actual state of the process.
- o At each level optimization methods are used to generate setpoints and targets for the underlaying level on the basis of targets obtained from a higher level and status information received from a lower level.

As it is indicated in the previous, the need for mathematical models, describing the dynamic behaviour of a (sub)process, grows with the evolution of the control systems applied. Especially in the third and fourth phase accurate mathematical models that describe the dynamics of MIMO sub-processes are desired.

1.3 Modelling of industrial processes for process control

Models that describe the dynamic behaviour of a process can be obtained in various ways. The main methods used for modelling a process are:

- Construction of the model by using physical, chemical laws and by making assumptions on the behaviour of the actual process in its working area. This method is mainly used for the modelling of mechanical systems (e.g. satellites, aircraft, robots, generators), electrical systems (e.g. electric power systems, electronic circuits) and chemical processes (e.g. chemical reactions). In general, if it is feasible to derive a model from the basic laws, this is done.
  In situations where complex industrial processes have to be modelled this approach, in general, leads to complex models with many unknown quantities. Because of the complexity of the physical and chemical models, the difficulties related to finding appropriate estimates for the unknown quantities, the high dimensionality of the models and the nonlinearity of the models, this method is very laborious for most industrial processes and often does not lead to useful results.
  Furthermore the physical and chemical models give a complete description of the process whereas one is often only interested in the (input/output) behaviour of the process in specific working areas.

- Modelling of a process on the basis of observations of the behaviour of the process in different working points. These methods are often denoted by 'black box' modelling techniques. A better name for these

methods would however be 'grey box' modelling techniques, because extensive use is made of available knowledge on the physics of the process to be modelled (cf. fig. 1.3).

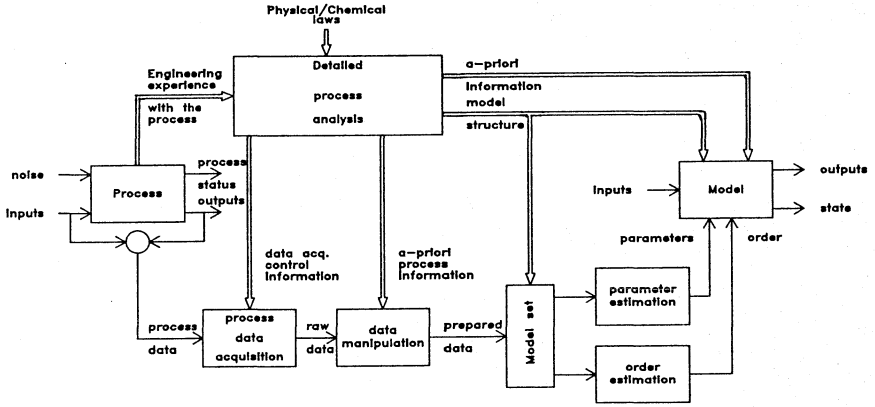

Fig. 1.3 Identification scheme

In fact the 'black box' part is related to the estimation of model parameters on the basis of observed input/output behaviour of the process. Determination of e.g. considered inputs and outputs, working points, signal characteristics, model sets, is mostly based on detailed analysis of the physical, chemical properties of the process. In the modelling traject several phases (cf. par. 2.2) have to be discerned in this method (cf. [Rademaker, 1984; Backx, 1985]):

- o First one tries to find the most relevant inputs and outputs of the process together with some characteristics on the behaviour of the process between these inputs and outputs. This information is obtained from a physical understanding of the behaviour of the process and from earlier experiences with the process.
- o Next a detailed investigation is made into the main characteristics of the process. Properties under consideration are: linearity, gain, bandwidth, disturbances, time delay, interactions, frequency dependent behaviour, time variance, sensitivity to changes in working point.
- o Information obtained from the previous phases is used as a-priori information for the actual identification of the process (cf. [Eykhoff, 1974]).

For the construction of the model of the process three basic choices have to be made:

- o Selection of the model set and its parametrization

- o Selection of the type of error used in the computation of the model parameters
- o Selection of the estimation method used during the estimation of the model parameters

On the basis of the information obtained from the detailed analysis of the process behaviour testsignals are designed and applied to the process. The responses to these signals are measured. The information obtained from these experiments is used for the actual estimation of the model parameters.

Grey box modelling techniques are mainly applied in situations, where it is very difficult to construct a model from basic laws with the accuracy needed for the application, and in situations, where only limited knowledge on the behaviour of the process is needed (e.g. input/output behaviour of a process in a specific working point).

1.4 Scope of this thesis

As an evolution is going on in industry towards an increasing automation of production processes and as high demands are put on their flexibility, a good understanding and knowledge of the (dynamic) behaviour of the processes is essential. In order to use this knowledge for automatic control it has to be available in mathematical models (cf. par. 1.2). Therefore techniques are required to enable the identification of multi-input multi-output industrial (sub)processes.

The **aim of the present study** is:

- To develop tools, based upon (dark) grey box modelling techniques, that enable identification of broad classes of multi-input multi-output industrial subprocesses.
- To test the developed tools in simulations.
- To test the tools with data obtained from measurements derived from experiments executed on industrial glass production processes, which are complex, distributed parameter systems and which may serve as examples of a broad class of industrial subprocesses.
- To design and test a multi-input multi-output control system based on the model obtained with the method developed in order to show its qualities in practice.

In chapter 2 an overview will be given of the techniques applied to come to a method that can be used for identification of a large class of industrial processes. As an introduction to the chapters 3, 4 and 5 some general notions relevant to model building will be given.

The next three chapters discuss the successive steps used to come to a model of the process.

Chapter 3 describes some techniques developed for the estimation of Markov parameters of a multi input multi output process together with auto-regressive noise model parameters.

Chapter 4 describes various techniques used for the determination of a suitable degree of the minimal polynomial for Minimal Polynomial Start Sequence Markov parameter (MPSSM) models. Furthermore some techniques are discussed that can be used for the estimation of MPSSM model parameters from a given, estimated Markov parameter model.

In chapter 5 properties of the various identification steps are analysed. Furthermore algorithms are developed for the estimation of MPSSM model parameters directly from available process input/output data. As will be indicated the developed algorithms require good initial values for the model parameters. Estimates for the MPSSM model parameters obtained with the methods discussed in chapter 4 in general satisfy the requirements.

For a successful identification of an industrial process, selection of the right process signals and thorough preparation of these signals before their use for parameter estimation are very important. Relevant items that have to be dealt with are the influence of selected process inputs on process outputs, linearity, time delays, trends in signals, spikes in signals, offsets, bandwidth of transfers. The preparation of the signals needed for a successful identification of a process is decribed in chapter 6.

The method developed in this thesis has been applied for modelling two different industrial processes.
The first process identified is the shaping part of a tube glass production process. This process is an example of a complex, distributed parameter type of system, as is often encountered in industrial practice. The outputs of the process, diameter and wall thickness of the tube, not only depend on the inputs used for the model, mandril pressure and drawing speed, but also on many other process parameters such as glass temperatures, furnace pressure, homogenity of the glass, etc.
The second process of which the identification is described is the feeder part of a production installation that is used to supply molten glass. The feeder is the part of the process installation that conditions the glass for shaping. The identified model has to describe the dynamic relations between the inputs of the feeder, two gas inputs and a cooling air input, and six temperatures measured at fixed points in a cross section of the feeder close to the spout. Also this process is a distributed parameter system.
Both processes represent many processes encountered in industrial practice.
Chapter 7 gives a summary of the various results obtained with the proposed identification method.

The model developed in chapter 7 has been used for the design of a control system for the shaping part of the tube glass production process. In chapter 8 this control system is described. Also the results obtained with this control system applied to the production process are given.

Finally, in chapter 9, some general conclusions are presented. Also the use of the developed method in industrial practice is discussed.

2. PROBLEM DESCRIPTION

2.1 Introduction

In this chapter an introduction will be given to the proposed method for the identification of multi-input multi-output industrial processes. As has been indicated in the introduction, the ongoing evolution in the control of industrial processes towards automatic control of MIMO subprocesses and total automatic control of factories requires sufficiently accurate mathematical models of those subprocesses. These models are for example needed for design of the MIMO control systems, for control of the processes and for on-line testing of process behaviour.
The required accuracy of the models highly depends on the demands put on the behaviour of the subprocesses that have to be controlled and monitored. A general problem corresponding to the indicated requirements concerning the identification of MIMO processes can be formulated as follows:

> Given a process with known inputs and outputs, construct a mathematical model that can predict the process output signals from measured, arbitrary input signals with a predetermined accuracy over a given time interval.

In this general problem formulation a need of mathematical models, which can predict the behaviour of the process in response to arbitrary input signals over a given time interval with a predetermined accuracy, is expressed. The two following examples may clarify this need.

Example 1: A process with delay times that are large compared to the process dynamics

As an example of such a process a tube glass production process can be considered (fig. 2.1). In this process the dimensions of the tube -wall thickness and diameter- are directly influenced by two process inputs: mandril pressure and drawing speed. The response of the process to changes of the inputs can only be measured after a rather long period of time compared to the process dynamics. This large delay time is caused by the fact that no sensors are available for measuring the tube dimensions (the process outputs) at the high temperatures of the tube during the shaping phase. Measurement of the dimensions is only possible after the tube has reached much lower temperatures. For the control of such a process a good model is required, especially as the delay times in the measurements of the tube dimensions are of the order of the process dynamics. For accurate control of tube dimensions the model needed in this case should be able to predict the process outputs over a large horizon based on known process inputs.

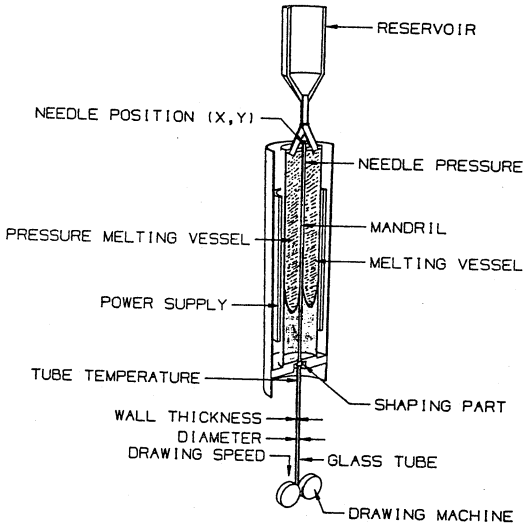

Fig. 2.1 Vello tube glass production process

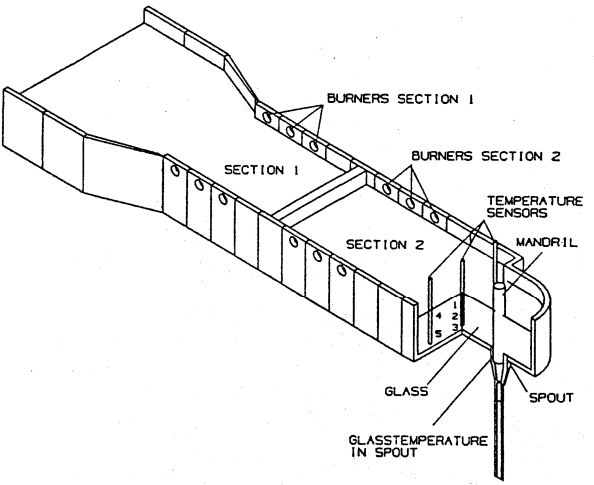

Fig. 2.2 A feeder

Example 2: Determination of the actual value of a process variable that cannot be measured continuously.

This problem refers to a situation often encountered in industrial practice that one needs to know the value of a specific process variable that can hardly be measured directly. Mostly one can measure variables related to the wanted variable, but, in this case, one needs to know the dynamic relation between the variable looked for and the ones that can be measured. As an example of this problem the measurement of a temperature at a specific spot (e.g. the spout) in a feeder of a process installation for melting glass can be considered (fig. 2.2). In this case input energies, material flows and temperatures in the feeder can be measured. These energies, flows and temperatures determine, through some process dynamics, the required temperature. So, if one knows this dynamic relationship, the desired temperature can be computed from the variables measured. In this case a model is needed that can be used for the prediction of the desired temperature from the known inputs and the present value of the measured variables with a predetermined accuracy.

The general problem, as formulated in the beginning of this section, can not be solved without a detailed, time-consuming study of the part of the process which the model has to describe. For many industrial processes it even appears to be impossible to construct such a general model with the required accuracy. Therefore the scope has to be restricted by making assumptions about the behaviour of the processes that are going to be identified.
To simplify the problem, the following assumptions are made with respect to the behaviour of the processes:

- Processes are assumed to be operated in the environments of a limited set of working points.

  This assumption restricts the problem of finding a mathematical model that describes the behaviour of the process in general to the problem of finding a set of mathematical models that describe the behaviour of the processes in the direct surroundings of the working points.

- Processes are assumed to stay near a certain working point for a long time compared to the largests process lags.

  This assumption allows neglection of the transitions between the various working points.

- In each working point, the process characteristics are considered to be time-invariant and causal.

  With this assumption it is possible to use time invariant, causal mathematical models for the description of the process.

- In each working point process characteristics are assumed to be stationary and ergodic.

  This assumption allows the identification of the process in its different working points on the basis of a limited number of recordings of the process behaviour.

- It is assumed that the behaviour of the processes in the different working points can be described with sufficient accuracy by linear models.

  This assumption allows the use of linear models.

- Only discrete time signals and models will be used.

  This assumption is imposed, because all process signals are sampled and all signal manipulations and computations are executed in discrete time. Furthermore, all results can be converted to the continuous time domain.

On the basis of these assumptions only linear, time-invariant, causal, discrete-time models will be considered in the sequel. They will be used to describe the dynamic behaviour of the industrial processes. A real process will never completely satisfy the assumptions made. A first step in the identification will therefore have to consist of a test of the behaviour of the process in the surroundings of the various working points with respect to the validity of the assumptions (cf. chapter 6).

2.2 Process identification: first steps

To solve a modelling problem for any industrial process, a procedure is developed consisting of several steps. Each step of this procedure is directed to obtain more detailed information about the dynamic behaviour of the process to be modelled. The information coming from previous steps is used as a-priori information for the next step in the procedure. As a preparation for the identification of a process the following sequence of investigations and experiments are undertaken:

- Analysis of the working point(s) used
- Selection of in- and outputs
- Experiments directed to obtaining more detailed information on (cf. chapter 6):
  - o linearity in the working points
  - o sensitivity of the process to changes in the inputs
  - o interaction between in- and outputs
  - o time delays in the transfers from inputs to outputs
  - o bandwidths of all transfers
  - o hysteresis
  - o disturbances present in in- and outputs
  - o time dependence of the process

In some of these experiments, test signals are applied to the process. Analysis of the recorded process behaviour during the various experiments results in two types of information:

- information with respect to the characteristics of the process installation.
- a-priori information for the identification of the process.

The first type of information can be used to detect malfunctioning of the process installation and to define required improvements of the process equipment. The second type of information is required for a successful identification of the process. For this identification two sets of experiments have to be carried out:

- experiments for process identification
  - o design of test sequences (e.g. pseudo random binary noise (PRBN) sequences) based on available information on the bandwidth, linearity and sensitivity of the process (cf. [Isermann, 1974]).
  - o excitation of the selected process inputs with the test signals.
- experiments for model validation
  - o excitation of the process with PRBN sequences that are linearly independent of previously applied PRBN sequences and that have the same characteristics as the ones directed to the estimation of the model.
  - o design of test signals with the same power spectrum as the input signals allowed for continuous operation of the process.
  - o application of the test signals to the process.

The latter set of test signals, i.e. the signals with the same power spectrum as the input signals allowed during continuous operation of the process, are used to test the simulation qualities of the models on signals which are allowed in practice.
The identification of the process is done on signals that have been prepared on the basis of knowledge, obtained from the detailed process analysis, to contain as much information as possible on the process to be modelled. Steps executed to prepare the signals for process identification are (cf. chapter 6):

- removal of spikes and other errors in the raw data
- removal of average values of the signals and trend correction without the introduction of phase errors
- shifting of in- and output signals to remove known time delays
- multiplication with weighting factors to make the energy contents of the signals equal
- filtering and decimation of the signals

2.3 Some general notions on estimation methods

To obtain a model based on signals that contain all relevant information on the dynamic behaviour of a process in a working point, basically three

choices have to be made:

- selection of the model set and its parametrization
- selection of the type of error used for the estimation of the model parameters
- selection of the estimation method used for the estimation of the model parameters

Throughout this thesis the following definitions will be used (cf. [Eykhoff, 1974; Isermann, 1974; Ljung, 1983; IEEE, 1984]):

Data set: A selection of information conveyors such as characters, analog quantities, samples to which a specific meaning might be assigned.

System: An integrated whole composed of one or more diverse, interacting structures that generates data sets possibly in relation to other data sets.

Model: A compact representation of the, for the application, essential aspects of an existing system that presents knowledge of that system in a usable form.

Model set: A selection of models that have similar representations.
- model parameters still have to be quantified

Size of a model set The minimum number of independent model parameters with the property that one model of the model set with a unique input/output behaviour is related to each chosen set of model parameter values.

Process: The relevant part of the physical system that has to be modelled.

Error: A data set which represents the deviations between a data set obtained from a process and the corresponding data set generated by the model, selected to be a representation of this process.

Estimation method: A mathematical function applied to the error, possibly with some assumptions on characteristics of the error or data sets used to generate the error, in order to select a model from the chosen model set (cf. fig. 2.3).

Estimation interval: Length of the data set used for the estimation of the model parameters.

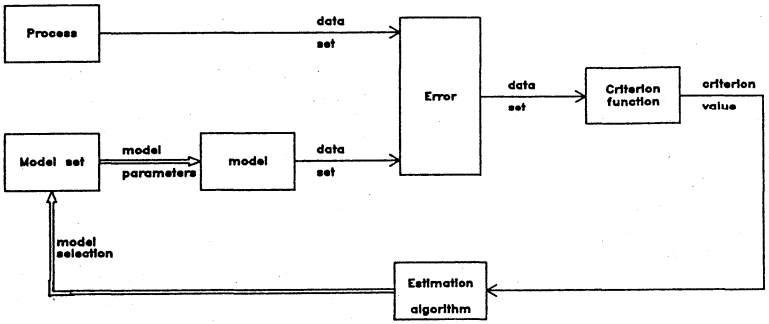

Fig. 2.3 Estimation method

Criterion function: Mathematical function of the error, based on the estimation method selected, that quantifies all possible models of a selected model set.

Mathematical model: A mathematical representation of the essential aspects of an existing system presenting knowledge of that system in a compact form.

Estimation algorithm: The computational method used to determine a model within a specified model set on the basis of a selected type of error, a selected estimation method as well as data sets and a-priori information obtained from the process which has to be represented by the model.

Identification: The determination by means of an estimation algorithm of a mathematical model of a process by using all available engineering expertise with the process, physical- and chemical laws and additional experimental information of the process to select a model set, a type of error and an estimation method and to prepare data sets obtained from the process.

In stead of 'criterion function' sometimes the term 'cost function' will be used in the sequel. Both terms have the same meaning.

2.3.1 Models and some general notions related to models

The model set is the collection of all possible models with given properties with respect to the transfer from input signals to output signals. The models contained in the model set can, for instance, be linear/nonlinear, causal/non causal, discrete time/continuous, time invariant/time varying [Janssen, 1986]. The choices made with respect to the model set and the parametrization of the models in this model set determine all models to be considered. Because each model describes the relation between input and output signals, also the set of all possible output signals that can be generated from a given input signal is directly related to the model set and the parametrization of the models chosen. Looking at the ability of the model to simulate the input/output behaviour of the process, it is clear that the ultimate quality to be obtained with a particular model from the model set is directly governed by the choice of the model set and its parametrization. In general, the choice of the model set and its parametrization has to be related to the intended use of the model and to the available a-priori knowledge of the process to be modelled. The more information one has of the behaviour of the process the smaller the model set can be. If only a rough knowledge of the dynamic behaviour of the process is available it is appropriate to make the set of all possible models as large as possible [Van den Boom, 1982; Eykhoff, 1974; Hajdasinski, 1982; Niederlinski, 1979].

Many different representations of models can be chosen [Hajdasinski, 1980]. Models that will be used in the sequel are:

- The **Finite Impulse Response** (FIR) model

$$y_k = \sum_{i=0}^{m} M_i \cdot u_{k-i} \qquad (2.1)$$

with: y_k output vector at time k — $\dim[y_k]$: q
u_i input vector at time i — $\dim[u_i]$: p
M_i i-th Markov parameter — $\dim[M_i]$: q × p

- The **Minimal Polynomial Start Sequence Markov Parameters** (MPSSM) model

$$y_k = \sum_{i=0}^{\infty} F(a_j, M_j \mid j \epsilon I) \cdot u_{k-i} \qquad I = 1,2, \ldots ,r \qquad (2.2)$$

with: F_i i-th Markov parameter — $\dim[F_i]$: q × p

a_j j-th coefficient of the minimal polynomial; cf. eq. (2.6)

r order of the minimal polynomial

$$\begin{cases} F_i = M_i & i \epsilon I,\ I = 1,2, \ldots ,r \\ F_{r+j} = \sum_{i=1}^{r} a_i \cdot F_{r+j-i} & j \epsilon J,\ J = 1,2,3, \ldots \text{ ; cf. eq. (2.7)} \end{cases}$$

- The **State Space** (SS) model

$$x_{k+1} = F \cdot x_k + G \cdot u_k \qquad (2.3a)$$

$$y_k = H \cdot x_k + D \cdot u_k \qquad (2.3b)$$

with:

x_k	state vector at time k	dim[x_k]: n
F	state matrix	dim[F]: n × n
G	input matrix	dim[G]: n × p
H	output matrix	dim[H]: q × n
D	direct feed through matrix	dim[D]: q × p

These models will be used to simulate the input/output behaviour of the process under study.
Both the FIR model and the MPSSM model can straightforwards be translated into corresponding State Space models. In general, there is not a one to one relation between a FIR model and a MPSSM model, because the FIR model covers a finite time horizon (cf. eq. (2.1)) and the MPSSM model has an infinite time horizon (cf. eq. (2.2)). Translation of a State Space model to a FIR is also impossible in general for the same time horizon reason. State Space models have always a corresponding MPSSM model and translation into each other can be done in a straightforward manner (cf. paragraph 4.2).
Important notions related to the last two mentioned types of models are the order n (MPSSM model and SS model), the realizability index r (MPSSM model and SS model) and the structural indices ν_i and μ_i (SS model) [Guidorzi, 1975, 1981].
The order (n) of a system is defined as the dimension of the state vector of the state space representation of the system. For minimal realizations of the system the system matrices satisfy the following conditions [Kailath, 1980]:

Controllability

$$\text{rank}\ [\ G\ ;\ (\lambda I - F)] = n \qquad \text{for all } \lambda,\ \lambda \epsilon C \qquad (2.4)$$

Observability

$$\text{rank}([H^t\ ;\ (\lambda I - F)^t]^t) = n \qquad \text{for all } \lambda,\ \lambda \epsilon C \qquad (2.5)$$

The realizability index r of the system is defined as the degree of the minimal polynomial of the state matrix F [Hajdasinski, 1980]. The minimal

polynomial is the annihilating polynomial of F of the lowest degree (cf. eq. (4.18)):

$$f(F) = F^r + a_1 \cdot F^{r-1} + \ldots + a_{r-1} \cdot F + a_r \cdot I = 0 \qquad (2.6)$$

Left multiplication of (2.6) with $H \cdot F^{j-1}$ and right multiplication with G gives:

$$M_{r+j} = - \sum_{i=1}^{r} a_i \cdot M_{r+j-i} \qquad \text{for all } j \geq 1 \qquad (2.7)$$

If a system satisfies eq. (2.6) it has a finite dimensional state space realization. A system that satisfies eq. (2.6) also satisfies eq. (2.7). Eq. (2.7) also implies eq. (2.6). As a result, a system that satisfies eq. (2.7) has a finite dimensional state space realization {F,G,H,D}. Eq. (2.7) is called the realizability criterion of the system (cf. [Tether, 1970]).

The structural indices ν_i belonging to the representation of a system in observability form can be found from the observability matrix of the system [Hajdasinski, 1980]:

$$Ob = [H^t ; F^t \cdot H^t ; \ldots ; (F^{n-1})^t \cdot H^t]^t \qquad (2.8)$$

From this matrix the invariants are found by looking for dependences in the ordered row vectors of Ob. An invariant ν_i has been found if an i-th vector of block matrix $H \cdot F^j$ is linearly dependant on previously selected vectors. As soon as a dependence has been found all i-th vectors of subsequent block matrices $H \cdot F^{j+1}$ can be ignored as they are dependent to the previously selected vectors. The selection goes on until all q indices have been determined. The same procedure can be used for the determination of the structural indices μ_i belonging to the controllability matrix:

$$Co = [G ; F \cdot G ; \ldots ; F^{n-1} \cdot G] \qquad (2.9)$$

Now the indices are found by searching for dependences in the column vectors of the matrix Co.
The indices selected this way are called Kronecker indices. The indices satisfy the following condition:

$$\sum_{i=1}^{q} \nu_i = n = \sum_{i=1}^{p} \mu_i \qquad (2.10)$$

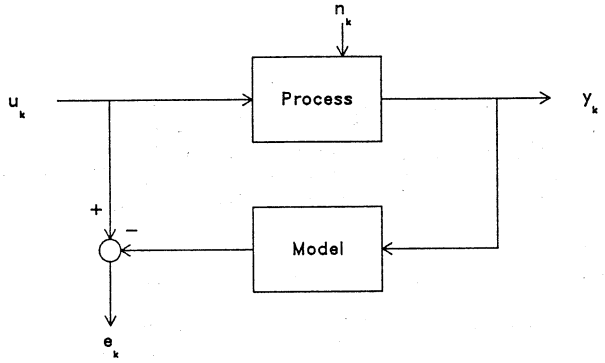

Fig. 2.4 Input error

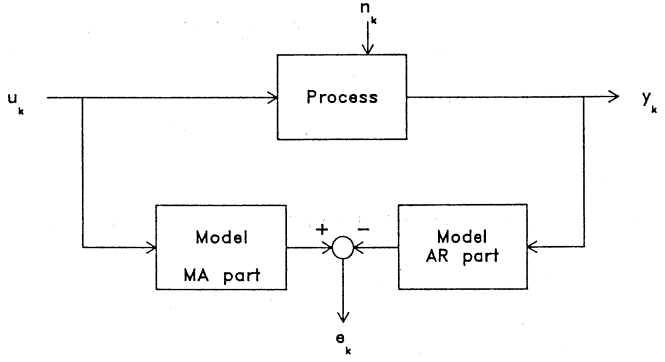

Fig. 2.5 Equation error

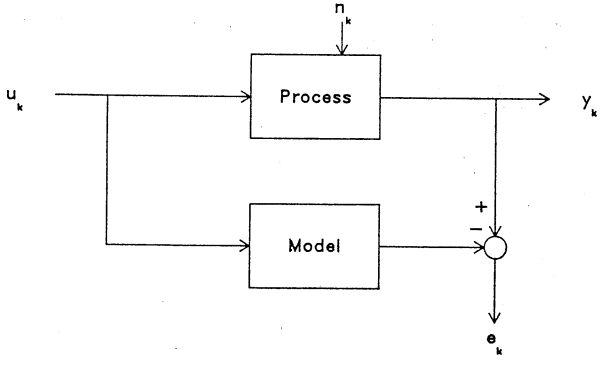

Fig. 2.6 Output error

2.3.2 Errors

In general, one will find a discrepancy between the actual measured process outputs and the output signals generated by the model. To make the actual measured signals and the simulated signals equivalent a conceptional error signal has to be added to the model signals. The position in the model where this extra signal, ε, is added defines the type of error used for the identification. Three possibilities are [Van den Boom, 1982]:

- **Input error:**

  The error signal ε_k is added to the model input signal (fig. 2.4):

$$y_k = S(y_i,(u_j - \varepsilon_j),\hat{\theta} \mid i,j \epsilon I) \qquad 0 \leq I \leq k \tag{2.11}$$

- **Equation error:**

  The error signal ε_k is fed into the model in such a way that for the computation of each new output sample all previously measured input and output samples can be used without correction with an error signal sample (fig. 2.5):

$$y_k = S(y_i,u_j,\hat{\theta} \mid i,j \epsilon I) + \varepsilon_k \qquad 0 \leq I \leq k \tag{2.12}$$

- **Output error:**

  The error signal ε_k is added to the output signal (fig. 2.6):

$$y_k = S((y_i - \varepsilon_i),u_j,\hat{\theta} \mid i,j \epsilon I) \qquad 0 \leq I \leq k \tag{2.13}$$

2.3.3 Estimation algorithms

For the computation of the model parameters θ various estimation methods can be used. The methods used in this thesis are:

- The **(Weighted) Least Squares method**
  A quadratic function of the error signal is minimized. For an impulse response model, using an output error, the quadratic cost function to be minimized can be obtained as follows:

$$y_k = \sum_{i=0}^{m} M_i \cdot u_{k-i} + \varepsilon_k$$

$$= \hat{y}_k(\theta,u_j \mid j \epsilon I) + \varepsilon_k \qquad (k-m) \leq I \leq k \tag{2.14}$$

$$\varepsilon_k = y_k - \hat{y}_k \tag{2.15}$$

$$V(\theta) = tr\{ E \cdot E^t \} \tag{2.16}$$

with: $E = [\varepsilon_k \ \varepsilon_{k+1} \ \cdots \ \varepsilon_{k+l}]$

θ representing the entries of M_i

The estimated parameters $\hat{\theta}$ are obtained by minimization of eq. (2.16) with respect to θ.
By applying a weighting W on the measurements the Weighted Least Squares method is obtained. The criterion function then becomes:

$$V(\theta) = tr\{ E \cdot W \cdot E^t \} \tag{2.17}$$

- The **Maximum Likelihood method**

For the application of this method the system to be modelled is assumed to be a member of the model set used. The joint probability density function P of ε_i is assumed to be known for the true system parameters θ_{true}:

$$P = P\{\varepsilon_k \ ; \ \varepsilon_{k+1} \ ; \ \cdots \ ; \ \varepsilon_{k+l}\}$$

$$= P\{y_i ; u_j ; \theta_{true} \mid i,j \in I\} \qquad I = k, k+1, k+2, \ \ldots \tag{2.18}$$

Because ε_k is a function of the measured process signals and the model parameters (cf. eq. (2.15)), this probability density function is a function of the unknown model parameters θ. The estimated parameter values are obtained by maximization of the likelihood function L. This likelihood function L is essentially the probability density function P with known values for the input and output signal samples. The cost function V is defined by:

$$V(\theta) = - \ln[\ L\{\theta \mid y_i, u_j\} \ ] \tag{2.19}$$

The estimates of the model parameters $\hat{\theta}$ are found by minimization of (2.19) with respect to θ, provided the assumptions on the true probability density function are valid.
If all assumed conditions are satisfied, the estimators, θ, for the model parameters are efficient. This means that the estimators are unbiased, have a finite variance and there do not exist other estimators θ^* for the model parameters whose variance is smaller than that of estimators θ (cf. [Kreyszig, 1970]).

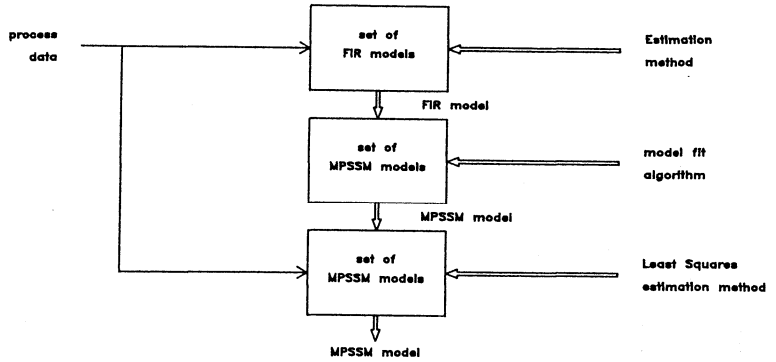

Fig. 2.7a Block diagram related to the three step identification approach

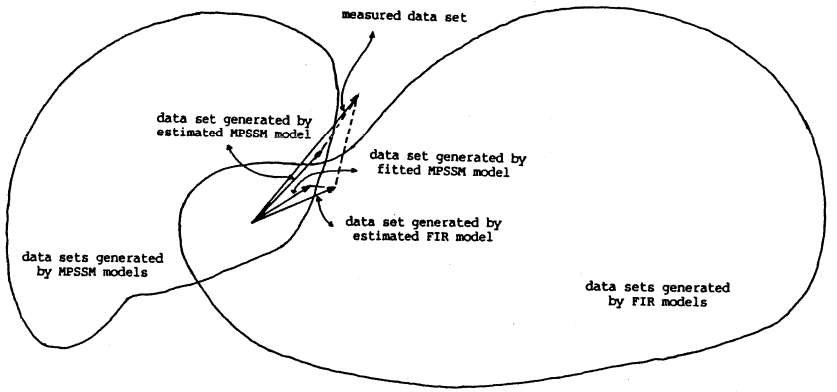

Fig. 2.7b Relations between the data set generated by the process and the data sets generated by the models

2.4 Process Identification: implementation

For the actual modelling of the process a three-step approach is chosen (cf. fig. 2.7):

- Estimation of finite impulse responses of the system from measured input/output data
- Determination of a MPSSM model from the estimated impulse responses
- Estimation of a MPSSM model directly from the input/output data, starting from the model obtained from the previous step.

This three-step approach is motivated by the fact that initially only little information on the process dynamics is available. Therefore the model set, initially used, has to be large. After the first identification the obtained model can be used to select a model from the much smaller set of MPSSM models. The third step finds the model of the relatively small MPSSM set that best fits to the data set used for the identification.

In the first step the model set - the set of finite impulse responses - is the set that has most degrees of freedom of all model sets that can be chosen for the modelling of stable systems. This model set is chosen for the first step because no detailed information on the order or on the structure of the process is needed. The only a-priori information needed for the execution of this step is the length of the impulse responses. In general, the quality of the models obtained with respect to their ability to simulate the output behaviour of the process on validation data sets is very good. A disadvantage of these models is found in their size. The computation power needed for doing simulations with these models is large due to the fact that for each output sample to be simulated a convolution has to be computed. Furthermore, these models are not very well suited for the analysis of process dynamics and for control system design. Control systems directly based on impulse responses require the computation of deconvolutions which are time-consuming (cf. [Richalet, 1978]).

In the second step the number of degrees of freedom of the model is significantly reduced. From the estimated impulse responses a degree of the minimal polynomial is determined and a MPSSM model [Gerth, 1972; Hajdasinski, 1976, 1978, 1980; Damen, 1982] of this degree is fitted to the estimated impulse responses. The advantages of this type of model are found in the enormous decrease in the number of parameters of the MPSSM model compared to number of parameters required by the finite impulse response model. For the MPSSM model no structure has to be determined as is required for MIMO (pseudo) canonical models. For most processes the structure used in MIMO (pseudo) canonical models has no direct relation with the process dynamics. As a consequence the determination of an appropriate structure for a model that has to reflect the dynamic properties of the process is very difficult. Especially the fact that no structure has to be determined for the MPSSM model is a great advantage. The model set of MPSSM models is still quite large because no fixed structure is used.
Furthermore the MPSSM type of model can be transformed directly into a corresponding state space model. As a result all available analysis and design tools for process analysis, process simulation and control system design, developed for state space models, can be applied [Kailath, 1980; Kuo, 1980; Aström, 1984].
An advantage resulting from the one to one correspondence of the MPSSM model with a relatively low order state space model is the reduced amount of computation time needed for simulations with this model compared to the time required with a finite impulse response model. In general, the simulation power of the MPSSM models obtained from this second step can be significantly improved by using the third step as will be shown later (see chapters 4, 5 and 7).

In the third step a MPSSM model is estimated directly from the available input/output data. The MPSSM model obtained in the second step is used as a start for this estimation. Numerical minimization procedures are used for the computation of the model parameters. The model obtained from this third step, in general, has the qualities of the impulse response model with respect to the accuracy of simulations and has all advantages mentioned for minimal polynomial start sequence Markov parameter models. A disadvantage of the third step is the computational effort required for the parameter estimation. This is due to the fact that a highly non-linear function of the polynomial coefficients has to be minimized.

2.5 Concluding remarks

This chapter was devoted to two steps towards the construction of mathematical models that describe the process' dynamics in the environment of its working points:

- A detailed investigation of the dynamic behaviour of the process in the environment of its working points in order to obtain insight into the properties of the process and the process installation (cf. chapter 6).
- The identification of the process to obtain mathematical models of the process that may be used for process control in the various working points.

These two steps are required to get sufficient a-priori information on the characteristics of the process installation to determine and improve the influence of the process equipment on the dynamic properties of the process and to improve the prospects of the modelling of the process dynamics.

The proposed identification approach consists of three steps.

The first step uses a large model set. The advantage of this large model set is that almost always an appropriate model can be found without much a-priori information on the process (cf. chapter 3). A disadvantage of the use of the FIR models is the large number of parameters in the models. This large number of parameters would imply great computational effort, if the model were to be used for simulation or control purposes.

The second identification step is directed to obtain a model of a MPSSM model set. This type of model has a much smaller number of parameters. The MPSSM model set is small compared to the FIR model set.
The MPSSM model does not require the determination of an appropriate structure as needed for (pseudo) canonical models.
The choice that has to be made with respect to the degree of the minimal polynomial of the MPSSM model set can be based on the a-priori information obtained from the previously determined FIR model.
A 'best' (cf. chapter 4) MPSSM model is fitted to the available FIR model. As a result a compact mathematical model is obtained that can be transformed one to one into a low order State Space model.

The third identification step is directed to the estimation of the MPSSM model parameters directly from available input/output data of the process (cf. chapter 5). This step uses the model parameters obtained from the second step as initial values for the parameter estimation. With this third step a better fit of the model to the data set can be reached compared to the fit of the FIR model due to the fact that the length of the impulse responses is no longer restricted to a given finite length any more.

Finally, due to the one to one relation that exists between MPSSM models and State Space models, all tools available for state space analysis, design and simulation may be used in conjunction with the model ultimately obtained from this type of identification.

3. ESTIMATION OF MARKOV PARAMETERS

3.1 Introduction

There are many ways of modelling a linear, time-invariant, discrete-time, stable MIMO process (cf. chapter 2). To attain a unique parameterisation of a model without the need of detailed information about the order and the structure of the process, an Impulse Response or Markov parameter model can be used [Gerth, 1972; Hajdasinski 1978, 1980, 1982].
For process analysis and the design of process control systems, in general, also a model of the noise characteristics is required.
In this chapter some techniques will be discussed that can be used for the estimation of the parameters of a Markov parameter process model and an auto regressive (AR) noise model from available process input/output data.

The Markov parameter- or Hankel model of a discrete time system is based on the impulse responses of this system. Because of the uniqueness of the impulse responses of a system this model always results in a parameterisation which produces unique parameters for a specific input/output behaviour. Assuming that the system is part of the model set, it can easily be shown that the estimated parameters are unbiased and independent of the colouring of the output noise, under the condition that the output noise and the input signal applied to the system are not correlated [Eykhoff, 1974; Van den Boom, 1982].
Besides a model that closely describes the process dynamics, in general, also insight in frequency dependent properties of the output noise of the process (such as the Power spectrum of the noise (cf. [Papoulis, 1977])) is important both for the analysis of the dynamic process behaviour and for the design of an appropriate control system for the process. To get information on the characteristics of the output noise, not only a process model but also a noise model is identified. A model that suits very well for modelling the process noise characteristics is the Auto regressive (AR) model. Similar to the Markov parameter model the AR model also produces unique parameters for a specific input/output behaviour. The AR model (cf. eq. (3.4)) describes the dynamics on the basis of autoregressions of the outputs of the system. This fits well to the case of modelling the output noise of a process where only estimates for the output noise samples of the noise process are available.
To allow a maximum-likelihood estimation of the process and of the noise parameters one extra Moving Average (MA) noise parameter (cf. eq. (3.14)) has to be used to make the input noise generators independent, as will be shown later (see paragraph 3.4). This extra parameter is needed to represent the direct coupling of the various noise sources that are assumed to be inter-channel independent.

In this chapter a few algorithms are developed for the estimation of model parameters based on least squares and maximum-likelihood estimation methods. The differences between these computational methods result from the ways in which the parameters are computed from the given set of input/output data. Various methods have been tested on a number of simulated multi-input multi-output processes. The simulated processes reflect some of the problems

encountered in practice, such as a big difference between largest and smallest eigenvalue, strong coupling between all inputs and outputs, coloured output noise. The results of the tests give an impression of the advantages and disadvantages of the methods tested.
For the maximum-likelihood method an assumption is made on the joint probability density function of the input noise of the noise model. That input noise is assumed to be stationary, white, ergodic, inter-channel independent, Gaussian.
If the process is in the model set and if the joint probability density function for the true system parameters satisfies the assumptions on its characteristics, the maximum-likelihood method is the only method of all estimation methods tested to result in an efficient estimation of the parameters [Cramer, 1961; Kreyszig, 1970; Aström, 1982; Damen, 1982].

3.2 Mathematical description of the process

If the process is assumed to fit into the class of Hankel models, its behaviour can be modelled by the following system [Niederlinski, 1979]:

$$Y = M \cdot \Omega + N \tag{3.1}$$

with:

Y	- output signal matrix	$\dim[Y]$: $q \times (l+1)$
Ω	- input signal matrix	$\dim[\Omega]$: $p \cdot (\kappa+1) \times (l+1)$
M	- Markov parameter matrix	$\dim[M]$: $q \times p \cdot (\kappa+1)$
N	- noise signal matrix	$\dim[N]$: $q \times (l+1)$

$$Y = [y_k ; y_{k+1} ; \cdots ; y_{k+l}]$$

$$\Omega = \begin{bmatrix} u_k & u_{k+1} & \cdots & u_{k+l} \\ u_{k-1} & u_k & \cdots & u_{k+l-1} \\ \cdot & \cdot & & \cdot \\ \cdot & \cdot & & \cdot \\ u_{k-\kappa} & u_{k-\kappa+1} & \cdots & u_{k-\kappa+l} \end{bmatrix}$$

$$M = [\, M_0 \; ; \; M_1 \; ; \; M_2 \; ; \; \cdots \; ; \; M_\kappa \,]$$

$$N = [\, n_k \; ; \; n_{k+1} \; ; \; \cdots \; ; \; n_{k+l} \,]$$

In this description only the outputs of the process are assumed to be corrupted with noise.
In eq. (3.1) only $\kappa+1$ Markov parameters are used. In general for a real physical system $(\kappa+1) \to \infty$. A model that includes the tails can be written as:

$$\hat{Y} = \hat{M}_m \cdot \Omega_m + \hat{M}_{tail} \cdot \Omega_{tail} \tag{3.2}$$

with: $\hat{M}_m = [\tilde{M}_0 \; ; \; \tilde{M}_1 \; ; \; \ldots \; ; \; \tilde{M}_m]$

$\hat{Y} = [\hat{y}_k \; ; \; \hat{y}_{k+1} \; ; \; \ldots \; ; \; \hat{y}_{k+l}]$

In this expression the term $\hat{M}_{tail} \cdot \Omega_{tail}$ describes the tail responses and the term $\hat{M}_m \cdot \Omega_m$ stands for the first m+1 parameters of the impulse responses. For many stable systems m can be chosen large enough to make the tail effects negligible provided the system does not have pure integrating action. If the system has pure integrating action extra auto regressive parameters may be included in the model to cover the tail effects [Eykhoff, 1974; Swaanenburg, 1983, 1985].
The model used for the estimation of the process behaviour can be written as:

$$\hat{Y} = \hat{M}_m \cdot \Omega_m \tag{3.3}$$

Not only the process, but also the colouring of the output noise can be modeled using an AR parameterisation. The model describing the colouring of the noise N is given by:

$$\hat{N} = \hat{A} \cdot \hat{H} + \hat{B}_0 \cdot \hat{\Xi} \tag{3.4}$$

with:

$\hat{H}$ – matrix containing the output error samples — dim[H] : $\nu q \times (l+1)$

$\hat{A}$ – AR noise parameter matrix — dim[A] : $q \times \nu q$

$\hat{\Xi}$ – matrix containing the Gaussian, white noise input samples of the noise colouring filter — dim[Ξ] : $q \times (l+1)$

$\hat{B}_0$ – matrix showing the coupling of the noise sources among the various channels — dim[B_0]: $q \times q$

$$\hat{H} = \begin{bmatrix} n_{k-1} & n_k & \cdots & n_{k+l-1} \\ n_{k-2} & n_{k-1} & \cdots & n_{k+l-2} \\ \cdot & \cdot & & \cdot \\ \cdot & \cdot & & \cdot \\ n_{k-\nu} & n_{k+1-\nu} & \cdots & n_{k+l-\nu} \end{bmatrix}$$

$$\hat{A} = [\, \tilde{A}_1 \; ; \; \tilde{A}_2 \; ; \; \dots \; ; \; \tilde{A}_\nu \,]$$

$$\hat{\Xi} = [\, \hat{\xi}_k \; ; \; \hat{\xi}_{k+1} \; ; \; \dots \; ; \; \hat{\xi}_{k+l} \,]$$

For this model, too, an infinite number of AR parameters is generally required to describe a real physical noise-colouring filter. Again the model is split into two parts, one describing the relevant behaviour and the other showing the tail effects. The basis is a filter that contains "all" spectral distributions feasible.

$$\hat{N} = \hat{A}_n \cdot \hat{H}_n + \hat{A}_{tail} \cdot \hat{H}_{tail} + \hat{B}_0 \cdot \hat{\Xi} \qquad (3.5)$$

Equations (3.2) and (3.5) combined give the complete model as it is used to describe the process behaviour:

$$\hat{Y} = \hat{M}_m \cdot \Omega_m + \hat{A}_n \cdot \hat{H}_n + \hat{B}_0 \cdot \hat{\Xi} + \hat{M}_{tail} \cdot \Omega_{tail} + \hat{A}_{tail} \cdot \hat{H}_{tail} \qquad (3.6)$$

For the estimation of the model parameters the tail effects are neglected. Neglection of the tail effects may influence the bias of the parameters. If the input signal is not "white noise" the parameters will be biased due to the correlation between the residual caused by the tails of the impulse responses and the input signal.
The <u>complete model</u> as it is used for estimation purposes can be written as:

$$\hat{Y} = \hat{\Theta} \cdot \hat{\Omega} + \hat{Z} \qquad (3.7)$$

with:

$$\hat{\Omega} = [\, \Omega_m^t \; ; \; \hat{H}_n^t \,]^t$$

$$\hat{H}_n = \begin{bmatrix} \hat{e}_{k-1} & \hat{e}_k & \cdots & \hat{e}_{k+l-1} \\ \hat{e}_{k-2} & \hat{e}_{k-1} & \cdots & \hat{e}_{k+l-2} \\ \cdot & \cdot & & \cdot \\ \cdot & \cdot & & \cdot \\ \hat{e}_{k-n} & \hat{e}_{k+1-n} & \cdots & \hat{e}_{k+l-n} \end{bmatrix}$$

$$\hat{\Theta} = [\, \hat{M}_m \; ; \; \hat{A}_n \,]$$

$$\hat{Z} = \hat{B}_0 \cdot \hat{\Xi}$$

In this expression the value $\hat{e}_i$ is the output error obtained for sample i.

If the system has pure integrating action or a large time constant the model has to be extended. In this case one or more AR parameters may be included to cover the tail effects. An alternative is to include an integrator or a low pass filter with to be estimated gain factors to integrate or to filter the inputs signal samples corresponding with the tail of the impulse responses (cf. [Eykhoff, 1974]). If AR parameters are included in the model to cover the tail effects and if one wants to keep the function to be minimized a quadratic function of the process model parameters, the criterion goes over from an output error criterion into an equation error criterion

3.3 Least squares parameter estimation

The least squares solution of eq. (3.7) is a parameter matrix $\hat{\Theta}$ chosen in such a way that the span of difference E (the output error matrix):

$$E = Y - \hat{Y} \tag{3.8}$$

is orthogonal to the span of matrix Ω. This solution can be found by minimizing function V:

$$V = \mathrm{tr}(E \cdot E^t) \tag{3.9}$$

with respect to parameter matrix $\hat{\Theta}$. Eq (3.9) gives the total energy of the difference between the measured output signals and the output signals estimated by the model. Substitution of E by eq. (3.8) and $\hat{Y}$ by $\hat{\Theta} \cdot \hat{\Omega}$ yields the expression of V as a function of parameters $\hat{\Theta}$.

$$V = \mathrm{tr}\{(Y - \hat{\Theta} \cdot \hat{\Omega}) \cdot (Y^t - \hat{\Omega}^t \cdot \hat{\Theta}^t)\} \tag{3.10}$$

Note that in this expression $\hat{\Omega}$, too, is a function of the estimated Markov parameters, because the output errors used for filling the "noise" matrix H_n are computed by means of the estimated Markov parameters. This implies that the set of equations to be solved is non-linear in the parameters. A necessary condition for the parameters to minimize V is that the derivative of V with respect to the parameters $\hat{\Theta}$ is equal to zero. The derivatives of

eq. (3.10) with respect to the parameters $\hat{\Theta}$ are (see Appendix A):

$$\frac{\partial V}{\partial \Theta} = 2 \cdot [\, X \; ; \; -\hat{A}_1^t \cdot X \; ; \; \ldots \; ; \; -\hat{A}_n^t \cdot X \,] \cdot \begin{bmatrix} \Omega_{m_k}^t & \hat{H}_n^t \\ \Omega_{m_{k-1}}^t & 0 \\ \cdot & \cdot \\ \cdot & \cdot \\ \Omega_{m_{k-n}}^t & 0 \end{bmatrix} = 0 \qquad (3.11)$$

with: $X = A_n^* \cdot (Y_m^{**} - M_m^{**} \cdot \Omega_m^{**})$

$$A_n^* = [-I \; ; \; \hat{A}_1 \; ; \; \ldots \; ; \; \hat{A}_n]$$

$$Y_m^{**} = [Y_k^t \; ; \; Y_{k-1}^t \; ; \; \ldots \; ; \; Y_{k-n}^t]^t$$

$$Y_{k-i} = [y_{k-i} \; ; \; y_{k-i+1} \; ; \; \ldots \; ; \; y_{k-i+l}]$$

$$M_m^{**} = \text{diag}\{ \hat{M}_m \} = \begin{bmatrix} \hat{M}_m & 0 & \ldots & 0 \\ 0 & \hat{M}_m & \ldots & 0 \\ \cdot & \cdot & & \cdot \\ \cdot & \cdot & & \cdot \\ 0 & 0 & \ldots & \hat{M}_m \end{bmatrix}$$

$$\Omega_m^{**} = [\Omega_m^t \; ; \; \Omega_{m_{k-1}}^t \; ; \; \ldots \; ; \; \Omega_{m_{k-n}}^t]^t$$

$$\Omega_{m_{k-i}} = \begin{bmatrix} u_{k-i} & u_{k-i+1} & \cdots & u_{k-i+l} \\ u_{k-i-1} & u_{k-i} & \cdots & u_{k-i+l-1} \\ \cdot & \cdot & & \cdot \\ \cdot & \cdot & & \cdot \\ u_{k-i-m} & u_{k-i+1-m} & \cdots & u_{k-i+l-m} \end{bmatrix}$$

Furthermore, for a set of parameters to minimize V the matrix with all second order derivatives, the Hessian, needs to be positive definite for the parameter values obtained from eq. (3.11). From eq. (3.11) the parameters

have to be solved. As eq. (3.11) is non-linear, the solution has to be computed by some iterative method.
A method for solving eq. (3.11) is based on a quadratic approximation of loss function V. The values previously computed for parameters $\hat{M}_m$ are used for the computation of $\hat{H}_n$ and matrix $\hat{H}_n$ is no longer considered a function of $\hat{M}_m$ during the minimization. In that case eq. (3.11) is reduced to a simple set of linear equations:

$$\left(Y - [\hat{M}_m \; ; \; \hat{A}_n] \cdot \begin{bmatrix} \mathcal{Q}_m \\ \hat{H}_n \end{bmatrix} \right) \cdot [\mathcal{Q}_m^t \; ; \; \hat{H}_n^t] = 0 \qquad (3.12)$$

It is easy to see that a unique solution for the parameters can be found from this set of equations as long as the matrix $[\mathcal{Q}_m^t \; ; \; \hat{H}_n^t]$ has full column rank. To start up matrix $\hat{H}_n$ is filled with the output error samples e_i obtained from a simulation on the available input/output data with a Markov parameter model estimated in a previous step (cf. eq. (3.7) and (3.8)).
Another method of finding the solution that minimizes eq. (3.10) is by using a numerical minimization method. A quasi Newton minimization method is to be preferred because of its efficiency and robustness (cf. [Fletcher, 1980]). In this case the problem defined by eq. (3.10) and (3.11) is solved with a numerical minimization method.
By the Least Squares method the expression $\hat{\Xi}^t \cdot \hat{B}_0^t \cdot \hat{B}_0 \cdot \hat{\Xi}$ is minimized as long as the tail effects may be neglected (cf. eq. (3.6) and (3.7)).

3.4 Maximum-likelihood estimation

The least squares estimation method, described in the previous section, has been derived without using any knowledge on the noise statistics. Only the energy of the difference between the measured outputs and the outputs simulated by the model was minimized in a quadratic sense.
The estimation of the parameters can also be viewed from a probabilistic point of view by making use of the maximum-likelihood method. The noise that interferes with the outputs of the process is assumed to be coloured and to have a direct coupling among the channels. So the output noise can be described as:

$$n_i = A_1 \cdot n_{i-1} + A_2 \cdot n_{i-2} + \ldots + A_n \cdot n_{i-n} + B_0 \cdot \xi_i \qquad (3.13)$$

Input noise ξ_i of the noise filter is assumed to be stationary, Gaussian, inter-channel independent and white. The noise representing the coupling

among the channels is given by:

$$\zeta_i = B_0 \cdot \xi_i \tag{3.14}$$

This noise is assumed to have the following properties:

$$R = E\{\zeta_i \cdot \zeta_j^t\} = \begin{cases} 0 & \text{for } i \neq j \quad (3.15) \\ \sigma^2 \cdot B_0 \cdot B_0^t & \text{for } i = j \quad (3.16) \end{cases}$$

$$p(\zeta) = \frac{1}{(2\pi)^{q/2}\{\det(R)\}^{1/2}} \cdot \exp\{-(\zeta^t \cdot R^{-1} \cdot \zeta)\} \tag{3.17}$$

with: q - the dimension of the vector ζ
R - the covariance matrix of the noise ($R = E\{\zeta \cdot \zeta^t\}$)
$p(\zeta)$ - the probability density function of the noise

The joint probability density function assumed for the complete set of noise samples obtained from the measurements is:

$$p(Z) = \frac{1}{(2\pi)^{q(l+1)/2}\{\det(R)\}^{(l+1)/2}} \cdot \exp\left(-1/2 \sum_{i=0}^{l} (\zeta_{k+i}^t \cdot R^{-1} \cdot \zeta_{k+i}) \right) \tag{3.18}$$

with: $Z = [\ \zeta_k\ ;\ \zeta_{k+1}\ ;\ \cdots\ ;\ \zeta_{k+l}\ ]$

In expression (3.18) ζ_{k+i} can be written as a function of the model parameters (cf. fig. 3.1):

$$\begin{aligned} \zeta_{k+i} &= y_{k+i} - M_0 \cdot u_{k+i} - M_1 \cdot u_{k+i-1} - \cdots - M_m \cdot u_{k+i-m} - \\ &\quad - A_1 \cdot e_{k+i-1} - \cdots - A_n \cdot e_{k+i-n} \\ &= y_{k+i} - \hat{y}_{k+i} \end{aligned} \tag{3.19}$$

If input/output samples of the process are available, eq. (3.18) can be regarded as a measure for the 'likelihood' of a particular value Z. Z is a function of the parameters of the system. Therefore eq. (3.18) gives for an available input/output data set of the process the 'likelihood' of each parameter set to cause the measured input/output behaviour.

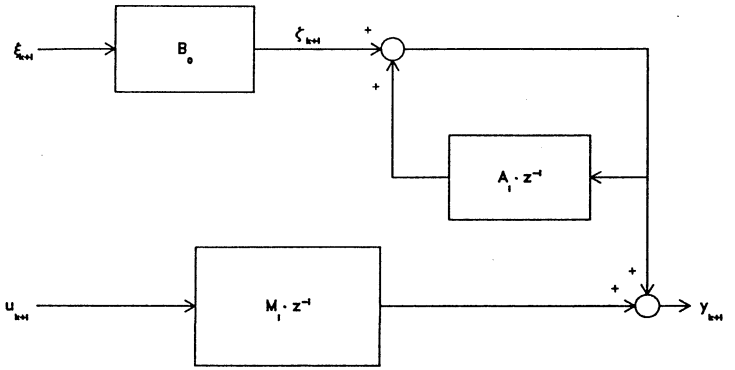

Fig. 3.1 Process and noise model

Substitution of eq. (3.19) in eq. (3.18) gives likelihood function L of the system (process and noise) parameters for a given set of input/output samples.

$$L(\hat{M}_m,\hat{A}_n|\ Y,U) = \frac{1}{(2\pi)^{q(l+1)/2}\cdot\{\det(\hat{R})\}^{(l+1)/2}}\cdot$$

$$\exp\Big(-1/2\ \sum_{i=0}^{l}(y^t_{k+i} - \hat{y}^t_{k+i})\cdot\hat{R}^{-1}\cdot(y_{k+i} - \hat{y}_{k+i})\Big) \qquad (3.20)$$

In this case the best estimate of the parameters is the one that maximizes L or minimizes -ln(L), which yields the same result. Necessary conditions for the parameters to minimize -ln(L) are:

$$\frac{\partial\{-\ln(L)\}}{\partial\hat{R}} = 0 \qquad (3.21)$$

and

$$\frac{\partial\{-\ln(L)\}}{\partial\hat{\Theta}} = 0 \qquad (3.22)$$

Furthermore the matrix with all second order partial derivatives of -ln(L)

needs to be positive semi definite. Eq. (3.21) results in:

$$\frac{\partial\{-\ln(L)\}}{\partial \hat{R}} = 1/2 \sum_{j=k}^{k+l} \left(-(\hat{R}^{-1})^t \cdot \hat{\zeta}_j \cdot \hat{\zeta}_j^t \cdot (\hat{R}^{-1})^t \right) + \frac{l+1}{2} \cdot (\hat{R}^{-1})^t = 0 \quad (3.23)$$

This yields:

$$\hat{R} = \frac{1}{l+1} \sum_{j=k}^{k+l} \hat{\zeta}_j \cdot \hat{\zeta}_j^t \quad (3.24)$$

as a necessary condition for the minimum of $-\ln(L)$. This expression can be substituted in eq. (3.20):

$$-\ln(L) = \frac{1}{2} \sum_{j=k}^{k+l} \hat{\zeta}_j^t \cdot \left(\frac{1}{l+1} \sum_{i=1}^{k+l} \hat{\zeta}_i \cdot \hat{\zeta}_i^t \right)^{-1} \cdot \hat{\zeta}_j + \frac{(l+1)q}{2} \cdot \ln(2\pi) +$$

$$+ \frac{l+1}{2} \ln\left(\det\left(\frac{1}{l+1} \sum_{i=k}^{k+l} \hat{\zeta}_i \cdot \hat{\zeta}_i^t\right) \right) \quad (3.25)$$

Since eq. (3.25) is a scalar equation, the first term to the right can be rewritten as:

$$\frac{l+1}{2} \operatorname{tr}\left\{ \sum_{j=k}^{k+l} \hat{\zeta}_j^t \cdot \left(\sum_{i=k}^{k+l} \hat{\zeta}_i \cdot \hat{\zeta}_i^t \right)^{-1} \cdot \hat{\zeta}_j \right\} =$$

$$= \frac{l+1}{2} \operatorname{tr}\left\{ \left(\sum_{j=k}^{k+l} \hat{\zeta}_i \cdot \hat{\zeta}_i^t \right)^{-1} \cdot \left(\sum_{j=k}^{k+l} \hat{\zeta}_j \cdot \hat{\zeta}_j^t \right) \right\} =$$

$$= \frac{l+1}{2} \cdot q \quad (3.26)$$

With this result eq. (3.25) becomes:

$$-\ln(L) = \frac{l+1}{2} \cdot \left\{ q + \ln\left(\det\left(\frac{1}{l+1} \cdot \sum_{i=k}^{k+l} \hat{\zeta}_i \cdot \hat{\zeta}_i^t \right) \right) + q \cdot \ln(2\pi) \right\} \quad (3.27)$$

From this expression the minimum of $-\ln(L)$ follows to be the minimum of:

$$\det\left(\sum_{i=k}^{k+l} \hat{\zeta}_i \cdot \hat{\zeta}_i^t \right) = \det(\hat{Z}^t \cdot \hat{Z}) \quad (3.28)$$

The parameters that minimize eq. (3.28) for a given set of input/output data are the maximum-likelihood estimates.

3.5 Various computational schemes

Estimation of the parameters of the model by means of the Least Squares Method implies the computation of the parameters of a non square set of linear equations in the form of least squares:

$$Y = \hat{\Theta} \cdot \hat{\Omega} + N \tag{3.29}$$

To find the least squares solution $\hat{\Theta}$ of eq. (3.29) the pseudo inverse of matrix $\hat{\Omega}$ has to be computed. If the covariance matrix R of the noise is known, the inverse of this covariance matrix may be used as a weighting matrix (cf. eq. (2.17)). In this case the Weighted Least Squares method is obtained. Weighting with the inverse of the covariance matrix makes the estimator efficient (cf. [Eykhoff, 1974; Van den Boom, 1982]).

Parameters $\hat{\Theta}$ are computed in such a way that the reconstructed outputs with this parameter matrix approximate the measured outputs as closely as possible. Difference E between the measured and reconstructed outputs is defined as:

$$E = Y - \hat{Y} = Y - \hat{\Theta} \cdot \Omega \tag{3.30}$$

The function that is minimized is:

$$V(\hat{\Theta}) = \mathrm{tr}(\, E \cdot E^t) = \mathrm{tr}\{(Y - \hat{\Theta} \cdot \Omega) \cdot (Y^t - \Omega^t \cdot \hat{\Theta}^t)\} \tag{3.31}$$

or, if a weighting matrix W ($= R^{-1}$) is applied:

$$V(\hat{\Theta}) = \mathrm{tr}(\, E \cdot W \cdot E^t) = \mathrm{tr}\{(Y - \hat{\Theta} \cdot \Omega) \cdot W \cdot (Y^t - \Omega^t \cdot \hat{\Theta}^t)\} \tag{3.32}$$

The analytic solution found is:

$$\hat{\Theta} = Y \cdot \Omega^t \cdot (\Omega \cdot \Omega^t)^{-1} \tag{3.33}$$

respectively:

$$\hat{\Theta} = Y \cdot W \cdot \Omega^t \cdot (\Omega \cdot W \cdot \Omega^t)^{-1} \tag{3.34}$$

To solve this Least Squares parameter estimation problem three different algorithms have been developed:

1. A recursive algorithm that also may be used for on-line estimation or update of the model parameters [Ljung, 1983; Sidar, 1976].
2. An algorithm based on the approximation of the non-linear problem given by eq. (3.12). Several iterations may be performed using the previously obtained parameter values to update the approximation.

3. An algorithm using a comprehensive quasi Newton minimization method to solve the non-linear set of equations given by eq. (3.10) and (3.11).

Besides the algorithms developed for solving the least squares estimation problem a fourth algorithm has been developed to solve the Maximum Likelihood estimation problem:

4. An algorithm using a comprehensive quasi Newton minimization method to solve the problem given by eq. (3.28).

First algorithm:

The first algorithm is based on the recursive computation of the inverse of $(\Omega \cdot \Omega^t)$. This inverse is computed through extension of the Ω and Y matrices with a new sample in each recursion step:

$$\hat{\Theta}_{j+1} = [Y_j \cdot \Omega_j^t + y_{j+1} \cdot \omega_{j+1}^t] \cdot [\Omega_j \cdot \Omega_j^t + \omega_{j+1} \cdot \omega_{j+1}^t]^{-1} \tag{3.35}$$

Using the matrix inversion lemma and some matrix manipulation, this equation is rewritten into:

$$\hat{\Theta}_{j+1} = \hat{\Theta}_j + [y_{j+1} - \hat{\Theta}_j \cdot \omega_{j+1}] \cdot [1 + \omega_{j+1}^t \cdot (\Omega_j \cdot \Omega_j^t)^{-1} \cdot \omega_{j+1}]^{-1} \cdot$$

$$[\omega_{j+1}^t \cdot (\Omega_j \cdot \Omega_j^t)^{-1}] \tag{3.36}$$

Similarly an expression is obtained for the inverse covariance matrix $(\Omega \cdot \Omega^t)^{-1}$:

$$[\Omega_{j+1} \cdot \Omega_{j+1}^t]^{-1} = [\Omega_j \cdot \Omega_j^t]^{-1} - [\Omega_j \cdot \Omega_j^t]^{-1} \cdot \omega_{j+1} \cdot$$

$$[1 + \omega_{j+1}^t \cdot (\Omega_j \cdot \Omega_j^t)^{-1} \cdot \omega_{j+1}]^{-1} \cdot \omega_{j+1}^t \cdot [\Omega_j \cdot \Omega_j^t]^{-1} \tag{3.37}$$

If Θ also contains parameters of the noise model, expression (3.36) provides a quadratic approach to the minimization of the cost function (eq. (3.31) or (3.32)). This is because the estimated noise model parameters depend on the estimated process model parameters. This dependence is neglected in eq. (3.36). For the computation of the output noise part of each new signal vector ω_{j+1} the parameter values obtained from the previous recursion step are used.
For this procedure to be improved, the part of the Ω matrix containing the prediction errors has to be updated completely after the computation of each estimated set of parameters $\hat{\Theta}$.

Second algorithm:

A better method of computing the estimates $\hat{\Theta}$ follows from eq (3.7) with $\hat{H}_1$ explicitly written as a function of the measured and the predicted outputs:

$$\hat{Y} = \hat{M}_m \cdot \Omega_m + \hat{A}_n \cdot \hat{H}_n \tag{3.7}$$

with:

$$\hat{H}_n = \begin{bmatrix} \hat{e}_{k-1} & \hat{e}_k & \cdots & \hat{e}_{k+l-1} \\ \hat{e}_{k-2} & \hat{e}_{k-1} & \cdots & \hat{e}_{k+l-2} \\ \cdot & \cdot & & \cdot \\ \cdot & \cdot & & \cdot \\ \hat{e}_{k-n} & \hat{e}_{k-n+1} & \cdots & \hat{e}_{k+l-n} \end{bmatrix} \tag{3.38}$$

and:

$$\hat{e}_i = y_i - \begin{bmatrix} \hat{M}_0 & \hat{M}_1 & \cdots & \hat{M}_m \end{bmatrix} \cdot \begin{bmatrix} u_i \\ u_{i-1} \\ \cdot \\ \cdot \\ u_{i-m} \end{bmatrix} \tag{3.39}$$

Using eq. (3.39) H_n can be written as (cf. eq. (3.11)):

$$H_n = Y^* - M_m^* \cdot \Omega_m^* \tag{3.40}$$

with:

$$Y^* = \begin{bmatrix} y_{k-1} & y_k & \cdots & y_{k+l-1} \\ y_{k-2} & y_{k-1} & \cdots & y_{k+l-2} \\ \cdot & \cdot & & \cdot \\ \cdot & \cdot & & \cdot \\ y_{k-n} & y_{k-n-1} & \cdots & y_{k+l-n} \end{bmatrix}$$

$$\Omega_m^* = \begin{bmatrix} \Omega_{m_{k-1}}^t & ; & \Omega_{m_{k-2}}^t & ; & \cdots & ; & \Omega_{m_{k-n}}^t \end{bmatrix}^t$$

$$M_m^* = \text{diag}\ (\hat{M}_m)$$

Substitution of (3.40) in (3.7) yields:

$$\hat{Y} = [\hat{M}_m ; \hat{A}_n] \cdot \begin{bmatrix} \Omega_{m_k} \\ Y^* - M_m^* \cdot \Omega_m^* \end{bmatrix} \qquad (3.41)$$

From this expression the function to be minimised can be found to be:

$$V = \text{tr}\{ \left(Y - \hat{M}_m \cdot \Omega_{m_k} - \hat{A}_n \cdot Y^* + \hat{A}_n \cdot M_m^* \cdot \Omega_m^* \right) \cdot$$

$$\left(Y^t - \Omega_{m_k}^t \cdot \hat{M}_m^t - Y^{*t} \cdot \hat{A}_n^t + \Omega_m^{*t} \cdot M_m^{*t} \cdot \hat{A}_n^t \right) \} \qquad (3.42)$$

This function is nonquadratic in parameters A_n and M_m. Consequently differentiation does not result in a set of linear equations. The equation to be solved is eq. (3.11).

Again in this expression $\hat{H}_n$ is a function of $\hat{M}_m$ as can be seen from eq. (3.40).
A method used to solve this problem is an iterative procedure based on succesive substitution in the form of least squares. This gives the second algorithm developed to solve the Least Squares estimation problem (algorithm 2a). The problem solved in each iteration cycle is:

$$Y = [\hat{M}_{m,i} ; \hat{A}_{n,i}] \cdot \begin{bmatrix} \Omega_{m,k} \\ \hat{H}_{n,i-1} \end{bmatrix} \qquad i=1,2,... \qquad (3.43)$$

For the computation of $\hat{H}_n$ the value of $\hat{M}_m$ computed in the previous iteration cycle is used. $\hat{H}_n$ is computed by means of eq. (3.40). The least squares solution can be computed using Householder transformations. In this case matrix $[\Omega_{m,k}^t ; \hat{H}_n^t]^t$ is transformed into a non-singular, upper triangular block matrix of dimension $((l+1)p+nq) \times ((l+1)p+nq)$. Matrix Y is transformed alike. The transformations are computed in such a way that the span of

difference E:

$$E = Y - \left[\hat{M}_{m,i} \; ; \; \hat{A}_{n,i} \right] \cdot \begin{bmatrix} \Omega_{m_k} \\ \hat{H}_{n,i-1} \end{bmatrix} \tag{3.44}$$

is orthogonal to $\left[\Omega^t_{m_k} \; ; \; \hat{H}^t_{n,i-1} \right]^t$.

A modified version of this method is provided by (algorithm 2b):

$$Y_k \cdot \left[\Omega^t_{m_k} ; \hat{H}^t_{n,i-1} \right] = \left[\hat{M}_{m_k} \; ; \; \hat{A}_{n,i} \right] \cdot \begin{bmatrix} \Omega_{m_k} \\ \hat{H}_{n,i-1} \end{bmatrix} \cdot \left[\Omega^t_{m_k} ; \hat{H}^t_{n,i-1} \right] \tag{3.45}$$

In this expression the product of matrices $\left[\Omega^t_{m_k} \; ; \; \hat{H}^t_{n,i-1} \right]^t$ and $\left[\Omega^t_{m_k} \; ; \; \hat{H}^t_{n,i-1} \right]$ has the same rank as matrix $\left[\Omega^t_{m_k} \; ; \; \hat{H}^t_{n,i-1} \right]^t$. If the matrix has full row rank, the set of equations eq. (3.45) has a unique solution. The solution found is the same as that for eq. (3.43). The advantage of using eq. (3.45) compared to eq. (3.43) is in the sizes of the matrices that have to be stored and handled. The size of the matrices is determined by the number of parameters and the number of samples.
Disadvantage of using eq. (3.45) is that the condition number of the product of the information matrix with its transpose is the square of the condition number of the matrix itself. Consequently, if the input signals are poorly conditioned or if the equation errors can be seen as the outputs of a low-pass filter with a large eigenvalue the solution computed with eq. (3.45) is generally worse than that found with eq. (3.43).

Third algorithm:

A different procedure is the minimization of eq. (3.42) by a comprehensive quasi Newton minimization method. For this method the first-order derivatives with respect to parameters (eq. (3.42)) have to be computed. As a starting value for the quasi Newton algorithm the solution found from eq. (3.43) is used.

Besides the algorithms that have been developed to solve the Least Squares parameter estimation problem a fourth algorithm has been developed to solve the maximum likelihood parameter estimation problem.

Fourth algorithm:

The last algorithm that has been developed is based on the computation of the maximum-likelihood estimate for the model parameters. The function to be minimized is given by eq. (3.28):

$$V = \det(Z^t \cdot Z)$$

Eq. (3.14) shows this is equal to:

$$V = \det\left\{ \left(\left(Y - \left[\hat{M}_m \; ; \; \hat{A}_n \right] \cdot \begin{bmatrix} \Omega_{m_k} \\ \\ \hat{H}_n \end{bmatrix} \right) \cdot \left(Y^t - \left[\Omega_{m_k}^t \; ; \; \hat{H}_n^t \right] \cdot \begin{bmatrix} \hat{M}_m^t \\ \\ \hat{A}_n^t \end{bmatrix} \right) \right) \right\} \tag{3.46}$$

Unlike in eq. (3.42) a determinant function has to be minimized instead of a trace function. For the minimization of this function, too, a comprehensive quasi Newton algorithm has been used. This algorithm computes approximations for the derivatives with respect to the parameters for each iteration cycle.

For the last three algorithms mentioned the following three matrices have to be computed once only (cf. [Vaessen, 1983]):

$$YSQ = Y_k \cdot Y_k^t \tag{3.47a}$$

$$SY = \Omega_{m_k} \cdot Y_k^t \tag{3.47b}$$

$$SSQ = \Omega_{m_k} \cdot \Omega_{m_k}^t \tag{3.47c}$$

Another three matrices are needed, which have to be updated in each iteration cycle or during each function call by the numerical minimization algorithm (see flow diagram fig. 3.2):

$$\hat{H}_n \cdot Y^t \tag{3.47d}$$

$$\hat{H}_n \cdot \Omega_{m_k}^t \tag{3.47e}$$

$$\hat{H}_n \cdot \hat{H}_n^t \tag{3.47f}$$

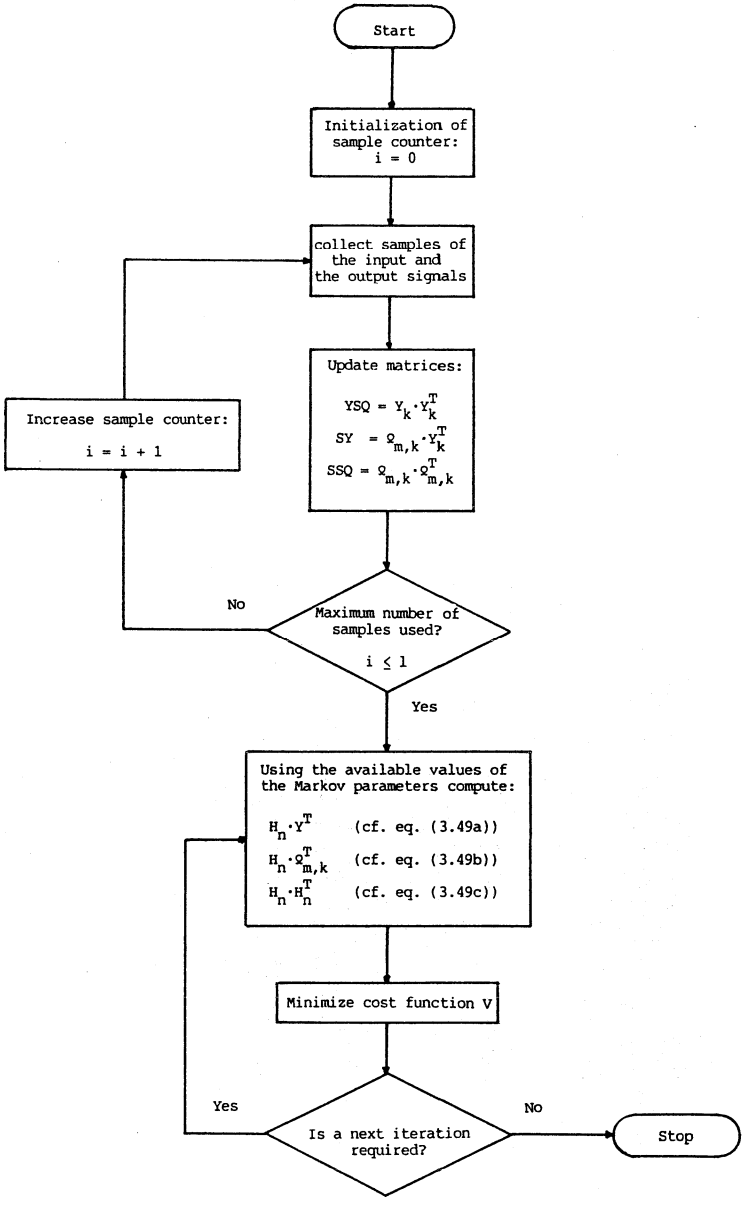

Fig. 3.2 Flow diagram for the computation of the estimates.

As a basis for this update the following matrices are computed once from the data-set:

$$YASY = \begin{bmatrix} Y_{k-1} \cdot Y_k^t \\ Y_{k-2} \cdot Y_k^t \\ \vdots \\ Y_{k-n} \cdot Y_k^t \end{bmatrix} \qquad SASY = \begin{bmatrix} \Omega_{m_{k-1}} \cdot Y_k^t \\ \Omega_{m_{k-2}} \cdot Y_k^t \\ \vdots \\ \Omega_{m_{k-n}} \cdot Y_k^t \end{bmatrix}$$

$$YASS = \begin{bmatrix} Y_{k-1} \cdot \Omega_{m_k}^t \\ Y_{k-2} \cdot \Omega_m^t \\ \vdots \\ Y_{k-n} \cdot \Omega_{m_k}^t \end{bmatrix} \qquad SASS = \begin{bmatrix} \Omega_{m_{k-1}} \cdot \Omega_{m_k}^t \\ \Omega_{m_{k-2}} \cdot \Omega_{m,k}^t \\ \vdots \\ \Omega_{m_{k-n}} \cdot \Omega_{m_k}^t \end{bmatrix}$$

$$YASYAS = \begin{bmatrix} Y_{k-1} \cdot Y_{k-1}^t & Y_{k-1} \cdot Y_{k-2}^t & \cdots & Y_{k-1} \cdot Y_{k-n}^t \\ Y_{k-2} \cdot Y_{k-1}^t & Y_{k-2} \cdot Y_{k-2}^t & \cdots & Y_{k-2} \cdot Y_{k-n}^t \\ \vdots & \vdots & & \vdots \\ Y_{k-n} \cdot Y_{k-1}^t & Y_{k-n} \cdot Y_{k-2}^t & \cdots & Y_{k-n} \cdot Y_{k-n}^t \end{bmatrix}$$

$$YASSAS = \begin{bmatrix} Y_{k-1} \cdot \Omega_{m_{k-1}}^t & Y_{k-1} \cdot \Omega_{m_{k-2}}^t & \cdots & Y_{k-1} \cdot \Omega_{m_{k-n}}^t \\ Y_{k-2} \cdot \Omega_{m_{k-1}}^t & Y_{k-2} \cdot \Omega_{m_{k-2}}^t & \cdots & Y_{k-2} \cdot \Omega_{m_{k-n}}^t \\ \vdots & \vdots & & \vdots \\ Y_{k-n} \cdot \Omega_{m_{k-1}}^t & Y_{k-n} \cdot \Omega_{m_{k-2}}^t & \cdots & Y_{k-n} \cdot \Omega_{m_{k-n}}^t \end{bmatrix}$$

$$SASSAS = \begin{bmatrix} \Omega_{m_{k-1}} \cdot \Omega^t_{m_{k-1}} & \Omega_{m_{k-1}} \cdot \Omega^t_{m_{k-2}} & \cdots & \Omega_{m_{k-1}} \cdot \Omega^t_{m_{k-n}} \\ \Omega_{m_{k-2}} \cdot \Omega^t_{m_{k-1}} & \Omega_{m_{k-2}} \cdot \Omega^t_{m_{k-2}} & \cdots & \Omega_{m_{k-2}} \cdot \Omega^t_{m_{k-n}} \\ \vdots & \vdots & & \vdots \\ \Omega_{m_{k-n}} \cdot \Omega^t_{m_{k-1}} & \Omega_{m_{k-n}} \cdot \Omega^t_{m_{k-2}} & \cdots & \Omega_{m_{k-n}} \cdot \Omega^t_{m_{k-n}} \end{bmatrix} \tag{3.48}$$

The updates for matrices $\hat{H}_n \cdot Y^t$, $\hat{H}_n \cdot \Omega^t_{m_k}$ and $\hat{H}_n \cdot \hat{H}^t_n$ can be computed simply from these matrices each time a new estimate for $\hat{M}_m$ is available as defined in:

$$\hat{H}_n \cdot Y^t = YASY - diag(\hat{M}_m) \cdot SASY \tag{3.49a}$$

$$\hat{H}_n \cdot \Omega^t_{m_k} = YASS - diag(\hat{M}_m) \cdot SASS \tag{3.49b}$$

$$\hat{H}_n \cdot \hat{H}^t_n = YASYAS - diag(\hat{M}_m) \cdot (YASSAS)^t - (YASSAS) \cdot diag(\hat{M}^t_m) + diag(\hat{M}_m) \cdot SASSAS \cdot diag(\hat{M}^t_m) \tag{3.49c}$$

3.6 Simulation examples and tests applied to examine the results

For testing of the two estimation methods -Least Squares method and Maximum Likelihood method- and for comparing the various computational diagrams four different simulated processes have been used. The simulated processes cover part of the problems also encountered in practice:

- process dynamics with clusters of eigenvalues
- coloured output noise
- coupling of process dynamics between various inputs and outputs

First simulated process:

The first simulated process is a simple process consisting of two independent SISO systems with different eigenvalues. The outputs of the process are disturbed with a coloured output noise. The eigenvalues of the noise colouring filter are larger than the eigenvalues of the process. A

state space description of this system is given by:

process:

$$F = \begin{bmatrix} 0.7 & 0.0 \\ 0.0 & 0.5 \end{bmatrix} \qquad G = H = \begin{bmatrix} 1.0 & 0.0 \\ 0.0 & 1.0 \end{bmatrix}$$

$$D = \begin{bmatrix} 0.0 & 0.0 \\ 0.0 & 0.0 \end{bmatrix}$$

noise colouring filter:

$$F_n = \begin{bmatrix} 0.85 & 0.0 \\ 0.0 & 0.75 \end{bmatrix} \qquad G_n = H_n = \begin{bmatrix} 1.0 & 0.0 \\ 0.0 & 1.0 \end{bmatrix}$$

$$D_n = \begin{bmatrix} 0.0 & 0.0 \\ 0.0 & 0.0 \end{bmatrix}$$

Second simulated process:

The second simulated process is a 4-th order, 3-input, 2-output MIMO process. The process has two clusters of eigenvalues. The output noise is coloured by a second order noise filter with eigenvalues close to the smallest eigenvalues of the process. A state space description of this process is given by:

process:

$$F = \begin{bmatrix} 0.7 & 0.0 & 0.0 & 0.0 \\ 0.0 & 0.6 & 0.0 & 0.0 \\ 0.0 & 0.0 & 0.2 & 0.0 \\ 0.0 & 0.0 & 0.0 & 0.1 \end{bmatrix}$$

$$G = \begin{bmatrix} 1.0 & 0.0 & 1.0 \\ -1.0 & 0.5 & 0.5 \\ 0.0 & 1.0 & -0.5 \\ 0.0 & 0.5 & -1.0 \end{bmatrix}$$

$$H = \begin{bmatrix} 0.5 & 0.0 & 1.0 & 1.0 \\ 1.0 & -0.5 & 0.5 & -0.5 \end{bmatrix}$$

$$D = \begin{bmatrix} 0.0 & 0.0 & 0.0 \\ 0.0 & 0.0 & 0.0 \end{bmatrix}$$

noise colouring filter:

$$F_n = \begin{bmatrix} 0.3 & 0.0 \\ 0.0 & 0.2 \end{bmatrix} \qquad G_n = H_n = \begin{bmatrix} 1.0 & 0.0 \\ 0.6 & 0.5 \end{bmatrix}$$

$$D_n = \begin{bmatrix} 0.0 & 0.0 \\ 0.0 & 0.0 \end{bmatrix}$$

Third simulated process:

The third simulated process is the same as the second simulated process except for the noise characteristics. Now the output noise is coloured by a noise filter with eigenvalues close to the largest eigenvalues of the process. Furthermore the noise filter gives a direct coupling among the channels. A state space description of this simulated process is:

process:

$$F = \begin{bmatrix} 0.7 & 0.0 & 0.0 & 0.0 \\ 0.0 & 0.6 & 0.0 & 0.0 \\ 0.0 & 0.0 & 0.2 & 0.0 \\ 0.0 & 0.0 & 0.0 & 0.1 \end{bmatrix}$$

$$G = \begin{bmatrix} 1.0 & 0.0 & 1.0 \\ -1.0 & 0.5 & 0.5 \\ 0.0 & 1.0 & -0.5 \\ 0.0 & 0.5 & -1.0 \end{bmatrix}$$

$$H = \begin{bmatrix} 0.5 & 0.0 & 1.0 & 1.0 \\ 1.0 & -0.5 & 0.5 & -0.5 \end{bmatrix}$$

$$D = \begin{bmatrix} 0.0 & 0.0 & 0.0 \\ 0.0 & 0.0 & 0.0 \end{bmatrix}$$

noise colouring filter:

$$F_n = \begin{bmatrix} 0.85 & 0.0 \\ 0.0 & 0.75 \end{bmatrix} \qquad G_n = H_n = \begin{bmatrix} 1.0 & 0.0 \\ 0.6 & 0.5 \end{bmatrix}$$

$$Dn = \begin{bmatrix} 1.0 & 0.3 \\ 0.6 & 0.4 \end{bmatrix}$$

Fourth simulated process:

The fourth simulated process again is a MIMO process with 3 inputs and 2 outputs. The eigenvalues of this process are larger than the eigenvalues of the previous processes. The time constant corresponding to the largest eigenvalue of the process is about 3 times as large as the largest time constant of simulated processes 2 and 3. The characteristics of the noise colouring filter are similar to those of the third simulated process. A

state space description of this process is given by:

process:

$$F = \begin{bmatrix} 0.9 & 0.0 & 0.0 & 0.0 \\ 0.0 & 0.8 & 0.0 & 0.0 \\ 0.0 & 0.0 & 0.3 & 0.0 \\ 0.0 & 0.0 & 0.0 & 0.2 \end{bmatrix}$$

$$G = \begin{bmatrix} 1.0 & 0.0 & 1.0 \\ -1.0 & 0.5 & 0.5 \\ 0.0 & 1.0 & -0.5 \\ 0.0 & 0.5 & -1.0 \end{bmatrix}$$

$$H = \begin{bmatrix} 0.5 & 0.0 & 1.0 & 1.0 \\ 1.0 & -0.5 & 0.5 & -0.5 \end{bmatrix}$$

$$D = \begin{bmatrix} 0.0 & 0.0 & 0.0 \\ 0.0 & 0.0 & 0.0 \end{bmatrix}$$

noise colouring filter:

$$F_n = \begin{bmatrix} 0.85 & 0.0 \\ 0.0 & 0.75 \end{bmatrix} \qquad G_n = H_n = \begin{bmatrix} 1.0 & 0.0 \\ 0.6 & 0.5 \end{bmatrix}$$

$$Dn = \begin{bmatrix} 1.0 & 0.3 \\ 0.6 & 0.4 \end{bmatrix}$$

The test signals used as input signals for both process and noise model are Gaussian, inter-channel independent, white noise sequences. All input signals have a mean value $\mu_i = 0$. The variances of the input signals are $\sigma_i^2 = 1$. The variances of the input signals offered to the noise filters are chosen such that the signal-to-noise ratio at each output is equal to S/N = 20 dB. For testing of the estimation procedures 20 different input/output data sequences have been used. Each sequence consists of 1000 samples for all inputs and outputs of the system.
The computational methods used are:

RECMAK - recursive estimation of the system parameters; eq. (3.36), (3.37)

MARKEST - a quadratic approximation of the non-linear estimation problem is solved. Both sides of the resulting set of linear equations are post-multiplied by the transposed of the information matrix. Only the first step of the iterative substitution of previously estimated Markov parameters is executed; eq. (3.45)

EXACTMARK - Again a quadratic approximation of the non-linear estimation problem is solved. Only the first step of the iterative substitution procedure is executed; eq. (3.43)

MARKEST-25 - The same as MARKEST-1. Now 25 cycles of the iterative substitution procedure are executed.

MARKMIN - The complete non-linear problem is solved by a comprehensive quasi Newton method; eq. (3.42), (3.11)

MARKMIND - maximum-likelihood estimation of the parameters by a comprehensive quasi Newton method, which also computes values for the derivatives with respect to the parameters; eq. (3.46)

To make tail effects small, the following numbers of parameters have been estimated for the various simulated processes:

system 1 - 15 Markov parameters and 2 AR noise parameters
system 2 - 20 Markov parameters and 2 AR noise parameters
system 3 - 20 Markov parameters and 2 AR noise parameters
system 4 - 50 Markov parameters and 2 AR noise parameters

The results obtained with the various algorithms and methods are compared with respect to:

- the value of the cost function obtained with the estimated parameters
- the total energy of the output error
- the fit of the estimated impulse responses to the real impulse responses

As a tool for comparing the impulse responses obtained with the various computational methods, with the impulse responses of the true simulated processes, an error, ERR, has been defined on the basis of the Hankel norm of the impulse responses. This Hankel norm of an impulse response is defined as the largest singular value of the doubly infinite block Hankel matrix H. This H is defined by (cf. eq. (2.1), (2.3), (2.8), (2.9)):

$$H = \tilde{O}b \cdot \tilde{C}o = \begin{bmatrix} M_1 & M_2 & \cdots & M_k & \cdot\cdot \\ M_2 & M_3 & \cdots & M_{k+1} & \cdot\cdot \\ \cdot & \cdot & & \cdot & \\ \cdot & \cdot & & \cdot & \\ M_k & M_{k+1} & \cdots & M_{2k-1} & \cdot\cdot \\ \cdot & \cdot & & \cdot & \\ \cdot & \cdot & & \cdot & \end{bmatrix} \qquad (3.50)$$

with: $\tilde{C}o = [\, G \;;\; F \cdot G \;;\; \ldots \;;\; F^{n-1} \cdot G \;;\; F^{n} \cdot G \;;\; \cdot\cdot \,]$

$$\tilde{O}b = [\, H^t \;;\; F^t \cdot H^t \;;\; \ldots \;;\; (F^{n-1})^t \cdot H^t \;;\; \cdot\cdot \,]^t$$

By definition (eq. (3.50)) the block Hankel matrix H can be interpreted as the mapping of past inputs to future outputs via state x_k (cf. eq. (2.3)):

$$x_k = \tilde{C}o \cdot \begin{bmatrix} u_{k-1} \\ u_{k-2} \\ . \\ . \end{bmatrix} \tag{3.51a}$$

$$\begin{bmatrix} y_k \\ y_{k+1} \\ . \\ . \end{bmatrix} = \tilde{O}b \cdot x_k \tag{3.51b}$$

The largest singular value, σ_1, of the doubly infinite Hankel matrix is equal to the maximum obtainable gain of past inputs to future outputs [Staar, 1982]:

$$||\tilde{Y}||_2 = \max_{||U||_2=1} ||Y||_2 = \max_{||U||_2=1} ||H \cdot U||_2 = ||H||_\infty = ||M||_H = \sigma_1$$

with: $\tilde{Y} = \left[\tilde{y}_k^t \; ; \; \tilde{y}_{k+1}^t \; ; \; \ldots \right]^t$

$$U = \left[u_{k-1}^t \; ; \; u_{k-2}^t \; ; \; \ldots \right]^t$$

To get a measure for the quality of the estimated impulse response models the maximum obtainable gain of the so called "error" system is determined. The impulse responses of the "error" system are defined as the difference of the impulse responses of the true system and the impulse responses obtained from the identification:

$$M_{err_i} = M_{t_i} - \tilde{M}_i \qquad \text{for all } i \epsilon I,\ I=0,1,2,\ \ldots \tag{3.53}$$

with: M_{err_i} - i-th sample of the impulse responses of the "error" system

M_{t_i} - i-th sample of the impulse responses of the true system

$\tilde{M}_i$ - i-th sample of the estimated impulse responses

Error ERR is defined as:

$$ERR = || M_t - \tilde{M} ||_H = \sigma_1(H - \tilde{H}) = \sigma_1(H_{err}) \tag{3.54}$$

with: H - the doubly infinite block Hankel matrix belonging to the true system

$\tilde{H}$ - the doubly infinite block Hankel matrix belonging to the system obtained from the identification

$\sigma_1(H - \tilde{H})$ - the maximum singular value of $H - \tilde{H}$

According to eq. (3.53) ERR is related to the maximum possible energy of the output signal obtained from the mapping of past inputs to future outputs of the "error" system. For computation of the maximum Hankel singular value σ_1 the observability and controllability gramians, P_{err} and Q_{err}, have to be determined. The controllability gramian is defined by:

$$P_{err} = \sum_{i=0}^{\infty} F_{err}^{i} \cdot G_{err} \cdot G_{err}^{t} \cdot (F_{err}^{t})^{i} \tag{3.55}$$

The observability gramian is defined by:

$$Q_{err} = \sum_{i=0}^{\infty} (F_{err}^{t})^{i} \cdot H_{err}^{t} \cdot H_{err} \cdot F_{err}^{i} \tag{3.56}$$

In these expressions F_{err}, G_{err} and H_{err} are matrices of a state space representation of the "error" system (cf. eq. (2.3) and fig. 2.6). The required state space representation of the estimated impulse response model can be obtained from a simple substitution of the estimated parameters in the state space matrices in observability canonical form (cf. [Kailath, 1980]).
The gramians satisfy the discrete time Lyapunov equations:

$$P_{err} - F_{err} \cdot P_{err} \cdot F_{err}^{t} = G_{err} \cdot G_{err}^{t} \tag{3.57}$$

$$Q_{err} - F_{err}^{t} \cdot Q_{err} \cdot F_{err} = H_{err}^{t} \cdot H_{err} \tag{3.58}$$

From the definitions of the block Hankel matrix, the observability and the controllability gramian, the singular values of the block Hankel matrix are

found to be equal to:

$$\sigma_j^2(H_{err}) = \lambda_j(H_{err}^t \cdot H_{err}) = \lambda_j(\tilde{C}o_{err}^t \cdot \tilde{O}b_{err}^t \cdot \tilde{O}b_{err} \cdot \tilde{C}o_{err}) =$$

$$= \lambda_j(\tilde{C}o_{err} \cdot \tilde{C}o_{err}^t \cdot \tilde{O}b_{err}^t \cdot \tilde{O}b_{err}) = \lambda_j(P_{err} \cdot Q_{err}) \qquad (3.59)$$

As a result the maximum singular value of the doubly infinite block Hankel matrix is equal to the square root of the maximum eigenvalue of the product of the controllability gramian and the observability gramian. If a balanced realization of the error system is computed both gramians will be equal and diagonal (cf. [Kailath, 1980]). In this case the maximum Hankel singular value of the error system is equal to the maximum diagonal element of the gramians.

Besides the Hankel norms of the "error" systems also the Frobenius norms of these systems are computed. The Frobenius norm of a system is defined as the square root of the sum of the squares of all Hankel singular values:

$$||H_{err}||_F = \sqrt{\sum_{i=1}^{n} \sigma_i^2} \qquad (3.60)$$

The meaning of both norms defined above and used for the judgement of the quality of the models obtained from the estimations is given by the following descriptions:

- The Hankel norm of the error system, defined by eq. (3.53), is the maximum value of the square root of the sum of all squared outputs (output energy) observed **from** a time instance T_0, that can be produced by the error system if worst case, unity input signals are applied **until** time instance T_0. The Hankel norm therefore may be interpreted as the worst case error that can occur in simulations.
- The Frobenius norm of the error system, defined by eq. (3.60), is the square root of the sum of all possible squared, independent sets of output vectors of the error system observed **from** a time instance T_0, if unity inputs are applied **until** time instance T_0. The Frobenius norm divided by the order of the error system may be interpreted as the average error that can occur in simulations.

For evaluation of the quality of the noise models obtained from the estimations two criteria are important with respect to the use of the noise models for the design of control systems:

- the total noise energy at the output of the system
- the frequency distribution of the noise

These criteria determine the demands that have to be put on the control system with respect to closed loop amplification and bandwidth of the closed loop system, if suppression of the noise is important.

The Power Spectrum of the noise (Fourier series of the autocorrelation of the noise) gives information on both the noise energy and the frequency distribution of the noise (cf. [Papoulis, 1977]).

3.7 Results

The estimation methods discussed in this chapter have been applied to the simulated processes discussed in the previous section. The values of the cost functions, together with the values obtained for the output errors are given in fig. 3.3 - 3.6. In these figures for each system the average values are shown of both the criterion values and of the output errors that have been computed from the results obtained from the 20 estimations. Around each value the standard deviation interval, computed from the 20 estimation results, is plotted.

In general, the cost function values obtained with the recursive estimation algorithm RECMAK are slightly bigger than the results obtained with the other algorithms. Especially in cases of multivariable systems that have coloured output noise with a bandwidth close to the bandwidth determined by the largest eigenvalues of the process ("low frequent" output noise; system 1, system 3 and system 4) the results obtained with the recursive algorithm are worse than the results obtained with the other algorithms.
The algorithm based on the iterative substitution of previously estimated Markov parameters (MARKEST-25) often appears to diverge for multivariable systems disturbed with "low frequent" output noise (cf. fig. 3.5 and 3.6).
The algorithms that use a numerical method for the minimization of the cost function could not be applied for system 4. This is due to the large number of parameters to be handled. The amount of processor time required for minimization of the cost function is at least a quadratic function of the number of parameters.

Examination of the results obtained for the output errors again indicates a poor behaviour of the recursive algorithm; the results are worse than the results obtained with the other algorithms.
Iterative solution of a quadratic approximation of the cost function using the Markov parameters obtained from a previous iteration sometimes deteriorates the results again for simulated process 3 (cf. fig. 3.5). For simulated process 4 this is almost always the case (cf. fig. 3.6).

The computed Hankel norms and Frobenius norms of the "error" systems (cf. eq. (3.53) - (3.60)) are given in fig. 3.7 - 3.10 respectively for simulated processes 1, 2, 3 and 4. The results presented are the average values of the norms computed from each of the 20 FIR models estimated for each system. Again the computed standard deviation intervals are indicated around the average values.

From the obtained values for the Hankels norms its clear that the recursive method gives results that are inferior to the results obtained with the other methods in cases of "low frequent" output noise (cf. fig. 3.7, 3.9 and 3.10).

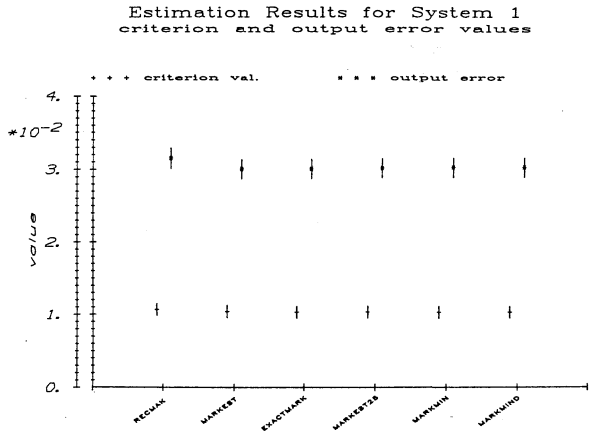

Fig. 3.3 Values of the estimation criterion and the output error obtained for system 1

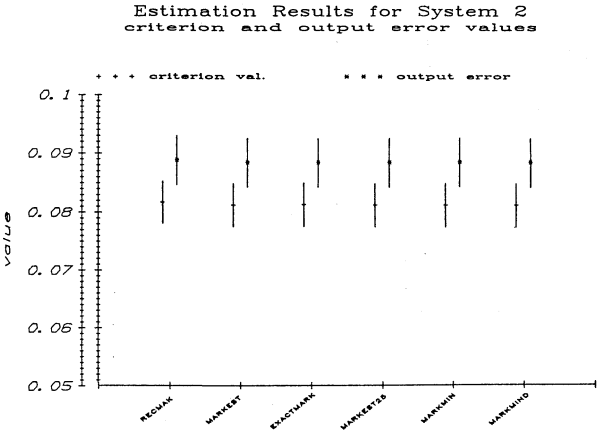

Fig. 3.4 Values of the estimation criterion and the output error obtained for system 2

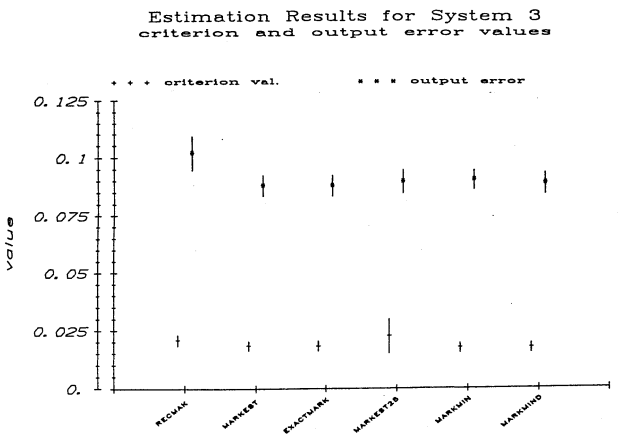

Fig. 3.5 Values of the estimation criterion and the output error obtained for system 3

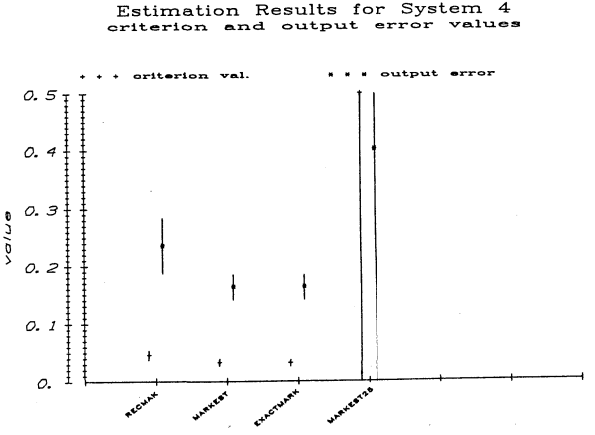

Fig. 3.6 Values of the estimation criterion and the output error obtained for system 4

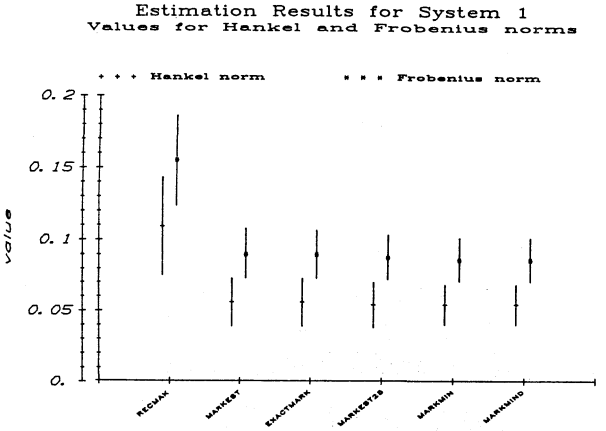

Fig. 3.7 Computed Hankel norms and Frobenius norms of the error systems resulting from the estimated FIR models for system 1

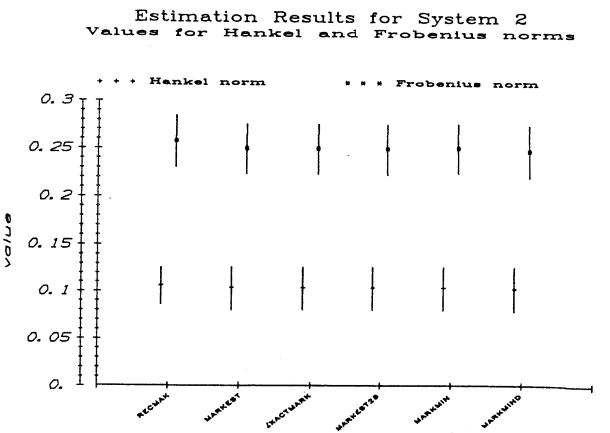

Fig. 3.8 Computed Hankel norms and Frobenius norms of the error systems resulting from the estimated FIR models for system 2

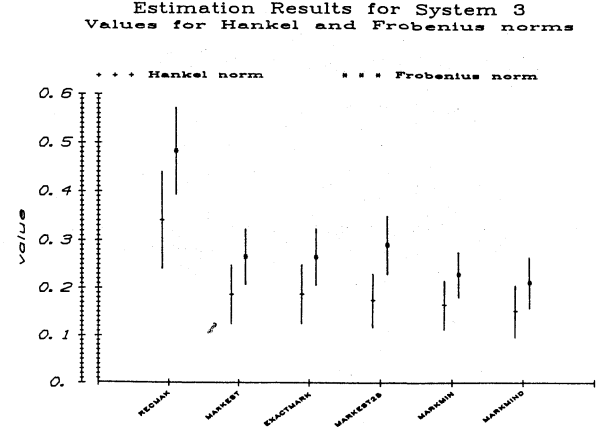

Fig. 3.9 Computed Hankel norms and Frobenius norms of the error systems resulting from the estimated FIR models for system 3

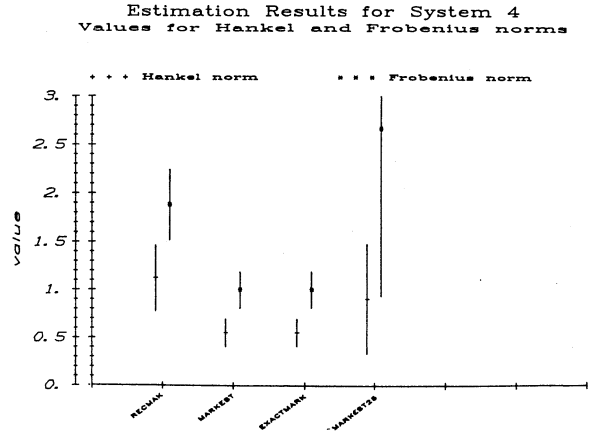

Fig. 3.10 Computed Hankel norms and Frobenius norms of the error systems resulting from the estimated FIR models for system 4

		Hankel norm	Frobenius norm
system 1:	true system	0.196E+01	0.237E+01
	RECMAK	0.109E+00	0.155E+00
	MARKEST	0.557E-01	0.896E-01
	EXACTMARK	0.556E-01	0.895E-01
	MARKEST25	0.536E-01	0.874E-01
	MARKMIN	0.539E-01	0.858E-01
	MARKMIND	0.540E-01	0.858E-01
system 2:	true system	0.336E+01	0.390E+01
	RECMAK	0.106E+00	0.258E+00
	MARKEST	0.104E+00	0.250E+00
	EXACTMARK	0.104E+00	0.250E+00
	MARKEST25	0.104E+00	0.250E+00
	MARKMIN	0.104E+00	0.251E+00
	MARKMIND	0.103E+00	0.248E+00
system 3:	true system	0.336E+01	0.390E+01
	RECMAK	0.340E+00	0.482E+00
	MARKEST	0.185E+00	0.264E+00
	EXACTMARK	0.185E+00	0.263E+00
	MARKEST25	0.172E+00	0.288E+00
	MARKMIN	0.162E+00	0.226E+00
	MARKMIND	0.150E+00	0.210E+00
system 4:	true system	0.874E+01	0.903E+01
	RECMAK	0.112E+01	0.188E+01
	MARKEST	0.543E+00	0.992E+00
	EXACTMARK	0.542E+00	0.993E+00
	MARKEST25	0.895E+00	0.266E+01

table 3.1 Norms of the true systems and average values of the norms computed for the error systems

In the case of coloured noise with a large bandwidth all methods perform almost equally (cf. fig. 3.8).
To give a reference table 3.1 shows the values of the Hankel norms and the Frobenius norms for each of the four systems together with the average values of the norms computed for the error systems. The results obtained for the various systems appear to be rather good.

The computed Frobenius norms of the "error" systems also indicate the inferiority of the recursive algorithm compared to the other algorithms in cases of "low frequent" output noise (cf. fig. 3.7, 3.9 and 3.10).
Fig. 3.10 clearly shows the bad performance of the method based on iterative substitution (MARKEST-25) for simulated process 4.

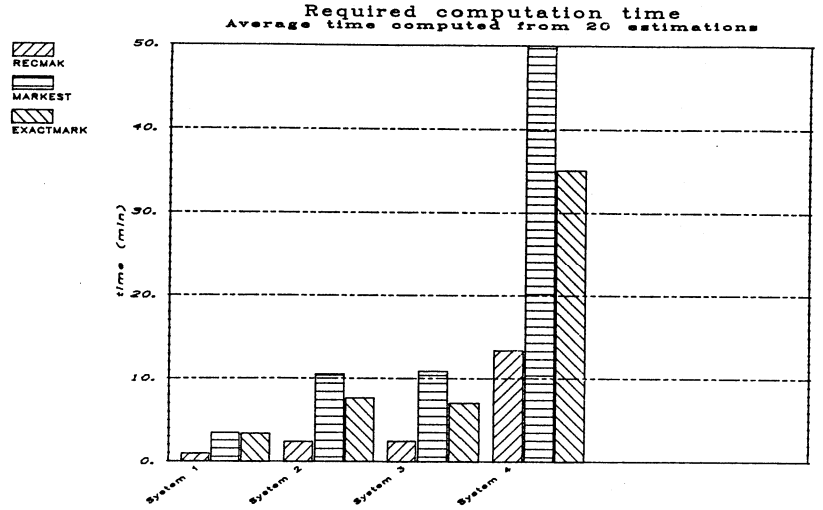

Fig. 3.11 Average processor time (VAX 11/750) used for the estimation of the FIR model parameters by RECMAK, MARKEST and EXACTMARK

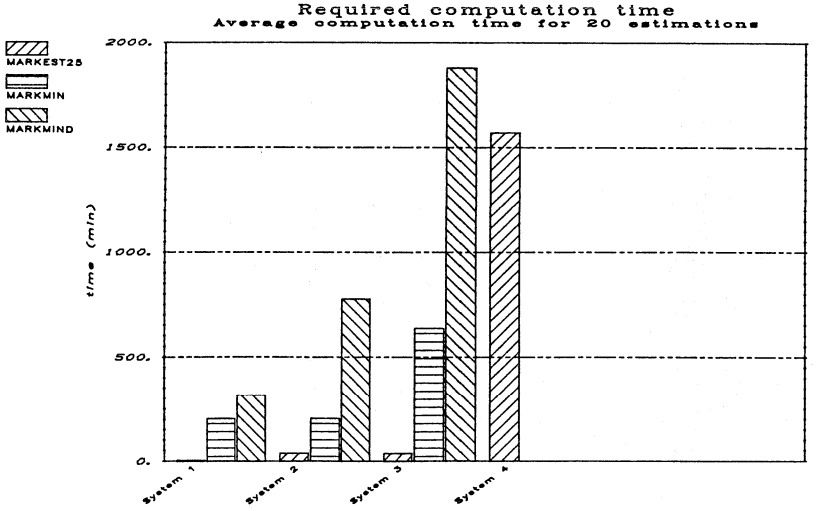

Fig. 3.12 Average processor time (VAX 11/750) used for the estimation of the FIR model parameters by MARKEST-25, MARKMIN and MARKMIND

Fig. 3.11 and 3.12 show the average processor time required on a VAX 11/750 computer system to do the estimations for the various simulated processes. With respect to the time required for the estimations the recursive algorithm (RECMAK) performs best. The average time required by the recursive estimation algorithm is about one third of the time required by the second best algorithm (EXACTMARK).
The algorithms that use numerical minimization methods perform much worse with respect to the required CPU time (cf. fig. 3.10 and 3.11). The average amount of processor time required by least squares algorithm MARKMIN is about 60 times as high as the average time used by EXACTMARK. The average time used by the maximum likelihood algorithm MARKMIND is even about 160 times as high as the average time used by EXACTMARK.

To be able to make a judgement on the quality of the estimated noise models the power spectral densities of white Gaussian noise passed through the noise colouring filters have been computed. The power spectral densities are scaled to the estimated output error energy. For comparison also the power spectral densities of the true noise colouring filters, used for the process simulations, have been computed.
For each system only the results obtained with the recursive algorithm and the results obtained from the program EXACTMARK are shown. The results obtained with the other algorithms hardly differ from the results obtained with EXACTMARK. The figures show the average PSD for each output together with the standard deviation interval.
Fig. 3.13 - 3.14 show the results obtained for system 1.
Fig. 3.15 - 3.16 show the results obtained for system 2.
The results obtained for simulated processes 3 and 4 are shown in fig. 3.17 - 3.18 and fig. 3.19 - 3.20 respectively.
In general, the results obtained with the estimated noise models come rather close to the true power spectral density functions. For the real multivariable processes the results obtained with the recursive estimation method appear to be slightly better than the results obtained with the other methods (cf. fig. 3.19 - 3.20). For control system design purposes the results obtained will usually be sufficient.

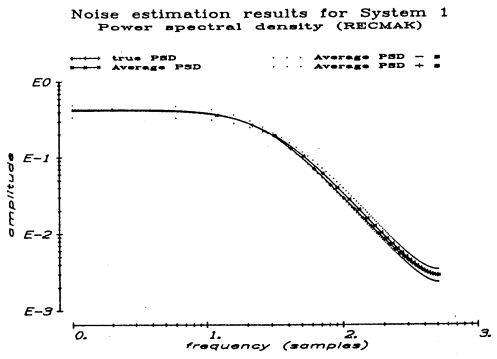

Fig. 3.13a Average Power Spectral Density of the noise of output 1 of system 1 resulting from the estimation with RECMAK

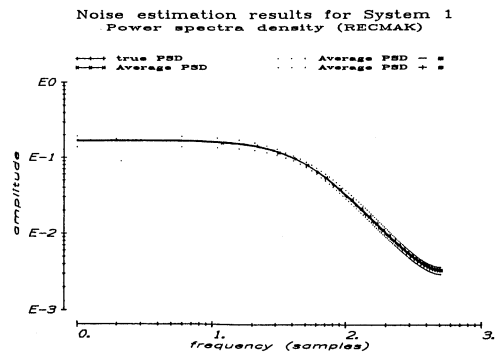

Fig. 3.13b Average Power Spectral Density of the noise of output 2 of system 1 resulting from the estimation with RECMAK

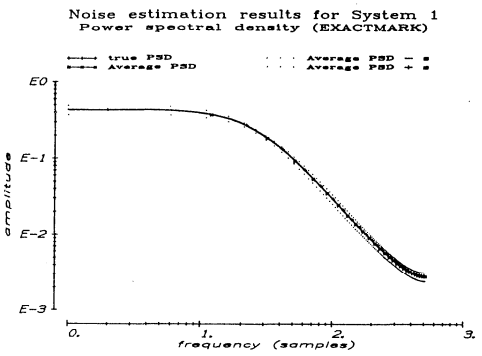

Fig. 3.14a Average Power Spectral Density of the noise of output 1 of system 1 resulting from the estimation with EXACTMARK

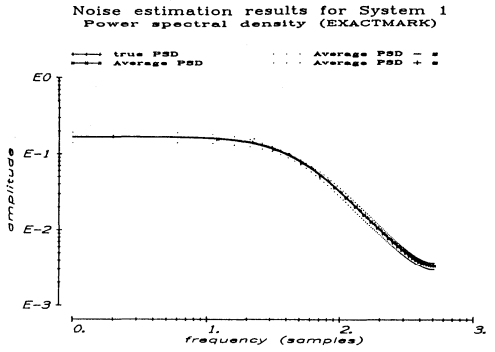

Fig. 3.14b Average Power Spectral Density of the noise of output 2 of system 1 resulting from the estimation with EXACTMARK

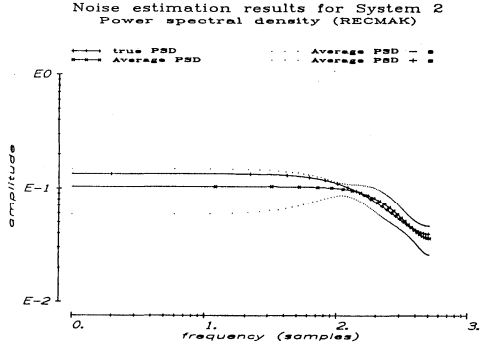

Fig. 3.15a Average Power Spectral Density of the noise of output 1 of system 2 resulting from the estimation with RECMAK

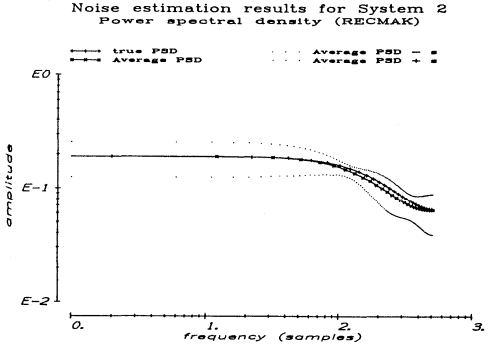

Fig. 3.15b Average Power Spectral Density of the noise of output 2 of system 2 resulting from the estimation with RECMAK

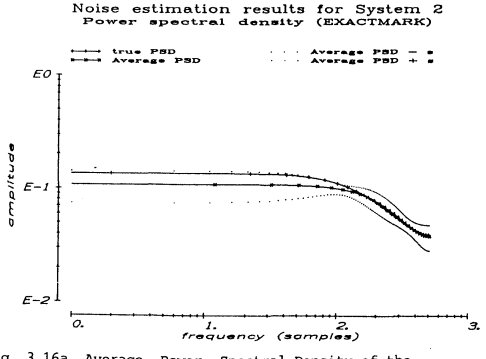

Fig. 3.16a Average Power Spectral Density of the noise of output 1 of system 2 resulting from the estimation with EXACTMARK

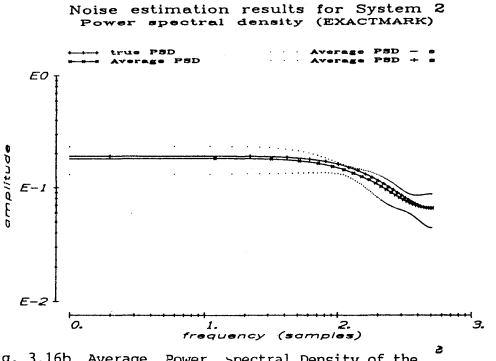

Fig. 3.16b Average Power Spectral Density of the noise of output 2 of system 2 resulting from the estimation with EXACTMARK

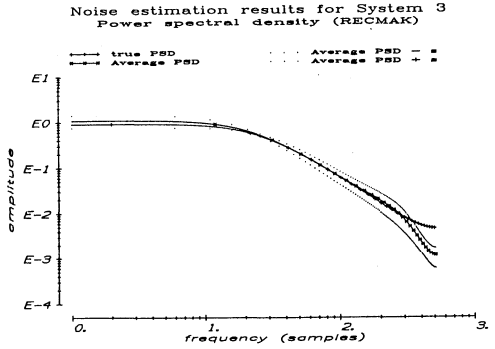

Fig. 3.17a Average Power Spectral Density of the noise of output 1 of system 3 resulting from the estimation with RECMAK

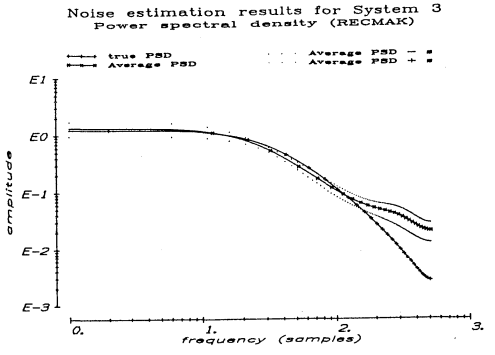

Fig. 3.17b Average Power Spectral Density of the noise of output 2 of system 3 resulting from the estimation with RECMAK

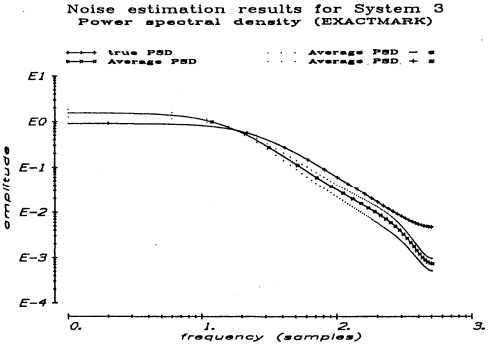

Fig. 3.18a Average Power Spectral Density of the noise of output 1 of system 3 resulting from the estimation with EXACTMARK

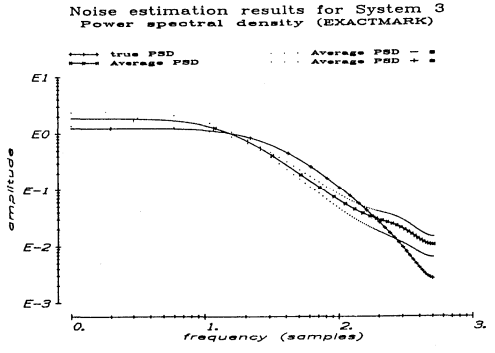

Fig. 3.18b Average Power Spectral Density of the noise of output 2 of system 3 resulting from the estimation with EXACTMARK

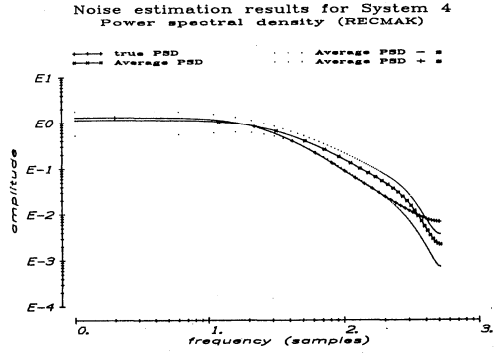

Fig. 3.19a Average Power Spectral Density of the noise of output 1 of system 4 resulting from the estimation with RECMAK

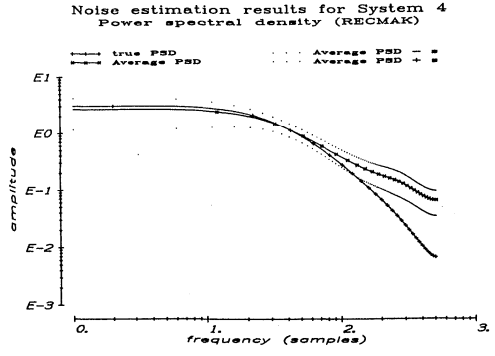

Fig. 3.19b Average Power Spectral Density of the noise of output 2 of system 4 resulting from the estimation with RECMAK

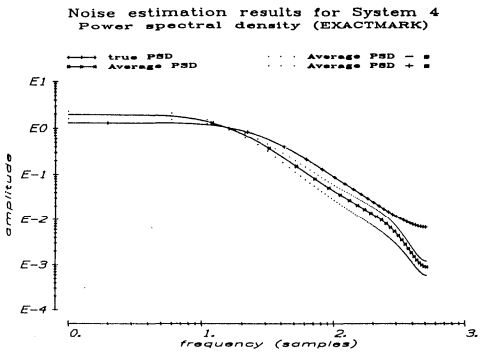

Fig. 3.20a Average Power Spectral Density of the noise of output 1 of system 4 resulting from the estimation with EXACTMARK

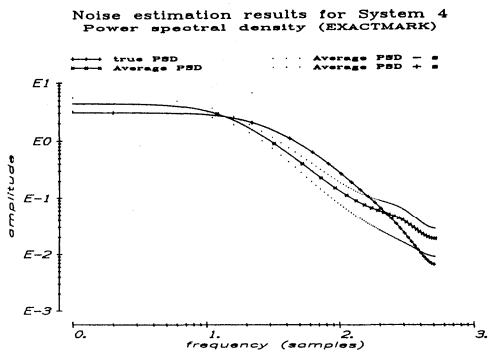

Fig. 3.20b Average Power Spectral Density of the noise of output 2 of system 4 resulting from the estimation with EXACTMARK

3.8 Concluding remarks

In this chapter various methods for the estimation of Finite Impulse Response (FIR) process models and Auto Regressive (AR) noise models have been discussed. Algorithms have been developed based on the (weighted) least squares and maximum likelihood method. The algorithms developed for those two different estimation methods have been compared for four different simulated processes. For the least squares method five different computational methods have been tested. For the maximum-likelihood method one algorithm has been used.
The algorithms have been tested on 20 data sets for each simulated process. The signal to noise ratio used for each data set is 20 dB.
The properties of the various methods observed from the simulation tests can be summarized as follows:

- In a situation where the eigenvalues of the noise colouring filter are close to the smallest eigenvalues of the simulated process all methods perform equally well.
- If the eigenvalues of the noise colouring filter are close to the largest eigenvalues of the simulated process, the recursive estimation method is inferior to the other estimation methods. Especially, if the model obtained from the identification has to be used for prediction of the process behaviour the recursive method is not to be preferred (cf. fig. 3.7 - 3.10).
- Iterative quadratic approximation of the cost function using Markov parameters obtained from a previous iteration for successive substitution often does not converge. In cases of many parameters the algorithm almost always diverges (cf. fig. 3.5 and 3.6).
- The methods using numerical methods for minimization of the cost function generally perform best. However, they can not be applied for processes with large time constants because of large number of parameters required for the FIR model and the related amount of processor time required.

- The recursive method performs best with respect to the processor time required for the parameter estimation. The method based on eq. (3.44) performs second best. The average time required for the parameter estimation by this method is about 3 times the time required by the recursive method. The maximum likelihood algorithm on the average takes about 500 times as much processor time as the recursive algorithm.
- The results obtained with the maximum likelihood estimation algorithm are slightly better than the results obtained with the least squares estimation algorithm that uses a numerical minimization method for minimization of the cost function.
- With respect to the modelling of the coloured output noise the recursive method performs slightly better than the other estimation methods. In general, the quality of the information obtained from all methods will be sufficient for control system design purposes.

Looking at the demands put on the simulation abilities of the models, the algorithm based on eq. (3.44) (EXACTMARK) is preferred for the initial estimation of impulse responses. This method performs best with respect to the quality of the estimation results and the amount of processor time required to obtain these results.

4. DETERMINATION OF A MINIMAL POLYNOMIAL START SEQUENCE MARKOV PARAMETERS (MPSSM) MODEL FROM A FIR MODEL

4.1 Introduction

This chapter describes some techniques that can be used for the determination of a Minimal Polynomial Start Sequence Markov (MPSSM) parameters model from estimated Finite Impulse Responses.
The description of a system by a start sequence of Markov parameters and corresponding minimal polynomial coefficients was first proposed by Ho [Ho, 1966]. The advantage of the use of an MPSSM model compared to the use of a FIR or a (pseudo) canonical model for the identification of a multivariable process is twofold.

First advantage:

- The model does not need information about the system structure. Only the degree r of the polynomial has to be determined.

Second advantage:

- The number of parameters n_m of a model of degree r with p inputs, q outputs and a D-matrix (cf. eq. (2.2)) is small compared to the number of parameters n_i needed for the description of the dynamics of the same system by means of its Markov parameters only (cf. eq. (2.1)):

$$n_m = (r + 1)\cdot p\cdot q + r \tag{4.1}$$

respectively:

$$n_i = (m + 1)\cdot p\cdot q \tag{4.2}$$

As a consequence of the first mentioned advantage, difficulties with respect to the determination from measured process signals of structural indices, as required for MIMO (pseudo) canonical models, are avoided.
The size of the MPSSM model set is large compared to the model set of (pseudo) canonical models with a given order and structure. In the set of MPSSM models of a given degree r several canonical modelsets of the same order with different structures are contained.
The MPSSM model set of degree r contains models of order n where n may be larger than the degree r of the minimal polynomial as will be shown later (cf. eq. (4.15)):

$$n \leq r\cdot\min(p,q) \tag{4.3}$$

A MPSSM model can be determined directly from measured input/output data. For the computation of the model parameters, however, a high order function of the polynomial coefficients has to be minimized (cf. chapter 5). To make

efficient use of numerical minimization algorithms for the minimization of this criterion function with its many minima good initial values for the MPSSM model parameters have to be computed first. This can be done by making use of 'curve fitting' techniques applied to the estimated finite impulse responses.

The purpose of this chapter is to develop some methods that can be used for the computation of initial values for the MPSSM model parameters from given, noise corrupted finite impulse responses.
For the estimation of the start sequence Markov parameters and minimal polynomial coefficients from estimated, noise corrupted Markov parameters five methods are discussed:

- Gerth's method [Gerth, 1972]
- a modified version of Gerth's method
- Approximate realization from the Hankel matrix [Hajdasinski, 1979; Damen, 1982]
- Approximate realization from the Page matrix [Damen, 1982]
- Determination of a reduced order model using a method developed by Glover [Glover, 1984]

As will be shown in chapter 5, section 5.2.2 the initially estimated FIR model and the impulse responses of the MPSSM model directly estimated from input/output data under the following assumptions are Frobenius norm approximations of the impulse responses of the true system:

- The input signals applied for the estimation of the model parameters are stationary, inter-channel independent, white noise signals.
- The ouput noise is not correlated with the input signals.
- A sufficient number of samples is used for the estimation of the model parameters.

The MPSSM models obtained with the method of Gerth and with the modified Gerth method are approximations of the MPSSM model of which the impulse responses are closest to the initial FIR model in Frobenius norm (cf. chapter 5, section 5.2.2).
The approximate realization methods (third and fourth method) result in MPSSM models with corresponding block Hankel (Page) matrices that are close to the optimal Frobenius norm approximations of the block Hankel (Page) matrix of the FIR model.
The method of Glover (fifth method) results in a MPSSM model that is an optimal Hankel norm approximation of the original FIR model.

Section 4.2 gives a general description of the MPSSM model and of its properties. Before polynomial coefficients and start sequence Markov parameters can be estimated first the degree of the minimal polynomial has to be determined. Section 4.3 is devoted to the techniques used for the estimation of an appropriate value for the degree of the minimal polynomial. A description of Gerth's method and the modified Gerth method for the determination of the MPSSM model parameters is given in section 4.4. The approximate realization methods and the method developed by Glover are described in section 4.5. A comparison of the results obtained with the

various methods is made in section 4.6. For the tests the same simulated processes are used as in chapter 3.

4.2 Mathematical description of the system

To derive the MPSSM model the state space model is used. This model has been introduced by eq. (2.3a) and (2.3b):

$$x_{k+1} = F \cdot x_k + G \cdot u_k$$

$$y_k = H \cdot x_k + D \cdot u_k$$

From this model the input/output behaviour can be written as:

$$y_k = H \cdot F^k \cdot x_0 + \sum_{i=1}^{k} H \cdot F^{i-1} \cdot G \cdot u_{k-i} + D \cdot u_k \qquad k \geq 0 \qquad (4.4)$$

with: x_0 - the initial value of the state vector

The model is assumed to be completely controllable and completely observable.

A model is called completely controllable if there exists a set control vectors u_i $(1 \leq i \leq n)$ that will bring the model from any given initial state $x_0 = x_{is}$ to an arbitrary, desired state $x_n = x_{ds}$ within n sample intervals.
A necessary and sufficient condition for a model to be completely controllable is (cf. [Kailath, 1980]):

$$\text{rank}(Co) = n \qquad (4.5)$$

with: Co: Controllability matrix
n: the size of state matrix F

A model is called completely observable if one can always reconstruct the value of the initial state x_0 of the system from a finite number l $(1 \leq l \leq n)$ observed past input signals u_l and output signals y_l of the system.
A necessary and sufficient condition for a system to be completely observable is (cf. [Kailath, 1980]):

$$\text{rank}(Ob) = n \qquad (4.6)$$

with: Ob: Observability matrix
n : size of state matrix F

In the sequel the initial value of the state vector x_0 will be assumed to be equal to zero.

In general, models obtained by using process identification techniques will be completely observable because they are based on the observed process responses on input signals applied to the process. The only information used for modelling the process is the information present in the changes of the state of the system that can be observed at the outputs of the system. A non-controllable part can belong to the model if the initial state of the system has not been equal to zero and the system is not completely controllable or if other inputs than the ones used for the modelling (noise inputs) excite non-controllable states.

If the initial state of the system is assumed to be equal to zero, the following expressions for the Markov parameters of the system are obtained from eq. (2.1) and eq. (4.4):

$$M_i = \begin{cases} D & i=0 \qquad (4.7a) \\ G \cdot F^{i-1} \cdot H & i>0 \qquad (4.7b) \end{cases}$$

To come to the MPSSM model a definition of an annihilating polynomial has to be given first. A scalar polynomial $f(\lambda)$ is called an annihilating polynomial of the square matrix F if the following equation is satisfied:

$$f(F) = 0 \qquad (4.8)$$

The Cayley-Hamilton theorem states that every square matrix satisfies its characteristic equation (cf. [Gantmacher, 1959]). The characteristic polynomial f_{cp} therefore is an annihilating polynomial. Application of the Cayley-Hamilton theorem to the state matrix F gives (cf. eq. (2.6)):

$$f_{cp}(F) = F^n + \alpha_1 \cdot F^{n-1} + \ldots + \alpha_{n-1} \cdot F + \alpha_n \cdot I = 0 \qquad (4.9)$$

Multiplication of eq. (4.9) with some power of state matrix F leads to the following recurrent relation that can be used for the computation of any power of F:

$$F^{j-1} = \sum_{i=1}^{n} -\alpha_i \cdot F^{j-i-1} \qquad (4.10)$$

Left multiplication of eq. (4.10) with the output matrix H and right multiplication with the input matrix G results in a recurrent relation for the Markov parameters:

$$M_j = \sum_{i=1}^{n} -\alpha_i \cdot M_{j-i} \qquad \text{for all } j>n \qquad (4.11)$$

According to the Cayley-Hamilton theorem every square matrix satisfies its characteristic equation. In general, however, the characteristic polynomial is not necessarily the polynomial of the lowest degree r with the property given by eq. (4.8):

$$f(F) = 0$$

It can be shown (cf. [Gantmacher, 1957]) that the polynomial of the lowest degree with this property is the polynomial that has the eigenvalues of state matrix F as zeros, where each distinct eigenvalue only is counted once.

definition: A distinct eigenvalue of matrix F is an eigenvalue that has a corresponding Jordan block, if matrix F is transformed into Jordan companion form.

The monic (highest order coefficient equal to one), annihilating polynomial of the lowest degree is called the minimal polynomial f_{mp}:

$$f_{mp}(\lambda) = (\lambda - \lambda_1)\cdot(\lambda - \lambda_2)\cdot \ \dots \ \cdot(\lambda - \lambda_r)$$

$$= \lambda^r + a_1\cdot\lambda^{r-1} + a_2\cdot\lambda^{r-2} + \ \dots \ + a_r = 0 \qquad (4.12)$$

with: r - the number of distinct eigenvalues of F

The minimal polynomial is unique. The relation between the characteristic polynomial and the minimal polynomial is given by (cf. [Gantmacher, 1957]):

$$f_{mp}(\lambda) = \frac{f_{cp}(\lambda)}{D_{n-1}(\lambda)} \qquad (4.13)$$

with: $D_{n-1}(\lambda)$ - the greatest common divisor of all the elements of the adjoint matrix $B(\lambda)$ of $(\lambda I - F)$

Because state matrix F also satisfies its minimal polynomial, the recurrence relation for the Markov parameters (eq. (4.11)) can be reduced to:

$$M_{r+j} = \sum_{i=1}^{r} -a_i\cdot M_{r+j-i} \qquad \text{for all } j\geq 1 \qquad (4.14)$$

with: r - the degree of the minimal polynomial
a_i - the coefficients of the minimal polynomial
$M_{r+j} = M_{r+j}(a_i, M_i \mid i\epsilon I) \qquad I=1,2,3, \ \dots \ ,r$

From eq. (4.14) it is clear that a complete description of the system only requires the first r Markov parameters -the so called start sequence of

Markov parameters- and the minimal polynomial coefficients that give, with eq. (4.14), the continuation of the sequence of Markov parameters. To identify a MPSSM model first the degree of the minimal polynomial has to be determined and next the polynomial coefficients as well as the start sequence of Markov parameters have to be estimated. The number of parameters to be estimated is given by eq. (4.1).

From the property of the minimal polynomial that its zeros are all distinct eigenvalues of the model with multiplicity one only, it is clear that, in general, the order of the model and the degree of the minimal polynomial are different. The relation between the order of the system in minimal state space representation and the degree of the minimal polynomial for the generic input/output model follows from (cf. [Backx, 1986]):

$$f_{cp}(\lambda) = [f_{mp}(\lambda)]^{\min(p,q)} \quad \text{with} \quad n = r \cdot \min(p,q) \tag{4.15}$$

with: p - the number of inputs of the system
q - the number of outputs of the system

To prove this a finite block Hankel matrix $H_{r,r}$ consisting of r block rows and r block columns filled with Markov parameters $\{M_i\}_{i=1,2,\ldots,2r-1}$ of the MPSSM model has to be constructed. From recurrence relation (4.14) it follows that:

$$\text{rank}(H_{r+i,r+j}) = \text{rank}(H_{r,r}) \quad \text{for all } i,j \geq 1 \tag{4.16}$$

Generically the Hankel matrix $H_{r,r}$ will have full rank since there will not occur any dependence in the estimated start sequence Markov parameters. With the realization algorithm of Ho-Kalman [Ho, 1966] the minimum state space dimension is:

$$\text{rank}(H_{r,r}) = r \cdot \min(p,q) = n \tag{4.17}$$

Based on $H_{r+1,r+1}$ a canonical state space realization can be constructed both in observability or in controllability form respectively by considering the row or column dependences in $H_{r+1,r+1}$. Due to the dependence in the Markov parameters (eq. (4.14)) this matrix will no longer have full rank. Because of the relation given by eq. (4.17) the dimension of the state space description of the model for $q \leq p$ will be equal to $r \cdot q$. In this case an expression for the F matrix of a state space realization in canonical observability form is obtained from a simple substitution of the minimal polynomial coefficients (cf. [Kailath, 1980]):

$$F = \text{diag}(F_1, F_2, \ldots, F_q) \tag{4.18}$$

with: $F_1 = F_2 = \ldots = F_q$

$$F_i = \begin{bmatrix} 0 & & \\ \vdots & & I_{r-1,r-1} \\ 0 & & \\ -a_r & -a_{r-1} \quad \ldots \quad & -a_1 \end{bmatrix}$$

Similarly, if $p \leq q$ the order of a minimal state space description will be $r \cdot p$. Now the F matrix of a realization in a canonical controllability form is (cf. [Kailath, 1980]):

$$F = \text{diag}(F_1, F_2, \ldots, F_p) \tag{4.19}$$

with: $F_1 = F_2 = \ldots = F_p$

$$F_i = \begin{bmatrix} 0 & \ldots & 0 & -a_r \\ & I_{r-1,r-1} & & -a_{r-1} \\ & & & \vdots \\ & & & -a_1 \end{bmatrix}$$

This gives as a result for the characteristic polynomial of F:

$$f_{cp}(\lambda) = \det(\lambda I - F) = [f_{mp}(\lambda)]^{\min(p,q)} \tag{4.20}$$

This implies that all zeros of the minimal polynomial (the eigenvalues of the system) occur in the state space model with multiplicity min(p,q).

4.3 Determination of the degree of the minimal polynomial

The determination of the degree of the minimal polynomial has to be done on the basis of available input/output data and/or with already estimated Markov parameters. A problem with the determination of the degree of the MPSSM model is found in the fact that, in industrial practice, the process in general does not fit in the model set. The choice of the model set -for the MPSSM models the choice of a degree r- simply has to be based on considerations with respect to the ability of models from that model set to simulate a measured process behaviour with a certain accuracy. Due to the complexity of the processes, in general, in industrial identification practice the model is not constructed on the basis of a thorough theoretical knowledge of the process dynamics. Hence, no direct relation can be found between the process to be modelled and the degree of the model to be chosen.

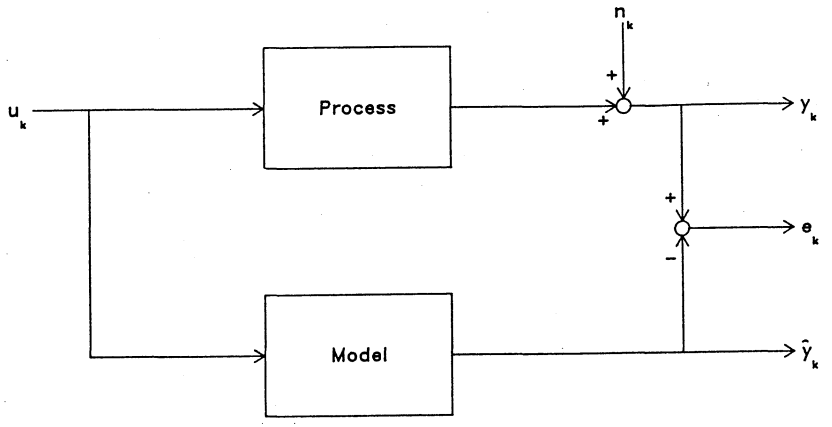

Fig. 4.1 Reconstruction of the output error

For the determination of the degree essentially two different approaches are used:

- Several models with different degrees are estimated. With each model the process outputs are simulated. By a comparison of the measured process outputs with the simulated outputs the output error (cf. eq. 3.8) is obtained (see fig. 4.1). An impression of the quality of a model is gained from tests applied to the reconstructed output errors.
- From an estimated sequence of Markov parameters consisting of the main part of the process impulse responses an order is determined by looking for (almost) dependences between the estimated parameters.

4.3.1 Tests applied to output errors obtained with models of different orders

Tests applied to the output errors are concentrating on the extraction of information still present in the output error that can be used to improve the model. For the generation of the output errors, estimated models of increasing degrees of the minimal polynomial are used. In general, the selected degree of the minimal polynomial will be kept as low as possible in accordance with the principle of parsimony. The degree will be chosen in such a way that a further increase of the degree will hardly give any improvement of the model. Of the output error the following properties are investigated:

- trace of the square of the output error matrix
- variance of the output error
- autocorrelation function of the output error

In the sequel a short description of the various tests will be given (cf. [Berben, 1985]).

Trace of the output error:
The function evaluated is (cf. eq. (3.9)):

$$V = \frac{1}{m} \cdot tr(E \cdot E^t) \tag{4.21}$$

This function gives information on the power present in the output error. By looking at V as a function of the degree of the MPSSM model insight is obtained in the degree that has to be used. When the degree of the model is chosen too low, still some process energy related to the applied input signals will be present in the reconstructed output error, because not enough degrees of freedom have been inserted in the model. An increase of the degree of the model will give more degrees of freedom to model the process dynamics and the result will be a better fit of the simulated outputs to the process outputs. This improvement of the fit will continue until the residue does not contain any more information that can be explained from the inputs used by the model. Further increase of the degree will hardly give a decrease of V. The degree of the MPSSM model is found from the change in the rate of decrease of V.

Variance of the output error:
From the output error samples obtained from a model of degree r an estimate for the covariance matrix is computed:

$$\hat{R} = \frac{1}{m-1} \cdot \sum_{i=1}^{m} (e_i - \bar{e}) \cdot (e_i - \bar{e})^t \tag{4.22}$$

with: e_i the residue for sample i

$\bar{e}$ average of the output error
m the number of samples used for the estimation

The estimated variances for each output are the diagonal elements of this covariance matrix $\hat{R}$. The decrease of the variances as a function of the order of the model gives information of the degree of the MPSSM model to be selected. The mechanism of this order test is based on the fact that too low an order of the model results in an extra contribution to the variance of the output error due to the fact that a part of the output signal can not be reconstructed by the model. Again, increase of the degree will result in less energy in the output error and therefore in a lower value for the variances. This will continue until all energy in the output signal, that can be explained from the inputs used by the model, is simulated by the model.

Autocorrelation of the output error
For each output j the normed autocorrelation function (cf. [Papoulis, 1977]) is evaluated as a function of the degree of the MPSSM model:

$$\rho_j(i) = \frac{(m-1)\cdot \sum_{k=1}^{m-i} \{e_k(j) - \bar{e}(j)\}\cdot\{e_{k+i}(j) - \bar{e}(j)\}}{(m-i-1)\cdot \sum_{k=1}^{m} \{e_k(j) - \bar{e}(j)\}^2} \qquad (4.23)$$

The order test is based on the computation of this normed autocorrelation of the output errors. For white Gaussian noise it has been shown (cf. [Van den Boom, 1982]) that the variance of the normed autocorrelation function calculated by using m samples is:

$$\mathrm{var}\{\rho_j(i)\} \simeq \frac{1}{m} \qquad (4.24)$$

This property can be used in order tests of systems with white Gaussian output noise. In this case the autocorrelation functions of the output errors are calculated for some range of k for different model orders. The shape of the functions gives information about the whiteness of the output errors. If the output errors are white, this means $\rho_j(i)$ corresponds to an impulse, an appropriate degree for the minimal polynomial can be found by looking for the degree r that gives a $\rho_j(i)$ with a majority of its values for i>0 below the value given by (4.24).
In most practical cases, however, the output error is not white because of the fact that the noise present on the process outputs is coloured. In this case an impression of the degree of the system can be obtained by evaluating the shape of the autocorrelation functions. The idea behind it is that the process part present in the signals decreases when the model order is increased. A proper degree r has been found, as soon as the shape of the autocorrelation function does not show a significant change any more when the degree of the minimal polynomial is further increased.

4.3.2 Order determination from estimated FIR models

The second type of order tests is based on the determination of (almost) dependences between estimated Markov parameters.
As has been shown in chapter 3 the doubly infinite block Hankel matrix maps all past inputs to, at the moment of observation, all future outputs of the system generated by these past inputs (cf. eq. (3.50) and (3.51)). The doubly infinite block Hankel matrix can be seen as a generalization of the FIR model that maps the past inputs to the next future output sample (cf. eq. (2.1)). An immediate consequence of eq. (4.14) is that the degree r of the minimal polynomial is equal to the number of independent block rows and block columns of the doubly infinite Hankel matrix. In this respect block rows (columns) are called dependent if recurrent relation eq. (4.14) also

holds for the Markov parameters replaced by complete block rows (columns) of the block Hankel matrix.
To determine the required degree r of the minimal polynomial the number of - due to the noise- almost dependent block rows/columns of the largest possible block Hankel matrix has to be found. To find an appropriate estimate for the degree r of the minimal polynomial the Markov parameters of the estimated FIR model can be written in vector form. Degree r is found from the (almost) dependences of the vectors obtained. In correspondence with eq. (4.17) the order of the MPSSM model generically will be $r \cdot \min(p,q)$. Basically two methods are applied to determine the degree r of the minimal polynomial from the block Hankel matrix consisting of Markov parameters in vector form:

- Construction of block matrices with a Hankel structure from an increasing number of Markov parameters in vector form. Computation of the determinants of the product of each of the constructed matrices with their transposes. Determination of the ratios of each two successive determinants and analysis of the obtained determinant ratios.
- Analysis of the singular values of an upper left block matrix with Hankel structure and with as many non-zero block rows and columns as possible built from all available, estimated Markov parameters in vector form.

As stated, both tests make use of information obtained from the block matrix with Hankel structure built from Markov parameters in vector form:

$$H_{i,j} = \begin{bmatrix} \mathrm{vec}(M_1) & \mathrm{vec}(M_2) & \cdots & \mathrm{vec}(M_j) \\ \mathrm{vec}(M_2) & \mathrm{vec}(M_3) & \cdots & \mathrm{vec}(M_{j+1}) \\ \vdots & \vdots & & \vdots \\ \mathrm{vec}(M_i) & \mathrm{vec}(M_{i+1}) & \cdots & \mathrm{vec}(M_{j+i-1}) \end{bmatrix} \qquad (4.25)$$

with: $\mathrm{vec}(M_i) = \left[M_{11,i}\ ,\ M_{21,i}\ ,\ \cdots\ ,\ M_{12,i}\ ,\ \cdots\ ,\ M_{1p,i}\ ,\ \cdots\ ,\ M_{qp,i}\right]^t$

The computation of the ratios of the determinants requires the computation of the following determinant ratio function:

$$d(k) = \frac{\det\left(H^t_{k+1,k+1} \cdot H_{k+1,k+1}\right)}{\det\left(H^t_{k,k} \cdot H_{k,k}\right)} \qquad (4.26)$$

An appropriate estimate for the degree r is found, if the determinant and, as a result, d(k) becomes small, because in that case an almost dependency occurs in the block Hankel matrix.
This method requires a lot of computational effort, because for each point of the function d(k) the computation of a determinant is needed. Furthermore the method is not very reliable with respect to its numerical behaviour.

This is due to the fact that the matrix $H_{k+1,k+1}$ of eq. (4.26) becomes almost singular when the right degree of the minimal polynomial is about to be found.

A better method to find dependences between the Markov parameters is based on the analysis of the singular spectrum of the block matrix with Hankel structure. For the determination of the degree r of the minimal polynomial the block matrix has to consist of as many of the estimated Markov parameters as possible. All information contained in the estimated FIR model for the mapping of inputs to outputs will also be used in the mapping by the Hankel matrix, if the Hankel matrix is constructed such that the first block row and the first block column consist of all available, estimated Markov parameters in vector form. To be able to find an appropriate value for the degree r, the block Hankel matrix has to contain at least more block rows and block columns than the expected degree of the minimal polynomial. The singular value decomposition of the block Hankel matrix can be written as:

$$H_{k,l} = U \cdot S \cdot V^t \qquad (4.27)$$

with: U – orthogonal matrix containing the left singular vectors of $H_{k,l}$

S – diagonal matrix containing the singular values of $H_{k,l}$

V – orthogonal matrix containing the right singular vectors of $H_{k,l}$

Eq. (4.27) can be rewritten into:

$$H_{k,l} = \sum_{j=1}^{m} \sigma_j \cdot u_j \cdot v_j^t \qquad (4.27a)$$

Because all singular vectors are orthonormal, each singular value is a weighting factor that gives the attenuation in the direction corresponding to singular vector u_j. A singular value that is almost zero indicates a non relevant direction in the mapping. An appropriate degree of the minimal polynomial is found from the number of singular values that significantly differs from zero.

A further analysis shows some properties of the order determination methods discussed. Observation of the block Hankel matrix reveals that due to the noise present on the estimated Markov parameters all singular values will be greater than zero. By writing each Markov parameter as the true Markov parameter Mtrue plus an added noise matrix N, it can be seen that to each element of the block matrix defined by eq. (4.25) an extra noise component is added.

$$M_i = Mtrue_i + N_i \quad \text{gives} \quad H_{i,j} = Htrue_{i,j} + Hnoise_{i,j} \qquad (4.28)$$

The noise on each entry of the estimated FIR Markov parameters is expected to be independent of the noise on each other entry, if the input signal used is zero mean, white noise (cf. Appendix D eq. (D.8) - (D.11)).

In general, the noise components will result in an increase of the singular values of the Hankel matrix. This implies that singular values corresponding to dependent column vectors of the block matrix with Hankel structure consisting of the noise free Markov parameters will still have a value >0 due to the noise.

If the energy in the singular values due to the noise is significantly smaller than the energy in the singular values related to the true system, the right degree r is found from a drop in the singular values as soon as the degree of the true system is reached. The singular spectrum can be splitted into two parts then:

- The first r singular values, related to the true system and increased due to the noise energy, that represent a total energy $E_1 = \sum_{i=1}^{r} \sigma_i^2$.
- The last m-r singular values, related to the noise only, that represent a part of the total noise energy present on the estimated Markov parameters equal to $E_2 = \sum_{i=r}^{m} \sigma_i^2$.

A drop in the singular values is found if E_2 is significantly smaller than E_1. In this case a rough estimate for the signal to noise ratio S_r of the deterministic part and the noise components of estimated FIR model parameters is given by:

$$S_r = \frac{E_1 - \frac{r}{m-r} \cdot E_2}{\frac{m}{m-r} \cdot E_2} \qquad (4.29)$$

Besides the drop that may occur in the singular values the decrease of the singular values generally becomes significantly smaller as soon as the noise level is reached. An explanation for this phenomenon is given by the following reasoning. In case the matrix Hnoise consists of independent, zero mean, white noise elements the condition number of this matrix, defined by the ratio of the largest and the smallest singular value, will tend to one because its rows (columns) will be almost perpendicular and of equal size (cf. Appendix D eq. (D.10) and (D.11)). This implies that the singular values related to Hnoise will be almost equal. Consequently the decrease of the singular values related to the noise on the estimated Markov parameters will be small. The decrease of the Hankel singular values related to the system generally will be larger. Moreover, the first singular values will decrease both due to a decrease of the Hankel singular values of the system and due to a (smaller) decrease of the singular values related to the noise on the estimated Markov parameters.

The fact that the noise, present on the entries of a Markov parameter, occurs at various positions in the block Hankel matrix hardly influences the results. In successive columns of the block Hankel matrix (cf. eq. (4.25)) each Markov parameter and also its noise components shift to the preceding block row. Within each block row the noise components are expected to be independent as long as the noise on the entries of the different Markov parameters is independent. So, if the noise on the Markov parameters is white, the columns of noise matrix Hnoise (cf. eq. (4.28)) are expected to be independent and the above reasoning will hold.
To increase the sensitivity for the detection of a step in the singular values and a change in the rate of decrease of the singular values the ratios of successive singular values can be used. This ratio is expected to tend to one, if the noise on the parameter entries is white.

4.4 Estimation of an MPSSM model using Gerth's method

The Gerth algorithm (cf. [Gerth, 1972]) makes explicit use of the existence of a finite dimensional realization of the system as given by eq. (4.14):

$$M_{r+j} = \sum_{i=1}^{r} -a_i \cdot M_{r+j-i}$$

Starting point for the algorithm are the Markov parameters $\tilde{M}_i$ estimated from process input/output data. A start sequence of Markov parameters and minimal polynomial coefficients are fitted to these estimated, noisy Markov parameters. For the computation of polynomial coefficients and start sequence Markov parameters Gerth proposed to solve two sets of linear equations in least squares sense (cf. [Gerth, 1972; Graham, 1981], Appendix C):

$$G \cdot a = v \qquad (4.30)$$

with:

$$G = \begin{bmatrix} \mathrm{vec}(M_1) & \mathrm{vec}(M_2) & \dots & \mathrm{vec}(M_r) \\ \mathrm{vec}(M_2) & \mathrm{vec}(M_3) & \dots & \mathrm{vec}(M_{r+1}) \\ \vdots & \vdots & & \vdots \\ \mathrm{vec}(M_{m-r}) & \mathrm{vec}(M_{m-r+1}) & \dots & \mathrm{vec}(M_{m-1}) \end{bmatrix}$$

$$v^t = [\mathrm{vec}(M_{r+1})^t \;\; \mathrm{vec}(M_{r+2})^t \;\; \dots \;\; \mathrm{vec}(M_m)^t]^t$$

$$\mathrm{vec}(M_i)^t = [M_{11,i}, M_{21,i}, \dots, M_{q1,i}, M_{12,i}, \dots, M_{q2,i}, \dots, M_{qp,i}]$$

$$a^t = -[a_r, a_{r-1}, \dots, a_1]^t$$

and:

$$H \cdot Mv = M \qquad (4.31)$$

with: $H^t = [I_r \; ; \; A \cdot E_r \; ; \; A^2 \cdot E_r \; ; \; \ldots \; ; \; A^{m-r} \cdot E_r]$

$$A = \begin{bmatrix} 0 & \ldots & 0 & -a_r \\ & & & -a_{r-1} \\ & I_{r-1,r-1} & & \cdot \\ & & & \cdot \\ & & & -a_1 \end{bmatrix}$$

$$E_r = \begin{bmatrix} 0 \\ 0 \\ \cdot \\ \cdot \\ 1 \end{bmatrix}$$

$$Mv^t = [\mathrm{vec}(M_1) \; \mathrm{vec}(M_2) \; \ldots \; \mathrm{vec}(M_r)]$$

$$M^t = [\mathrm{vec}(M_1) \; \mathrm{vec}(M_2) \; \ldots \; \mathrm{vec}(M_m)]$$

Equation (4.30) is used for the estimation of the minimal polynomial coefficients. Equation (4.31) gives the start sequence Markov parameters by making use of the computed polynomial coefficients. Because both matrix G and vector v are constructed using the earlier estimated Markov parameters, the criterion used for the computation of the "autoregressive" polynomial coefficients basically is an equation error criterion (cf. eq. (2.12)). This implies that the algorithm will have properties belonging to equation error methods (cf. [Van den Hof, 1985]). The start sequence Markov parameters of the model will be asymptotically unbiased estimates of the noise corrupted input Markov parameters.
For the minimal polynomial coefficients Gerth used the solution of the set of equations (4.30) in least squares sense (cf. [Gerth, 1972]). The minimal polynomial coefficients computed this way approximate the vector v as closely as possible without changes of matrix G. This means that only vector v is assumed to be corrupted with noise. This assumption is not in correspondance with reality, because all Markov parameters used for the construction of both G and v were obtained from an earlier estimation of the Markov parameters of the system. All Markov parameters, and consequently also all the elements of G and v, will therefore be corrupted with noise. In this case a better approach is the solution of eq. (4.30) in a Total Least Squares sense (cf. [Golub, 1980; Senning, 1982; Van Huffel, 1985, 1987]). For the computation of the total least squares solution of (4.30) both G and v are assumed to be corrupted with noise. The solution looked for is the

solution of the set $\tilde{G}$, $\tilde{v}$ that is as close as possible in Frobenius norm to the original set G, v and where the set $\tilde{G}$, $\tilde{v}$ has to have an exact solution. To find the Total Least Squares solution of eq. (4.30) the equation is approximated by:

$$(G + \Delta G)\cdot a - (v + \Delta v) = 0 \tag{4.32}$$

with: ΔG - adjustment of matrix G
Δv - adjustment of vector v

Now the problem that has to be solved can be written as:

$$([G\ v] + [\Delta G\ \Delta v])\cdot \begin{bmatrix} a \\ -1 \end{bmatrix} = [\tilde{G}\ \tilde{v}]\cdot \begin{bmatrix} a \\ -1 \end{bmatrix} = 0 \tag{4.33}$$

with: $[\tilde{G}\ \tilde{v}]$ the singular matrix that is closest to matrix [G v] in Frobenius norm

Matrix $[\tilde{G}\ \tilde{v}]$ can be found by computation of the singular value decomposition of [G v]:

$$[G\ v] = U\cdot\Sigma\cdot V^t \tag{4.34}$$

and making the smallest singular value of Σ equal to zero. This gives a singular diagonal matrix $\tilde{\Sigma}$. As a result the set of equations:

$$[\tilde{G}\ \tilde{v}]\cdot \begin{bmatrix} a \\ -1 \end{bmatrix} = U\cdot\tilde{\Sigma}\cdot V^t\cdot \begin{bmatrix} a \\ -1 \end{bmatrix} = 0 \tag{4.35}$$

has exactly one non-trivial solution: the last column of matrix V scaled with its last element. This non-trivial solution is the Total Least Squares solution of eq. (4.30). The solution found for the minimal polynomial coefficients can be substituted in eq. (4.31) for the computation of the corresponding start sequence of Markov parameters. This equation is solved in least squares sense. The previously estimated polynomial coefficients are not changed any more.

The matrix [G v] used to obtain the estimates for the minimal polynomial coefficients is a block Hankel matrix of the Markov parameters in vector form. This means that the computation of the total least squares solution involves the computation of a matrix of rank equal to the column rank of this block Hankel matrix minus one, that is closest to the block Hankel matrix in Frobenius norm. The matrix obtained from this approximation is not a block Hankel matrix any more. If it had the Hankel structure the result of the approximation could immediately be used for the computation of both the polynomial coefficients and the start sequence Markov parameters. Now the extra step indicated -the solution of eq. (4.31)- is required to obtain

an estimate for the start sequence Markov parameters. In general, the complete solution found this way will not be the solution of the given order that is closest to the originally estimated Markov parameters in Frobenius norm.

4.5 Approximate realization of the estimated Markov parameters

A different method to obtain estimates for the start sequence Markov parameters and minimal polynomial coefficients from the earlier estimated sequence of Markov parameters is based on the computation of a state space realization (F, G, H, D) from the estimated Markov parameters (cf. [Ho, 1966; Zeiger, 1974; Hajdasinski, 1979; Damen, 1982; Glover, 1984]). What is looked for is a state space system of a given order k that approximates the estimated Markov parameters as closely as possible in Frobenius norm or in Hankel norm (cf. chapter 3, section 3.6). The order k of the approximate model has to be determined by means of one of the methods discussed in section 4.3. Once a state space model is available, start sequence Markov parameters and minimal polynomial coefficients can be computed by making use of relations (4.7) to (4.14).
Three different approximate realization algorithms are tested:

- The algorithm of Zeiger and McEwen. This algorithm is based on the singular value decomposition of a block Hankel matrix. The algorithm results in a balanced state space realization (cf. [Zeiger, 1974]).
- An algorithm developed by Damen, Hajdasinski and Van den Hof, based on the singular value decomposition of the so called "Page" matrix. This Page matrix is, like the block Hankel matrix, sequentially filled with Markov parameters in such a way that each Markov parameter only has one block entry in the matrix (cf. [Damen, 1982]).
- The last approximate realization algorithm used is an algorithm developed by Glover. This algorithm computes the state space model of order k that is closests in Hankel norm to the estimated FIR model (cf. [Glover, 1984]).

4.5.1 Approximate realization algorithm of Zeiger and McEwen

The method developed by Zeiger and McEwen starts from a block Hankel matrix. This block Hankel matrix is constructed from the estimated Markov parameters:

$$H_{k,k} = \begin{bmatrix} M_1 & M_2 & \cdots & M_k \\ M_2 & M_3 & \cdots & M_{k+1} \\ \cdot & \cdot & & \cdot \\ \cdot & \cdot & & \cdot \\ M_k & M_{k+1} & \cdots & M_{2k-1} \end{bmatrix} \qquad (4.36)$$

If the block Hankel matrix (4.36) has the proper dimensions all system information (i.e. order, structure, system input- output characteristics) can be obtained from this matrix. The block Hankel matrix has the proper dimensions if further extension of the matrix with extra block rows and/or columns does not increase the rank of the matrix (cf. eq. (4.16)). The order n of the system immediately follows from dependences between the rows (columns) of the block Hankel matrix (cf. eq. (2.3) - (2.10)). As a first step to obtain state space matrices F, G, H, D, the block Hankel matrix is decomposed into an observability and a controllability matrix (cf. eq. (2.8), (2.9)) by computation of its singular value decomposition.

$$H_{k,k} = U \cdot S \cdot V^t = (U_1 \cdot S_1^{1/2}) \cdot (S_1^{1/2} \cdot V_1^t) = Ob \cdot Co \tag{4.37}$$

with: S_1 - the full rank nxn upper left block of S

U_1 - the first n columns of U

V_1 - the first n columns of V

From this observability matrix the output matrix H is found as the matrix consisting of the first q rows of Ob. The input matrix G is immediately obtained from the controllability matrix Co. It consists of the first p columns of Co. This follows from the definitions of the observability and the controllability matrices (see eq. (2.8, 2.9)):

$$G = S_1^{1/2} \cdot V_1^t \cdot E_{kp} \tag{4.38}$$

$$H = E_{kq} \cdot U_1 \cdot S_1^{1/2} \tag{4.39}$$

with: $E_{kp} = [\, I_p \; 0 \cdot I_p \; \ldots \; 0 \cdot I_p \,]^t$ $\qquad \dim[E_{kp}]: kp \times p$

$E_{kq} = [\, I_q \; 0 \cdot I_q \; \ldots \; 0 \cdot I_q \,]$ $\qquad \dim[E_{kq}]: q \times kq$

An estimate for the D matrix of the system is the originally estimated direct transfer from inputs to outputs of the system. For the computation of an estimate for the state matrix F a shifted block Hankel matrix ($H^s_{k,k}$) of the same dimension as $H_{k,k}$ has to be constructed from the estimated Markov parameters. This matrix, also having order n, can be obtained by appending one extra block row (column) to the Hankel matrix given by eq. (4.36) and deleting the first block row (column) of that matrix:

$$H^{s}_{k,k} = \begin{bmatrix} M_2 & M_3 & \cdots & M_{k+1} \\ M_3 & M_4 & \cdots & M_{k+2} \\ \cdot & \cdot & & \cdot \\ \cdot & \cdot & & \cdot \\ M_{k+1} & M_{k+2} & \cdots & M_{2k} \end{bmatrix} \tag{4.40}$$

With eq. (4.37) and the properties of the block Hankel matrices $H^{s}_{k,k}$ can be decomposed into:

$$H^{s}_{k,k} = Ob \cdot F \cdot Co \tag{4.41}$$

With eq. (4.37) and (4.41) the system matrix F can be computed:

$$F = S_1^{-1/2} \cdot U_1^{t} \cdot H^{s}_{k,k} \cdot V_1 \cdot S_1^{-1/2} \tag{4.42}$$

If condition (4.17) -block Hankel matrices $H_{k,k}$ and $H^{s}_{k,k}$ having proper dimensions- is fulfilled, the matrices F, G and H exactly reconstruct the Markov parameters used for the construction of the block Hankel matrices. This can easily be seen by computation of the Markov parameters with eq. (4.7) and by substitution of these Markov parameters in eq. (4.36) and (4.40). Comparison of the block Hankel matrices obtained this way with the block Hankel matrices constructed from the original Markov parameters gives the result.
A problem arises if the block Hankel matrices constructed from the previously estimated, noisy Markov parameters do not obey rank condition (4.17). In this case only a part of the Markov parameters that compile $H_{k,k}$ can be reconstructed. This can be seen by considering the rank of the matrices obtained in (4.37):

$$\text{rank}(Ob) = \min(\text{rank}(U_1), \text{rank}(S_1^{1/2})) = \text{rank}(U_1) = n \tag{4.43}$$

$$\text{rank}(Co) = \min(\text{rank}(S_1^{1/2}), \text{rank}(V_1^{t})) = \text{rank}(V_1^{t}) = n \tag{4.44}$$

$$\text{rank}(H_{k,k}) = \min(\text{rank}(Ob), \text{rank}(Co)) = n \tag{4.45}$$

According to the fact that (4.17) is not satisfied due to the noise on the entries of the estimated Markov parameters:

$$n = \text{rank}(H_{k,k}) < \text{rank}(H_{k+1,k}) = \text{rank}(H_{k,k+1}) \leq \text{rank}(H_{\infty}) \tag{4.46}$$

To be able to reconstruct all the Markov parameters of the system the rank has to be equal to the rank of the infinite Hankel matrix H_∞. Eq. (4.45), (4.46) and (4.14) imply that not all Markov parameters can be reconstructed using the information contained in the constructed observability and controllability matrices. In eq. (4.41) relation (4.14) is implicitly assumed with n equal to the rank of block Hankel matrix $H_{k,k}$ (eq. 4.45). As a result only the first k Markov parameters of the system will be reconstructed exactly by the obtained state space system F, G, H, D. The parameters $M_{k+i}\{i\epsilon I \mid I>0\}$ will almost satisfy eq. (4.14) using the coefficients $a_i\{i\epsilon I \mid 1\leq i\leq n-1\}$ of the minimal polynomial of F. This problem will always be met in practice. Due to the noise on the estimated Markov parameters the rank of the constructed block Hankel matrices will always be:

$$\text{rank}(H_{k,k}) = \min(p\cdot k, q\cdot k) \tag{4.47}$$

Extension of the size of the block Hankel matrix implies an increase of the rank of the matrix. This corresponds with eq. (4.46).

Another problem that arises in practice is that the order resulting from eq. (4.36) to (4.42) is large. Therefore a low order approximation to the system is constructed. The order to be used, n_r, is obtained from one of the order estimation methods described in section 4.3. To obtain this low order approximation to the system a matrix $\tilde{H}_{k,k}$ of rank n_r is computed that is as close as possible to matrix $H_{k,k}$ in Frobenius norm:

$$H_{err} = \min_{\text{rank}(\tilde{H}_{k,k})=r} ||H_{k,k} - \tilde{H}_{k,k}||_F \tag{4.48}$$

To get an expression for this matrix $\tilde{H}_{k,k}$ only the first r singular values of S (eq. (4.37)) are taken into account:

$$\tilde{H}_{k,k} = U_2\cdot S_2\cdot V_2^t \tag{4.49}$$

with: $\text{diag}(S_2) = \text{diag}(S)_r$

U_2 the first r columns of U

V_2 the first r columns of V

Again this matrix can be decomposed into an "observability" matrix and a "controllability" matrix:

$$\tilde{H}_{k,k} = U_2\cdot S_2^{1/2}\cdot S_2^{1/2}\cdot V_2^t = \tilde{O}b\cdot\tilde{C}o \tag{4.50}$$

From the matrices $\tilde{O}b$, $\tilde{C}o$ and the shifted Hankel matrix $H^{s}_{k,k}$ a state space system of order r can be computed as indicated in (4.37) to (4.42). With this approach a problem is that, in general, matrix $\tilde{H}_{k,k}$ does not have the required Hankel structure. This implies that the block elements of $\tilde{O}b$ and $\tilde{C}o$ in general can not be decomposed into blocks $H \cdot F^{i-1}$ and $F^{i-1} \cdot G$ and consequently the block elements of $\tilde{H}_{k,k}$ certainly will not satisfy eq. (4.14):

$$(\tilde{O}b)_i \neq H \cdot F^{i-1} \qquad \text{for } i \in I,\ I=1,2,\ \ldots\ ,k \tag{4.51}$$

$$(\tilde{C}o)_i \neq F^{i-1} \cdot G \qquad \text{for } i \in I,\ I=1,2,\ \ldots\ ,k \tag{4.52}$$

Therefore the block Hankel matrix reconstructed with state space matrices F, G and H will not be equal to $\tilde{H}_{k,k}$. This implies that, in general, the state space system obtained from this approximation process does not satisfy the condition that it is the closest Frobenius norm approximation to the system described by the estimated Markov parameters. In fact, it is not clear in what sense the state space system obtained approximates the system described by the estimated Markov parameters.

4.5.2 Method of the Page matrix

A modification to the algorithm of Zeiger and McEwen has been suggested by Damen, Hajdasinski and Van den Hof (cf. [Damen, 1982]). With the modification suggested by Damen et al. each Markov parameter is used only once. To this end a new matrix, the Page matrix, is introduced:

$$P_{\eta,\mu} = \begin{bmatrix} M_1 & M_2 & M_3 & \cdots & M_{\mu} \\ M_{\mu+1} & M_{\mu+2} & M_{\mu+3} & \cdots & M_{2\mu} \\ \cdot & \cdot & \cdot & \cdots & \cdot \\ \cdot & \cdot & \cdot & \cdots & \cdot \\ M_{(\eta-1)\mu+1} & M_{(\eta-1)\mu+2} & M_{(\eta-1)\mu+3} & \cdots & M_{\eta\mu} \end{bmatrix} \tag{4.53}$$

In the approach using the Page matrix the low order approximation of the block Hankel matrix $P_{\eta,\mu}$ by $\tilde{P}_{\eta,\mu}$ results in a unique set of Markov parameters because each Markov parameter only has one block entry in the Page matrix. As each Markov parameter only has one block entry in the Page matrix there is a constant weighting factor for each Markov parameter in stead of the triangular weighting from the Hankel matrix. Consequently also each noise sample, present on each entry of the Markov parameters, appears only once. This Page matrix can be decomposed into an observability matrix

of the system (F^{μ}, G, H) and a controllability matrix of the system (F, G, H) similarly as the block Hankel matrix:

$$P_{\eta,\mu} = \begin{bmatrix} H \\ H\cdot F^{\mu} \\ H\cdot F^{2\mu} \\ \cdot \\ \cdot \\ H\cdot F^{(\eta-1)\mu} \end{bmatrix} \cdot \begin{bmatrix} G & F\cdot G & F^2\cdot G & F^3\cdot G & \ldots & F^{\mu-1}\cdot G \end{bmatrix} \qquad (4.54)$$

As an alternative to this Page matrix the so called "Chinese Page" matrix can be used. In this Chinese Page matrix the Markov parameters are written column wise whereas they are ordered row wise in the Page matrix. Decomposition of the Chinese Page matrix results in an Observability matrix of the system (F, G, H) and a Controllability matrix of the system (F^{μ}, G, H).

For the computation of a minimum realization (F, G, H) from the Page matrix the same algorithm may be applied as for the computation of a minimum realization from the block Hankel matrix. So also the shifted Page matrix is required:

$$P^{s}_{\eta,\mu} = \begin{bmatrix} M_2 & M_3 & M_4 & \cdots & M_{\mu+1} \\ M_{\mu+2} & M_{\mu+3} & M_{\mu+4} & \cdots & M_{2\mu+1} \\ \cdot & \cdot & \cdot & \cdots & \cdot \\ \cdot & \cdot & \cdot & \cdots & \cdot \\ M_{(\eta-1)\mu+2} & M_{(\eta-1)\mu+3} & M_{(\eta-1)\mu+4} & \cdots & M_{\eta\mu+1} \end{bmatrix} \qquad (4.55)$$

For the computation of G and H the Page matrix is decomposed into:

$$P_{\eta,\mu} = U_3\cdot S_3^{1/2}\cdot S_3^{1/2}\cdot V_3^{t} = (Ob_{\mu})\cdot(Co) \qquad (4.56)$$

with: S_3 – a square, diagonal matrix containing all non-zero singular values of $P_{\eta,\mu}$

U_3 – matrix containing the left singular vectors corresponding with the singular values of S_3

V_3 – matrix containing the right singular vectors corresponding with the singular values of S_3

With eq. (4.56) the matrices G and H can be computed:

$$G = S_3^{1/2}\cdot V_3^{t}\cdot E_{\mu p} \qquad (4.57)$$

$$H = E_{\eta q} \cdot U_3 \cdot S_3^{1/2} \tag{4.58}$$

with: $E_{\mu p} = [I_p \; 0 \cdot I_p \; \ldots \; 0 \cdot I_p]^t$ $\qquad$ $\dim[E_{\mu p}]$: $\mu p \times p$

$E_{\eta q} = [I_q \; 0 \cdot I_q \; \ldots \; 0 \cdot I_q]$ $\qquad$ $\dim[E_{\eta q}]$: $q \times \eta q$

State matrix F is obtained by making use of the following property of the shifted Page matrix:

$$P^s_{\eta,\mu} = Ob_\mu \cdot F \cdot Co \tag{4.59}$$

From eq. (4.56) and (4.59) F is found to be equal to:

$$F = S_3^{-1/2} \cdot U_3^t \cdot P^s_{\eta,\mu} \cdot V_3 \cdot S_3^{-1/2} \tag{4.60}$$

A necessary condition for the existence of this realization is that the extended observability matrix Ob_μ has full rank n. This condition is equivalent to the condition that the system (F^μ, G, H) has to be completely observable. It has been shown [Damen, 1982] that the system (F^μ, G, H) is completely observable if the following condition does <u>not</u> hold:

Condition:

(i) Either for some i: $\lambda_i = 0$ and r(i)>1 <u>or</u> for some i≠j: $\lambda_i^\mu = \lambda_j^\mu$

<u>and</u>

(ii) For each i the set of r(i) q-dimensional column vectors h_{1i1}, h_{1i2}, ... , $h_{1ir(i)}$ of the rearranged Jordan form for F^μ, which are the columns of H corresponding to the independant states of the model, is a linearly dependent set.

with: Jordan canonical form of the system given by

$$F_J = \begin{bmatrix} F_1 & 0 & \ldots & 0 \\ 0 & F_2 & \ldots & 0 \\ . & . & \ldots & . \\ 0 & 0 & \ldots & F_\nu \end{bmatrix} \qquad \dim[F_J]: n \times n$$

$$H_J = [\, H_1 \; H_2 \; \ldots \; H_\nu \,] \qquad \dim[H_J]: q \times n$$

$$F_i = \begin{bmatrix} F_{i1} & 0 & \dots & 0 \\ 0 & F_{i2} & \dots & 0 \\ . & . & \dots & . \\ 0 & 0 & \dots & F_{ir(i)} \end{bmatrix} \qquad \dim[F_i]: n_i \times n_i$$

$$H_i = \begin{bmatrix} H_{i1} & H_{i2} & \dots & H_{ir(i)} \end{bmatrix} \qquad \dim[H_i]: q \times n_i$$

$$F_{ij} = \begin{bmatrix} \lambda_i & 1 & 0 & \dots & 0 \\ 0 & \lambda_i & 1 & \dots & 0 \\ 0 & 0 & 0 & \vdots & 1 \\ 0 & 0 & 0 & \dots & \lambda_i \end{bmatrix} \qquad \dim[F_{ij}]: n_{ij} \times n_{ij}$$

$$H_{ij} = \begin{bmatrix} h_{1ij} & h_{2ij} & \dots & h_{nij} \end{bmatrix} \qquad \dim[H_{ij}]: q \times n_{ij}$$

In cases where the Page matrix fails, the Chinese Page matrix can be used.

A reduced order state space model can be obtained in a similar way as from the Hankel matrix (cf. eq. (4.49), (4.50)). A low order approximation to the Page matrix $\tilde{P}_{\eta,\mu}$ is computed that is as close as possible to matrix $P_{\eta,\mu}$ in Frobenius norm. This approximating Page matrix of order r is obtained by making all singular values with indexes that exceed r equal to zero.

A nice property of the Page matrix is related to the influence of the noise, present on the Markov parameters, on the singular values of the matrix. If the noise on the entries of the Markov parameters is assumed to be stationary, white, signal independent, inter-channel independent, additive, Gaussian noise the following holds (cf. [Damen, 1982]):

$$\hat{P} = P + \Xi_p \tag{4.61}$$

with: Ξ_p - the matrix containing the noise samples
P - the Page matrix of the noise free Markov parameters $\qquad \dim[P]: h \times m$

If $h \leq m$ consider $\hat{P} \cdot \hat{P}^t$, else continue with $\hat{P}^t \cdot \hat{P}$:

$$\hat{P} \cdot \hat{P}^t = P \cdot P^t + \Xi_p \cdot \Xi_p^t + \Xi_p \cdot P^t + P \cdot \Xi_p^t \tag{4.62}$$

with: $E\{\Xi_p\} = 0 \cdot I_{h,m}$

$$E\{\Xi_p \cdot \Xi_p^t\} = m \cdot \sigma^2 \cdot I_h$$

This results in:

$$E\{\hat{P}\cdot\hat{P}^t\} = P\cdot P^t + m\cdot\sigma^2\cdot I_h \tag{4.63}$$

With:

$$P = U_p\cdot S_p\cdot V_p^t \tag{4.64}$$

eq. (4.68) becomes:

$$E\{\hat{P}\cdot\hat{P}^t\} = U_p\cdot(S_p^2 + m\cdot\sigma^2\cdot I_h)\cdot U_p^t \tag{4.65}$$

The dual derivation for $\hat{P}^t\cdot\hat{P}$ can be made for the case h>m. Consequently in this sense the singular values of $\hat{P}$ are increased as:

$$\hat{S}_p = S_p + \sigma\cdot\max(h,m)\cdot I_{\min(h,m)} \tag{4.66}$$

The noise on the singular values of the Page matrix is independent if $N\to\infty$. The total noise energy is proportional to the rank of the Page matrix.

The advantages of the Page matrix compared with the block Hankel matrix for the computation of an approximate minimum realization from the estimated Markov parameters are:

- Determination of the order of the system on the basis of the singular values of the Page matrix is simpler since all noisy data only appear once in the Page matrix. For stationary, white, signal independent, inter-channel independent, additive, Gaussian noise, the non relevant singular values of the Page matrix are independent.
- The approximating Page matrix P , with matrix P a closest approximation of $P_{\eta,\mu}$ in Frobenius norm, consists of a unique set of Markov parameters, because also in $\tilde{P}_{\eta,\mu}$ all Markov parameters appear only once. Because of the independence of the non relevant singular values the expected reduction in noise energy is equal to a factor f:

$$f = \frac{n\cdot\max(h,m)\cdot\sigma^2}{h\cdot m\cdot\sigma^2} = \frac{n}{\min(h,m)} \tag{4.67}$$

with: n – rank of the approximating Page matrix $\tilde{P}_{\eta,\mu}$
h – number of rows of the Page matrix
m – number of columns of the Page matrix

- The saving attained in the computational effort required for the computation of a minimum realization, due to the much smaller dimensions of the Page matrix compared with the block Hankel matrix.

Although the approximating Page matrix $\tilde{P}_{\eta,\mu}$ is a closest approximation to $P_{\eta,\mu}$ in Frobenius norm and although it gives a unique set of Markov parameters, the obtained order r state space realization (F, G, H) of the model, described by the estimated Markov parameters, still is not the closest possible approximation in Frobenius norm. This is due to the fact that $\tilde{P}_{\eta,\mu}$ does not have any structure; the entries in $\tilde{P}_{\eta,\mu}$ are not necessarily Markov parameters of a model of dimension r. The "observability" matrix and "controllability" matrix obtained from the singular value decomposition of $\tilde{P}_{\eta,\mu}$ can therefore <u>not</u> be written as:

$$Ob_{\mu} = \begin{bmatrix} H \\ H \cdot F^{\mu} \\ \vdots \\ H \cdot F^{(\eta-1)\mu} \end{bmatrix} \tag{4.68}$$

and

$$Co = \begin{bmatrix} G & F \cdot G & \dots & F^{\mu-1} \cdot G \end{bmatrix} \tag{4.69}$$

So, also in this approach, it is not clear in what sense the state space model obtained approximates the model described by the estimated parameters.

4.5.3 Optimal Hankel norm approximation

Another way to approximate the system, described by the estimated Markov parameters, is developed by Glover (cf. [Glover, 1984]). The approximating state space realization (F, G, H) obtained by this method is an optimal approximation to the originally estimated Markov parameters in Hankel norm. The method of Glover is based on the result that for infinite dimensional Hankel matrices with:

$$N_{r\infty} = || H_{err\infty} || = || H_{\infty} - \tilde{H}_{\infty} ||_{\infty} = \sigma_1(H_{\infty} - \tilde{H}_{\infty}) \tag{4.70}$$

with: $\tilde{H}_{\infty}$ - an order r approximation of the order n Hankel matrix H_{∞}

the restriction that $\tilde{H}_{\infty}$ needs to be a Hankel matrix does not affect the achievable error $N_{r\infty}$. This result was first obtained by Adamjan, Arov and Krein (cf. [Adamjan, 1971]) for single input, single output systems. The

significance of this result for the model reduction problem in systems theory is first noted by Dewilde as mentioned in Kailath (cf. [Kailath, 1980]). The result has been extended for multivariable systems and applied to the model reduction problem by various authors [Silverman, 1980; Genin, 1981; Kung, 1981]. Glover first developed an approximation algorithm only using linear algebra. Furthermore he derived all solutions to the optimal Hankel norm approximation problem and explained them to be a simple function of a balanced realization. Glover developed his algorithm for continuous time systems, but he showed, however, that for a discrete time system the solution found for the equivalent continuous time problem immediately generates the solution to the discrete time problem in the sense that the Hankel singular values of the errors and the frequency responses are the same, if the bilinear transformation is applied for conversions between discrete and continuous time domain.
Starting point for the application of this model reduction algorithm is a continuous time, balanced state space model. To attain this continuous time, balanced state space realization first a high order discrete time state space model in canonical observability form (cf. eq. (4.18)) is constructed from the available, previously estimated Markov parameters. The construction involves:

- Substition of the estimated Markov parameters in input matrix G (cf. eq. (5.57c))
- Construction of state matrix F with a structure given by eq. (4.18) and all coefficients $a_i=0$
- Construction of output matrix H as given by eq. (5.57b)
- Copy direct feed through matrix D from the estimated D matrix

The order n of this realization is equal to $\min(p \cdot n_m, q \cdot n_m)$ with n_m the number of Markov parameters originally estimated. In a second step the obtained discrete time state space system is converted to a corresponding continuous time state space system $(\tilde{A}, \tilde{B}, \tilde{C}, \tilde{D}_c)$ with (see: Appendix B):

$$\tilde{A} = (I + F)^{-1} \cdot (F - I) \tag{4.71a}$$

$$\tilde{B} = \sqrt{2}\ (I + F)^{-1} \cdot G \tag{4.71b}$$

$$\tilde{C} = \sqrt{2}\ H \cdot (I + F)^{-1} \tag{4.71c}$$

$$\tilde{D}_c = D_d - H \cdot (I + A)^{-1} \cdot G \tag{4.71d}$$

In a next step the obtained continuous time state space system $(\tilde{A}, \tilde{B}, \tilde{C}, \tilde{D}_c)$ is transformed into a balanced state space system (A, B, C, D_c) (cf. [Laub, 1980]). The realization obtained is a balanced realization with the same observability and controllability gramians as its corresponding balanced discrete time system (cf. Appendix D). As a consequence both realizations

have the same Hankel singular values and the same McMillan degree (cf. [Gevers, 1986; Kailath, 1980]). The Hankel singular values of the system are equal to the square roots of the eigenvalues of the product of the controllability gramian and observability gramian. These Hankel singular values are also equal to the singular values obtained from the singular value decomposition of the finite block Hankel matrix used for the computation of a balanced state space representation of the system from the earlier estimated FIR model.
To the continuous time state space system (A, B, C, D_c) the model reduction algorithm of Glover can be applied. With this algorithm an optimal Hankel norm, order k realization is computed from the available order n realization ($n \geq k$).
The algorithm developed by Glover is based on a main result on the approximation of systems that states that the minimal Hankel norm of the error system -the system that describes the differences between the order n system and the approximating order k system- is equal to Hankel singular value σ_{k+1} of the original n-th order system, when a k-th order approximation is determined (see [Glover, 1984] for a proof):

Result

Given a stable, rational, qxp, transfer function G(s) with McMillan degree n then:

$$(1)\quad \sigma_{k+1}(G(s)) = \inf_{F(s)\in H_-^\infty,\hat{G}(s)} || G(j\omega) - \hat{G}(j\omega) - F(j\omega) ||_{L^\infty} \qquad (4.72)$$

with: McMillan degree $(\hat{G}(s)) \leq k$
$F(s)$ - an anti-causal transfer function
$\hat{G}(s)$ - a causal transfer function

(2) If G(s) has Hankel singular values $\sigma_1 \geq \sigma_2 \cdots \geq \sigma_k > \sigma_{k+1} = \sigma_{k+2} \cdots = \sigma_{k+r} > \sigma_{k+r+1} \geq \cdots \geq \sigma_n > 0$ then $\hat{G}(s)$ of McMillan degree k is an optimal Hankel norm approximation to G(s) if and only if there exists $F(s) \in H_-^\infty$ (whose McMillan degree can be chosen $\leq n-k-r$) such that $E(s) = G(s) - \hat{G}(s) - F(s)$ satisfies:

$$E(s)\cdot E^*(-\bar{s}) = \sigma_{k+1}^2 \cdot I \qquad (4.73)$$

and consequently:

$$||G(s) - \hat{G}(s)||_H = \sigma_{k+1} \qquad (4.74)$$

(3) Let $G(s)$ be as given in (2), then an optimal Hankel norm approximation of McMillan degree k, $\hat{G}(s)$, can be constructed as follows. Let (A, B, C, D_c) be a balanced realization of $G(s)$ with corresponding gramians $\Sigma = \text{diag}(\Sigma_1, \sigma_{k+1}\cdot I_r) = \text{diag}(\sigma_1, \sigma_2, \cdots, \sigma_k, \sigma_{k+r+1}, \cdots, \sigma_n, \sigma_{k+1}, \cdots, \sigma_{k+r})$, and define $(\hat{A}, \hat{B}, \hat{C}, \hat{D})$ by:

$$\hat{A} = \Gamma^{-1}\cdot(\sigma_{k+1}^2\cdot A_{11}^* + \Sigma_1\cdot A_{11}\cdot\Sigma_1 - \sigma_{k+1}\cdot C_1^*\cdot U\cdot B_1^*) \tag{4.75}$$

$$\hat{B} = \Gamma^{-1}\cdot(\Sigma_1\cdot B_1 + \sigma_{k+1}\cdot C_1^*\cdot U) \tag{4.76}$$

$$\hat{C} = C_1\cdot\Sigma_1 + \sigma_{k+1}\cdot U\cdot B_1^* \tag{4.77}$$

$$\hat{D} = D_c - \sigma_{k+1}\cdot U \tag{4.78}$$

with: $A = \begin{bmatrix} A_{11} & A_{12} \\ A_{21} & A_{22} \end{bmatrix}$ $\quad \dim[A_{11}]: k \times k$

$B = \begin{bmatrix} B_1 \\ B_2 \end{bmatrix}$ $\quad \dim[B_1]: k \times p$

$C = \begin{bmatrix} C_1 & C_2 \end{bmatrix}$ $\quad \dim[C_1]: q \times k$

$\Gamma = \Sigma_1\cdot\Sigma_1 - \sigma_{k+1}^2\cdot I$

$B_2 = -C_2^*\cdot U$

$U^*\cdot U \leq I$

Then:

$$\hat{G}(s) + F(s) = \hat{D} + \hat{C}\cdot(sI - \hat{A})^{-1}\cdot\hat{B} \tag{4.79}$$

With: $\hat{G}(s)\epsilon H_+^\infty$, a causal transfer function

$F(s)\epsilon H_-^\infty$, an anti-causal transfer function

The above mentioned result in fact is based on the following observations:

- the transfer function $E(s)=G(s)-\hat{G}(s)-F(s)$ obtained from the construction given by eq. (4.75) - (4.78) is an all-pass transfer function
- all-pass transfer functions have Hankel singular values which are all equal
- the Hankel singular values of $E(s)$ are equal to σ_{k+1}
- approximating state matrix $\hat{A}$ exactly has k stable eigenvalues and n-k-r unstable eigenvalues

Part (3) of the above mentioned result describes the construction of a k-th order, optimal Hankel norm approximation of the n-th order system. The algorithm based on this result consists of three steps.

First step:

- ordering of the balanced realization in order to seperate Hankel singular values σ_{k+1} - σ_{k+r}:

$$\tilde{A} = \begin{bmatrix} A_{11} & A_{12} \\ A_{21} & A_{22} \end{bmatrix} \qquad \dim[A_{11}]: (n-r) \times (n-r) \tag{4.80a}$$

$$\tilde{B} = \begin{bmatrix} B_1 \\ B_2 \end{bmatrix} \qquad \dim[B_1]: (n-r) \times p \tag{4.80b}$$

$$\tilde{C} = \begin{bmatrix} C_1 & C_2 \end{bmatrix} \qquad \dim[C_1]: q \times (n-r) \tag{4.80c}$$

$$\begin{aligned} \tilde{\Sigma} &= \mathrm{diag}(\sigma_1, \sigma_2, \ldots, \sigma_k, \sigma_{k+r+1}, \ldots, \sigma_n, \sigma_{k+1}, \sigma_{k+2}, \ldots, \sigma_{k+r}) \\ &= \mathrm{diag}(\Sigma_1, \sigma_{k+1} \cdot I_r) \end{aligned} \tag{4.81}$$

The partioning of A, B and C is conform the partioning of gramian Σ. Reordering of the matrices is done by performing an orthogonal state transformation.

Second step:

- Determination of the sum of the approximating causal transfer function $\hat{G}(s)$ and the anticausal $F(s)$ according to eq. (4.75) - (4.79):

$$U = - C_2 \cdot B_2^{*+} \tag{4.82}$$

$$\Gamma = (\Sigma_1^2 - \sigma_{k+1}^2 I_{n-1}) \tag{4.83}$$

$$\hat{A} = \Gamma^{-1} \cdot (\sigma_{k+1}^2 \cdot A_{11}^* + \Sigma_1 \cdot A_{11} \cdot S_1 - \sigma_{k+1} \cdot C_1^* \cdot U \cdot B_1) \tag{4.75}$$

$$\hat{B} = \Gamma^{-1} \cdot (\Sigma_1 \cdot B_1 + \sigma_{k+1} \cdot C_1^* \cdot U) \tag{4.76}$$

$$\hat{C} = C_1 \cdot \Sigma_1 + \sigma_{k+1} \cdot U \cdot B_1^* \tag{4.77}$$

$$\hat{D} = D_c - \sigma_{k+1} \cdot U \tag{4.78}$$

The matrices $\hat{A}$, $\hat{B}$, $\hat{C}$ and $\hat{D}$ are the state space realization of $\hat{G}(s)+F(s)$

Third step:

- Separation of the causal and the anti-causal part of the state space realization obtained in the second step. This requires the following actions:
- Block diagonalization of $\hat{A}$ by reduction of $\hat{A}$ to real upper Schur form

$$\hat{A}_s = V_1^t \cdot \hat{A} \cdot V_1 \tag{4.84}$$

with: V_1 such that $V_1^t \cdot V_1 = I_{n-r}$

- Re-ordering of the eigenvalues of the real Schur matrix $\hat{A}_s$ by pre- and post-multiplication of $\hat{A}_s$ with an orthogonal matrix V_2 in such a way that the upper left block contains all left plane eigenvalues and the lower right block contains all right half plane eigenvalues:

$$V_2^t \cdot \hat{A}_s \cdot V_2 = \begin{bmatrix} \hat{A}_{11} & \hat{A}_{12} \\ 0 & \hat{A}_{22} \end{bmatrix} \qquad \dim[\hat{A}_{11}]: k \times k \tag{4.85}$$

with: $\mathrm{Re}(\lambda_i(\hat{A}_{11}))<0$

$\mathrm{Re}(\lambda_i(\hat{A}_{22}))>0$

In this form matrix $\hat{A}_{11}$ already is the state matrix of the k-th order optimal Hankel norm approximation of (A, B, C, D_c). For this ordering of the eigenvalues algorithms developed by G. Stewart or by

P. Van Dooren (cf. [Stewart, 1976; Van Dooren, 1982]) can be used. By writing:

$$\begin{bmatrix} I_k & -X \\ 0 & I_{n-k-r} \end{bmatrix} \cdot \begin{bmatrix} \hat{A}_{11} & \hat{A}_{12} \\ 0 & \hat{A}_{22} \end{bmatrix} \cdot \begin{bmatrix} I_k & X \\ 0 & I_{n-k-r} \end{bmatrix} \tag{4.86}$$

$$= \begin{bmatrix} \hat{A}_{11} & \hat{A}_{11} \cdot X - X \cdot \hat{A}_{22} + \hat{A}_{12} \\ 0 & \hat{A}_{22} \end{bmatrix}$$

it can be seen that X has to be determined such in a way that the upper right block of (4.86) becomes zero.

- determination of the solution $X \epsilon R^{k \times (n-k-r)}$ of the Sylvester equation:

$$\hat{A}_{11} \cdot X - X \cdot \hat{A}_{22} + \hat{A}_{12} = 0 \tag{4.87}$$

This solution can be found with an algorithm developed by Golub, Nash and Van Loan [Golub, 1979]

- finally, the transformation matrices T and S have to be computed in order to obtain the appropriate input- and output matrices B and C:

$$T = V_1 \cdot V_2 \cdot \begin{bmatrix} I_k & X \\ 0 & I_{n-k-r} \end{bmatrix} = [T_1 \; T_2] \tag{4.88}$$

$$S = \begin{bmatrix} I_k & -X \\ 0 & I_{n-k-r} \end{bmatrix} \cdot V_2^t \cdot V_1^t = \begin{bmatrix} S_1 \\ S_2 \end{bmatrix} \tag{4.89}$$

- determination of the input- and output matrices $\hat{B}_1$, $\hat{B}_2$, $\hat{C}_1$ and $\hat{C}_2$:

$$\hat{B}_1 = S_1 \cdot \hat{B} \tag{4.90}$$

$$\hat{B}_2 = S_2 \cdot \hat{B} \tag{4.91}$$

$$\hat{C}_1 = \hat{C} \cdot T_1 \tag{4.92}$$

$$\hat{C}_2 = \hat{C} \cdot T_2 \tag{4.93}$$

The state space system given by the matrices $\hat{A}_{11}$, $\hat{B}_1$, $\hat{C}_1$, $\hat{D}$ is a minimal realization of the causal, k-th order, optimal Hankel norm approximation of

the n-th order system. For the optimal Hankel norm approximation of the system described by the estimated Markov parameters the choice of the D-matrix is arbitrary since it does not influence the Hankel norm.
Next the obtained continuous time domain realization has to be converted back to the discrete time domain using bilinear transformation. The corresponding discrete time balanced realization is obtained with (see: Appendix B):

$$H_k = \sqrt{2}\ \hat{C}_1 \cdot (I_k - \hat{A}_{11})^{-1} \tag{4.94a}$$

$$G_k = \sqrt{2}\ (I_k - \hat{A}_{11})^{-1} \cdot \hat{B}_1 \tag{4.94b}$$

$$F_k = (I_k - \hat{A}_{11})^{-1} \cdot (I_k + \hat{A}_{11}) \tag{4.94c}$$

$$D_k = D_c + \hat{C}_1 \cdot (I_k - \hat{A}_{11})^{-1} \cdot \hat{B}_1 \tag{4.94d}$$

The start sequence Markov parameters and the corresponding minimal polynomial coefficients are directly obtained from this discrete time state space realization (F_k, B_k, C_k, D_k).

4.6 Simulation results

The various methods discussed in this chapter have been applied to the estimation results obtained with the program EXACTMARK discussed in chapter 3 on the simulated processes defined in section 3.6. The FIR models used for system 1 contained 15 estimated Markov parameters. The models used for systems 2 and 3 consisted of 20 Markov parameters. The models used for system 4 had 50 Markov parameters.

The order determination tests discussed in section 4.3 have been tested on the results obtained for the four simulated systems.
Output error tests have been applied to the output errors obtained with models of increasing order computed with the Gerth method.
Using the different models obtained with Gerth's method, for each autocorrelation function 1000 samples of the output errors have been computed on the basis of the same set of input signals as the set that has been used for the estimation of the FIR model parameters. For each evaluation the average of the results obtained for approximate models computed on the basis of 5 different, estimated FIR models is used.
For each system the computed autocorrelation functions of the output errors obtained with models of increasing orders are presented in fig. 4.2 - 4.5. For system 1 the autocorrelation of the outputs does not change any more for orders above 2. For systems 2, 3 and 4 only minor changes in the autocorrelation functions are found between second, third and fourth order systems.

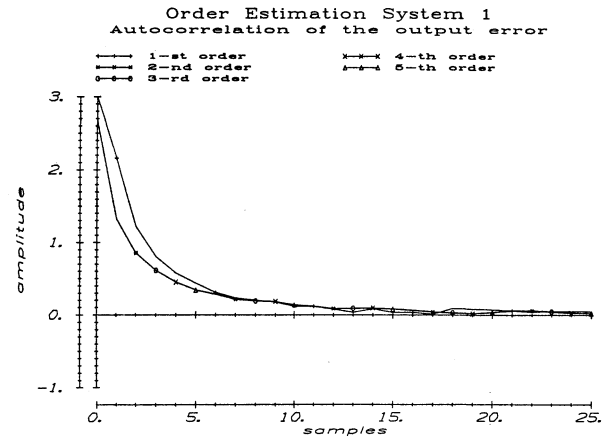

Fig. 4.2a Estimation of the degree of the minimal polynomial on the basis of the autocorrelation of the output error. Results obtained for output 1 of system 1.

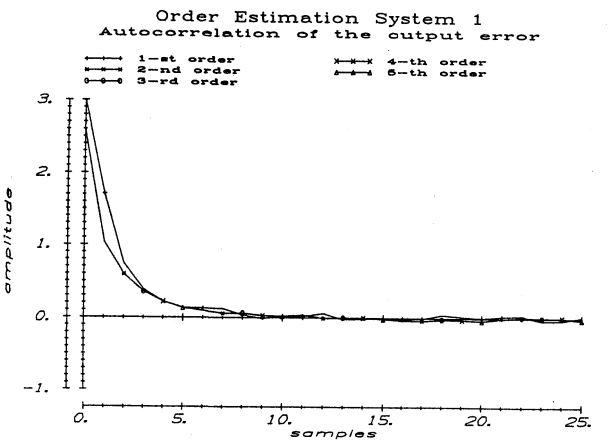

Fig. 4.2b Estimation of the degree of the minimal polynomial on the basis of the autocorrelation of the output error. Results obtained for output 2 of system 1.

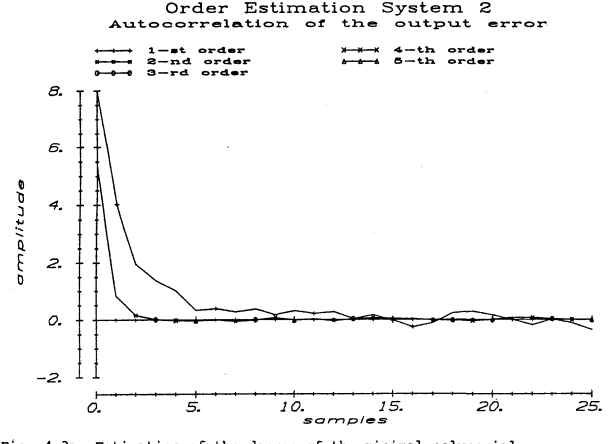

Fig. 4.3a Estimation of the degree of the minimal polynomial on the basis of the autocorrelation of the output error. Results obtained for output 1 of system 2.

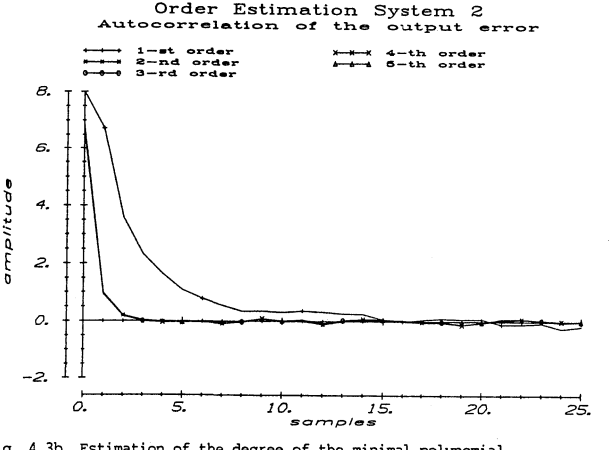

Fig. 4.3b Estimation of the degree of the minimal polynomial on the basis of the autocorrelation of the output error. Results obtained for output 2 of system 2.

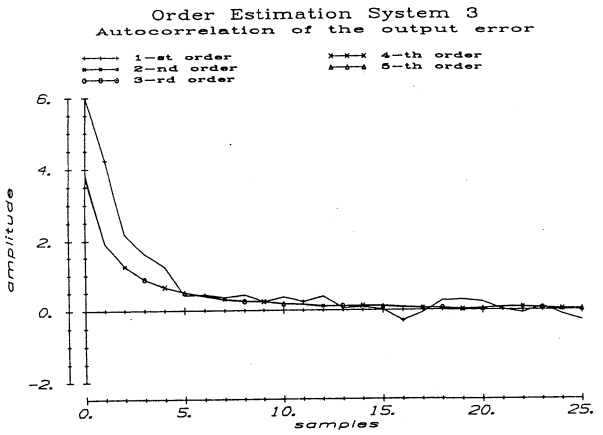

Fig. 4.4a Estimation of the degree of the minimal polynomial on the basis of the autocorrelation of the output error. Results obtained for output 1 of system 3.

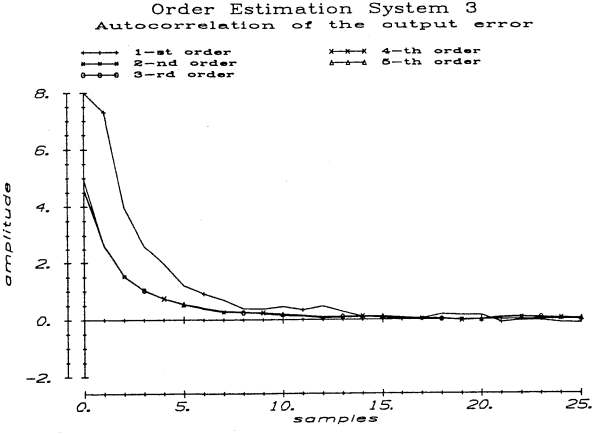

Fig. 4.4b Estimation of the degree of the minimal polynomial on the basis of the autocorrelation of the output error. Results obtained for output 2 of system 3.

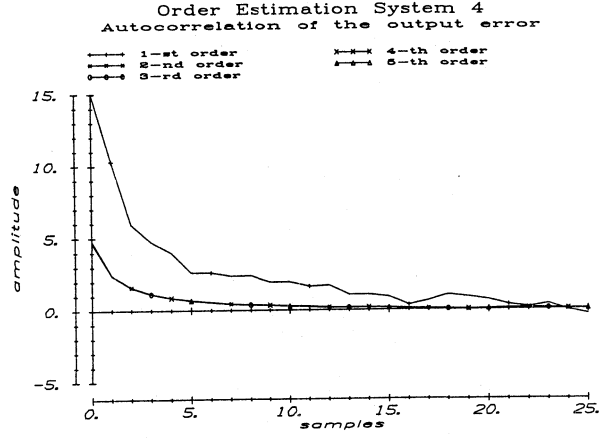

Fig. 4.5a Estimation of the degree of the minimal polynomial on the basis of the autocorrelation of the output error. Results obtained for output 1 of system 4.

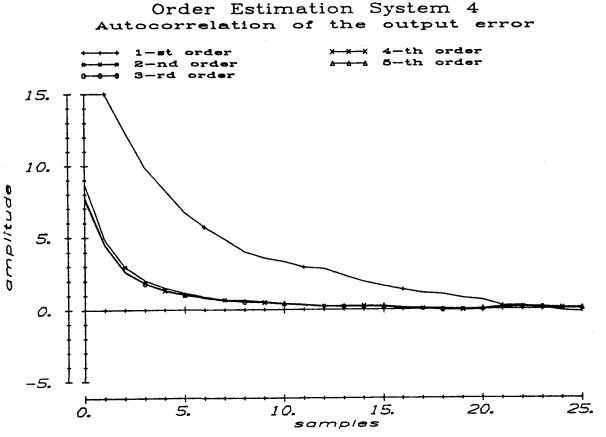

Fig. 4.5b Estimation of the degree of the minimal polynomial on the basis of the autocorrelation of the output error. Results obtained for output 2 of system 4.

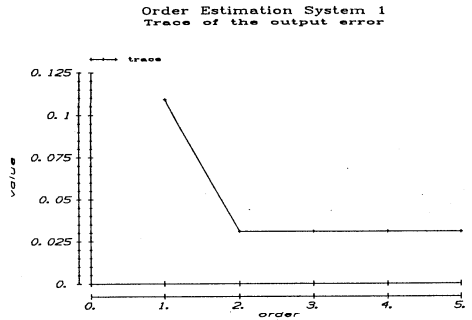

Fig. 4.6a Trace of the output error as function of the degree of the minimal polynomial of the MPSSM model of system 1.

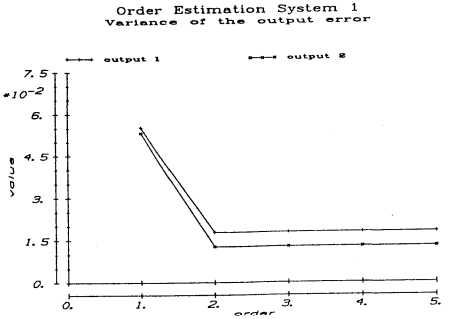

Fig. 4.6b Variance of the error of each output as function of the degree of the minimal polynomial of the MPSSM model of system 1.

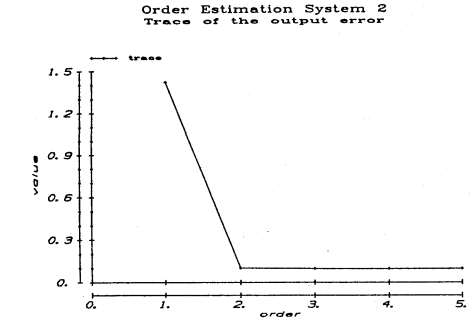

Fig. 4.7a Trace of the output error as function of the degree of the minimal polynomial of the MPSSM model of system 2.

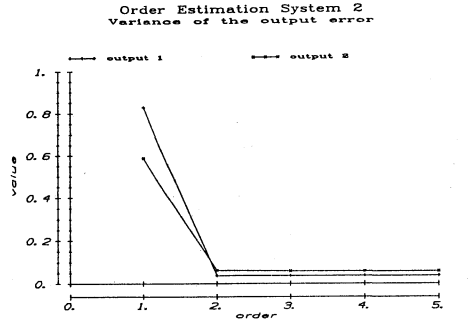

Fig. 4.7b Variance of the error of each output as function of the degree of the minimal polynomial of the MPSSM model of system 2.

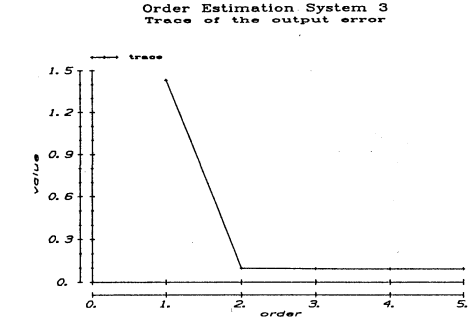

Fig. 4.8a Trace of the output error as function of the degree of the minimal polynomial of the MPSSM model of system 3.

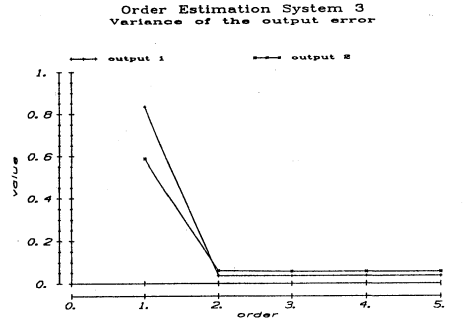

Fig. 4.8b Variance of the error of each output as function of the degree of the minimal polynomial of the MPSSM model of system 3.

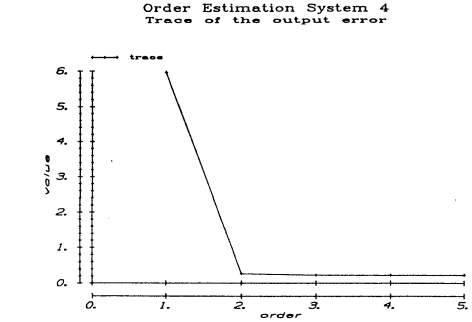

Fig. 4.9a Trace of the output error as function of the degree of the minimal polynomial of the MPSSM model of system 4.

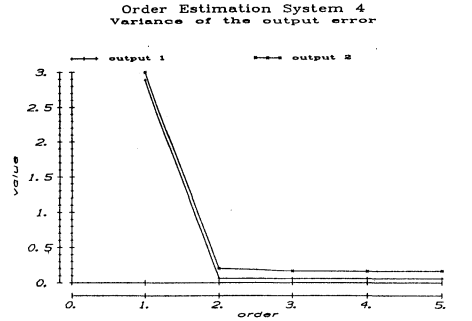

Fig. 4.9b Variance of the error of each output as function of the degree of the minimal polynomial of the MPSSM model of system 4.

Values computed for the traces and the variances of the output errors are presented in fig. 4.6 - 4.9. Again, for system 1 no change in both the trace and the variance values is found for orders above 2. For systems 2, 3 and 4 only a minor decrease between the values obtained for second, third and fourth order models is found. For orders above 4 no decrease in the values is found any more.
The results are well in agreement with the expectations, for according to eq. (4.15) a second order minimal polynomial generically already results in a fourth order system if the minimum of the number of inputs and outputs equals two. In the cases of the systems 2, 3 and 4, which have two clusters of poles, a second order minimal polynomial with poles at each cluster already gives good results. The results obtained show that the minimal polynomials of second order approximations have eigenvalues at each of the clusters. Third order approximations typically have an eigenvalue close to the two largest eigenvalues of the true system, an eigenvalue at the cluster of smallest eigenvalues of the true system and an eigenvalue between both clusters. Table 4.1 shows a typical example of the eigenvalues obtained for a second, third and fourth order approximation of a 4-th order system with two clusters of eigenvalues. In the example results are given of approximations of a FIR model estimated for system 3. Also the eigenvalues of 4-th order approximate state space realizations computed with the method of Zeiger and McEwen on the basis of the 2-nd, 3-rd and 4-th order MPSSM models are given.

order	roots minimal polynomial			
2	0.690E+00	0.143E+00	0.000E+00	0.000E+00
3	0.669E+00	0.388E+00	0.121E+00	0.000E+00
4	0.676E+00	0.523E+00	0.122E+00	-0.325E+00
	Eigenvalues of corresponding 4-th order approximate state space realizations			
2	0.143E+00	0.143E+00	0.690E+00	0.690E+00
3	0.470E-01	0.169E+00	0.587E+00	0.681E+00
4	0.776E-01	0.178E+00	0.592E+00	0.687E+00
	Eigenvalues of system 3			
	0.200E-01	0.300E-01	0.600E-01	0.700E-01

table 4.1 Characteristic example (system 3) of the eigenvalues of computed MPSSM models with resp. 2-nd, 3-rd and 4-th order minimal polynomials (Gerth method) and the eigenvalues of their approximate 4-th order state space realizations.

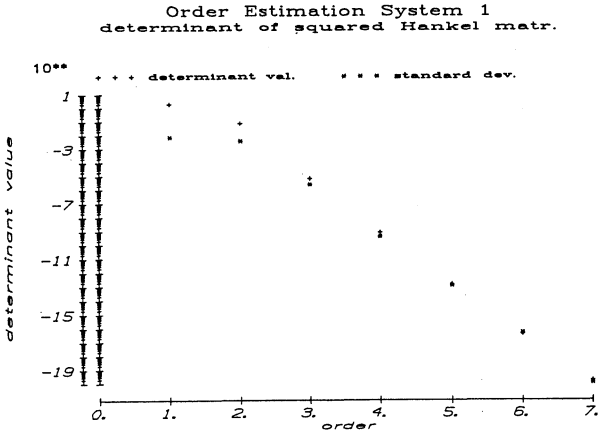

Fig. 4.10a Determinant values of squared block Hankel matrices built with an increasing number of Markov parameters in vector form of the FIR model of system 1.

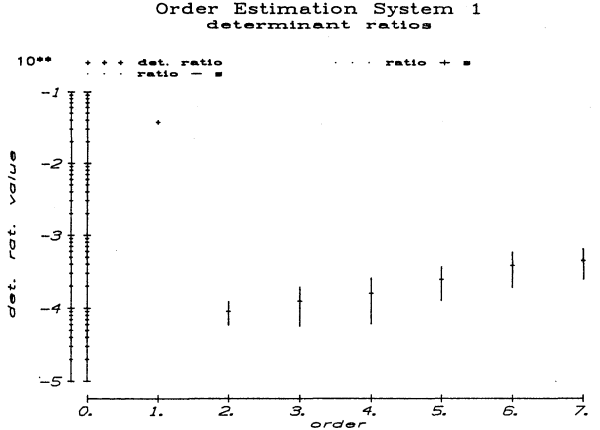

Fig. 4.10b Ratios of consecutive determinant values of squared block Hankel matrices built with an increasing number of Markov parameters in vector form of the FIR model of system 1.

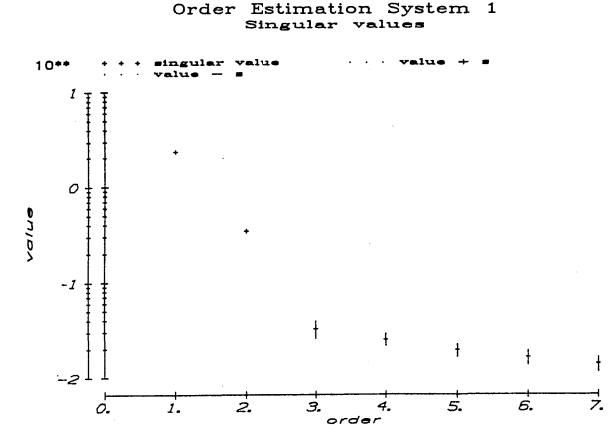

Fig. 4.10c Singular values of block Hankel matrices built with Markov parameters in vector form of the FIR model of system 1.

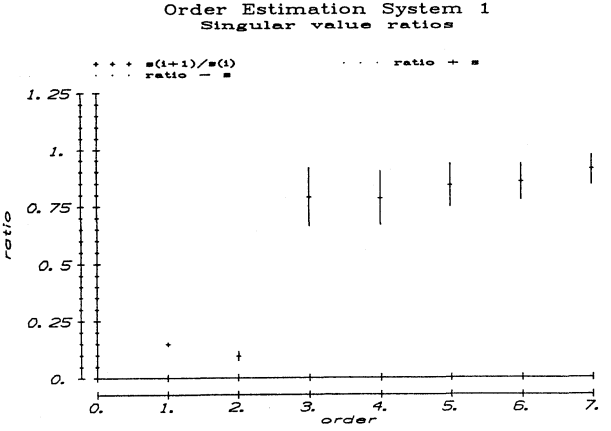

Fig. 4.10d Ratios of consecutive singular values of block Hankel matrices built with Markov parameters in vector form of the FIR model of system 1.

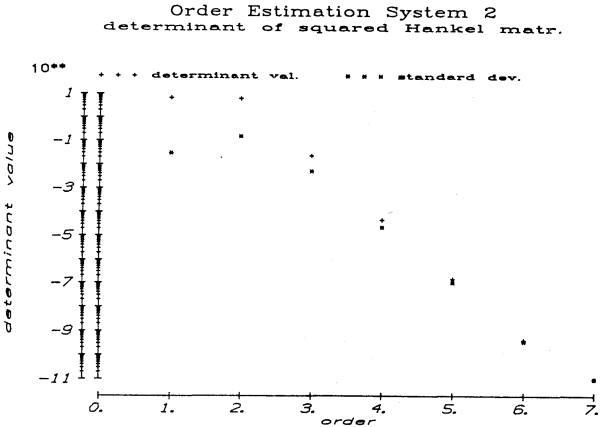

Fig. 4.11a Determinant values of squared block Hankel matrices built with an increasing number of Markov parameters in vector form of the FIR model of system 2.

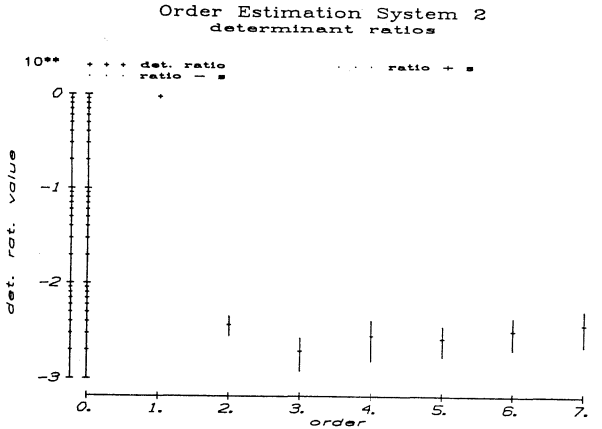

Fig. 4.11b Ratios of consecutive determinant values of squared block Hankel matrices built with an increasing number of Markov parameters in vector form of the FIR model of system 2.

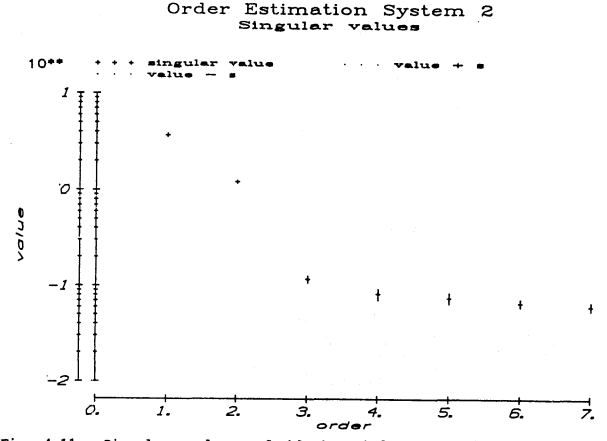

Fig. 4.11c Singular values of block Hankel matrices built with Markov parameters in vector form of the FIR model of system 2.

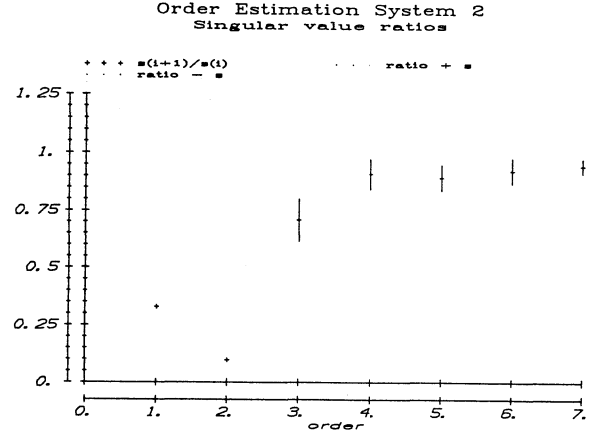

Fig. 4.11d Ratios of consecutive singular values of block Hankel matrices built with Markov parameters in vector form of the FIR model of system 2.

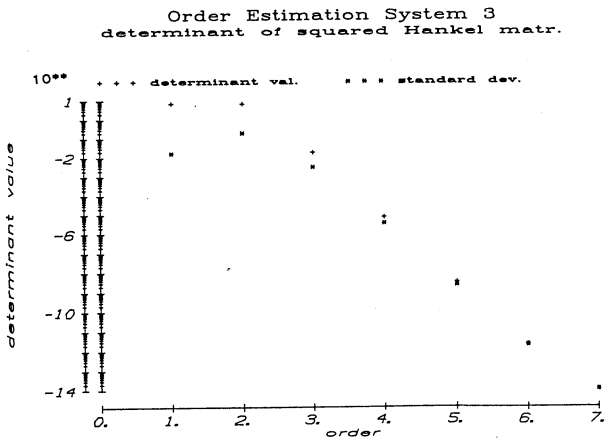

Fig. 4.12a Determinant values of squared block Hankel matrices built with an increasing number of Markov parameters in vector form of the FIR model of system 3.

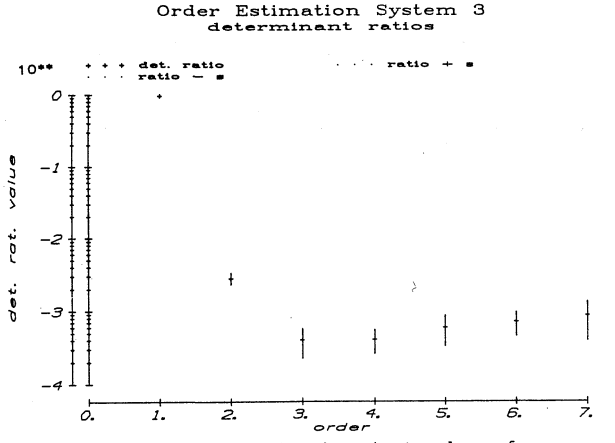

Fig. 4.12b Ratios of consecutive determinant values of squared block Hankel matrices built with an increasing number of Markov parameters in vector form of the FIR model of system 3.

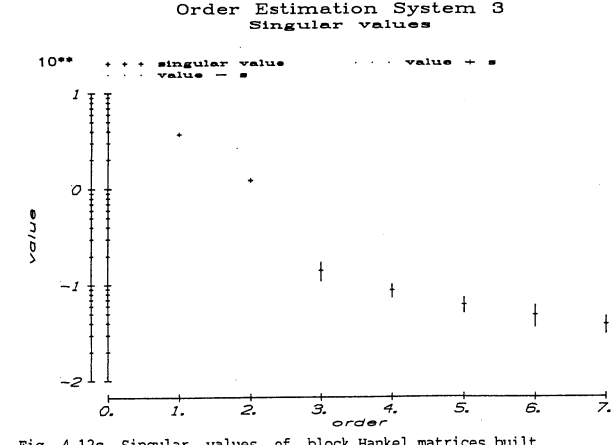

Fig. 4.12c Singular values of block Hankel matrices built with Markov parameters in vector form of the FIR model of system 3.

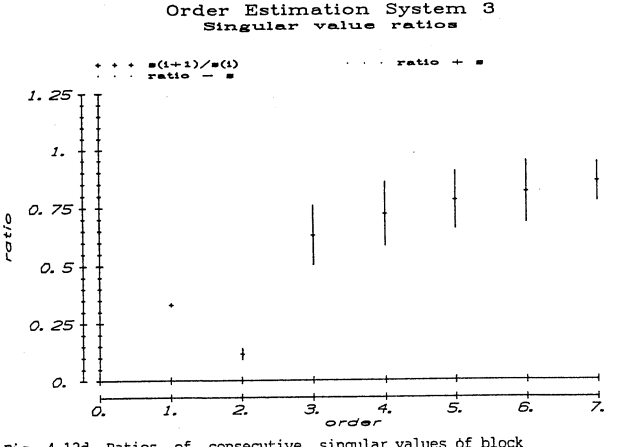

Fig. 4.12d Ratios of consecutive singular values of block Hankel matrices built with Markov parameters in vector form of the FIR model of system 3.

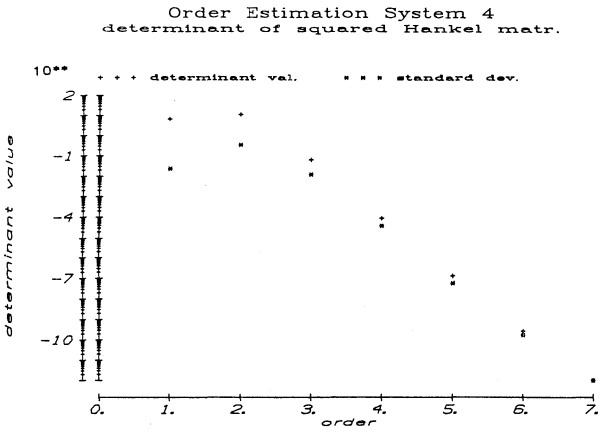

Fig. 4.13a Determinant values of squared block Hankel matrices built with an increasing number of Markov parameters in vector form of the FIR model of system 4.

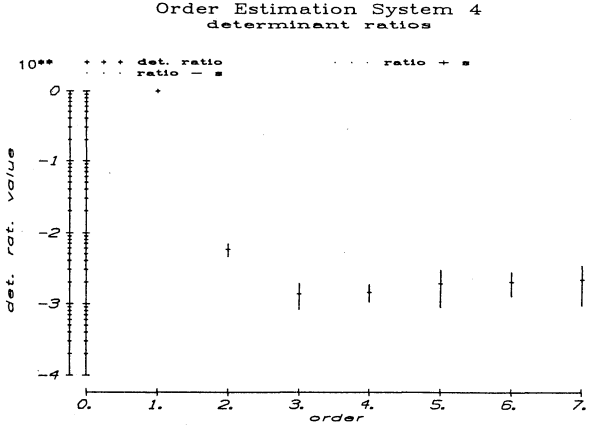

Fig. 4.13b Ratios of consecutive determinant values of squared block Hankel matrices built with an increasing number of Markov parameters in vector form of the FIR model of system 4.

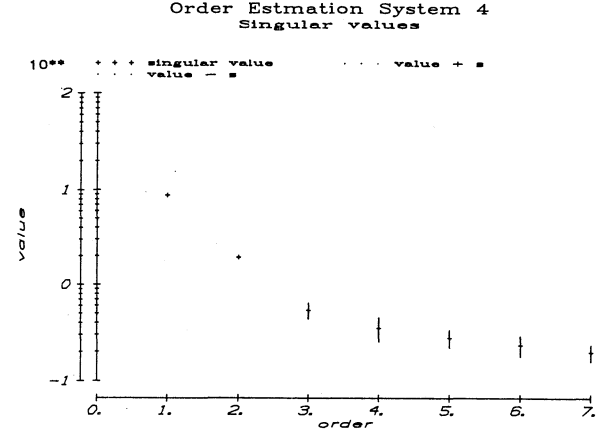

Fig. 4.13c Singular values of block Hankel matrices built with Markov parameters in vector form of the FIR model of system 4.

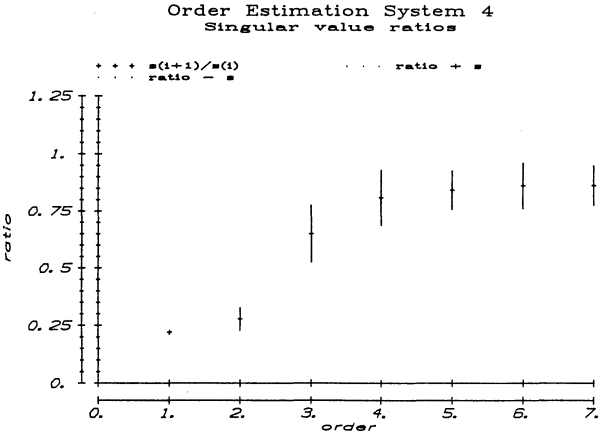

Fig. 4.13d Ratios of consecutive singular values of block Hankel matrices built with Markov parameters in vector form of the FIR model of system 4.

The second type of order tests, discussed in section 4.3.2, is also applied to the FIR models. For determination of the order of the minimal polynomial the determinants, determinant ratios, singular values and singular value ratios of the block Hankel matrix have been computed. The results are given in fig. 4.10 - 4.13 for system 1, 2, 3 and 4 respectively.
Also these tests indicate for system 1 an order 2 to be appropriate. For systems 2, 3 and 4 a third order for the minimal polynomial is indicated as a best choice. All methods applied give the same results. However, the clearest indication of the order to be used is given by the methods based on the ratios of successive values. Of the four methods tested (determinant, determinant ratio, singular values and singular value ratio) the method based on the ratios of singular values is preferred because of its numerical reliability, its speed and the clearness of the results.

Of all order estimation methods tested the methods based on the analysis of a block Hankel matrix consisting of the estimated FIR model parameters in vector form (cf. eq. (4.25)) give the best results.

The various approximate realization methods discussed in this chapter have been tested on the FIR models obtained from EXACTMARK for the four simulated processes. For each system all 20 FIR models estimated for the analysis of chapter 3 have been used as input models. For the tests the same orders have been used both for the minimal polynomials (Gerth method and modified Gerth method) and for the state space descriptions (Approximate realization from the Hankel matrix, Approximate realization from the Page matrix and optimal Hankel norm approximation). The orders used for the various systems are:

system 1 - order 2
system 2 - order 4
system 3 - order 4
system 4 - order 4

To be able to compare the results obtained with the Gerth method, the modified Gerth method (cf. section 4.4), the realization from a block Hankel matrix, the realization from the Page matrix and the method developed by Glover (cf. section 4.5) all approximating MPSSM models are compared with the estimated FIR models which were used as inputs for the various algorithms.
For all models both the Hankel norm and the Frobenius norm of the error systems -the systems that describe the differences between the estimated FIR models and the obtained approximate models- have been computed (cf. eq. (3.50) - (3.60)).
To recapture the meaning of these norms:

- The Hankel norm is a measure for the worst case error in the transfer of past inputs to future outputs by the approximate model compared to the transfer given by the original model.
- The Frobenius norm divided by the number of Hankel singular values of a minimal realization of the error system is a measure for the average error of the transfer of past inputs to future outputs.

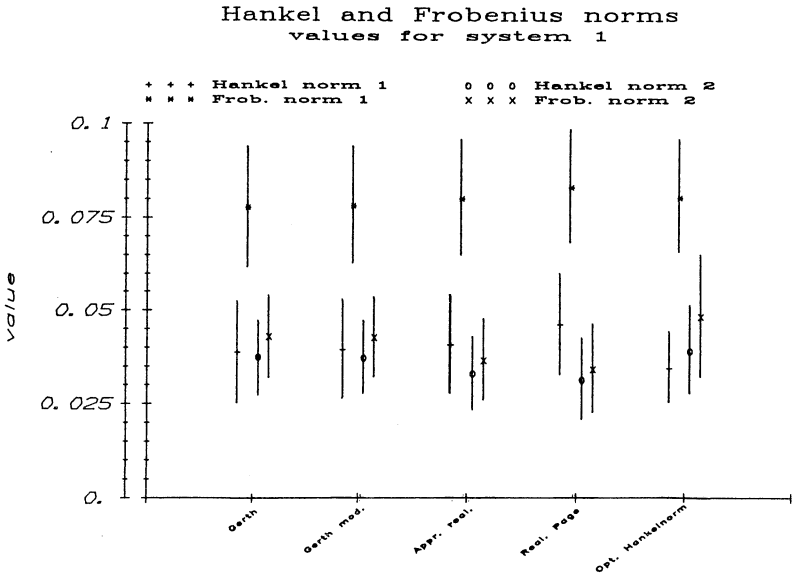

Fig. 4.14 Average values of the norms of the error systems obtained for system 1 with the method of Gerth, the modified Gerth method, the approximate realization methods on the basis of the Hankel matrix and the Page matrix and the optimal Hankel norm approximation mehod.

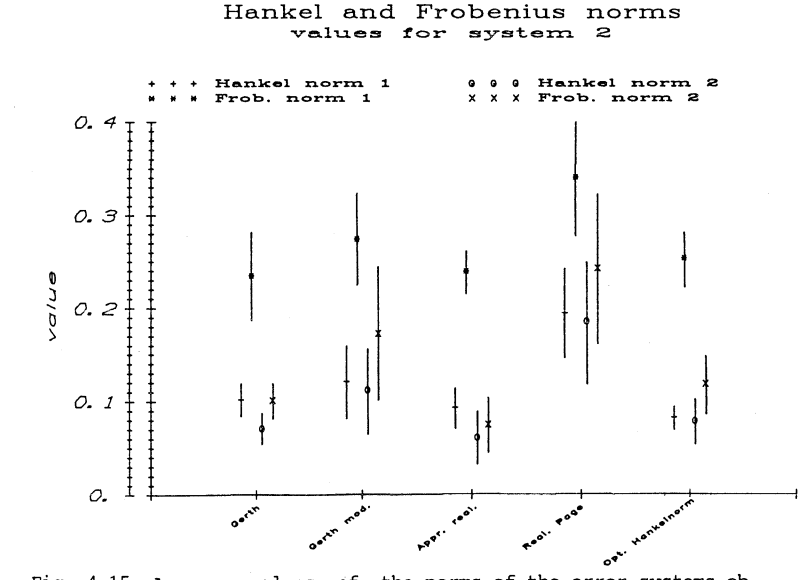

Fig. 4.15 Average values of the norms of the error systems obtained for system 2 with the method of Gerth, the modified Gerth method, the approximate realization methods on the basis of the Hankel matrix and the Page matrix and the optimal Hankel norm approximation mehod.

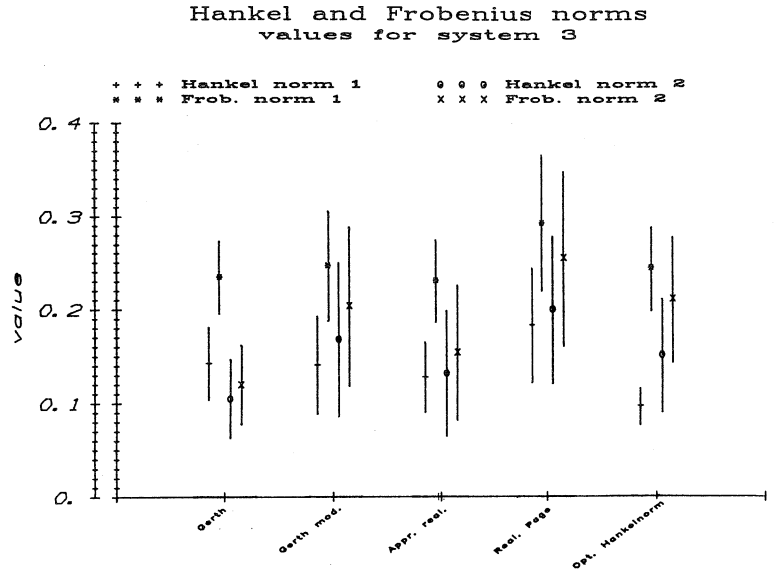

Fig. 4.16 Average values of the norms of the error systems obtained for system 3 with the method of Gerth, the modified Gerth method, the approximate realization methods on the basis of the Hankel matrix and the Page matrix and the optimal Hankel norm approximation mehod.

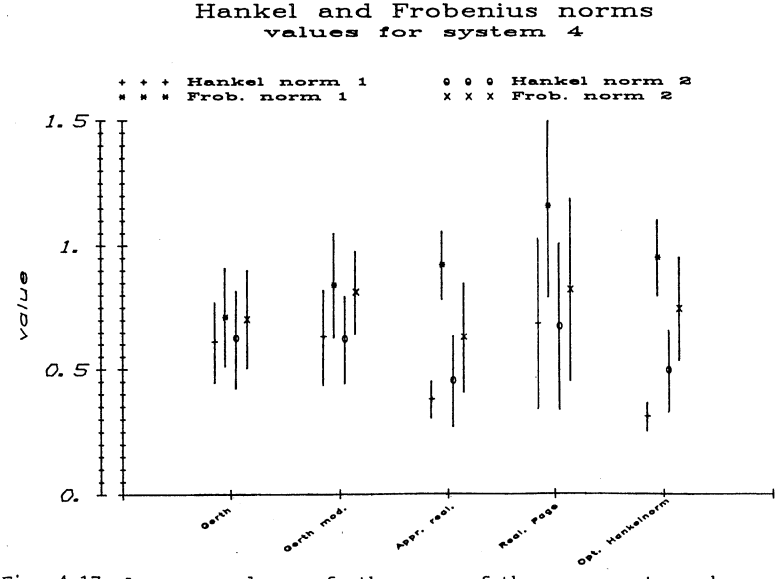

Fig. 4.17 Average values of the norms of the error systems obtained for system 4 with the method of Gerth, the modified Gerth method, the approximate realization methods on the basis of the Hankel matrix and the Page matrix and the optimal Hankel norm approximation mehod.

Besides the differences between the estimated FIR models and the approximate realizations also the differences between the approximate realizations and the true systems have been analysed. Also of the error systems defined by the differences of true systems and approximate realizations the Hankel norms and the Frobenius norms have been computed.
The results are presented in fig. 4.14 - 4.17. In these figures the various norms depicted are:

- Hankel norm 1: The Hankel norm of the error system that describes the differences between the estimated FIR model and the approximate realization
- Frobenius norm 1: The Frobenius norm of the error system defined by the differences between the estimated FIR model and the approximate realization
- Hankel norm 2: The Hankel norm of the error system defined by the differences between the true system and the approximate realization
- Frobenius norm 2: The Frobenius norm of the error system defined by the true system and the approximate realization

The figures show the average values of the errors of 20 approximate realizations plus and minus the computed standard deviation of the obtained values.

First the fit of the approximate models to the originally estimated FIR input models is discussed. As expected, the method developed by Glover gives the best results in Hankel norm when the resulting models are compared with the originally estimated FIR models. In Frobenius norm, the norm that is a measure for the overall fit of the models, both the Gerth method and the approximate realization method developed by Zeiger and McEwen give better results than the optimal Hankel norm approximation method of Glover.
In general, the Gerth method performs slightly better than the aproximate realization from the block Hankel matrix. This difference can be explained from the fact that the order r MPSSM model used in the Gerth method generically leads to a $r \cdot \min(p,q)$ order state space model compared to the order n (with: $n<r \cdot \min(p,q)$) of the balanced realization obtained from the Hankel matrix. Consequently the MPSSM has some more freedom in shaping the systems responses.
Analysis of the results obtained for the error models described by the differences between true systems and approximate realizations shows a change in the Hankel norm results in favour of both the Gerth method and the method of Zeiger and McEwen. Comparison of the results shows that the method developed by Glover does not perform so well any more.
Table 4.2 summarizes the average results obtained for the Hankel norms and the Frobenius norms for each of the 4 systems and for all approximate realization mehods. To show the quality of the results also the Hankel norms and Frobenius norms of the true systems are given.

	Hankel norm	Frobenius norm
system 1: true system	0.196E+01	0.237E+01
Gerth	0.374E-01	0.428E-01
Gerth modified	0.372E-01	0.426E-01
Appr. real. Hankel	0.330E-01	0.365E-01
Appr. real. Page	0.313E-01	0.341E-01
Opt. Hankelnorm	0.390E-01	0.482E-01
system 2: true system	0.336E+01	0.390E+01
Gerth	0.710E-01	0.101E+00
Gerth modified	0.112E+00	0.173E+00
Appr. real. Hankel	0.612E-01	0.749E-01
Appr. real. Page	0.186E+00	0.243E+00
Opt. Hankelnorm	0.783E-01	0.118E+00
system 3: true system	0.336E+01	0.390E+01
Gerth	0.105E+00	0.120E+00
Gerth modified	0.168E+00	0.204E+00
Appr. real. Hankel	0.132E+00	0.154E+00
Appr. real. Page	0.200E+00	0.255E+00
Opt. Hankelnorm	0.151E+00	0.211E+00
system 4: true system	0.874E+01	0.903E+01
Gerth	0.625E+00	0.704E+00
Gerth modified	0.622E+00	0.813E+00
Appr. real. Hankel	0.455E+00	0.631E+00
Appr. real. Page	0.676E+00	0.823E+00
Opt. Hankelnorm	0.496E+00	0.745E+00

table 4.2 Norms of the true systems and norms computed for the error systems

Overall the approximate realization method developed by Zeiger and McEwen and the method developed by Gerth perform almost equal.
At first sight the modified Gerth method and the method based on the Page matrix perform significantly worse than the other methods. A closer look at the results obtained for each model shows that these bad results are mainly caused by the fact that these methods sometimes give results that are very bad compared to the results obtained with the other methods. Further research is required to find out why these methods sometimes perform that badly.

4.7 Concluding remarks

In this chapter various methods have been discussed for the determination of approximate MPSSM and State Space models from FIR models.
MPSSM and State Space models respectively require the estimation of the degree of the minimal polynomial and of the order of the system. To get an estimate for the degree of the minimal polynomial basically two different types of methods have been examined:

- methods based on the analysis of the output errors that remain when increasing degrees for the computed approximate model are used.
- methods based on an immediate analysis of the available FIR models.

To test the various order estimation methods earlier estimated FIR models (cf. chapter 3 section 3.6) have been used as input models.
For the test of the first type of order estimation methods for each of the four simulated processes (cf. chapter 3 section 3.6) five times five approximate MPSSM models with minimal polynomials of degrees 1, 2 ,3 ,4 and 5 have been computed using Gerth's method. With these models output signals were simulated and output error signals consisting of 1000 samples for each output have been computed. Of the obtained output error signals autocorrelation functions, variances and traces were analysed.
For the test of the second type of order estimation methods all FIR models estimated with the program EXACTMARK for the examples of chapter 3 (cf. section 3.6) were used as input models. Of each of the FIR models determinants, determinant ratio's, singular values and singular value ratio's of block Hankel matrices constructed from the estimated Markov parameters in vector form (cf. eq. (4.25)) have been computed.

The results of the tests can be summarized as follows:

- The second type of order tests needs much less computational effort than the first type of order test methods
- The second type of order test methods gives a better discrimination between the various degrees of the minimal polynomial
- Of the methods of the second type tested the methods based on the computation of singular values of the block Hankel matrix need less computational effort and are numerically more reliable than the methods based on the computation of determinants of almost singular matrices

As a result of the tests the second type of order estimation methods is selected as the best because of the less computational effort required and the higher level of discrimination obtained between the various degrees of the minimal polynomial. Of these methods the method based on the computation of ratios of successive singular values of the block Hankel matrix (eq. (4.25)) is preferred.

For the computation of approximate realizations of initially estimated FIR models five methods have been investigated. The methods can be divided into two different types:

- Methods based on Minimal Polynomial Start Sequence Markov parameter (MPSSM) models. Methods that fit into this class are:
  - . two step method for the estimation of minimal polynomial coefficients and start sequence Markov parameters developed by Gerth (cf. eq. (4.29) - (4.30))
  - . modified Gerth method (cf. eq. (4.32) - (4.35))
- Methods based on state space models. The methods that fit into this class are:
  - . balanced approximate realization of the finite block Hankel matrix (cf. eq. (4.36) - (4.42))
  - . approximate realization of the Page matrix (cf. eq. (4.53) - (4.60)
  - . optimal Hankel norm approximation (cf. eq. (4.70) - (4.94))

The method of Gerth and the modified Gerth method give as a result MPSSM models of degree r that are close to the MPSSM model of the same degree r with impulse responses that are closest (measured in Frobenius norm) to the estimated finite impulse responses (cf. chapter 5, section 5.2.2). The approximate realizations of order r determined from the finite block Hankel (Page) matrix are close to the state space systems of order r which have a block Hankel (Page) matrix that is closest to the original Hankel (Page) matrix measured in Frobenius norm (cf. section 4.5.1, 4.5.2). The optimal Hankel norm approximation of order r results in a state space model of order r with the property that the error system, defined by the difference of the original high order system and the order r approximate realization, has a largest Hankel singular value equal to the (r+1)-st Hankel singular value of the original system (cf. section 4.5.3).

To be able to compare the results obtained with the various methods two quality criteria have been applied to the error systems defined by the difference between the approximate realizations and the estimated FIR models and to the error systems defined by the difference between the approximate realizations and the true simulated processes:

- the Hankel norms of the error systems (cf. eq. (3.50) - (3.59))
- the Frobenius norms of the error systems (cf. eq. (3.60))

The results obtained from the tests are summarized by the following conclusions:

- As expected the optimal Hankel norm approximation method gives the best results measured in Hankel norm of the error system defined by the differences between the input, estimated FIR model and the obtained approximate realization
- With respect to the error system defined by the differences between approximate realization and the true simulated process the method of Gerth and the approximate realization from the finite block Hankel matrix are the best methods measured in Hankel norm
- Measured in Frobenius norm the method of Gerth and the approximate realization method based on the finite block Hankel matrix perform best

- In general, the Gerth method performs slightly better than the method based on the computation of an approximate realization from the finite block Hankel matrix, because the MPSSM model of degree r has some more degrees of freedom for shaping the systems responses than a minimal state space realization of the same order r (cf. (4.12) - (4.20))
- The modified Gerth method and the method based on the computation of an approximate realization from the Page matrix sometimes perform very badly.
- Overall looking at the quality of the models obtained, measured in both Hankel norm and in Frobenius norm of the error systems, of all models obtained with the various methods, the models resulting from the computation of a balanced state space realization from a finite block Hankel matrix (method of Zeiger and McEwen) generally are the best.

Regarding the computation time required and the quality of the models with respect to the overall fit to the original FIR model and to the true system both the method of Gerth (cf. eq. (4.30) and (4.31)) and the method of Zeiger and McEwen (cf. eq. (4.36) - (4.42)) are good methods. These methods are preferred above the other methods tested.
Further research is required to find out why the modified Gerth method and the method based on the realization from Page matrix sometimes perform bad.

5. DIRECT ESTIMATION OF THE MPSSM MODEL PARAMETERS FROM INPUT/OUTPUT DATA

5.1 Introduction

In the previous chapters first methods have been developed for the estimation of Markov parameters from a given set of process input/output data. Next the estimated Markov parameter model has been used for the determination of a best fitting MPSSM model.
The motivation for first estimating a Markov parameter model has been found in the size of the set (cf. section 2.3) of the Markov parameter models, the little a-priori knowledge required for the estimation of a Markov parameter model and the simplicity of the algorithms needed for the determination of a Markov parameter model with a Least Squares or Maximum Likelihood estimation method using an output error criterion. Due to the size of the model set, the quality of the model obtained is almost always very good. The model itself, however, is in general not very useful in practice because of this very size.
The second step results in a model, the MPSSM model, that has a much smaller number of parameters. To find the best fitting MPSSM model, the knowledge of the dynamic behaviour of the process, obtained from the estimated Markov parameter model in the first step, is exhaustively used for the selection of the model set (i.e. selection of the order of the minimal polynomial, selected inputs and outputs). The MPSSM model resulting from this second step is, however, purely based on the earlier estimated FIR model. The available process information, the process input/output data, is not used for the determination of this initial MPSSM model.
In this chapter a method, called the direct estimation method, will be developed for the adjustment of the initial MPSSM model to get a better fit of the model to the available process input/output data in Least Squares sense on the basis of an output error criterion. The method will appear to be rather demanding with respect to the computational effort required. This is caused by the fact that the function to be minimized is highly non-linear in the minimal polynomial coefficients. To solve the minimization problem numerical minimization techniques have to be applied. Application of such numerical techniques implies the need for good initial values for the parameters if one wants to find the right minimum of the function in an acceptable period of computation time. In addition to the fact that the available information on the process behaviour is used in the previous steps to choose a good fitting model set and that the models obtained in the first two steps may be useful too, this is a motivation for the work done in the previous chapters: it provides us with a good initial MPSSM model.

In this chapter section 2 is devoted to the analysis of some important properties of and interrelations between the three identification steps proposed. In section 3 the basic formulas, required for the direct estimation of the MPSSM model parameters, are derived. Section 4 describes two algorithms for the direct estimation of the model parameters. In section 5 the direct estimation method, developed in this chapter, is used for the estimation of MPSSM model parameters for the simulated processes described in section 3.6. For these estimations the same input/output data are used as

for the earlier estimations of the FIR models described in chapter 3. The results obtained with the approximate realization algorithm of Zeiger and McEwen, described in chapter 4, are used as initial values for the MPSSM model parameters after transformation of the state space models to MPSSM models. Finally, in section 6, a summary is given of the main conclusions related to the direct estimation method.

5.2 Some important properties of the identification steps proposed

The MPSSM model is defined by a unique set of start sequence Markov parameters and a polynomial of order r (eq. (2.2)):

$$y_k = \sum_{i=0}^{\infty} F_i(\hat{a}_j, \hat{M}_j \mid j \epsilon I) \cdot u_{k-i} \quad I=1,2, \ \ldots \ ,r$$

with: $F_0 = \hat{M}_0 = \hat{D}$ the direct transfer from inputs to outputs (5.1)

$$F_i = \hat{M}_i \qquad i \epsilon I,\ I=1,2, \ \ldots \ ,r \tag{5.2}$$

$$F_{r+i} = \sum_{j=1}^{r} -a_j \cdot F_{r+i-j} \qquad i \epsilon I,\ I=1,2, \ \ldots \tag{5.3}$$

Remark: In the sequel $F(\hat{a}_j, \hat{M}_j \mid j \epsilon I)$ $I=1,2, \ \ldots \ ,r$ will be denoted by $F(\hat{\underline{a}}, \hat{\underline{M}})$ for notational convenience.

For the estimation of the parameters of the MPSSM model it is assumed that the process can be described by the following input/output relation (cf. eq. (3.1)):

$$Y = M_{kp} \cdot \Omega + N \tag{5.4}$$

with:
- Y - the output signal matrix — dim[Y]: $q \times (l+1)$
- Ω - the input signal matrix — dim[Ω]: $p \cdot (\kappa+1) \times (l+1)$
- M_{kp} - the process Markov parameter matrix — dim[M]: $q \times p \cdot (\kappa+1)$
- N - the additive output noise signal matrix — dim[N]: $q \times (l+1)$
- κ - length of the impulse responses of the process expressed in number of samples, in general $\kappa \to \infty$

$$Y = [y_k,\ y_{k+1},\ y_{k+2},\ \ldots \ ,y_{k+l}]$$

$$M_{Kp} = [M_0,\ M_1,\ M_2,\ \ldots\ ,M_K]$$

$$\Omega = \begin{bmatrix} u_k & u_{k+1} & u_{k+2} & \cdots & u_{k+l} \\ u_{k-1} & u_k & u_{k+1} & \cdots & u_{k+l-1} \\ \cdot & \cdot & \cdot & \cdots & \cdot \\ \cdot & \cdot & \cdot & \cdots & \cdot \\ u_{k-K} & u_{k-K+1} & u_{k-K+2} & \cdots & u_{k-K+l} \end{bmatrix}$$

$$N = [n_k \quad n_{k+1} \quad n_{k+2} \quad \cdots \quad n_{k+l}]$$

A rough analysis of the various steps performed in the identification shows that the MPSSM model obtained from the two step method (FIR model estimation and Gerth method applied to the FIR model) is expected to be the same as the MPSSM model obtained with the direct estimation method as long as tail effects can be neglected and under the assumption that the impulse responses generated by the MPSSM model obtained with the Gerth algorithm are as close as possible to the estimated FIR's measured in Frobenius norm.
If no noise model is included, the FIR model parameters are found by minimizing the following criterion (cf. eq. (3.10)):

$$\min_{\tilde{M}} \arg V_\alpha = \min_{\tilde{M}} \arg \| Y - \tilde{M}\cdot\Omega \|_F \rightarrow \tilde{M} = Y\cdot\Omega^t\cdot(\Omega\cdot\Omega^t)^{-1} \qquad (5.5)$$

If eq. (4.30) and (4.31) are iteratively solved with matrix G (cf. eq. (4.30)), starting from the second iteration, filled with Markov parameters generated by the MPSSM model of the preceeding iteration and if the iterative process converges, the MPSSM model parameters obtained with the Gerth method iteratively applied are expected to satisfy:

$$\min_{\hat{\underline{a}},\hat{\underline{M}}} \arg V_\beta = \min_{\hat{\underline{a}},\hat{\underline{M}}} \arg \| \tilde{M} - F(\hat{\underline{a}},\hat{\underline{M}}) \|_F \qquad (5.6)$$

with: $\hat{\underline{a}},\hat{\underline{M}}$ the MPSSM model parameters that minimize V_β and that are expected to be equal to the MPSSM model parameters obtained from the Gerth algorithm

Direct estimation from input/output data of the MPSSM model parameters involves the computation of:

$$\min_{\hat{\underline{a}},\hat{\underline{M}}} \arg V_\gamma = \min_{\hat{\underline{a}},\hat{\underline{M}}} \arg \| Y - F(\hat{\underline{a}},\hat{\underline{M}})\cdot\Omega \|_F \qquad (5.7)$$

with: $\hat{\underline{a}},\hat{\underline{M}}$ the MPSSM model parameters obtained from direct estimation on the basis of input/output data.

Substitution of the solution of eq. (5.5) in eq. (5.6) and working out the criterion gives:

$$\min_{\hat{\underline{a}},\hat{\underline{M}}} \arg V_\beta = \min_{\hat{\underline{a}},\hat{\underline{M}}} \arg [\mathrm{tr}\{Y\cdot\Omega^t\cdot(\Omega\cdot\Omega^t)^{-2}\cdot\Omega\cdot Y^t - 2\cdot Y\cdot\Omega^t\cdot(\Omega\cdot\Omega^t)^{-1}\cdot F(\hat{\underline{a}},\hat{\underline{M}})^t + F(\hat{\underline{a}},\hat{\underline{M}})\cdot F(\hat{\underline{a}},\hat{\underline{M}})^t\}] \quad (5.8)$$

Working out eq. (5.7) results in:

$$\min_{\hat{\underline{a}},\hat{\underline{M}}} \arg V_\gamma = \min_{\hat{\underline{a}},\hat{\underline{M}}} \arg [\mathrm{tr}\{Y\cdot Y^t - 2\cdot Y\cdot\Omega^t\cdot F(\hat{\underline{a}},\hat{\underline{M}})^t + F(\hat{\underline{a}},\hat{\underline{M}})\cdot\Omega\cdot\Omega^t\cdot F(\hat{\underline{a}},\hat{\underline{M}})^t\}] \quad (5.9)$$

As the first terms of eq. (5.8) and (5.9) are no functions of the parameters they do not influence the minimization. If the input signal matrix Ω satisfies the following condition:

$$\Omega\cdot\Omega^t = I \quad (5.10)$$

both MPSSM models will be the same. Zero mean, white noise sequences are input signals that satisfy eq. (5.10) asymptotically. If, however, the input signal matrix does not satisfy eq. (5.10), use of a weighting matrix $\Omega\cdot\Omega^t$ in the computation of the MPSSM model on the basis of the estimated FIR model parameters (cf. eq. (5.6)) results in (cf. eq. (5.8) and (5.9)):

$$\min_{\hat{\underline{a}},\hat{\underline{M}}} \arg V_\beta = \min_{\hat{\underline{a}},\hat{\underline{M}}} \arg [\mathrm{tr}\{Y\cdot\Omega^t\cdot(\Omega\cdot\Omega^t)^{-1}\cdot\Omega\cdot Y^t - 2\cdot Y\cdot\Omega^t\cdot F(\hat{\underline{a}},\hat{\underline{M}})^t + F(\hat{\underline{a}},\hat{\underline{M}})\cdot\Omega\cdot\Omega^t\cdot F(\hat{\underline{a}},\hat{\underline{M}})^t\}] \quad (5.11)$$

As can be seen from eq. (5.11), the terms depending on the MPSSM model parameters have become the same as the terms in the criterion function belonging to the direct estimation from input/output data (cf. eq. (5.9)). The MPSSM model parameters are therefore expected to be the same for both approaches.

Before rewriting the estimation problem into a form that can be used for the computation of the model parameters, it is advisable to analyse the convergence properties of the impulse responses generated by the model to the true systems impulse responses as far as they exist (cf. [Ljung, 1987]).

A motivation for this analysis is found in the observation that application of the model for model reference type control purposes requires that the model can be used for prediction of the deterministic process behaviour over an interval at least equal to the delay time of the process. This implies that the simulation properties of the model have to be signal independent. As a consequence the impulse responses generated by the model have to be as close as possible to the true systems impulse responses measured in some to be specified norm.

5.2.1 Convergence of the MPSSM models

To be able to do the convergence analysis first some assumptions have to be made on the characteristics of the signals. The input signals of the process are assumed to be stationary, white, inter channel independent, zero mean, Gaussian noise with covariance matrix Σ_u:

$$E\{u \cdot u^t\} = \Sigma_u = \sigma^2 \cdot I_p \qquad \dim[\Sigma_u]: p \times p \tag{5.12}$$

$$E\{u\} = 0 \tag{5.13}$$

$$E\{u_i \cdot u_j^t\} = 0 \cdot I_p \qquad i,j \in I,\ i \neq j,\ I=0,1,2,\ \ldots \tag{5.14}$$

The additive output noise is assumed not to be correlated with the input signal applied to the process:

$$E\{u_i \cdot n_j^t\} = 0 \cdot I_{p,q} \qquad \text{for all } i,j \in I,\ I=0,1,2,\ \ldots \tag{5.15}$$

Furthermore the additive output noise is assumed to be zero mean:

$$E\{n\} = 0 \tag{5.16}$$

Starting point for the analysis is the criterion function used for the estimation of the model parameters:

$$V = tr\{\frac{1}{I+1} \cdot (Y - \hat{Y}) \cdot (Y^t - \hat{Y}^t)\} \tag{5.17}$$

with: $\hat{Y} = [\hat{y}_k, \hat{y}_{k+1}, \ldots, \hat{y}_{k+l}]$ outputs simulated by the model

$Y = [y_k, y_{k+1}, \ldots, y_{k+l}]$ measured process outputs

Substitution of the true system characteristics (eq. (5.4)) and the model

(eq. (2.2)) in eq. (5.17) gives the following expression:

$$V = \mathrm{tr}\{\frac{1}{l+1}\cdot(M_{mp}\cdot\Omega_m + M_{tail}\cdot\Omega_{tail} + N - F(\hat{\underline{a}},\hat{\underline{M}})\cdot\Omega_m)$$

$$(M_{mp}\cdot\Omega_m + M_{tail}\cdot\Omega_{tail} + N - F(\hat{\underline{a}},\hat{\underline{M}})\cdot\Omega_m)^t\}$$

$$= \mathrm{tr}\{\frac{1}{l+1}\cdot((M_{mp} - F(\hat{\underline{a}},\hat{\underline{M}}))\cdot\Omega_m\cdot\Omega_m^t(M_{mp}^t - F(\hat{\underline{a}},\hat{\underline{M}})^t) +$$

$$2\cdot M_{tail}\cdot\Omega_{tail}\cdot\Omega_m^t\cdot(M_{mp}^t - F(\hat{\underline{a}},\hat{\underline{M}})^t) + M_{tail}\cdot\Omega_{tail}\cdot\Omega_{tail}^t\cdot M_{tail}^t +$$

$$2\cdot N\cdot\Omega_m^t\cdot(M_{mp}^t - F(\hat{\underline{a}},\hat{\underline{M}})^t) + N\cdot N^t + 2\cdot N\cdot\Omega_{tail}\cdot M_{tail})\} \qquad (5.18)$$

with: $M_{mp} = [M_0, M_1, M_2, \ldots, M_m]$ main parameters of the true system

$$F(\hat{\underline{a}},\hat{\underline{M}}) = [\hat{M}_0, \hat{M}_1, \hat{M}_2, \ldots, \hat{M}_r, \hat{F}_{r+1}(\hat{a}_j,\hat{M}_j \mid j\epsilon I), \ldots,$$

$$\hat{F}_m(\hat{a}_j,\hat{M}_j \mid j\epsilon I)] \qquad I=1,2,\ldots,r$$

Markov parameters obtained from the MPSSM model

$M_{tail} = [M_{m+1}, M_{m+2}, \ldots, M_K]$ tail parameters of the true system

$$\Omega_m = \begin{bmatrix} u_k & u_{k+1} & u_{k+2} & \cdots & u_{k+l} \\ u_{k-1} & u_k & u_{k+1} & \cdots & u_{k+l-1} \\ \cdot & \cdot & \cdot & & \cdot \\ \cdot & \cdot & \cdot & & \cdot \\ u_{k-m} & u_{k+1-m} & u_{k+2-m} & \cdots & u_{k+l-m} \end{bmatrix}$$

$$\Omega_{tail} = \begin{bmatrix} u_{k-m-1} & u_{k-m} & u_{k+1-m} & \cdots & u_{k+l-m-1} \\ u_{k-m-2} & u_{k-m-1} & u_{k-m} & \cdots & u_{k+l-m-2} \\ \cdot & \cdot & \cdot & & \cdot \\ \cdot & \cdot & \cdot & & \cdot \\ \cdot & \cdot & \cdot & & \cdot \\ u_{k-K} & u_{k+1-K} & u_{k+2-K} & \cdots & u_{k+l-K} \end{bmatrix}$$

$N = [n_k, n_{k+1}, \ldots, n_{k+l}]$

In this expression the products of the various signal matrices can be written as:

$$\Omega_m \cdot \Omega_m^t = (l+1) \cdot (\sigma^2 \cdot I_{(m+1)\cdot p} + E_1) \tag{5.19}$$

$$\Omega_{tail} \cdot \Omega_m^t = (l+1) \cdot E_2 \tag{5.20}$$

$$N \cdot \Omega_m^t = (l+1) \cdot E_3 \tag{5.21}$$

$$\Omega_{tail} \cdot \Omega_{tail}^t = (l+1) \cdot (\sigma^2 \cdot I_{(K-m-1)\cdot p} + E_4) \tag{5.22}$$

$$N \cdot N^t = (l+1) \cdot \Psi_n \tag{5.23}$$

$$N \cdot \Omega_{tail}^t = (l+1) \cdot E_5 \tag{5.24}$$

Because of the characteristics of the input signals and the noise signals (cf. eq. (5.12) - (5.16)) the probability limits of the matrices E_1, E_2, E_3, E_4 and E_5 are equal to zero:

$$\operatorname*{plim}_{l\to\infty} [E_1] = 0 \cdot I_{(m+1)\cdot p} \tag{5.25}$$

$$\operatorname*{plim}_{l\to\infty} [E_2] = 0 \cdot I_{(K-m-1)\cdot p,(m+1)\cdot p} \tag{5.26}$$

$$\operatorname*{plim}_{l\to\infty} [E_3] = 0 \cdot I_{q,(m+1)\cdot p} \tag{5.27}$$

$$\operatorname*{plim}_{l\to\infty} [E_4] = 0 \cdot I_{(K-m-1)\cdot p} \tag{5.28}$$

$$\operatorname*{plim}_{l\to\infty} [E_5] = 0 \cdot I_{q,(K-m-1)\cdot p} \tag{5.29}$$

In case the input signal does not satisfy eq. (5.12) - (5.14) matrices E_1, E_2 and E_4 will not have a probability limit equal to zero. If eq. (5.15) does not hold the probability limit of matrices E_3 and E_5 will not be equal to zero.

Substitution of eq. (5.19) - (5.24) in eq. (5.18) gives:

$$V = tr\{\sigma^2 \cdot (M_{mp} - F(\hat{\underline{a}},\hat{\underline{M}})) \cdot I_{(m+1)\cdot p} \cdot (M_{mp}^t - F(\hat{\underline{a}},\hat{\underline{M}})^t) +$$

$$(M_{mp} - F(\hat{\underline{a}},\hat{\underline{M}})) \cdot E_1 \cdot (M_{mp}^t - F(\hat{\underline{a}},\hat{\underline{M}})^t) +$$

$$2 \cdot M_{tail} \cdot E_2 \cdot (M_{mp}^t - F(\hat{\underline{a}},\hat{\underline{M}})^t) + \sigma^2 \cdot M_{tail} \cdot I_{(\kappa-m-1)\cdot p} \cdot M_{tail}^t +$$

$$M_{tail} \cdot E_4 \cdot M_{tail}^t + 2 \cdot E_3 \cdot (M_{mp}^t - F(\hat{\underline{a}},\hat{\underline{M}})^t) + \Psi_n +$$

$$2 \cdot E_5 \cdot M_{tail}\} \qquad (5.30)$$

According to eq. (5.25) - (5.29) the terms containing one of the matrices E_1, E_2, E_3, E_4 or E_5 will have a probability limit equal to a zero matrix. Using the definition of the probability limit (cf. [Goldberger, 1964]), this implies that for arbitrarily small (ε,δ) there exists a value l_0 for the number of samples considered such that for all $l>l_0$:

$$P(||E_i|| > \varepsilon) < \delta \qquad i=1,2, \ldots ,5 \qquad (5.31)$$

The limit process only regards the number of samples used for the construction of the criterion function V. As a result it can be expected that the contribution of these terms becomes negligibly small if the number of samples used is taken high. The number of samples that has to be used will depend on the specific characteristics of the input- and noise signals. In general, if an inner product of a zero mean, white noise sequence with some coloured noise sequence is computed, many periods of the lowest frequency components of the coloured noise sequence have to be part of the signal or the low frequency components have to have low amplitudes to assure that the result is almost equal to zero (cf. chapter 6 section 6.2). The parameter matrices do not influence the limit process.
Fig. 5.1a shows a typical course of the inner product divided by the length of the sequences of two finite sequences of samples obtained from a generator that generates white, zero mean, Gaussian noise with variance equal to one as a function of the number of samples used. Fig. 5.1b is a typical result of the inner product divided by the number of samples of a sequence of white, zero mean, Gaussian noise samples and a sequence of white noise samples filtered by a first order low pass filter with a time constant equal to λ=0.8 as a function of the number of samples used.
Using Slutsky's theorem (cf. [Goldberger, 1964]) the probability limit of

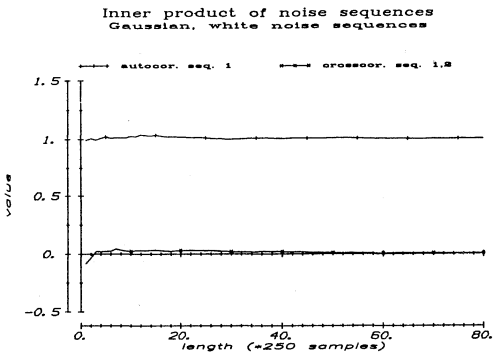

Fig. 5.1a Overview of the inner product of two finite length, zero mean, white, Gaussian noise sequences divided by the number of samples as function of the number of samples.

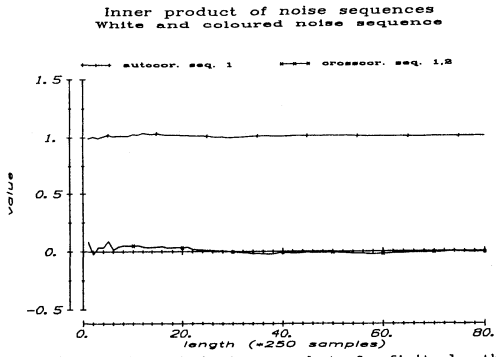

Fig. 5.1b Overview of the inner product of a finite length, zero mean, white, Gaussian noise sequence and a low pass filtered (1-st order, λ=0.8) finite length, zero mean, white, Gaussian noise sequence divided by the number of samples as function of the number of samples.

the criterion function V becomes:

$$\operatorname*{plim}_{l\to\infty} [V] = \mathrm{tr}\{\sigma^2 \cdot (M_{mp} - F(\hat{\underline{a}},\hat{\underline{M}})) \cdot (M_{mp}^t - F(\hat{\underline{a}},\hat{\underline{M}})^t) + \sigma^2 \cdot M_{tail} \cdot M_{tail}^t + \Psi_n\} \qquad (5.32)$$

In eq. (5.32) the terms $\sigma^2 \cdot M_{tail} \cdot M_{tail}^t$ and Ψ_n are no functions of the MPSSM model parameters $(\hat{a}_j, \hat{M}_j \mid j=1,2, \ldots ,r)$. Consequently, if a criterion function V, built of enough samples (cf. eq. (5.31)) with properties given by eq. (5.12) - (5.16), is minimized as a function of the MPSSM model parameters $(\hat{a}_j, \hat{M}_j \mid j=1,2, \ldots ,r)$, the parameter values obtained are expected to belong to a minimum of the function V_1:

$$V_1 = \mathrm{tr}\{(M_{mp} - F(\hat{\underline{a}},\hat{\underline{M}})) \cdot (M_{mp}^t - F(\hat{\underline{a}},\hat{\underline{M}})^t)\} \qquad (5.33)$$

This implies that the Markov parameters of the model, computed from the MPSSM model parameters that minimize V, will be as close as possible to the true system Markov parameters.

In eq. (5.33) the Markov parameters given by function $F(\hat{\underline{a}},\hat{\underline{M}})$ are polynomial functions of the polynomial coefficients a_j $(j=1,2, \ldots ,r)$ (cf. eq. (5.2), (5.3)). Using eq. (5.3), criterion function V_1 clearly is seen to be a polynomial function of the polynomial coefficients of degree $(m-r)^2$.

Consequently V_1 and also V will not have one, unique minimum, but at least $\mathrm{Int}(((m-r)^2 - 1)/2)$ minima.
If numerical techniques are used for minimization of the criterion function V, the minimum found will not necessarily be the global minimum of V. In general, the algorithm will converge to a local minimum of V. Tests with initial MPSSM model parameters equal to zero have confirmed this conjecture. The minimum found will highly depend on the initial values used for the model parameters. Therefore the minimization process has to be started with initial model parameter values that are obtained from earlier applied estimation algorithms which result in Markov parameters that are close to the true system parameters. Eq. (5.5) - (5.11) indicate that MPSSM model parameters obtained from the Gerth algorithm can be used as initial values for the model parameters.

5.2.2 Properties of the FIR model and the initial MPSSM model

To get an impression of the qualities of the initial model parameter values obtained with the preferred algorithms described in chapters 3 and 4, the convergence properties of these algorithms also have to be analysed.
Again the input/output behaviour of the process is assumed to be given by eq. (5.4). The input signals and the noise on the process outputs are assumed to satisfy the properties given by eq. (5.12) - (5.16).

The input/output behaviour of the FIR model is assumed to be given by eq. (3.3):

$$\tilde{Y} = \tilde{M}_{mp} \cdot \Omega_m$$

According to the results derived in appendix D (cf. eq. (D.14)) the model parameters are expected to converge to the true system parameters, if the process dynamics fit into the set of FIR models used for the identification. In case also AR noise parameters are estimated simultaneously, the estimated Markov parameters of the FIR model will converge to the true system parameters, if the output error matrix $\tilde{H}_n$ is computed with Markov parameters that are close to the true system Markov parameters (cf. appendix D eq. (D.21)).
However, if the process behaviour can not exactly be described by a FIR model of the model set used, the model obtained still is a model that simulates output signals that are closest to the measured process outputs in Frobenius norm due to the fact that the square of the output errors is minimized (eq. (3.9)):

$$V = \mathrm{tr}\{E \cdot E^t\} = \mathrm{tr}\{(Y - \tilde{Y}) \cdot (Y^t - \tilde{Y}^t)\} =$$

$$\mathrm{tr}\{(Y - \tilde{M}_{mp} \cdot \Omega_m) \cdot (Y^t - \Omega_m^t \cdot \tilde{M}_{mp}^t)\}$$

Consequently, the FIR model obtained will be a model that simulates outputs that are closest to the measured process outputs in Frobenius norm for the specific input signal applied.

If the applied input signal is a Gaussian, white noise sequence that satisfies eq. (5.12) - (5.14) and if the output noise satisfies eq. (5.15) and (5.16), the derivation done for the analysis of the asymptotic properties of the MPSSM model (cf. eq. (5.17) - (5.33)) can also be made for the FIR model. As a result the following expression is obtained for the criterion used for the estimation of the FIR model parameters in case no AR noise parameters are estimated:

$$\min_{\tilde{M}_{mp}} \arg V = \min_{\tilde{M}_{mp}} \arg \mathrm{tr}\{ (Y - \hat{Y})\cdot(Y^t - \hat{Y}^t) \} =$$

$$\min_{\tilde{M}_{mp}} \arg \mathrm{tr}\{ (M_{mp} - \tilde{M}_{mp})\cdot(M_{mp}^t - \tilde{M}_{mp}^t) \} \qquad (5.34)$$

As can be seen the estimated FIR model parameters are indeed expected to converge to the true system Markov parameters. If also an AR noise model is estimated and if both the process and the true colouring filter of the noise are in the model sets, the estimator is equal to the maximum likelihood estimator. In this case the parameters are also expected to the true parameters.

The FIR model obtained from this first step is used as a basis for the computation of a MPSSM model. Two of the methods tested in chapter 4 have been selected as preferred methods for this approximate model computation (cf. section 4.7).
The first of the methods preferred is the method developed by Gerth. In this two step method first minimal polynomial coefficients are fitted in least squares sense to the available Markov parameters of the FIR model (cf. eq. 4.30):

$$\hat{\underline{\tilde{a}}} = \arg \min_{\underline{\tilde{a}}} ||v - G\cdot\underline{\tilde{a}}||_F \qquad (5.35)$$

with: $v^t = [\mathrm{vec}(\tilde{M}_{r+1})^t \;\; \mathrm{vec}(\tilde{M}_{r+2})^t \;\; \ldots \;\; \mathrm{vec}(\tilde{M}_m)^t]^t$

$$G = \begin{bmatrix} \text{vec}(\tilde{M}_1) & \text{vec}(\tilde{M}_2) & \dots & \text{vec}(\tilde{M}_r) \\ \text{vec}(\tilde{M}_2) & \text{vec}(\tilde{M}_3) & \dots & \text{vec}(\tilde{M}_{r+1}) \\ \vdots & \vdots & & \vdots \\ \text{vec}(\tilde{M}_{m-r}) & \text{vec}(\tilde{M}_{m-r+1}) & \dots & \text{vec}(\tilde{M}_{m-1}) \end{bmatrix}$$

In the second step of Gerth's method start sequence Markov parameters are computed that generate, with the minimal polynomial coefficients obtained from the first step, impulse responses that are closest to the FIR in least squares sense (cf. eq. (4.31)):

$$\hat{\tilde{M}}_v = \arg\min_{\hat{\tilde{M}}_v} ||\tilde{M} - H \cdot \hat{\tilde{M}}_v||_F \qquad (5.36)$$

with: $\tilde{M}^t = [\text{vec}(\tilde{M}_1)\ \text{vec}(\tilde{M}_2)\ \dots\ \text{vec}(\tilde{M}_m)]^t$ Estimated FIR parameters

$\hat{\tilde{M}}_v^t = [\text{vec}(\hat{\tilde{M}}_1)\ \text{vec}(\hat{\tilde{M}}_2)\ \dots\ \text{vec}(\hat{\tilde{M}}_r)]^t$ Start Sequence Markov parameters

$H^t = [I_r, \hat{\tilde{A}} \cdot E_r, \hat{\tilde{A}}^2 \cdot E_r, \dots, \hat{\tilde{A}}^{m-r} \cdot E_r]$

$$\hat{\tilde{A}} = \begin{bmatrix} 0 & \dots & 0 & -\hat{\tilde{a}}_r \\ & & & -\hat{\tilde{a}}_{r-1} \\ & I_{r-1} & & \vdots \\ & & & -\hat{\tilde{a}}_1 \end{bmatrix}$$

$$E_r = \begin{bmatrix} 0 \\ 0 \\ \vdots \\ 1 \end{bmatrix}$$

Because the two steps are executed seperately, the MPSSM model obtained with this method, in general, will not be the model of the selected MPSSM model set that is closest to the original FIR model in least squares sense. However, if the order selected corresponds with the order obtained from the order test (cf. section 4.3.2) and if the noise on the estimated FIR

parameters is small compared to the amplitudes of the parameters, the results obtained with this algorithm, in general, come close to the true least squares approximation of the FIR model.

At this moment it is good to analyse the meaning of a least squares approximation of the impulse responses of an approximating model to given initial impulse responses. Minimization of the square of the difference between the two impulse responses implies:

$$\arg \min_{\hat{\underline{a}},\hat{\underline{M}}} || \tilde{M}_{mp} - F(\hat{\underline{a}},\hat{\underline{M}}) ||_F =$$

$$\arg \min_{\hat{\underline{a}},\hat{\underline{M}}} \mathrm{tr}\{ (\tilde{M}_{mp} - F(\hat{\underline{a}},\hat{\underline{M}}))\cdot(\tilde{M}_{mp} - F(\hat{\underline{a}},\hat{\underline{M}}))^t\} =$$

$$\arg \min_{\hat{\underline{a}},\hat{\underline{M}}} \mathrm{tr}\{ (\tilde{M}_{mp} - F(\hat{\underline{a}},\hat{\underline{M}}))\cdot\Omega_m\cdot\Omega_m^t(\tilde{M}_{mp} - F(\hat{\underline{a}},\hat{\underline{M}}))^t\}$$

$$\arg \min_{\hat{\underline{a}},\hat{\underline{M}}} \mathrm{tr}\{ (\tilde{Y} - F(\hat{\underline{a}},\hat{\underline{M}})\cdot\Omega_m)\cdot(\tilde{Y} - \Omega_m^t\cdot F(\hat{\underline{a}},\hat{\underline{M}}))^t\} \qquad (5.37)$$

with: Ω_m - any orthogonal matrix satisfying $\Omega_m\cdot\Omega_m^t = I$

A set of input signals that satisfies this condition, at least asymptotically, is a Gaussian, zero mean, inter-channel independent, white noise sequence with variance equal to one. Another set of input signals that satisfies this condition is a set of impulses not simultaneously put on the different inputs of the system.
Eq. (5.37) implies that the least squares approximation of the original impulse responses results in a least squares approximation of the process output signals in case a special type of input signal is used (e.g. a Gaussian, zero mean, inter channel independent, white noise sequence).

At this moment the results so far obtained can be summarized by:

i) Direct Estimation of MPSSM model parameters from input/output data (cf. eq. (5.33)):

$$\arg \min_{\hat{\underline{a}},\hat{\underline{M}}} V = \arg \min_{\hat{\underline{a}},\hat{\underline{M}}} || Y - F(\hat{\underline{a}},\hat{\underline{M}})\cdot\Omega_m ||_F$$

$$\simeq \arg \min_{\hat{\underline{a}},\hat{\underline{M}}} || M_{mp} - F(\hat{\underline{a}},\hat{\underline{M}}) ||_F$$

conditions: u - stationary, inter channel independent, zero mean, white noise
n - not correlated with u
- sufficient number of input/output samples used (cf. eq. (5.30), (5.32)

remark: Due to the high degree of the minimal polynomial coefficients in the criterion function the function will have more than one minimum. Therefore good initial values for the MPSSM model parameters are required.

ii) FIR model parameter estimation from input/output data (cf. eq. (5.34)):

$$\arg \min_{\tilde{M}_{mp}} V = \arg \min_{\tilde{M}_{mp}} || Y - \tilde{M}_{mp} \cdot \Omega_m ||_F$$

$$\simeq \arg \min_{\tilde{M}_{mp}} || M_{mp} - \tilde{M}_{mp} ||_F$$

conditions: u - stationary, inter channel independent, zero mean, white noise
n - not correlated with u
- sufficient number of input/output samples used to allow substitution of products of signal matrices by their probability limits

iii) Least squares approximation of the FIR model with a MPSSM model (cf. eq. (5.37)):

$$\arg \min_{\hat{\tilde{\underline{a}}},\hat{\tilde{\underline{M}}}} V = \arg \min_{\hat{\tilde{\underline{a}}},\hat{\tilde{\underline{M}}}} || \tilde{M}_{mp} - F(\hat{\tilde{\underline{a}}},\hat{\tilde{\underline{M}}}) ||_F$$

$$\simeq \arg \min_{\hat{\tilde{\underline{a}}},\hat{\tilde{\underline{M}}}} || \tilde{Y} - F(\hat{\tilde{\underline{a}}},\hat{\tilde{\underline{M}}}) \cdot \Omega_m ||_F$$

with: $\tilde{Y}$ - the outputs simulated with the FIR model

condition: $\Omega_m \cdot \Omega_m^t = I$

The second of the preferred methods for the computation of a MPSSM model on the basis of an available FIR model is the computation of a balanced state space realization from the largest possible block Hankel matrix that can be constructed from the available FIR Markov parameters. For the computation of the observability and controllability matrices of a low order (n) state space realization this block Hankel matrix of order $\min(m \cdot p, m \cdot q)$ is approximated with an order n matrix ($\tilde{H}$) that is as close as possible to the block Hankel matrix in Frobenius norm. For the computation of this approximation the singular value decomposition of $H_{m,m}$ is used:

$$H_{m,m} = U \cdot S \cdot V^t \quad \Rightarrow \quad \tilde{H} = U_1 \cdot S_1 \cdot V_1^t \tag{5.38}$$

with: $\dim[U]$: $m \cdot q \times \min(m \cdot p, m \cdot q)$

$\dim[S]$: $\min(m \cdot p, m \cdot q) \times \min(m \cdot p, m \cdot q)$

$\dim[V]$: $m \cdot p \times \min(m \cdot p, m \cdot q)$

U_1 - the first n columns of U $\quad \dim[U_1]$: $m \cdot q \times n$

S_1 - the upper left block of S $\quad \dim[S_1]$: $n \times n$

V_1 - the first n columns of V $\quad \dim[V_1]$: $m \cdot p \times n$

The problem encountered here is that this approximating matrix does not have the required block Hankel structure any more. As a consequence the obtained state space realization with the algorithm of Zeiger and McEwen (cf. eq. (4.36) - (4.42)) will only result in a block Hankel matrix with the required block Hankel structure that approximates the earlier computed optimal Frobenius norm approximant $\tilde{H}$ of the original block Hankel matrix. The results obtained in chapter 4 show, however, that the obtained model with this method comes close to the original FIR model measured in Frobenius norm.

At this moment it is good to recall the meaning of the Frobenius norm of the difference between the Hankel matrices generated by the original system and the one generated by the approximate realization. The Frobenius norm is defined as the square root of the sum of the squares of all elements of the difference matrix of both Hankel matrices. This is equal to the square root of the sum of squares of the Hankel singular values (cf. eq. (3.60)):

$$|| H_\infty - \hat{H}_\infty ||_F = || \Delta H_\infty ||_F = \sqrt{\left(\sum_{i=1}^{s} \sigma_i^2 \right)} \tag{5.39}$$

with: $s = (m+1) \cdot \min(p,q) + n$ the order of the error system

σ_i - the Hankel singular values of the error system

Because the infinite Hankel matrix is the operator that maps past inputs of the system to future outputs (cf. eq. (3.50), (3.51)), the Frobenius norm of the error system divided by the number of Hankel singular values of the error system (s) is a measure for the average distance between the mapping from all possible past inputs to their corresponding future outputs by the model that describes the differences between the FIR model and the approximating order n state space model.
The Frobenius norm of the error system therefore gives information on the average qualities of the approximating model referred to the simulation on any set of input signals.

5.2.3 Influence of an over estimated degree of the minimal polynomial on the estimation results

In case the degree r selected for the minimal polynomial is over estimated, dependencies have to occur in the system resulting from the identification. To analyse the influence of an over estimation of the order the true system is assumed to have an order r_0 minimal polynomial. If for the estimation of the system parameters an order r_1 is used for the minimal polynomial, the following equations have to hold for the expected parameter values:

$$M_i = - a_1 \cdot M_{i-1} - a_2 \cdot M_{i-2} - \ldots - a_{r_0} \cdot M_{i-r_0} \tag{5.40}$$

$$M_{i+1} = - a_1 \cdot M_i - a_2 \cdot M_{i-1} - \ldots - a_{r_0} \cdot M_{i-r_0+1} \tag{5.41}$$

The estimated model of order r_1 satisfies (assume for simplicity $r_1 = r_0 + 1$):

$$M_{i+1} = - \tilde{a}_1 \cdot M_i - \tilde{a}_2 \cdot M_{i-1} - \ldots - \tilde{a}_{r_0} \cdot M_{i-r_0+1} - \tilde{a}_{r_1} \cdot M_{i-r_1+1} \tag{5.42}$$

The polynomial coefficients of eq. (5.42) have to imply both eq. (5.40) and (5.41). As a result eq. (5.42) has to be equivalent to the equation that results from addition of eq. (5.40) and (5.41) after multiplication of eq. (5.40) with an arbitrary factor δ:

$$M_{i+1} = - (a_1 + \delta) \cdot M_i - (a_2 + \delta \cdot a_1) \cdot M_{i-1} - \ldots - \delta \cdot a_{r_0} \cdot M_{i-r_0} \tag{5.43}$$

The minimal polynomial corresponding to eq. (5.43) is given by:

$$z^{r_0+1} + (a_1+\delta) \cdot z^{r_0} + (a_2+\delta \cdot a_1) \cdot z^{r_0-1} + \ldots + \delta \cdot a_{r_0} = 0 \tag{5.44}$$

The minimal polynomial of the true system is:

$$z^{r_0} + a_1 \cdot z^{r_0-1} + a_2 \cdot z^{r_0-2} + \ldots + a_{r_0} = 0 \qquad (5.45)$$

Division of eq. (5.44) by eq. (5.45) results in an extra pole for the system at the position $z = -\delta$. This extra pole next to the true system poles is the result of the too high order used.
In general, when the order r_1 used for the minimal polynomial exceeds the order r_0 of the minimal polynomial of the true system, the polynomial obtained can always be divided by the minimal polynomial of the true system. This result immediately follows from the fact that the polynomial of order r_1 is formed by the weigthed sum of $(r_1 - r_0)$ shifted minimal polynomial of the true systems (cf. eq. (5.40), (5.41) and (5.43)). The number of extra poles introduced will be equal to difference between the order used for the minimal polynomial of the model and the order of the minimal polynomial of the true system. The location of the extra poles depends on the weighting factors used for the summation.
The extra poles introduced by this increase of the order will not contribute to the input output transfer characteristics of the system as can be seen from the expression obtained for the order r_1 minimal polynomial:

$$\begin{aligned} M_{i+1} = &- a_1 \cdot M_i - a_2 \cdot M_{i-1} - \ldots - a_{r_0} \cdot M_{i-r_0+1} - \\ &\delta_1 \cdot (M_i + a_1 \cdot M_{i-1} + a_2 \cdot M_{i-2} + \ldots + a_{r_0} \cdot M_{i-r_0}) - \ldots - \\ &\delta_{r_1-r_0} \cdot (M_{i-r_1+r_0+1} + a_1 \cdot M_{i-r_1+r_0} + \ldots + a_{r_0} \cdot M_{i-r_1+2}) \end{aligned} \qquad (5.46)$$

In this expression each of the terms multiplied with a weigthing factor δ_j is equal to zero, because each term has the minimal annihilating polynomial of the true system built in (cf. eq. (4.9)):

$$\begin{aligned} &M_j + a_1 \cdot M_{j-1} + a_2 \cdot M_{j-2} + \ldots + a_{r_0} \cdot M_{j-r_0} = \\ &H \cdot F^{j-r_0-1} \cdot (F^{r_0} + a_1 \cdot F^{r_0-1} + \ldots + a_{r_0} \cdot I) \cdot G = 0 \cdot I_{q,p} \end{aligned} \qquad (5.47)$$

As a result the extra poles introduced by increasing the order of the minimal polynomial are canceled by zeros in the input output transfers.

Summarizing we can say that over estimation of the order of the minimal polynomial will introduce dummy poles at any location in the complex plane. However, these extra poles will not contribute to the input output transfer characteristics of the model because their influence will be, due to the noise partly, compensated by transmission zeros. The extra poles are expected to disappear when a reduced order approximate realization is computed for the model.

5.2.4 Approximate realization of the MPSSM model

The MPSSM is a model that inherently has distinct, multiple eigenvalues for a MIMO system (cf. eq. (4.20)). In general, not all of these eigenvalues will give a significant contribution to the input/output characteristics of the model. Therefore it is attractive with respect to the size of the model to do one more step after the MPSSM model is obtained. This final step is the computation of an approximate realization of the estimated MPSSM model to get rid of non-relevant parts in the input/output transfers of the MPSSM model.

For the computation of an approximate realization of the MPSSM model the techniques described in chapter 4, section 4.5 can be used. The preferred methods are the approximate realization based on the Frobenius norm approximation of the Hankel matrix (cf. the realization algorithm of Zeiger and McEwen section 4.5.1) and the optimal Hankel norm approximation algorithm of Glover (cf. section 4.5.3).
In cases of systems with eigenvalues that are close to the unit circle problems may arise in applying the algorithm of Zeiger and McEwen for the computation of an approximate realization. Cause of the problem is the required size of the finite block Hankel matrix of rank $r \cdot \min(p,q)$ of which the largest singular values and corresponding singular vectors have to be computed. The discrepancy between the dimensions of this block Hankel matrix and its low rank may result in a bad convergence of the singular value decomposition algorithm. An alternative for the algorithm of Zeiger and McEwen is developed by Moore and further investigated by Pernebo and Silverman [Moore, 1981; Pernebo, 1982].
As the MPSSM model can be translated in a corresponding state space model for the computation of an approximate realization also a model reduction method can be used that is based on deleting the least controllable and least observable part of a state space model (cf. [Moore, 1981; Pernebo, 1982]). To solve this problem the stable, reachable and observable state space model has to be transformed into a balanced state space representation first, which implies that after the coordinate transformation both the controllability and the observability gramian (cf. eq. (3.55), (3.56)) of the system will be diagonal and equal (cf. [Laub, 1980]). It has been shown that each state space system can be transformed into a balanced form (cf. [Moore, 1981]).
The gramians of the system are the unique positive definite solutions of the

Lyapunov equations (cf. eq. (3.57), (3.58)):

$$P - F \cdot P \cdot F^t = G \cdot G^t$$

and

$$Q - F^t \cdot Q \cdot F = H^t \cdot H$$

The approximate realization can be obtained by partitioning the state space system in accordance with the partitioning of the gramians made in order to delete respectively the least controllable and the least observable part of the model:

$$\begin{bmatrix} P_1 & 0 \\ 0 & P_2 \end{bmatrix} - \begin{bmatrix} F_{11} & F_{12} \\ F_{21} & F_{22} \end{bmatrix} \cdot \begin{bmatrix} P_1 & 0 \\ 0 & P_2 \end{bmatrix} \cdot \begin{bmatrix} F_{11}^t & F_{21}^t \\ F_{12}^t & F_{22}^t \end{bmatrix} = \begin{bmatrix} G_1 \\ G_2 \end{bmatrix} \cdot \begin{bmatrix} G_1^t & G_2^t \end{bmatrix} \tag{5.48a}$$

and

$$\begin{bmatrix} Q_1 & 0 \\ 0 & Q_2 \end{bmatrix} - \begin{bmatrix} F_{11}^t & F_{21}^t \\ F_{12}^t & F_{22}^t \end{bmatrix} \cdot \begin{bmatrix} Q_1 & 0 \\ 0 & Q_2 \end{bmatrix} \cdot \begin{bmatrix} F_{11} & F_{12} \\ F_{21} & F_{22} \end{bmatrix} = \begin{bmatrix} H_1^t \\ H_2^t \end{bmatrix} \cdot \begin{bmatrix} H_1 & H_2 \end{bmatrix} \tag{5.48b}$$

with: $P = Q = \Sigma$ the diagonal gramians of the state space system

The approximate realization is obtained from these expressions by retaining the subsystem (F_{11}, G_1, H_1). Pernebo and Silverman have proven that the approximation obtained will always be stable, reachable and observable (cf. [Pernebo, 1982]).
The n-th order approximate realization computed with the method of Moore and Pernebo has n Hankel singular values that are equal to the first n Hankel

singular values of the infinite block Hankel matrix of the original system (cf. eq. (3.59)):

$$\lim_{k\to\infty} \sigma_j^2(H_{k,k}) = \lim_{k\to\infty} \lambda_j(H_{k,k}^t \cdot H_{k,k}) = \lambda_j(P\cdot Q) = \lambda_j(\Sigma^2) = \sigma_j^2 \qquad (5.49)$$

with: $j = 1,2, \ldots ,n$

$P = Q = \Sigma$ the diagonal gramians of the balanced state space system representation

$H_{k,k}$ the block Hankel matrix of block dimensions k,k

σ_j the j-th Hankel singular value of the system

$\lambda_j(X)$ the j-th ordered eigenvalue of symmetric non-negative matrix X

The Moore-Pernebo approximation will give simulation results that, on the average, come close to the results obtained with the original MPSSM model (cf. section 5.2.2).

If for the computation of the approximate realization the method of Zeiger and McEwen is used, it is important to use a block Hankel matrix of appropriate dimensions. The first block row and block column of the matrix have to contain as much as possible of the complete impulse responses of the system. Tail effects have to be kept negligibly small. For the computation of the singular value decomposition of the block Hankel matrix an algorithm is preferred that only computes the first $\min(p,q)\cdot r$ singular values and corresponding singular vectors (cf. [Staar, 1982]) while the system generically only has an order equal to $\min(p,q)\cdot r$ (cf. eq. (4.15)).

The optimal Hankel norm approximation of the MPSSM model, results in a model with the smallest worst case error in the simulation of outputs on the basis of past inputs. Even for worst case input signals the resulting model will give quite good simulation results compared to the results obtained with the original MPSSM model (cf. eq. (4.74)).

5.3 Derivation of basic formulas for direct estimation of MPSSM model parameters

For Least Squares estimation of the model parameters directly from available input/output data, the sum of all squared differences between measured outputs and the outputs simulated by the model, the output errors e_k, has to be minimized. The output error matrix E is defined by:

$$E = Y - \hat{Y} = Y - F(\hat{\underline{a}},\hat{\underline{M}})\cdot \Omega_m \qquad I=1,2, \ldots ,r \qquad (5.50)$$

with: $E = [e_k, e_{k+1}, \ldots ,e_{k+l}]$

The function $V(\underline{a},\underline{M})$ that has to be minimized can therefore be written as:

$$V(\underline{a},\underline{M}) = \text{tr}\ \{E\cdot E^t\} \quad I=1,2,\ \ldots\ ,r \tag{5.51}$$

Substitution of eq. (5.50) in eq. (5.51) gives:

$$\begin{aligned} V &= \text{tr}\ \{(Y - \hat{Y})\cdot(Y^t - \hat{Y}^t)\} \\ &= \text{tr}\{Y\cdot Y^t - Y\cdot\underline{\varrho}_m^t\cdot F(\hat{\underline{a}},\hat{\underline{M}})^t - F(\hat{\underline{a}},\hat{\underline{M}})\cdot\underline{\varrho}_m\cdot Y^t + \\ &\qquad F(\hat{\underline{a}},\hat{\underline{M}})\cdot\underline{\varrho}_m\cdot\underline{\varrho}_m^t\cdot F(\hat{\underline{a}},\hat{\underline{M}})^t\} \end{aligned} \tag{5.52}$$

This function V has to be minimized with respect to the minimal polynomial coefficients and the start sequence Markov parameters. Necessary conditions for a set of parameters $(\hat{a}_i,\ \hat{M}_i \mid i\cdot\epsilon I)$, I=1,2, ... ,r,) to be in a (local) minimum of V are:

$$\frac{\partial V}{\partial \hat{a}_i} = 0 \qquad \text{for all } i\epsilon I,\ I=1,2,\ \ldots\ ,r \tag{5.53}$$

$$\frac{\partial V}{\partial \hat{M}_i} = 0_{q,p} \qquad \text{for all } i\epsilon I,\ I=1,2,\ \ldots\ ,r \tag{5.54}$$

These conditions are not sufficient for the function to reach a minimum. For the conditions to become sufficient an extra condition has to be fulfilled. The matrix K consisting of all second order partial derivatives of V with respect to the parameters $\hat{a}_i$ and $\hat{M}_{\alpha\beta,i}$, the Hessian, in addition has to be positive definite in the point obtained from eq. (5.53) and (5.54):

$$K(\hat{a}_i,\hat{M}_{\alpha\beta,i}) = \left[\ \frac{\partial^2 V}{\partial z_i\,\partial z_j}\ \right] > 0 \tag{5.55}$$

with: $z_i\ \epsilon\ \{a_j,\ M_{\alpha\beta,j}\}$ $\quad j=1,2,\ \ldots\ ,r$

$\alpha=1,2,\ \ldots\ ,q$

$\beta=1,2,\ \ldots\ ,p$

$i=1,2,\ \ldots\ ,(p\cdot q+1)\cdot r$

dim[K]: $(p\cdot q+1)\cdot r \times (p\cdot q+1)\cdot r$

Using a state space description defined by eq. (2.3a,b) the output simulated

by the model at sample moment t can be written as (cf. eq. (4.4)):

$$\hat{y}_t = \sum_{i=0}^{\infty} F(\hat{\underline{a}},\hat{\underline{M}})_i \cdot u_{t-i} = \sum_{i=1}^{\infty} H \cdot F^{i-1} \cdot G \cdot u_{t-i} + D \cdot u_t \qquad (5.56)$$

with: (F,G,H,D) matrices of a state space model that has the same input/output behaviour as the MPSSM model defined by $(\hat{a}_j, \hat{M}_j \mid j \in I)$, I=1,2, ... ,r

In this expression the initial value of the state vector, x_0, is assumed to be zero. For $q \leq p$ a minimal state space model that satisfies eq. (5.56) is the canonical observability form (cf. eq. (4.18)) given by:

$$F = \mathrm{diag}(\hat{F}_1, \hat{F}_2, \ldots, \hat{F}_q) \qquad (5.57a)$$

with: $\hat{F}_1 = \hat{F}_2 = \ldots = \hat{F}_q$

$$\hat{F}_i = \begin{bmatrix} 0 & & \\ \vdots & & I_{r-1} \\ & & \\ -\hat{a}_r & -\hat{a}_{r-1} \cdots & -\hat{a}_1 \end{bmatrix}$$

$$H = \begin{bmatrix} 1\ 0 \ldots 0 & 0\ 0 \ldots 0 & & 0\ 0 \ldots 0 \\ 0\ 0 \ldots 0 & 1\ 0 \ldots 0 & & 0\ 0 \ldots 0 \\ \cdot\ \cdot & \cdot\ \cdot & & \cdot\ \cdot \\ \cdot\ \cdot & \cdot\ \cdot & \cdots & \cdot\ \cdot \\ \cdot\ \cdot & \cdot\ \cdot & & \cdot\ \cdot \\ 0\ 0 \ldots 0 & 0\ 0 \ldots 0 & & 0\ 0 \ldots 0 \\ 0\ 0 \ldots 0 & 0\ 0 \ldots 0 & & 1\ 0 \ldots 0 \end{bmatrix} \qquad (5.57b)$$

$$G = \begin{bmatrix} \hat{M}_{11,1} & \hat{M}_{12,1} & \cdots & \hat{M}_{1p,1} \\ \hat{M}_{11,2} & \hat{M}_{12,2} & \cdots & \hat{M}_{1p,2} \\ \cdot & \cdot & & \cdot \\ \cdot & \cdot & & \cdot \\ \hat{M}_{11,r} & \hat{M}_{12,r} & \cdots & \hat{M}_{1p,r} \\ \hat{M}_{21,1} & \hat{M}_{22,1} & \cdots & \hat{M}_{2p,1} \\ \cdot & \cdot & & \cdot \\ \cdot & \cdot & & \cdot \\ \hat{M}_{q1,1} & \hat{M}_{q2,1} & \cdots & \hat{M}_{qp,1} \\ \cdot & \cdot & & \cdot \\ \cdot & \cdot & & \cdot \\ \hat{M}_{q1,r} & \hat{M}_{q2,r} & \cdots & \hat{M}_{qp,r} \end{bmatrix} \qquad (5.57c)$$

$$D = \hat{M}_0 \qquad (5.57d)$$

If $p \leq q$, similarly, the canonical controllability form (cf. eq. (4.19)) can be used to obtain a unique, minimal state space representation of the MPSSM model. In this case the state space representation consists of a block diagonal state matrix F with p blocks similar to the transposes of the ones defined by eq. (5.57a), a G matrix with unit row vector e_i ($1 \leq i \leq p$) at row $j=(r\cdot(i-1)+1)$, zero row vectors at all other rows and a H matrix filled with the elements of the start sequence Markov parameters $\hat{M}_i$.

In the sequel the number of outputs q is assumed to be less than or equal to the number of inputs p. For q>p a similar derivation can be made by taking the canonical controllability form for the state space representation of the MPSSM model. Using eq. (5.52) and (5.56) the cost function can be written as:

$$V(\hat{\underline{a}},\hat{\underline{M}}) = \mathrm{tr}\{Y\cdot Y^t - Y\cdot\Omega_m^t\cdot F(\hat{\underline{a}},\hat{\underline{M}})^t - F(\hat{\underline{a}},\hat{\underline{M}})\cdot\Omega_m\cdot Y^t + F(\hat{\underline{a}},\hat{\underline{M}})\cdot\Omega_m\cdot\Omega_m^t\cdot F(\hat{\underline{a}},\hat{\underline{M}})^t\} \qquad (5.58)$$

with: $F(\hat{\underline{a}},\hat{\underline{M}}) = [D \quad H\cdot G \quad H\cdot F\cdot G \quad \ldots \quad H\cdot F^{m-1}\cdot G]$

$$F = \mathrm{diag}\{\hat{F}(\hat{\underline{a}}) \quad \hat{F}(\hat{\underline{a}}) \quad \ldots \quad \hat{F}(\hat{\underline{a}})\}$$

$$\hat{F}(\hat{\underline{a}}) = \begin{bmatrix} 0 & & \\ \vdots & I_{r-1,r-1} & \\ -\hat{a}_r & -\hat{a}_{r-1} \cdots & -\hat{a}_1 \end{bmatrix}$$

$$G = G(\hat{\underline{M}}) = [G_1^t \; G_2^t \; \ldots \; G_q^t]^t$$

$$G_i = \begin{bmatrix} \hat{M}_{i1,1} & \hat{M}_{i2,1} & \cdots & \hat{M}_{ip,1} \\ \hat{M}_{i1,2} & \hat{M}_{i2,2} & \cdots & \hat{M}_{ip,2} \\ \cdot & \cdot & & \cdot \\ \cdot & \cdot & & \cdot \\ \hat{M}_{i1,r} & \hat{M}_{i2,r} & \cdots & \hat{M}_{ip,r} \end{bmatrix}$$

From eq. (5.58) it is clear that the cost function is quadratic in the start sequence Markov parameters. The partial derivative of $V(\underline{a},\underline{M})$ with respect to these start sequence Markov parameters will therefore be a linear function of the parameters $\hat{\underline{M}}$. Of the minimal polynomial coefficients, however, the cost function is a polynomial expression of degree $(m-r)^2$. Also the derivative to these coefficients will therefore be of a high degree. This implies that an analytic solution for the parameters cannot be found. A numerical minimization method has to be used to find the parameter values that minimize V.

For numerical methods it is advantageous to have analytic expressions for the gradients eq. (5.53) and (5.54) (cf. [Fletcher, 1980; Stoer, 1980]). The rate of convergence in general increases and, consequently, the number of function calls that has to be made in the search process for the minimum of the function can be significantly reduced this way. Analytic expressions for the partial derivatives can be obtained by making use of matrix calculus (cf. [Graham, 1981], Appendix C)). For the computation of the partial derivatives the following property of the derivative of a trace function is used (cf. Appendix C, eq. (C.23)):

$$\frac{\partial \, \mathrm{tr}\{(Y - \hat{Y}) \cdot (Y^t - \hat{Y}^t)\}}{\partial \, M_{\alpha\beta,i}} = \mathrm{tr}\{ \frac{\partial \, [(Y - \hat{Y}) \cdot (Y^t - \hat{Y}^t)]}{\partial \, M_{\alpha\beta,i}} \} \qquad (5.59)$$

First the partial derivatives of V with respect to the D-matrix parameter

entries are computed (cf. Appendix E, eq. (E.11)):

$$\frac{\partial V}{\partial \hat{M}_{\alpha\beta,0}} = 2 \sum_{j=0}^{l} e_\beta^t \cdot u_{k+j} \cdot \left[\left(u_{k+j}^t \otimes e_\alpha^t \right) \cdot \mathrm{vec}(D) + \left(\sum_{i=1}^{m} u_{k+j-i}^t \otimes e_1^t \cdot \hat{F}(\hat{\underline{a}})^{i-1} \right) \cdot \mathrm{vec}(G_\alpha) - e_\alpha^t \cdot y_{k+j} \right] \qquad (5.60)$$

Similarly an expression can be derived for the partial derivatives of V with respect to the start sequence Markov parameters (cf. Appendix E, eq. (E.14)):

$$\frac{\partial V}{\partial \hat{M}_{\alpha\beta,i}} = 2 \sum_{t=0}^{l} \left(\sum_{j=1}^{m} e_1^t \cdot \hat{F}(\hat{\underline{a}})^{j-1} \cdot E_{i\beta} \cdot u_{k+t-j} \right) \cdot \left[\left(u_{k+t}^t \otimes e_\alpha^t \right) \cdot \mathrm{vec}(D) + \left\{ \sum_{s=1}^{m} \left(u_{k+t-s}^t \otimes \left(e_1^t \cdot \hat{F}(\hat{\underline{a}})^{s-1} \right) \right) \right\} \cdot \mathrm{vec}(G_\alpha) - e_\alpha^t \cdot y_{k+t} \right] \qquad (5.61)$$

Also partial derivatives of V with respect to the minimal polynomial coefficients $\hat{a}_i$ have to be derived (cf. Appendix E, eq. (E.21)):

$$\frac{\partial V}{\partial a_i} = \frac{\partial\, \mathrm{tr}\{(Y - \hat{Y}) \cdot (Y - \hat{Y})^t\}}{\partial a_i} = 2\, \mathrm{tr}\left\{ \frac{\partial \hat{Y}}{\partial a_i} \cdot (\hat{Y}^t - Y^t) \right\} =$$

$$= 2 \sum_{\alpha=1}^{q} \sum_{t=0}^{l} \left(\sum_{j=2}^{m} \sum_{s=0}^{j-2} e_1^t \cdot \hat{F}(\hat{\underline{a}})^s \cdot E_{r,r-i+1} \cdot \hat{F}(\hat{\underline{a}})^{j-s-2} \cdot G_\alpha \cdot u_{k-j+t} \right) \cdot \left(e_\alpha^t \cdot D \cdot u_{k+t} + \sum_{s=1}^{m} e_1^t \cdot \hat{F}(\hat{\underline{a}})^{s-1} \cdot G_\alpha \cdot u_{k-s+t} - e_\alpha^t \cdot y_{k+t} \right) \qquad (5.62)$$

As indicated before cost function V (eq. (5.52)) is a $(m-r)^2$-th order polynomial function of the polynomial coefficients. With the expressions for V and for the gradients of V the minimum of this cost function V can be found by using a quasi-Newton algorithm. The algorithm in this case still has to do a local search when a minimum is expected to be found, because no analytic expression for the gramian is available.
Searching for the minimum of the function this way requires the algorithm to minimize with respect to all MPSSM model parameters. The total number of parameters of the model is equal to $(r+1) \cdot p \cdot q + r$ (cf. eq. (4.1)). The number of minimal polynomial coefficients is equal to r. The remaining $(r+1) \cdot p \cdot q$ parameters are the start sequence Markov parameters. As can be seen from eq.

(5.60) and (5.61) the start sequence Markov parameters that minimize V can be expressed as a function of the minimal polynomial coefficients by solving a set of linear equations. Necessary condition for a set of parameters to correspond with a local minimum of (5.52) is that equations (5.60), (5.61) and (5.62) are equal to zero for all α,β,i (α=1,2, ... ,q ; β=1,2, ... ,p ; i=1,2, ... ,r). The number of parameters to be used in the numerical minimization can be reduced significantly by computation of an analytic solution for eq. (5.54). If the start sequence Markov parameters are solved from eq. (5.60) and (5.61) for all α, β and i, they can be expressed as an analytic function of the minimal polynomial coefficients. Substitution of this expression in eq. (5.62) gives the gradient of V expressed as a function of the minimal polynomial coefficients only.
Rewrite eq. (5.60) for this purpose:

$$\frac{\partial V}{\partial M_{\alpha\beta,0}} = 2\left\{ \sum_{t=0}^{l} e_\beta^t \cdot u_{k+t} \cdot \left[u_{k+t}^t \left(\sum_{s=1}^{m} u_{k+t-s}^t \otimes e_1^t \cdot \hat{F}(\hat{\underline{a}})^{s-1} \right) \right] \right\} \cdot \begin{bmatrix} D^t \cdot e_\alpha \\ \mathrm{vec}(G_\alpha) \end{bmatrix} - 2\left[\sum_{t=0}^{l} e_\beta^t \cdot u_{k+t} \cdot y_{k+j}^t \cdot e_\alpha \right] \qquad (5.63)$$

Eq. (5.61) can be rewritten similarly:

$$\frac{\partial V}{\partial M_{\alpha\beta,i}} = 2\left\{ \sum_{t=0}^{l} \left(\sum_{j=1}^{m} e_1^t \cdot \hat{F}(\hat{\underline{a}})^{j-1} \cdot E_{i\beta} \cdot u_{k+t-j} \right) \cdot \left[u_{k+t}^t \left(\sum_{s=1}^{m} u_{k+t-s}^t \otimes e_1^t \cdot \hat{F}(\hat{\underline{a}})^{s-1} \right) \right] \right\} \cdot \begin{bmatrix} D^t \cdot e_\alpha \\ \mathrm{vec}(G_\alpha) \end{bmatrix}$$

$$- 2\left[\sum_{t=0}^{l} \left(\sum_{j=1}^{m} e_1^t \cdot \hat{F}(\hat{\underline{a}})^{j-1} \cdot E_{i\beta} \cdot u_{k+t-j} \right) \cdot y_{k+j}^t \cdot e_\alpha \right] \qquad (5.64)$$

The set of equations that has to be solved to find the analytic expression

for the start sequence Markov parameters is:

$$
\begin{bmatrix}
\frac{\partial \hat{V}}{\partial M_{11,0}} & \frac{\partial \hat{V}}{\partial M_{21,0}} & \cdots & \frac{\partial \hat{V}}{\partial M_{q1,0}} \\
\frac{\partial \hat{V}}{\partial M_{12,0}} & \frac{\partial \hat{V}}{\partial M_{22,0}} & \cdots & \frac{\partial \hat{V}}{\partial M_{q2,0}} \\
\vdots & \vdots & & \vdots \\
\frac{\partial \hat{V}}{\partial M_{1p,0}} & \frac{\partial \hat{V}}{\partial M_{2p,0}} & \cdots & \frac{\partial \hat{V}}{\partial M_{qp,0}} \\
\frac{\partial \hat{V}}{\partial M_{11,1}} & \frac{\partial \hat{V}}{\partial M_{21,1}} & \cdots & \frac{\partial \hat{V}}{\partial M_{q1,1}} \\
\frac{\partial \hat{V}}{\partial M_{12,1}} & \frac{\partial \hat{V}}{\partial M_{22,1}} & \cdots & \frac{\partial \hat{V}}{\partial M_{q2,1}} \\
\vdots & \vdots & & \vdots \\
\frac{\partial \hat{V}}{\partial M_{1p,1}} & \frac{\partial \hat{V}}{\partial M_{2p,1}} & \cdots & \frac{\partial \hat{V}}{\partial M_{qp,1}} \\
\vdots & \vdots & & \vdots \\
\vdots & \vdots & & \vdots \\
\frac{\partial \hat{V}}{\partial M_{11,r}} & \frac{\partial \hat{V}}{\partial M_{21,r}} & \cdots & \frac{\partial \hat{V}}{\partial M_{q1,r}} \\
\frac{\partial \hat{V}}{\partial M_{12,r}} & \frac{\partial \hat{V}}{\partial M_{22,r}} & \cdots & \frac{\partial \hat{V}}{\partial M_{q2,r}} \\
\vdots & \vdots & & \vdots \\
\frac{\partial \hat{V}}{\partial M_{1p,r}} & \frac{\partial \hat{V}}{\partial M_{2p,r}} & \cdots & \frac{\partial \hat{V}}{\partial M_{qp,r}}
\end{bmatrix} =
$$

$$
=2\left[\begin{array}{c}
\sum_{t=0}^{l} e_1^t \cdot u_{k+t} \cdot \left[u_{k+t}^t \left(\sum_{s=1}^{m} u_{k+t-s}^t \otimes e_1^t \cdot \hat{F}(\hat{\underline{a}})^{s-1} \right) \right] \\
\sum_{t=0}^{l} e_2^t \cdot u_{k+t} \cdot \left[u_{k+t}^t \left(\sum_{s=1}^{m} u_{k+t-s}^t \otimes e_1^t \cdot \hat{F}(\hat{\underline{a}})^{s-1} \right) \right] \\
\vdots \\
\sum_{t=0}^{l} e_p^t \cdot u_{k+t} \cdot \left[u_{k+t}^t \left(\sum_{s=1}^{m} u_{k+t-s}^t \otimes e_1^t \cdot \hat{F}(\hat{\underline{a}})^{s-1} \right) \right] \\
\sum_{t=0}^{l} \left(\sum_{j=1}^{m} e_1^t \cdot \hat{F}(\hat{\underline{a}})^{j-1} \cdot E_{11} \cdot u_{k+t-j} \right) \cdot \left[u_{k+t}^t \left(\sum_{s=1}^{m} u_{k+t-s}^t \otimes e_1^t \cdot \hat{F}(\hat{\underline{a}})^{s-1} \right) \right] \\
\vdots \\
\sum_{t=0}^{l} \left(\sum_{j=1}^{m} e_1^t \cdot \hat{F}(\hat{\underline{a}})^{j-1} \cdot E_{1p} \cdot u_{k+t-j} \right) \cdot \left[u_{k+t}^t \left(\sum_{s=1}^{m} u_{k+t-s}^t \otimes e_1^t \cdot \hat{F}(\hat{\underline{a}})^{s-1} \right) \right] \\
\vdots \\
\sum_{t=0}^{l} \left(\sum_{j=1}^{m} e_1^t \cdot \hat{F}(\hat{\underline{a}})^{j-1} \cdot E_{r1} \cdot u_{k+t-j} \right) \cdot \left[u_{k+t}^t \left(\sum_{s=1}^{m} u_{k+t-s}^t \otimes e_1^t \cdot \hat{F}(\hat{\underline{a}})^{s-1} \right) \right] \\
\vdots \\
\sum_{t=0}^{l} \left(\sum_{j=1}^{m} e_1^t \cdot \hat{F}(\hat{\underline{a}})^{j-1} \cdot E_{rp} \cdot u_{k+t-j} \right) \cdot \left[u_{k+t}^t \left(\sum_{s=1}^{m} u_{k+t-s}^t \otimes e_1^t \cdot \hat{F}(\hat{\underline{a}})^{s-1} \right) \right]
\end{array}\right]
$$

$$
\cdot \left[\begin{array}{c} D^t \\ \text{vec}(G_1) \quad \text{vec}(G_2) \quad \ldots \quad \text{vec}(G_q) \end{array} \right] -
$$

$$
-2\sum_{t=0}^{l}\begin{bmatrix} e_1^t\cdot u_{k+t} \\ \vdots \\ e_p^t\cdot u_{k+t} \\ \sum_{j=1}^{m} e_1^t\cdot\hat{F}(\hat{\underline{a}})^{j-1}\cdot E_{11}\cdot u_{k+t-j} \\ \vdots \\ \sum_{j=1}^{m} e_1^t\cdot\hat{F}(\hat{\underline{a}})^{j-1}\cdot E_{1p}\cdot u_{k+t-j} \\ \vdots \\ \sum_{j=1}^{m} e_1^t\cdot\hat{F}(\hat{\underline{a}})^{j-1}\cdot E_{r1}\cdot u_{k+t-j} \\ \vdots \\ \sum_{j=1}^{m} e_1^t\cdot\hat{F}(\hat{\underline{a}})^{j-1}\cdot E_{rp}\cdot u_{k+t-j} \end{bmatrix}\cdot y_{k+t}^t
$$

$$
= 2\,\Phi\cdot\Theta - 2\Upsilon = 0_{(r+1)p,q} \qquad (5.65)
$$

with: dim[Φ]: $(r+1)p \times (r+1)p$
dim[Θ]: $(r+1)p \times q$
dim[Υ]: $(r+1)p \times q$

Because of the characteristics of the input signal applied to the process and the minimal polynomial coefficients that result from an estimation, matrices Υ and Φ will have full rank. The start sequence Markov parameters that minimize V immediately follow from eq. (5.65):

$$
\Theta(\underline{a}) = \begin{bmatrix} D^t \\ \mathrm{vec}(G_1) \quad \mathrm{vec}(G_2) \quad \ldots \quad \mathrm{vec}(G_q) \end{bmatrix} = \Phi(\underline{a})^{-1}\cdot\Upsilon(\underline{a}) \qquad (5.66)
$$

Rewriting of eq. (5.62) into:

$$\frac{\partial V}{\partial \hat{a}_i} =$$

$$2 \sum_{\alpha=1}^{q} \sum_{t=0}^{l} \left(\sum_{j=2}^{m} \sum_{s=0}^{j-2} \left(u_{k-j+t}^{t} \otimes e_1^t \cdot \hat{F}(\hat{\underline{a}})^s \cdot E_{r,r-i+1} \cdot \hat{F}(\hat{\underline{a}})^{j-s-2} \right) \cdot \mathrm{vec}(G_\alpha) \right) \cdot$$

$$\left(u_{k+t}^{t} \cdot D^t \cdot e_\alpha + \sum_{s=1}^{m} \left(u_{k-s+t}^{t} \otimes e_1^t \cdot \tilde{F}^{s-1} \right) \cdot \mathrm{vec}(G_\alpha) - e_\alpha^t \cdot y_{k+t} \right) \qquad (5.67)$$

allows for immediate substitution of the result obtained from eq. (5.66). After this substitution eq. (5.67) is a function of the minimal polynomial coefficients only. As a consequence of the results obtained a quasi Newton minimization algorithm can be applied which only needs to minimize the function with respect to the r minimal polynomial coefficients.

At this moment it is good to recall the meaning of the various formulas obtained so far. First the partial derivatives of cost function $V(\hat{\underline{a}},\hat{\underline{M}})$ with respect to the D-matrix and the start sequence Markov parameters (eq. (5.60) and (5.61)) and with respect to the minimal polynomial coefficients (eq. (5.62)) have been computed. Next the observation that $V(\hat{\underline{a}},\hat{\underline{M}})$ is a quadratic function of the start sequence Markov parameters is used to derive an analytic expression for the start sequence Markov parameters (eq. (5.66)):

$$\frac{\partial V(\hat{\underline{a}},\hat{\underline{M}})}{\partial \hat{\underline{M}}} = 0 \quad \rightarrow \quad \hat{M}_j = \hat{M}_j(\hat{a}_i) \qquad j,i \epsilon I, \quad I=1,2, \ldots ,r \qquad (5.68)$$

With this analytic expression for the start sequence Markov parameters cost function $V(\hat{\underline{a}},\hat{\underline{M}})$ can implicitly be written as a function of the minimal polynomial coefficients only. To find a minimum of $V(\hat{\underline{a}},\hat{\underline{M}})$ the partial derivative of $V(\hat{\underline{a}},\hat{\underline{M}})$ with respect to the minimal polynomial coefficients is required:

$$\frac{\partial V(\hat{\underline{a}},\hat{\underline{M}}(\hat{\underline{a}}))}{\partial \hat{a}_j} = \frac{\partial V(\hat{\underline{a}},\hat{\underline{M}})}{\partial \hat{a}_j} + \sum_{\alpha,\beta,k} \frac{\partial V(\hat{\underline{a}},\hat{\underline{M}})}{\partial \hat{M}_{\alpha\beta,k}} \cdot \frac{\partial \hat{M}_{\alpha\beta,k}(\hat{\underline{a}})}{\partial \hat{a}_j} \qquad (5.69)$$

with: $\alpha=1,2, \ldots ,q \quad \beta=1,2, \ldots ,p \quad i,j,k \epsilon I, \quad I=1,2, \ldots ,r$

With the partial derivative of $V(\hat{\underline{a}},\hat{\underline{M}})$ to the entries of the start sequence Markov parameters being equal to zero (cf. eq. (5.60), (5.61), (5.66) and (5.66)) eq. (5.67) goes over into:

$$\frac{\partial V(\hat{\underline{a}},\hat{\underline{M}}(\hat{\underline{a}}))}{\partial a_j} = \frac{\partial V(\hat{\underline{a}},\hat{\underline{M}})}{\partial a_j} + 0 \qquad i,j\epsilon I,\ I=1,2,\ \ldots\ ,r \tag{5.70}$$

In this expression the values obtained for the start sequence Markov parameters from eq. (5.66) have to be substituted. However, eq. (5.66) can only be solved for given numeric values for the minimal polynomial coefficients. This implies that each evaluation of the function value of $V(\hat{\underline{a}},\hat{\underline{M}}(\hat{\underline{a}}))$ and of its derivative to the minimal polynomial coefficients requires the computation of start sequence Markov parameters using eq. (5.66). These evaluations of function values and first derivatives are done by the quasi Newton algorithm to estimate the required second derivative of $V(\hat{\underline{a}},\hat{\underline{M}}(\hat{\underline{a}}))$. If for each evaluation of function value and first derivative the $\hat{\underline{M}}(\hat{\underline{a}})$ computed from eq. (5.66) are used, an algorithm is obtained that needs to minimize a function $V(\hat{\underline{a}},\hat{\underline{M}}(\hat{\underline{a}}))$ only with respect to the minimal polynomial coefficients $\hat{\underline{a}}$.

5.4 Various algorithms

Two algorithms have been developed for the computation of the MPSSM model parameters directly from given process input/output data. Both algorithms make use of a comprehensive quasi-Newton algorithm for minimization of cost function $V(\hat{\underline{a}},\hat{\underline{M}})$ (eq. (5.51)). The minimization process is started with a set of MPSSM model parameters obtained from the methods described in chapters 3 and 4. The quasi-Newton method is chosen for its proven efficiency with respect to the number of function evaluations required, the amount of computational effort needed and its robustness with respect to convergence (cf. [Fletcher, 1980]).

The first algorithm developed minimizes cost function $V(\hat{\underline{a}},\hat{\underline{M}})$ without making use of the analytic expression for the start sequence Markov parameters as a function of the minimal polynomial coefficients (eq. (5.66)) (cf. [Van der Weijden, 1984]). The minimization procedure applied therefore has to minimize with respect to all $r\cdot(p\cdot q+1)$ model parameters.

Minimization of V with a quasi-Newton method requires expressions for computation in a given point of both the function value and the first derivatives with respect to the model parameters. For the computation of the derivatives eq. (5.60), (5.61) and (5.62) are used. The output errors are computed by simulation of the model outputs with a state space model given by eq. (2.3a,b) with matrices F, G, H and D defined by eq. (5.57a,b,c,d).

The function value for a given set of parameters is then obtained by computation of the sum of the squared output errors.
The algorithm only allows for stable systems. Reason for not taking into account unstable systems is that the industrial processes considered all are stable processes. A test is build in to check for the position of the largest eigenvalue of the minimal polynomial. This eigenvalue has to be inside the unit disk. If one wants to allow unstable processes, the initial state of the process needs to be estimated as extra set of parameters. Moreover the contribution of the initial state has to be included in the formulas for V and its partial derivatives derived in the previous section.

The second algorithm developed, only uses the minimization procedure for minimization of V with respect to the r minimal polynomial coefficients (cf. [Oudbier, 1986]). The start sequence Markov parameters that minimize V are computed by making use of the analytic expressions derived for the start sequence Markov parameters as a function of the minimal polynomial coefficients eq. (5.66). The algorithm again uses a quasi-Newton minimization method for minimization of V with respect to the minimal polynomial coefficients. During each evaluation of both the function value and the derivative of V with respect to the minimal polynomial coefficients first eq. (5.66) is solved for the proposed set of minimal polynomial coefficients. This gives the start sequence Markov parameters that minimize V for the given set of minimal polynomial coefficients. Next the start sequence Markov parameters obtained are substituted in eq. (5.67). Using eq. (5.67) the derivatives with respect to the minimal polynomial coefficients are computed. Finally the function value for the given set of minimal polynomial coefficients and the start sequence Markov parameters obtained from eq. (5.66) is computed using the state space representation given by (F, G, H, D).
This algorithm too only allows for stable systems. Also systems with negative real parts of the eigenvalues can be rejected by the algorithm. These last types of systems can be excluded by this algorithm because they, in general, do not correspond with the continuous time processes modelled. Normally eigenvalues with a negative real part are found due to over estimation of the order of the minimal polynomial, noise on the measured process signals or remainders of non relevant high frequency signal components. A reason for not wanting a model with eigenvalues that have a negative real part is given by the application of the model for control purposes. In these applications such a model may give rise to process input signals with inacceptable large amplitude changes every sample. Again, if unstable systems need to be modelled, also the initial state of the system has to be estimated as an extra set of parameters and the formulas derived for V and its derivatives have to be extended with initial state contributions.

Both algorithms developed, use, during simulation of the model outputs for the computation of the output error, the first part of the data set to reduce the effects of a wrong value for the initial state of the model. The

number of samples used for this purpose depends upon:

- the a priory knowledge of the length of the impulse responses
- the known accuracy of the measured process signals

To derive the number of samples to be used for the initialisation of the system, the state space representation of the system (eq. (2.3a,b)) is used. By selecting another basis the system can be written as:

$$\tilde{x}_{k+1} = T^{-1} \cdot F \cdot T \cdot \tilde{x}_k + T^{-1} \cdot G \cdot u_k = \tilde{F} \cdot \tilde{x}_k + \tilde{G} \cdot u_k \tag{5.71a}$$

$$y_k = H \cdot T \cdot \tilde{x}_k + D \cdot u_k = \tilde{H} \cdot \tilde{x}_k + D \cdot u_k \tag{5.71b}$$

with: $\tilde{F}$, $\tilde{G}$, $\tilde{H}$, D - a Jordan canonical form of the system (cf. section 4.5)

In the sequel the system is assumed to have distinct eigenvalues. The input output behaviour of the system is given by (cf. eq. (4.4)):

$$\begin{aligned} y_k &= H \cdot F^k \cdot x_0 + \sum_{i=1}^{k} H \cdot F^{i-1} \cdot u_{k-i} + D \cdot u_k \\ &= \tilde{H} \cdot \tilde{F}^k \cdot \tilde{x}_0 + \sum_{i=1}^{k} \tilde{H} \cdot \tilde{F}^{i-1} \cdot u_{k-i} + D \cdot u_k \end{aligned} \tag{5.72}$$

To find an estimate for the number of samples that will be required to make the influence of the initial state sufficiently small, the input signal is assumed to be equal to zero for all sample instances and the initial state is assumed to be $x_0 \neq 0$. Furthermore the initial state is assumed to be scaled so that:

$$\max_{||x_0||=1} || \tilde{H} \cdot x_0 ||_2 = \sigma_1 \tag{5.73}$$

with: σ_1 - the maximum singular value of $\tilde{H}$

With these assumptions eq. (5.72) becomes:

$$y_k = H \cdot F^k \cdot x_0 = \tilde{H} \cdot \tilde{F}^k \cdot \tilde{x}_0 \tag{5.74}$$

Now a value k_0 has to be determined that satisfies:

$$\frac{\| \tilde{H} \cdot \tilde{F}^k \cdot x_0 \|_2}{\| \tilde{H} \cdot x_0 \|_2} < \varepsilon \qquad \text{for all } k \geq k_0 \tag{5.75}$$

A value of k_0 that satisfies eq. (5.75) can be found from:

$$\frac{\| \tilde{H} \cdot \tilde{F}^k \cdot x_0 \|_2}{\| \tilde{H} \cdot x_0 \|_2} \leq \frac{\sigma_1 \cdot \lambda_{max}^k}{\sigma_1} < \varepsilon \tag{5.76}$$

with: λ_{max} - the maximum eigenvalue of the system ($\lambda_{max} < 1$)

From eq. (5.76) an expression is obtained for the determination of k_0:

$$k_0 \geq \frac{| \log \varepsilon |}{| \log \lambda_{max} |} \tag{5.77}$$

with: k_0 - number of samples used for initialisation
ε - relative accuracy wanted
λ_{max} - maximum eigenvalue of the approximate realization obtained from the first estimated FIR model

As a consequence of this approach the first k_0 samples of the data set may not be used for the system identification. In practice, however, this is no problem, because the number of samples available in the data sets, in general, largely exceeds the number of samples required for the identification.

5.5 Simulation results

The algorithms developed have been applied to input/output datasets generated with the 4 simulated processes introduced in chapter 3 (cf. section 3.6 system 1, 2, 3 and 4).
To test the algorithms MPSSM model parameters have been estimated for systems with minimal polynomial degrees equal to the degrees indicated by the order tests (cf. section 4.6, fig. 4.10 - 4.13)):

- System 1 degree of the minimal polynomial r=2
- System 2 degree of the minimal polynomial r=3
- System 3 degree of the minimal polynomial r=3
- System 4 degree of the minimal polynomial r=3

This implies that three of the four simulated processes (viz. system 2, 3 and 4) are not contained in the MPSSM modelsets used for the estimations.

To generate start values for the MPSSM model parameters, both the algorithm of Gerth (cf. eq. (4.30), (4.31)) and the algorithm of Zeiger and McEwen (cf. eq. (4.36) - (4.42)) have been applied. For the computation of these approximate realizations, for each of the 4 simulated processes the 20 FIR models, obtained from EXACTMARK, have been used (cf. section 3.6).

The MPSSM model parameters have been estimated twice. The first time using the parameters obtained from the Gerth algorithm as start values. The second time using the parameters obtained from the algorithm of Zeiger and McEwen as initial values. The input/output data sets used for the parameter estimations are the same as the ones used for the estimation of the finite impulse responses (see: section 3.6).
For the estimation of the MPSSM model parameters only the samples 500 - 1000 of the data sets have been used. However, the trace of the squared output errors is computed over the full sample interval (1 - 1000). This implies that the figures obtained for the output errors partly consist of model validation results and partly of estimation results.

Both algorithms discussed in section 5.4 have been appplied for the tests:

- The algorithm that minimizes cost function $V(\hat{\underline{a}},\hat{\underline{M}})$ without using the analytic expression for the computation of start sequence Markov parameters (eq. (5.66)) in the minimum of V.
- The algorithm that uses the derived analytic expression for the computation of the start sequence Markov parameters as a function of the minimal polynomial coefficients. Consequently the parameters to be handled for numerical minimization are the minimal polynomial coefficients only.

The only difference between the two algorithms is found in the amount of processor time required for the minimization of V. The second algorithm needs for the parameter estimation on the average about 20% of the processor time required by the first algorithm. Both methods gave exactly the same estimation results. In the sequel no further distinction will be made between the two methods.

For each of the MPSSM models an approximate realization has been computed of order 2 for system 1 and of order 4 for systems 2, 3 and 4. For the computation of the approximate realizations the algorithm of Zeiger and McEwen has been used. The block dimensions (number of block rows and number of block columns) of the finite block Hankel matrices used for the computation of the approximate realizations for the various systems are:

- System 1: 20
- System 2: 20
- System 3: 20
- System 4: 50

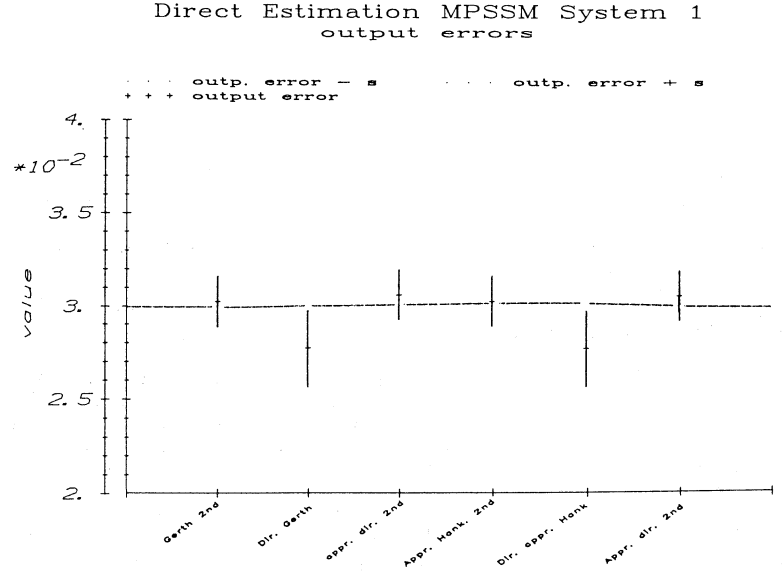

Fig. 5.2 Average output error values obtained with the 6 different models for system 2. The value obtained with the estimated FIR model is indicated with a dotted line.

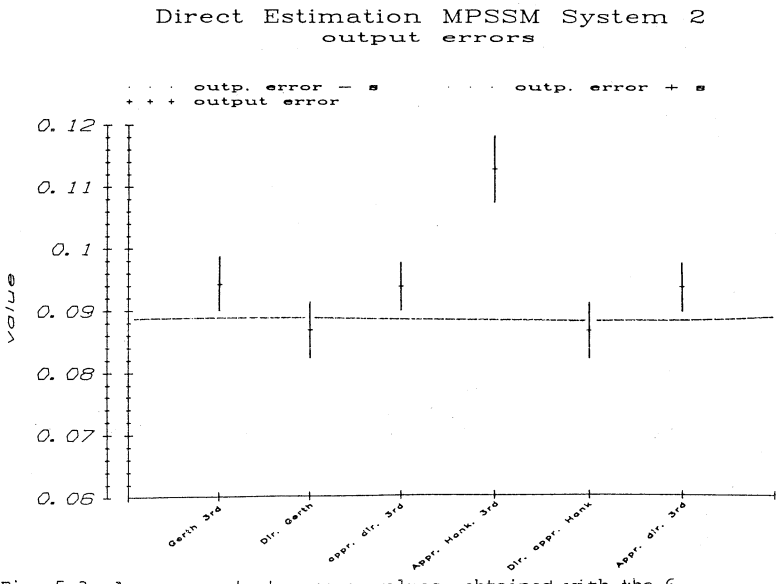

Fig. 5.3 Average output error values obtained with the 6 different models for system 3. The value obtained with the estimated FIR model is indicated with a dotted line.

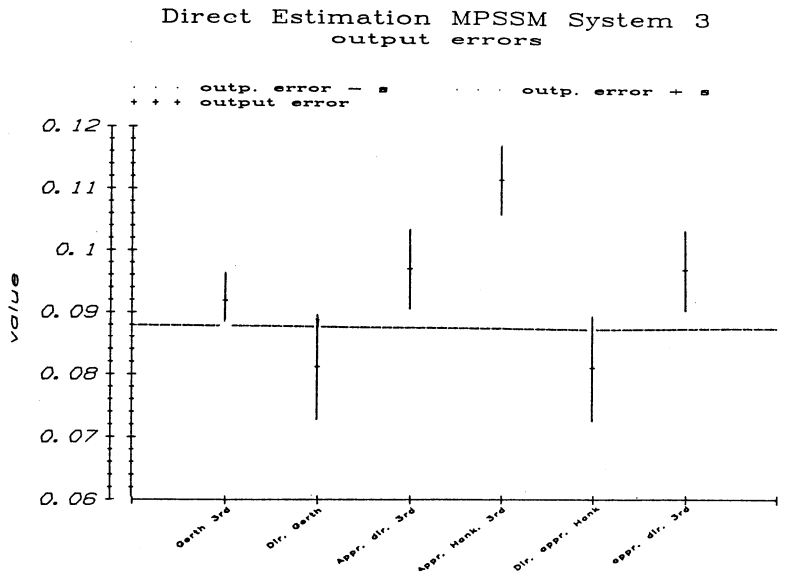

Fig. 5.4 Average output error values obtained with the 6 different models for system 4. The value obtained with the estimated FIR model is indicated with a dotted line.

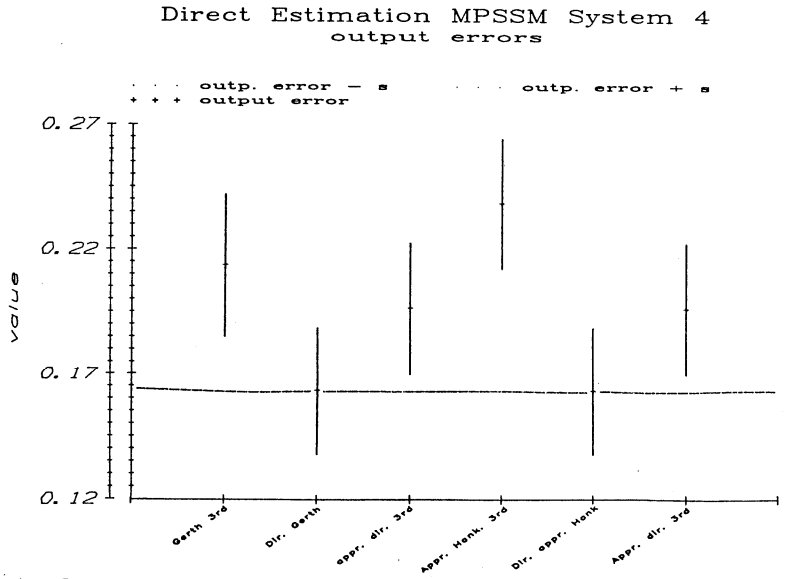

Fig. 5.5 Subsequent identification steps and the use of obtained model parameters in an identification step as initial values for a next step

To get an impression of the quality of the models obtained from the direct estimation and the corresponding approximate realizations, both the Hankel norm and the Frobenius norm of the error systems, defined by the difference between estimated or approximate model and the true system, have been computed (cf. eq. (3.50) - (3.60)).

The estimation results obtained are given in fig. 5.2 - 5.5. These figures show the average value of the traces of the output errors plus and minus the computed standard deviations. To make comparison with earlier obtained results easy, the average values of the output errors of the FIR models estimated with EXACTMARK are plotted in the figures as dotted lines. The presented values are computed from 20 estimation results for each system.

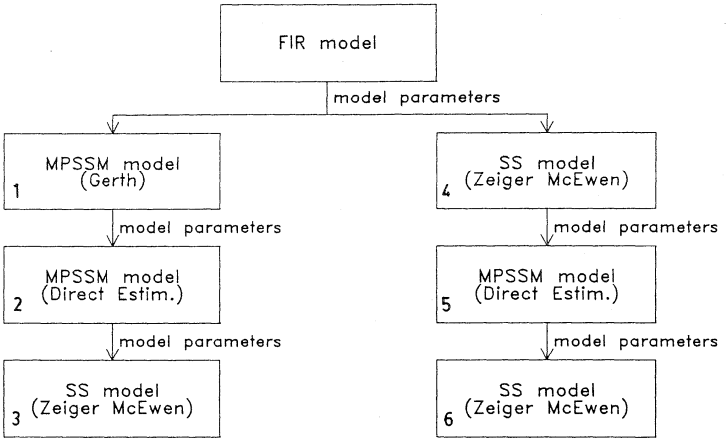

Fig. 5.6 Sequence of estimations done for each of the simulated processes

The output errors given are respectivley computed from the models obtained with (cf. fig. 5.6):

1. the Gerth algorithm applied to the FIR models estimated with the EXACTMARK algorithm (cf. eq. (3.43))
2. the Direct Estimation method, discussed in this chapter, using the MPSSM model parameters, computed with the Gerth algorithm, as start values
3. the approximate realization algorithm based on finite block Hankel matrices applied to the MPSSM models estimated with the Gerth model parameters as initial values

4. the approximate realization algorithm of Zeiger and McEwen applied to the FIR models estimated with the EXACTMARK algorithm (cf. eq. (3.43))
5. the Direct Estimation method using the approximate realization model parameters, computed with the algorithm of Zeiger and McEwen, as start values
6. the approximate realization algorithm applied to the MPSSM models estimated with the model parameters of the approximate realizations as initial values

In the figures the following names are used for the indication of each of the 6 steps (cf. fig. 5.6):

1. Gerth xxx	to indicate the results obtained with the method of Gerth using a MPSSM model of degree xxx
2. Dir. Gerth	to indicate the results obtained from the Direct Estimation method with the model parameters of 1 as initial parameter values
3. Appr. dir. Gerth	to indicate the results obtained with the approximate realization of the MPSSM model obtained from 2
4. Appr. Hank.	to indicate the results obtained with the model resulting from application of the algorithm of Zeiger and McEwen to the FIR model
5. Dir. Appr. Hank.	to indicate the results obtained from the Direct Estimation method with MPSSM model parameters of 4 as initial parameter values
6. Appr. dir.	to indicate the results obtained with the approximate realization of the MPSSM model obtained from 5

Although the output errors have been computed over the full range of 1000 samples while only samples 500 - 1000 have been used for the estimation of the model parameters with the Direct Estimation method, the output errors computed with the models obtained from the Direct Estimation method (2 and 5) are the smallest for all systems. The computed output error values are almost equal to the output error values obtained with the estimated FIR models (cf. dotted lines). Except for system 1, the approximate realizations (4) computed from the FIR models give the largest output errors.
The models obtained from the Direct Estimation method (2 and 5) are the same for both sets of initial values used for the model parameters (models obtained from Gerth's method (1) and models obtained from the approximate realization algorithm based on finite block Hankel matrices (4)). This implies that both sets of initial values for the MPSSM model parameters lead to the same minimum of the criterion function.

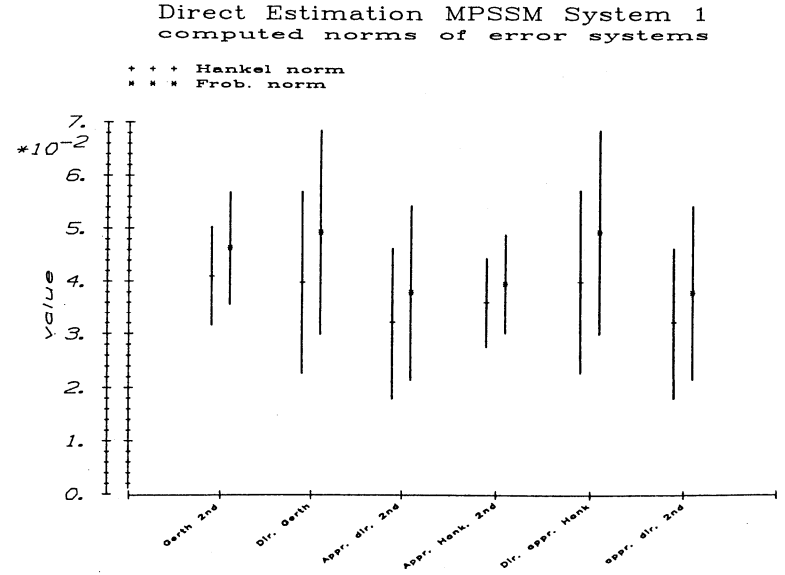

Fig. 5.7 Average values of the Hankel norm and of the Frobenius norm of the error systems computed with the various approximate realizations for system 1.

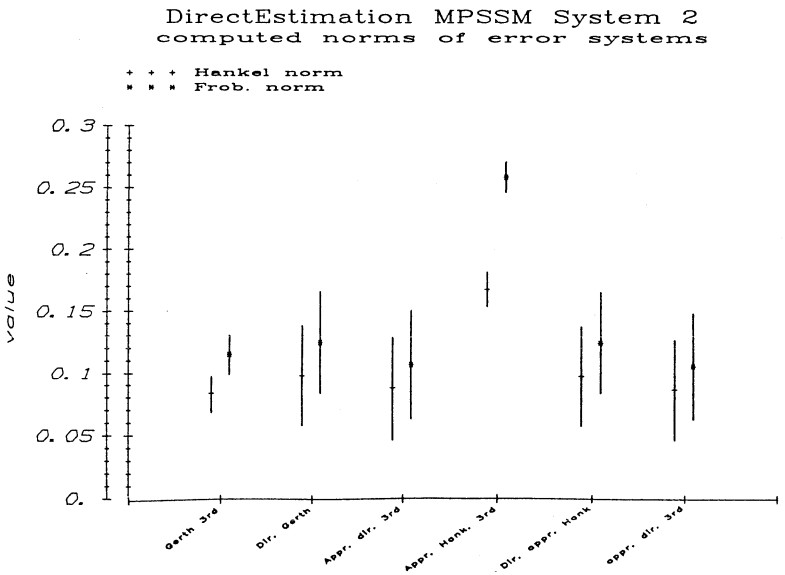

Fig. 5.8 Average values of the Hankel norm and of the Frobenius norm of the error systems computed with the various approximate realizations for system 2.

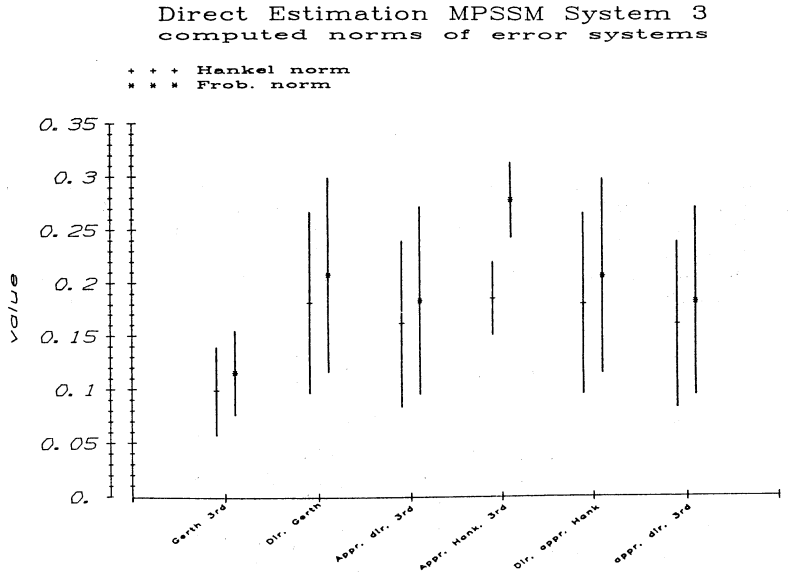

Fig. 5.9 Average values of the Hankel norm and of the Frobenius norm of the error systems computed with the various approximate realizations for system 3.

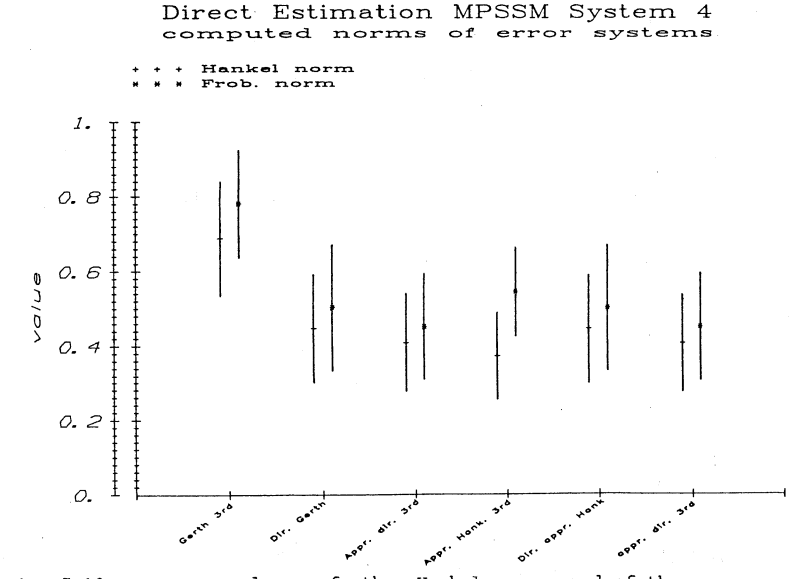

Fig. 5.10 Average values of the Hankel norm and of the Frobenius norm of the error systems computed with the various approximate realizations for system 4.

The values computed for the Hankel norms and the Frobenius norms of the error systems are given in fig. 5.7 - 5.10. Each figure shows the average values plus and minus the computed standard deviations. For each system the values have been computed from 20 estimation results. The average values obtained for the Hankel and Frobenius norms of the error systems are also summarized in table 5.1.

	Hankel norm	Frobenius norm
system 1: true system	0.196E+01	0.237E+01
Gerth 2-nd order	0.410E-01	0.464E-01
Direct Est. Gerth	0.399E-01	0.494E-01
appr. real. direct	0.322E-01	0.380E-01
Appr. Hankel 2-nd ord.	0.361E-01	0.396E-01
Direct Est. Appr. real	0.399E-01	0.494E-01
appr. real. direct	0.322E-01	0.380E-01
system 2: true system	0.336E+01	0.390E+01
Gerth 3-rd order	0.836E-01	0.116E+00
Direct Est. Gerth	0.990E-01	0.125E+00
appr. real. direct	0.884E-01	0.108E+00
Appr. Hankel 3-rd ord.	0.168E+00	0.259E+00
Direct Est. Appr. real	0.986E-01	0.125E+00
appr. real. direct	0.869E-01	0.106E+00
system 3: true system	0.336E+01	0.390E+01
Gerth 3-rd order	0.982E-01	0.115E+00
Direct Est. Gerth	0.181E+00	0.207E+00
appr. real. direct	0.161E+00	0.183E+00
Appr. Hankel 3-rd ord.	0.185E+00	0.278E+00
Direct Est. Appr. real	0.181E+00	0.207E+00
appr. real. direct	0.161E+00	0.183E+00
system 4: true system	0.874E+01	0.903E+01
Gerth 3-rd order	0.688E+00	0.781E+00
Direct Est. Gerth	0.448E+00	0.504E+00
appr. real. direct	0.409E+00	0.452E+00
Appr. Hankel 3-rd ord.	0.374E+00	0.546E+00
Direct Est. Appr. real	0.448E+00	0.504E+00
appr. real direct	0.409E+00	0.452E+00

table 5.1 Norms of the true systems and norms computed for the error systems

Strictly speaking, comparison of the results obtained from the Direct Estimation method (2 and 5) with the approximate realizations (1 and 4) used as starting values for the Direct method is not fair, for only 500 samples

have been used for the direct estimation of the MPSSM model parameters, while the approximate realizations have been computed from FIR models that have been estimated on the basis of 1000 samples.

In general, the results obtained for the approximate realizations (3 and 6) computed from the models estimated with the Direct Estimation method are better than the results obtained for the MPSSM models resulting from the estimation with the Direct Estimation method (2 and 5). This phenomenon may be explained by the observation that insignificant modes in the input/output behaviour of the MPSSM models (modes with a small transfer gain) can have an important influence on the computed Hankel and Frobenius norms for the error systems, for input signals that exclusively excite these modes fully contribute to the output error of the system, while significant modes of the true system are for a great deal compensated by the estimated significant modes of the estimated MPSSM models. In the computed approximate realizations of the MPSSM models (3 and 6) only the relevant modes, indicated by the largest Hankel singular values, are retained; insignificant modes are removed from the models and therefore do not contribute to the norms of the error systems any more.
Except for system 3, the results obtained for the approximate realizations (3 and 6) computed from the estimated MPSSM models are better than or comparible with the results obtained for the initial models. For system 3 the models obtained with Gerth's algorithm are clearly best.
Although the simulated processes do not fit in the model sets used for the estimation of the MPSSM model parameters (systems 2, 3 and 4), the results obtained with the approximate realizations of the estimated MPSSM models are almost equal to the results obtained with the approximate realizations computed on the basis of the FIR models in chapter 4 (cf. section 4.6, fig. 4.14 - 4.17).

5.6 Concluding remarks

In this chapter a method has been developed for the estimation of MPSSM model parameters directly from input/output data using a least squares method applied to the output error.

It has been shown that the criterion function $V(\hat{a}_i, \hat{M}_i \mid i \epsilon I)$, I=1,2, ... ,r, is a quadratic function of the start sequence Markov parameters $\hat{M}_i$ and a high order polynomial function of the minimal polynomial coefficients $\hat{a}_i$ (cf. eq. (5.56) - (5.58)). As a result an analytic expression has been derived for the computation of the start sequence Markov parameters, written as a function of the minimal polynomial coefficients $\hat{M}(\hat{a}_j \mid j \epsilon I)$ that minimize $V(\hat{a}_i, \hat{M}_i \mid i \epsilon I)$ (cf. eq. (5.66)).
To find a complete set of MPSSM model parameters that minimize $V(\hat{a}_i, \hat{M}_i(\hat{a}_j) \mid i,j \epsilon I)$ a numerical minimization method has to be used. The

remaining function $V(\hat{a}_i, \hat{M}_i(\hat{a}_j) \mid i,j \in I)$ that has to be minimized with a numerical minimization method in fact only is a function of the r minimal polynomial coefficients. This is an advantage of the MPSSM model set compared to (pseudo) canonical state space and MFD models, which generally have many more parameters that have to be minimized by a numerical minimization method, because they occur with a higher degree than two in the criterion function if an output error criterion is applied.

It has been shown that the impulse responses generated by the MPSSM model obtained from an estimation will be asymptotically as close as possible, measured in Frobenius norm, to the true systems impulse responses under the following conditions:

- it is assumed that the proces dynamics can be described by impulse responses
- the input test signal applied to the process is assumed to be stationary, white, inter-channel independent, zero mean noise
- the output noise is assumed not to be correlated with the input signals applied.
- the number of samples used is assumed to be sufficient large to allow the approximation of eq. (5.30) by eq. (5.32)

It also has been shown that the initial two step approach -estimation of FIR model parameters and, on the basis of the estimated FIR model, approximation in Frobenius norm of the FIR's by impulse responses generated by a MPSSM model- is expected to give the same results as the Direct Estimation method under the assumption that tail effects can be neglected (cf. eq. (5.5) - (5.11), section 5.2.1 and section 5.2.2). The Gerth algorithm is an approximation for the second step: fit of impulse responses generated by a to be determined MPSSM model to estimated finite impulse responses.

The MPSSM model generically has r multiple, distinct eigenvalues of multiplicity $\min(p,q)\cdot r$ (cf. eq. (4.20)). In general this implies that irrelevant modes are part of the estimated MPSSM model. During estimation these irrelevant modes will be used to model the process output noise partly. Generally this implies that the quality of the model will decrease. This effect has been found in the estimation results obtained from the Direct Estimation method (cf. fig. 5.7 - 5.10). To remove the irrelevant modes, a lower order approximate realization has to be computed on the basis of the estimated MPSSM model. For the computation of the approximate realization the following methods are well suited:

- The method based on the computation of a balanced realization from the finite block Hankel matrix (algorithm of Zeiger and McEwen cf. eq. (4.36) - (4.42))
- The approximation of a balanced state space representation of the MPSSM model by the subsystem that is best controllable and observable (cf. section 5.2.4, eq. (5.48), (5.49))
- The optimal Hankel norm approximation (algorithm of Glover cf. eq. (4.70) - (4.94))

The algorithm of Zeiger and McEwen results in an approximate realization that is close to the optimal Frobenius norm approximation of the original MPSSM model if the dimensions of the finite block Hankel matrix are chosen such that the first block row and the first block column include the impulse responses of the system with negligible tail effects. The resulting approximate realization will simulate outputs on the basis of past inputs that are, on the average, almost closest to the outputs simulated by the original MPSSM on the basis of the same past inputs.
The approximation of the MPSSM model by the best observable and controllable sub system also is close to a Frobenius norm approximation of the system.
The k-th order ($k<\min(p,q)\cdot r$) optimal Hankel norm approximation results in an approximation where the Hankel norm of the error system defined by the difference between the original MPSSM model and the approximate realization is equal to the (k+1)-st Hankel singular value of the MPSSM model. As a result the worst case difference between the outputs simulated by the original MPSSM model and the outputs simulated by its k-th order approximate realization will be smaller than or equal to the difference obtained with any other k-th order approximation.

The Direct Estimation method has been tested on the 4 simulated processes defined in chapter 3 (section 3.6). For the estimation of the MPSSM models the following degrees of the minimal polynomials have been used (cf. order estimation results chapter 4, section 4.6, fig. 4.10 - 4.13):

- System 1: degree of the minimal polynomial r=2
- System 2: degree of the minimal polynomial r=3
- System 3: degree of the minimal polynomial r=3
- System 4: degree of the minimal polynomial r=3

This implies that the simulated processes Systems 2, 3 and 4 are not contained in the MPSSM model sets used for the estimations.
For the estimation of the model parameters the same input/output data has been used as for the estimation of the FIR models (cf. chapter 3, section 3.6). For the actual estimation of the model parameters only samples 500 - 1000 of the data sets have been used. As initial values for the MPSSM model parameters the values obtained with the Gerth algorithm (cf. eq. (4.29) - (4.30)) and parameter values obtained from the approximate realization on the basis of finite block Hankel matrices using the algorithm of Zeiger and McEwen (cf. eq. (4.36) - (4.42)) have been used.

To be able to compare the results obtained with previously obtained estimation results, the following criteria have been used:

- Output error computed with the different models
- Hankel norm of the error systems defined by the differences between the estimated models and the true, simulated processes
- Frobenius norm of the error systems defined by the differences between the estimated models and the true, simulated processes

The results obtained from the tests can be summarized by the following conclusions (cf. fig. 5.2 - 5.5 and fig. 5.7 - 5.10):

- The output errors computed with the MPSSM models obtained from the Direct Estimation method are always the smallest
- The output error values obtained are almost equal to or slightly better than the output error values obtained with the FIR models estimated with EXACTMARK (cf. fig. 5.2 - 5.5)
- The estimation results obtained are the same for both sets of initial model parameters used (Gerth method and approximate realization from the block Hankel matrix)
- As can be expected from the fact that the estimated MPSSM will contain irrelevant modes that dissappear when an approximate realization is computed, both the Hankel norm and the Frobenius norm computed from the error systems determined on the basis of the approximate realizations of the estimated MPSSM models are always smaller than the norms computed from the error systems based on the estimated MPSSM models
- With one exception for system 3 (cf. fig. 5.9) the average values of the Frobenius norms of the error systems, defined by the difference between the approximate realization of the MPSSM model and the true system, are the smallest.
- The values obtained for both the Hankel norms and the Frobenius norms of the error systems based on the approximate realizations tested in chapter 4 (cf. section 4.6, fig. 4.14 - 4.17) are almost equal to the values obtained for the approximate realizations computed from the estimated MPSSM models, although the true processes did not fit in the MPSSM model sets used for the estimations with the Direct Estimation method.
- Estimation of MPSSM directly from input/output data requires quite some processor time due to the fact that a numerical minimization method has to be used for minimizing $V(\hat{a}_i,\hat{M}_i(\hat{a}_j)|\ i,j\epsilon I)$, $I=1,2,\ \ldots\ ,r$, with respect to the minimal polynomial coefficients $\hat{a}_i$. The average processor time used for an estimation of a MPSSM model was about 5 hours on a VAX 11/750 processor.
- For the estimation of MPSSM model parameters good initial values for the models parameters are required. The reason for this is that the cost function $V(\hat{a}_i,\hat{M}_i(\hat{a}_j)|\ i,j\epsilon I)$, $I=1,2,\ \ldots\ ,r$, is a high order polynomial function of the coefficients $\hat{a}_i$ (cf. eq. (5.58)). This polynomial function has many minima and convergence to the global minimum is not likely unless proper initial values for the parameters are used. Tests with zero initial values for the MPSSM model parameters have confirmed this conjecture. Tests with initial parameter values computed with the method of Gerth and initial parameter values computed with the algorithm of Zeiger and McEwen resulted in the same MPSSM models for all 20 estimations done for

each of the 4 systems (cf. fig. 5.6, table 5.1, fig. 5.1 - 5.5, fig. 5.7 - 5.10).

The method developed in this chapter for direct estimation of MPSSM model parameters from input/output data together with the computation of an approximate realization on the basis of the obtained MPSSM appears to be a promising method for modelling the dynamic behaviour of processes. In a next step the method will be tested on data obtained from real industrial processes to prove its value in industrial practice.

6. SIGNAL PREPARATION FOR THE IDENTIFICATION OF INDUSTRIAL PROCESSES

6.1 Introduction

In the preceeding chapters an identification method has been developed that allows the construction of a compact model of a MIMO process in a sequence of steps, with each step directed to improve the model on the basis of information obtained from previous steps. The method developed can very well be applied to the modelling of processes that can hardly be modelled from basic physical and chemical laws. It is not necessary that the process to be modelled belongs to the model sets chosen in the various steps. The ultimate model will be that model in the last chosen model set which can simulate outputs as closely as possible to the measured process outputs in a least squares sense. The selection of the model set is done on the basis of the accuracy of the model simulations wanted.

Because output error criteria are applied, only the process inputs are needed for these simulations. It is clear, however, that the quality of the simulations and, related to this, the quality of the process model will highly depend on the characteristics of the signals offered to the identification algorithms. The criterion used for the adjustment of the model parameters puts a penalty on deviations of simulated outputs from measured process outputs (cf. fig. 4.1). The quality of the model obtained will be governed by the disturbances present in the signals. Disturbances with a bad influence on the quality of the models are, for example, spikes, drifts, offsets, significant differences in powers of the various input and output signals. Because of their negative influence on the quality of the models and because almost all industrial process data will be corrupted by these types of 'noise', it is advisable to try to reduce these disturbances as much as possible. For this purpose dedicated signal processing techniques have been developed.

Another problem encountered in industrial practice is the presence of, often relatively long, time delays in the measured process transfers. If the signals applied to the identification algorithms are not corrected for these time delays, the delays have to be estimated by the algorithms. In most cases this implies that many extra parameters, corresponding to these time delays, have to be used for the modelling. This too has a deteriorating influence on the quality of the models ultimately obtained. Therefore it is preferred to estimate the time delays separately from the parameter identification and to correct the signals for the estimated time delays as far as possible.

This chapter describes techniques that have been developed to do the various signal manipulations required to improve modelling of industrial processes.
Section 6.2 gives a description of the method used for the removal of trends from signals without the introduction of unwanted signal components.
Section 6.3 pays attention to the removal of spikes from signals.
In section 6.4, the estimation of time delays is briefly reviewed.

Section 6.5 is used to describe tests for process non-linearity and to examine possibilities for linearization.
Section 6.6 is devoted to the subjects filtering and decimation of the process signals.
In section 6.7 some examples will be given to show the influence of the various signal manipulations on estimation results.

6.2 Trend determination and correction

In practical situations the (sub)process behaviour one wants to model for control purposes is mostly determined by a set of inputs and outputs that satisfy the following conditions:

- On-line measurement of the inputs and outputs must be feasible.
- The selected inputs should have a direct (short time delay) and, if possible, large influence on the process outputs.
- The inputs have to be available for manipulation.
- The inputs have to allow full control of the outputs.
- The permitted changes of the inputs have to enable measurable process responses with amplitudes and dynamic ranges that exceed those of the disturbances in the outputs.

The choice made with respect to the inputs does, in general, not include all process variables that influence the outputs selected. The inputs that have not been selected for the modelling may, however, contribute to the changes found at the outputs of the (sub)process. During the modelling these changes are considered as coloured output noise. Often the characteristics of these contributions to the output noise are known and in many cases the effects are slow variations of the outputs: trends. These trends have a bad influence on the quality of the model obtained from the identification due to the limited length of the data set used for the identification. In general only part of a period to a few periods of the trend signal will be present in the data interval used for the parameter estimation. To show this influence of limited sample size, the output signal of the process is split into two parts:

$$Y = Y_p + Y_{tr} \qquad (6.1)$$

with: Y_p - the process outputs without trend
Y_{tr} - the trend signal added to the process outputs

Consider for example the estimation of a FIR model. Using a least squares

estimation method, the model parameters are found by (cf. eq. (3.33)):

$$\hat{\Theta} = Y \cdot \Omega_m^t \cdot (\Omega_m \cdot \Omega_m^t)^{-1}$$

$$= Y_p \cdot \Omega_m^t \cdot (\Omega_m \cdot \Omega_m^t)^{-1} + Y_{tr} \cdot \Omega_m^t \cdot (\Omega_m \cdot \Omega_m^t)^{-1} \qquad (6.2)$$

The influence of the trend in the signal on the estimated parameters is given by the second term of eq. (6.2):

$$Y_{tr} \cdot \Omega^t = \left[y_{tr_k} , y_{tr_{k+1}} , \cdots , y_{tr_{k+l}} \right] \cdot$$

$$\begin{bmatrix} u_k^t & u_{k-1}^t & \cdots & u_{k-m}^t \\ u_{k+1}^t & u_k^t & \cdots & u_{k+1-m}^t \\ \cdot & \cdot & & \cdot \\ \cdot & \cdot & & \cdot \\ u_{k+l}^t & u_{k+l-1}^t & \cdots & u_{k+l-m}^t \end{bmatrix} \qquad (6.3)$$

$$= \left[\sum_{i=0}^{l} y_{tr_{k+i}} \cdot u_{k+i}^t , \sum_{i=0}^{l} y_{tr_{k+i}} \cdot u_{k+i-1}^t , \cdots , \sum_{i=0}^{l} y_{tr_{k+i}} \cdot u_{k+i-m}^t \right] \qquad (6.4)$$

In the limit case where $l \to \infty$ these sums will tend to zero because the trend signal is not correlated with the input signal. Owing to the fact that the spectrum of the trend may have significant components with wavelengths far below the test-signal period, and because of the low frequency components present in the input signal, the sums in eq. (6.4) will not be equal to zero and even can be rather large compared to Y_p if the amplitude of the trend is large. As a consequence, the trend signal may have a significant influence on the estimated model parameter values.

A possible approach to separate a trend from a signal is based on the determination of the trend by filtering the signal with a-low pass filter and subtraction of the obtained trend from the signal. However, filtering of the signal with a low pass filter introduces a phase shift between the original signal and the trend signal obtained (see fig. 6.1a). Subtraction of this shifted trend from the original signal leaves undesired signal components in the corrected signal (see fig. 6.1b). To overcome this problem the signal can be filtered twice: once with a causal low-pass filter and a second time with the corresponding anti-causal low-pass filter. The average of the sum of the two filtered signals obtained will not be shifted in phase any more compared to the original signal (see fig. 6.1c). Mathematically

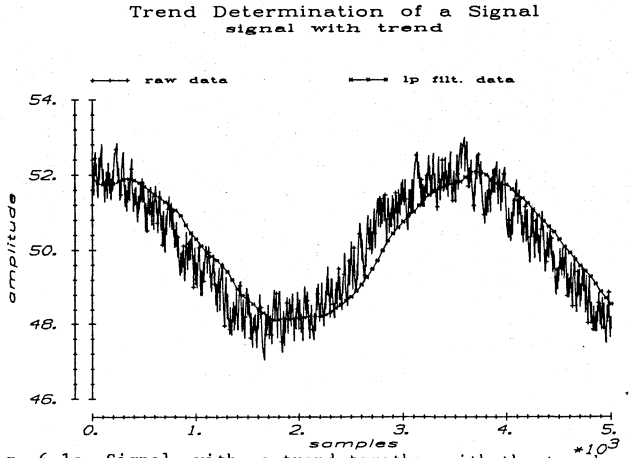

Fig. 6.1a Signal with a trend together with the trend computed by means of a low pass filter

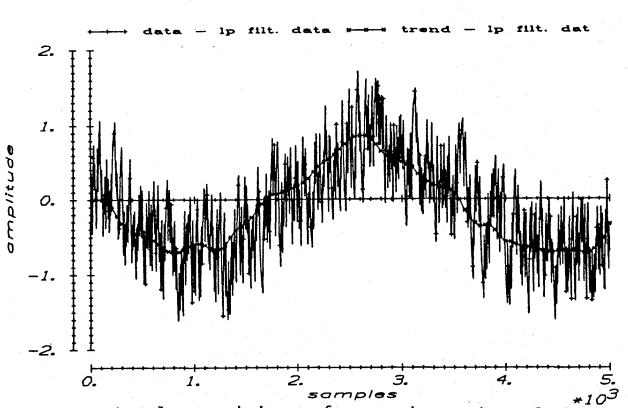

Fig. 6.1b Signal remaining after subtraction of the trend computed with a low pass filter.

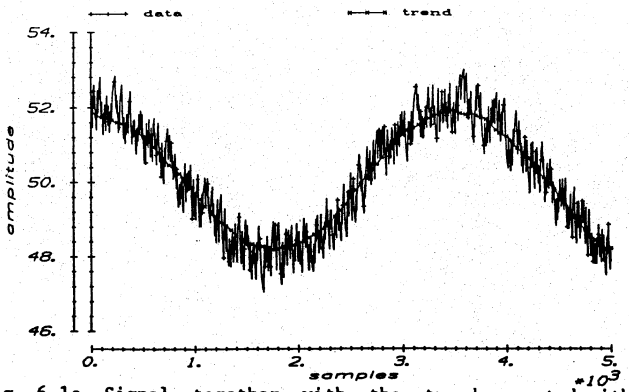

Fig. 6.1c Signal together with the trend computed with a filter that does not introduce a phase shift

this can be expressed by:

$$y_{tr_k} = \sum_{i=0}^{\infty} h_i^c \cdot y_{k-i} + \sum_{i=-\infty}^{-1} h_i^{ac} \cdot y_{k-i} = \boxed{\sum_{i=-\infty}^{\infty} h_i \cdot y_{k-i}} \qquad (6.5)$$

with: h^c the causal filter impulse response
h^{ac} the anti-causal filter impulse response

and:

$$h_i^c = h_{-i}^{ac} \qquad \text{for } 1 \leq i < \infty \qquad (6.6)$$

Subtraction of the trend signal obtained from eq. (6.5) from the original output signal results in eq. (6.4) being zero. Therefore the model obtained should no longer be a function of the trend signal caused by ignored input signals. The filter characteristic of the low-pass filter has to be designed so that the trends will be determined as accurately as possible and that no relevant process output signal information gets lost by the trend correction. In practice the filter design will almost always be a compromise between these two demands.

As can be seen from eq. (6.2), (6.3) and (6.4), offsets in the output signals have almost the same influence on the estimated parameters as a trend has. Also offsets at the input signals have a similar influence. Input signal offsets produce an output signal offset equal to the static gain of the process times the input offset signal.
Because of this influence also offsets need to be subtracted from the output signals and the input signals, especially since offsets on industrial data can be rather large compared to the signal changes used for the identification. A temperature in a glass melting tank may be considered as an example. The nominal value of such a temperature will be in the range up to 1600 ^{o}C, whereas the changes considered may be ± 1 ^{o}C.
The offsets can be included in the equation that describes the process input/output relation (cf. eq. (5.4)):

$$Y = M_{Kp} \cdot \Omega + \underline{Y_{os}} + N \qquad (6.7)$$

with: Y_{os} - matrix with the output offsets $\quad \dim[Y_{os}]: q \times (l+1)$

The offsets are assumed to be signal values that are constant in time. The changes due to the process dynamics are added to these offset levels. Therefore the offsets can be included in parameter matrix F_{Kp} by extending the parameter matrix with a first column containing the offset vector and

the input signal matrix with a first row of ones:

$$Y = \left[Y_{os} \quad F_{KP} \right] \cdot \begin{bmatrix} 1 & 1 & \ldots & 1 \\ & & \Omega & \end{bmatrix} + N \qquad (6.8)$$

As a result the offsets of the outputs can be estimated as an extra set of parameters. In practice, however, it is advisable to first subtract the main part of the offsets both from the input signals and from the output signals, because these offsets may be large and large offsets may lead to a loss of computational accuracy. The remaining offset can be included in the set of parameters to be estimated as indicated by eq. (6.8).

6.3 Peak shaving

Another problem often met in industrial practice is the disturbance of measured signals with spikes. These noise contributions may be introduced in the sensors and the (often long) leads from the sensors to the measuring equipment by switching actions of some high power process machinery. The amplitudes of these noise spikes, in general, are very large compared to the signal changes obtained from the process (cf. fig. 6.2a). Most of the time the spikes last from one sample to some tens of samples. If these spikes are not removed from the signals, they may form an important part of the noise energy. As a consequence the spikes can have a considerable influence on the ultimate model although they have no relation with the process itself. This a-priori knowledge has to be used for reducing the influence of the spikes. This can be done by signal treatment in the following four steps:

- Clip the signal amplitudes to values never reached by the real process signals (cf. fig. 6.2b):

$$\tilde{s}_k = f_{cl} \cdot s_k \qquad (6.9)$$

with: $\tilde{s}_k$ - the clipped signal

s_k - the measured signal corrupted with spikes

$$f_{cl} = \begin{cases} s_{max} \cdot \left(\frac{1}{s_k} \right) & \text{for: } s_k \geq s_{max} \\ 1 & \text{for: } s_{min} \leq s_k \leq s_{max} \\ s_{min} \cdot \left(\frac{1}{s_k} \right) & \text{for: } s_k \leq s_{min} \end{cases}$$

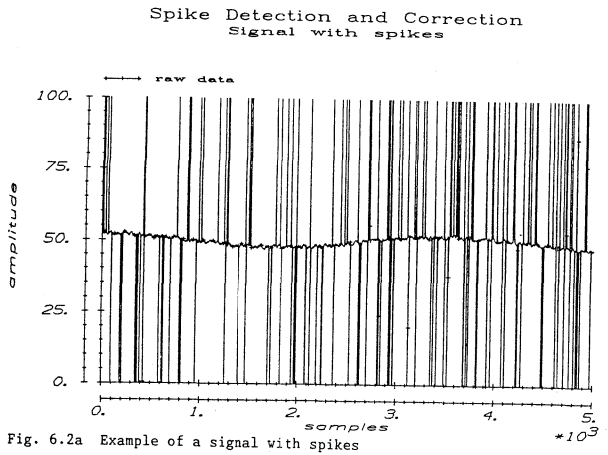

Fig. 6.2a Example of a signal with spikes

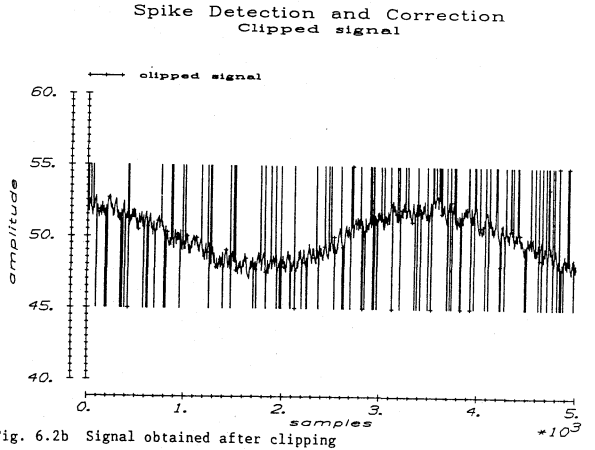

Fig. 6.2b Signal obtained after clipping

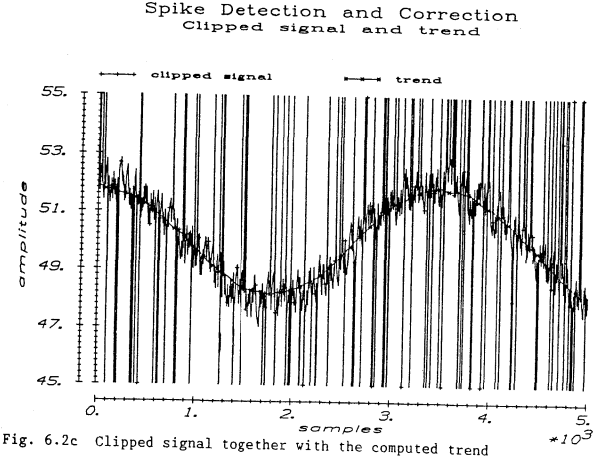

Fig. 6.2c Clipped signal together with the computed trend

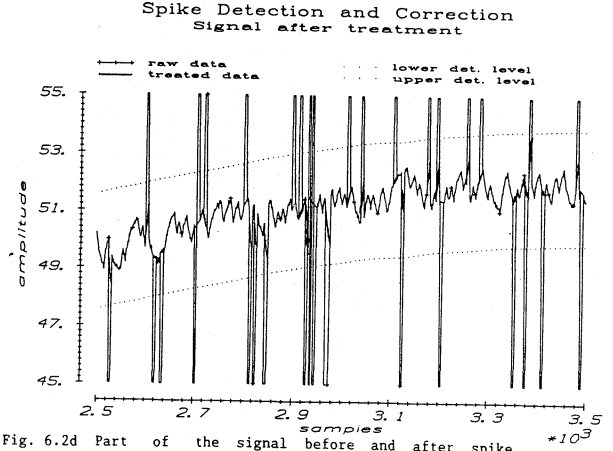

Fig. 6.2d Part of the signal before and after spike correction. Levels used to detect spikes are indicated by dotted lines.

- Compute a trend signal from the clipped signal as indicated in the previous section eq. (6.5) (cf. fig. 6.2c):

$$\bar{s}_k = \sum_{i=k-l}^{k} h_i \cdot \tilde{s}_{k-i} \qquad (6.10)$$

- Compute the standard deviation of the trend-corrected, clipped signal:

$$s = \sqrt{\sum_{i=0}^{l} \left(\tilde{s}_i - \bar{s}_i \right)^2} \qquad (6.11)$$

- Interpolate all samples of the original signal that are outside a band defined by the trend signal plus and minus α times the standard deviation obtained from the previous step (cf. fig. 6.2d). The permitted signal band is now given by:

$$x_k = \begin{cases} \bar{s}_k + \alpha \cdot s & \text{upper limit} \\ \\ \bar{s}_k - \alpha \cdot s & \text{lower limit} \end{cases} \qquad (6.12)$$

All consecutive sample values that are outside the permitted band are replaced by values obtained from a linear interpolation starting from the last accepted sample value and reaching to the first sample value within the permitted band after the spike.

In the last step the multiplication factor α has to be chosen such that no process signal values are outside the permitted signal range. The noise energy caused by the spikes is reduced significantly. Because of the interpolation the signal is kept at the average process signal level at those sample moments where no real process information is available. Using this signal treatment the influence of the spikes on the model ultimately obtained can be neglected.

6.4 Estimation of time delays

In industry one is often confronted with the problem that the signals to be used for process analysis and process modelling can only be measured with, sometimes significant, time delays. The measurement of tube dimensions in a tube glass production process may serve as an example. In this case the sensors used cannot withstand the high temperatures at the place where the shaping of the tube takes place. As a consequence, the tube dimensions can only be measured after the glass tube has reached a temperature the sensors can resist. This cooling takes time and this time will appear as an extra

time delay in the measured responses to applied process input signals. This type of transport delays occur in many processes.

If measured process responses contain time delays and if the signals are not corrected for these time delays before using them for process identification, the time delays have to be estimated as part of the process model. Although they are part of the model, the time delays do not contribute to the further description of the dynamic behaviour of the process. They just indicate after what times the responses at the outputs of the process are becoming perceptible after an input signal has been applied. Because the time delays involve extra model parameters (one extra Markov parameter for each delay sample), the number of parameters to be estimated increases when the modelling of the time delays has to be done by the identification algorithms. This increase in the number of parameters can be rather large if the delays are not modelled specifically, especially for the MPSSM model. The computational effort required for the modelling of the process will increase with the increased number of parameters to be estimated and the expected accuracy of the model will decrease because more parameters have to be estimated from the same data.
A good approach to overcome this time delay problem is estimation of the time delays separately from and prior to the model parameter estimation. The information obtained can then be used as a-priori knowledge to correct the measured process signals for these time delays as much as possible. Later, when the model is obtained, the time delays can easily be included in the model.
Estimation of the delays in process input/output transfers can be done with correlation techniques. One method is based on the analysis of the cross-correlation between process input and output signals. For this purpose the process under investigation is assumed to be ergodic. The input signal applied to the process is assumed to be a stationary, white, inter-channel independent, zero mean noise sequence with covariance matrix R:

$$E\{u \cdot u^t\} = R = \sigma^2 \cdot I_p \tag{6.13}$$

Then the autocorrelation function of the input signal becomes:

$$\psi_{uu}(\tau) = \lim_{l \to \infty} \frac{1}{l+1} \cdot \sum_{i=0}^{l} u_{i+\tau} \cdot u_i^t = \begin{cases} \sigma^2 \cdot I_p & \tau = 0 \quad (6.14a) \\ 0 & \tau \neq 0 \quad (6.14b) \end{cases}$$

Furthermore the input signal is assumed not to be correlated with the output noise signal. The process response to an arbitrary input signal may be written as:

$$y_k = \sum_{i=0}^{\infty} M_i \cdot u_{k-i} + n_i \tag{6.15}$$

The cross-correlation between process output and process input is given by:

$$\psi_{yu}(\tau) = \lim_{l\to\infty} \frac{1}{l+1} \cdot \sum_{i=0}^{l} y_{k+i+\tau} \cdot u_{k+i}^{t} \qquad (6.16)$$

Substitution of eq. (6.15) into eq. (6.16) gives:

$$\psi_{yu}(\tau) = \lim_{l\to\infty} \frac{1}{l+1} \cdot \sum_{i=0}^{l} \sum_{j=0}^{\infty} M_j \cdot u_{k+i+\tau-j} \cdot u_{k+i}^{t} +$$

$$\lim_{l\to\infty} \frac{1}{l+1} \cdot \sum_{i=0}^{l} n_{k+i+\tau} \cdot u_{k+i}^{t} \qquad (6.17)$$

Using the properties of the input signal u and the property that the input signal is not correlated with the output noise n, the following expression is obtained for the cross-correlation between outputs and inputs:

$$\psi_{yu}(\tau) = \sum_{j=0}^{\infty} \lim_{l\to\infty} \frac{1}{l+1} \cdot \sum_{i=0}^{l} M_j \cdot u_{k+i+\tau-j} \cdot u_{k+i}^{t} + \psi_{nu}(\tau)$$

$$= \sum_{j=0}^{\infty} M_j \cdot \psi_{uu}(j-\tau) \qquad (6.18)$$

In this expression the parameters M_j are the elements of the process impulse responses including the time delays. Substitution of eq. (6.14) into eq. (6.18) gives:

$$\psi_{yu}(\tau) = \sigma^2 \cdot M_\tau \qquad (6.19)$$

Consequently the cross-correlation function obtained will have the shape of the impulse responses in case the input signal is a stationary, white, inter-channel independent, zero mean noise sequence. Otherwise the cross-correlation function is the convolution of the impulse responses with the auto-correlation function of the input signal.

The time delays can be found from the cross-correlation function by looking for the beginning of a sequence of values that differ significantly from zero. Due to the finite length of the data sequence used for the computation of the cross-correlation function, the first elements of the computed cross-correlation function will not be equal to zero even if they represent a pure time delay. An example of a cross-correlation function obtained from real process data is given in fig. 6.3. The estimated time delay from this figure

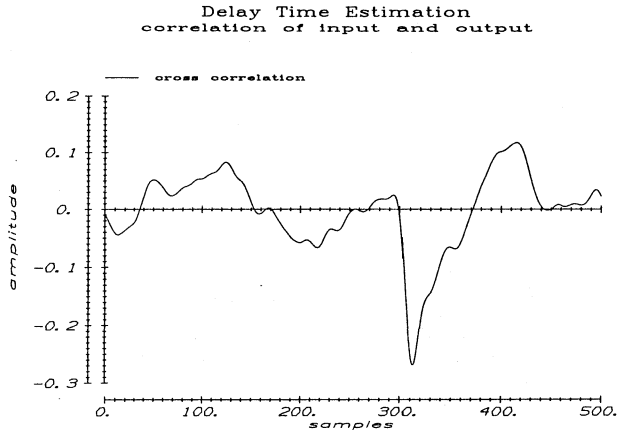

Fig. 6.3 Example of a cross correlation function computed from a finite set of input/output data of a tube glass production process. The input has been excited with a PRBN sequence.

is about 295 samples. Starting from sample 295 the figure is a noisy representation of the expected impulse response of the investigated input/ouput transfer.

For a process with p inputs and q outputs, in general, p·q different time delays will be found. Correction of the signals for the time delays is done by shifting the signals in time with respect to each other. Because only p + q signals are available only (p + q - 1) time delays can be compensated. The remaining delays have to be estimated as part of the model during the model parameter estimation.

6.5 Test for linearity

The methods developed here for modelling the dynamic behaviour of processes use linear models. No industrial process, however, is linear. An important step in the modelling process is the test whether the amplitude ranges applied to the process inputs are allowable without violating the assumption of linearity in practice. For a process to have a linear transfer the following condition has to be fulfilled (superposition theorem):

$$u_1 \rightarrow y_1 \quad \text{and} \quad u_2 \rightarrow y_2 \quad \Rightarrow \quad \alpha \cdot u_1 + \beta \cdot u_2 \rightarrow \alpha \cdot y_1 + \beta \cdot y_2 \qquad (6.20)$$

with: u_1 - input signal with an arbitrary amplitude ($u_1 \neq 0$)

y_1 - the process response to input u_1
u_2 - a second input signal ($u_2 \neq 0$)
y_2 - the process response to input u_2
α, β - arbitrary constants

A first test to be done is the test for steady state linearity of the process in the surroundings of the working point. If a process has non-linear steady-state responses then in most situations linearization is possible with simple linearizing polynomial functions.
A test signal that may be applied to each input of the process separately for testing steady-state linearity is the staircase signal (see fig. 6.4):

$$u_k = \alpha \cdot \sum_{i=0}^{s} [\, U(k-i\cdot\tau) - U(k-(s+1+i)\cdot\tau) - U(k-(2s+2+i)\cdot\tau) + U(k-(3s+3+i)\cdot\tau) \,] \qquad (6.21)$$

with: U(j) - a unit step at sample moment j

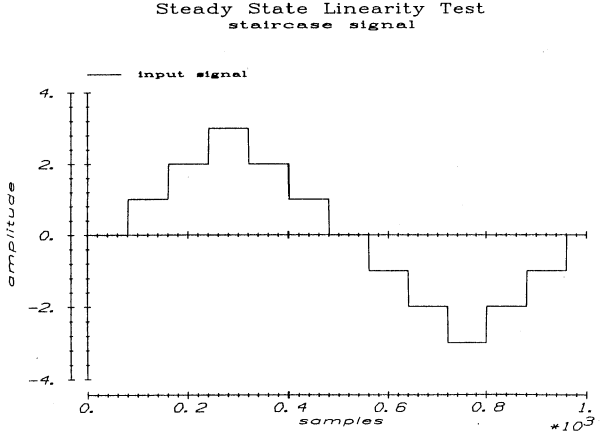

Fig. 6.4 Example of a staircase input signal that may be applied for steady-state linearity analysis of an input/output transfer of a process

The time interval τ between the steps must be chosen in accordance with the response time of the process. For the analysis of the steady-state behaviour

the process must reach a steady-state for each step applied. The maximum amplitude of the signal $(s+1)\cdot\alpha$ has to exceed the amplitude range that has to be covered by the model. Because each separate step in the signal has the same amplitude, also the responses to the different steps need to have the same amplitude if the process is steady-state linear. To test the linearity of the steady-state responses a polynomial can be fitted through the average steady-state amplitudes:

$$\beta_\mu \cdot u_j^\mu + \beta_{\mu-1} \cdot u_j^{\mu-1} \ \ldots + \beta_2 \cdot u_j^2 + u_j =$$

$$= \alpha_\nu \cdot y_i^\nu + \alpha_{\nu-1} \cdot y_i^{\nu-1} + \ldots + \alpha_1 \cdot y_i + \alpha_0 \qquad (6.22)$$

with: u_j - the scaled, offset corrected input signal at input j

y_i - the scaled, offset corrected, measured steady-state output signal at output i as a response to input u_j

According to eq. (6.22) the steady-state input/output behaviour of the system for the points measured has to satisfy:

$$\begin{bmatrix} u_j(0)^\mu & u_j(0)^{\mu-1} & \ldots\ u_j(0) & -y_i(0)^\nu & \ldots\ -y_i(0) & -1 \\ u_j(1)^\mu & u_j(1)^{\mu-1} & \ldots\ u_j(1) & -y_i(1)^\nu & \ldots\ -y_i(1) & -1 \\ \cdot & \cdot & \cdot & \cdot & \cdot & \cdot \\ \cdot & \cdot & \cdot & \cdot & \cdot & \cdot \\ u_j(2s+1)^\mu & u_j(2s+1)^{\mu-1} & \ldots\ u_j(2s+1) & -y_i(2s+1)^\nu & \ldots\ -y_i(2s+1) & -1 \end{bmatrix} \cdot$$

$$\begin{bmatrix} \beta_\mu \\ \beta_{\mu-1} \\ \cdot \\ \cdot \\ 1 \\ \alpha_1 \\ \cdot \\ \cdot \\ \alpha_0 \end{bmatrix} = P \cdot \beta = 0_{2s+1,1} \qquad (6.23)$$

with: $u_j(\iota)$ - the input amplitude of step ι of the staircase signal applied to input j

$y_i(\iota)$ - the steady-state amplitude at output i corresponding to input $u_j(\iota)$

α_K - polynomial coefficient corresponding to y_i^K

β_K - polynomial coefficient corresponding to u_j^K

In general, eq. (6.23) will not hold exactly if the order selected for the polynomials is less than the number of amplitude levels applied to the process. In that case polynomial coefficients have to be determined that satisfy (least squares approximation):

$$(P^t \cdot P \cdot \beta = 0_{2s+1,1} \qquad (6.24)$$

In most practical cases a third order polynomial will be sufficient as a describing curve. For example, a third order polynomial very well describes the beginning of saturation.

By comparing the polynomial terms $\beta_K \cdot u_j^K$ $(2 \leq K \leq k)$ and $\alpha_K \cdot y_i^K$ $(2 \leq K \leq 1)$ with the corresponding linear terms u_j and $\alpha_1 \cdot y_i$ for the maximum amplitude of the input signal, an impression is obtained of the steady-state non-linearity of the process in the direct surroundings of its working point. The coefficient α_0 is a measure for the offset remaining at the outputs.

Besides the steady-state non-linearities, also dynamic non-linearities have to be investigated. A similar test for dynamic non-linearities as the one discussed for the steady-state characterics is based on the same staircase test signal, but now as the envelope of an amplitude modulated sinusoidal signal. Application of similar test signals with different frequencies of the carrier wave, gives insight in the non-linearities at the different frequencies. The analyses discussed for the steady-state behaviour can also be done for the various frequency points. However, in practice linearization of dynamic non-linearities will be more difficult than linearization of static non-linearities.

Another test that can be used for the detection of dynamic non-linearities is based on the analysis of process responses on Pseudo Random Binary Noise (PRBN) sequences of different amplitudes. The cross-correlation functions of the applied PRBN input signals and the corresponding, measured process responses for the various amplitudes (cf. eq. (6.16) - (6.19)) give an impression of the behaviour of the process in response to different amplitudes. Non-linearities are indicated by significant changes in the computed correlation functions.

If non-linearities are found in the steady-state behaviour of the process, linearizing polynomial functions can be designed to linearize the behaviour. Most non-linearities encountered in practice are caused by sensors (e.g. thermocouples) and actuators (e.g. valves). Compensation for these

non-linearities can be done by application of a linearizing polynomial function to the corresponding output or input signal.
In practice many of these non-linearities appear to be linearized already by low-level control systems that are used for the closed loop control of primary functions in the process (cf. chapter 1, section 1.2). Practical experience shows that most processes can be considered to be linear in the direct surroundings of their working points.

For systems with the number of inputs, p, or the number of outputs, q, greater than one and different non-linearities in the various transfers, complete linearization, by application of linearizing polynomial functions (steady-state linearization) at the inputs and outputs, is not possible (cf. time delay correction). This can be seen from the set of equations that describe the steady-state transfer from the input of the input linearization block, u^*, to the output of the output linearization block y^* (cf. fig. 6.5):

$$y^* = L_o(y) = L_o\{F(u)\} = L_o[F\{L_i(u^*)\}] \tag{6.25}$$

$$= \begin{bmatrix} \sum_{\alpha=1}^{p}\sum_{\beta=1}^{q} l_{o_{1,\beta}}\{f_{\beta,\alpha}(l_{i_{\alpha,1}}(u_1^*))\} & \cdots & \sum_{\alpha=1}^{p}\sum_{\beta=1}^{q} l_{o_{1,\beta}}\{f_{\beta,\alpha}(l_{i_{\alpha,p}}(u_p^*))\} \\ \sum_{\alpha=1}^{p}\sum_{\beta=1}^{q} l_{o_{2,\beta}}\{f_{\beta,\alpha}(l_{i_{\alpha,1}}(u_1^*))\} & \cdots & \sum_{\alpha=1}^{p}\sum_{\beta=1}^{q} l_{o_{2,\beta}}\{f_{\beta,\alpha}(l_{i_{\alpha,p}}(u_p^*))\} \\ \vdots & & \vdots \\ \sum_{\alpha=1}^{p}\sum_{\beta=1}^{q} l_{o_{q,\beta}}\{f_{\beta,\alpha}(l_{i_{\alpha,1}}(u_1^*))\} & \cdots & \sum_{\alpha=1}^{p}\sum_{\beta=1}^{q} l_{o_{q,\beta}}\{f_{\beta,\alpha}(l_{i_{\alpha,p}}(u_p^*))\} \end{bmatrix}$$

with: L_i - the set of linearizing functions applied at the inputs
L_o - the set of linearizing functions applied at the outputs

As can be seen from this expression, a linearizing function applied to one specific input covers the transfers to all outputs and a linearizing function applied to an output signal of the system extends over the transfers from all inputs. In this case approximate linearizing functions have to be applied.

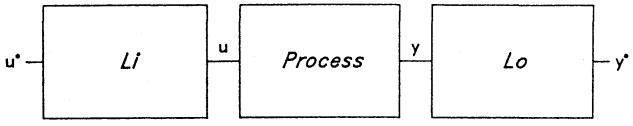

Fig. 6.5 Linearizing functions applied to the inputs and outputs of the process

6.6 Filtering and decimation

For modelling the dynamic behaviour of a process with identification techniques quite some experiments have to be done with the process. Experiments are required for getting the appropriate a priori information (e.g. relevant inputs and outputs, global dynamic properties of the transfers, sensitivities of outputs for input changes, disturbance characteristics, ...) and for collection of the process data that have to be used for the estimation of model parameters. It is very important that the information obtained from these experiments is reliable. To make sure that the collected process data represent the true process characteristics reliably, filtering of the data is required. Filtering has to prohibit aliasing effects and has to reduce influences of disturbances on the measured process signals. On the other hand filtering of the data may give rise to undesirable loss of relevant process data. Therefore the design of appropriate filters is an important step in the configuration of the measuring equipment.

As has been indicated in the previous sections quite some polishing of the signals is required to make it possible to find a good model for describing the process dynamics. All polishing actions carried out on the signals are directed to increase the ratio of relevant information on the process dynamics to disturbances blurring that information.
Many of the disturbances entering the recorded process signals do not have their sources in the process or even have not passed the process at all. Therefore these disturbances have no relation with the part of the signals

relevant for modelling the process. To reduce the influences of the disturbances two measures can be taken:

- Filter out all irrelevant information during the recording of the process data.
- Record extra information of the process in order to use part of that information to increase the ratio between relevant process information and blurring disturbances.

The first measure implies a filtering action, generally low-pass, applied to the recorded signals. The filters are designed such that only signals are passed in the frequency range that is relevant for the identification of the process dynamics. The design of the filters is based on a priori information on the bandwidth of the various transfers from inputs to outputs and on the noise characteristics at the outputs of the process. If this information is not available, it is determined via dedicated experiments.
The filters are also needed for making aliasing effects after sampling negligibly small.
The design of the filters is mainly governed by the following constraints:

- In the pass-band the filters are not allowed to have noticeable influence on the signal characteristics. In practice up to second order filters with a flat frequency response are used.
- The cut-off frequency of the filters has to be chosen so high that the filters do not introduce a significant damping at frequencies covered by the process dynamics.
- Disturbances at frequencies beyond the bandwidth of the process have to be removed as much as possible.

The second measure involves sampling of the process signals at a frequency higher than the frequency essentially needed for identification of the process. The sampling rate is chosen 5 to 10 times higher than the bandwidth of the process. Because in our case the test signals applied to the process are PRBN sequences, tuned to the process dynamics with respect to their frequency span, the recorded samples will have much redundancy that may be used for signal processing.

The signals recorded with this high sampling frequency will not contain much power at frequencies outside the baseband excited by the PRBN testsignal. If these signals are used for parameter estimation, problems occur at high frequencies. Especially at half the sampling frequency, problems are to be expected if the signals are immediately used for parameter estimation, because the input signals have but little power at this frequency, while the recorded output signals sometimes have considerable components at this frequency due to quantization effects. This generally implies that the obtained model will have poles with a negative real part. The gain at frequencies corresponding with these poles can become high if the input signal power is low compared to the power in the output signals at these frequencies. This implies that a reduction of the sampling frequency, in correspondence with the power contents of the PRBN test sequences used, is required before the signals are suited for parameter estimation.

The redundancy in the recorded signals is used for:

- Removal of trends and subtraction of average values of both input and output signals.
- Removal of spikes from the signals.
- Estimation and compensation of time delays.
- Scaling of the input and output signals.

After these signal manipulations have been carried out the signals have to be decimated to assure that the spectrum of the decimated input signals is flat. The decimation is executed in accordance with the characteristics of the PRBN input sequences applied to the process inputs. Of each step of the PRBN sequence at least one sample has to be retained. After the decimation step the data set has to consist of a set of input signals, that excite the process with equal power over its full frequency range, and the process responses corresponding with the applied process input signals. A convenient choice in practice for the decimation factor is 5 - 10. The redundancy in the recorded process signals is no longer needed as it has been used for the elimination of blurring information as far as possible.

The model obtained from process identification will only reflect the part of the process dynamics that was contained in the data used for the identification. For that reason it is very important to assure that information is included in the signals used for modelling of the process on the complete dynamic behaviour of the process that has to ber covered by the model (cf. [Eykhoff, 1974; Isermann, 1974]).

6.7 Scaling of signals and subtraction of average signal values

All identification methods discussed use the minimization of a cost function as a mechanism for the estimation of the model parameters (cf. eq. (3.10), (3.28), (5.10)). This cost function is a function of error signals obtained from process outputs and model outputs. The algorithms developed minimize the cost function by adjustment of the model parameters. This adjustment of the model parameters results in an adjustment of the outputs simulated by the model:

$$V = V(E) = V(Y - \hat{Y}) = V(Y - \hat{F} \cdot \Omega_m) \qquad (6.26)$$

with: $Y = [\, y_k \; y_{k+1} \cdots y_{k+1} \,]$ measured process outputs

$\hat{Y} = [\hat{y}_k \; \hat{y}_{k+1} \cdots \hat{y}_{k+1} \,]$ simulated model outputs

$$\Omega_m = \begin{bmatrix} u_k & u_{k+1} & \cdots & u_{k+l} \\ u_{k-1} & u_k & \cdots & u_{k+l-1} \\ \cdot & \cdot & & \cdot \\ \cdot & \cdot & & \cdot \\ u_{k-m} & u_{k-m+1} & \cdots & u_{k-m+l} \end{bmatrix}$$

$$\hat{F} = \begin{cases} [M_0 , M_1 , \ldots , M_m] & \text{FIR model} \\ [M_0 , M_1 , \ldots , M_r , F_{r+j}(a_i, M_i \mid i \in I) , \ldots , F_m(a_i, M_i \mid i \in I)] & \\ \qquad I=1,2, \ldots ,r & \text{MPSSM model} \end{cases}$$

In industrial practice not all inputs and outputs have the same order of magnitude. The figures obtained from the measurements are related to physical quantities, which, in general, even don't have the same dimension. The numerical values obtained for each of the measured quantities may differ significantly. For example, in a tube glass production process two important outputs, the tube diameter and wall thickness, may differ a factor 50 in magnitude. If these signals are used for the estimation of the model parameters by minimization of cost function V (eq. (6.26)) the signals with the highest numerical values will be considered as most important in the minimization process, because they contribute most to V.

Besides the differences in amplitudes of the signals also the nominal values or offsets of the signals may be a cause of problems. Sometimes the nominal value and the amplitude of the signal corresponding with the process dynamics differ several decades (cf. section 6.2). A melting tank for glass is a typical example. In a melting tank for glass nominal temperatures are about 1500 ^{o}C. Temperature changes related to the process dynamics are of the order of a few to a few tens of degrees. Loss of accuracy may occur due to the non zero nominal values of the signals (cf. eq. (6.2) and (6.4)). As indicated in section 6.2 offsets need to be subtracted from the signals. Estimation of offset residues (cf. eq. (6.8)) as an extra parameter vector may further improve the results.
After subtraction of the offset values the problem with respect to the differences in amplitudes of the various signals remains. If large differences in numerical values of the signals occur and no actions are taken to decrease such differences, the model obtained for the description of the process dynamics will be good for the input/output combination with the largest numerical values and bad for the input/output combinations with the smallest numerical values. Of course this is an undesired situation. The model looked for, in general, has to simulate all outputs with the same relative accuracy if possible. A way to solve this problem is by scaling of all inputs and outputs. If the signal to noise ratio is about equal for all outputs, scaling of the signals can best be done with respect to the power

contents of the signals, for the function that is minimized, in general, is related to the power of the error signal (e.g. cf. eq. (3.10), (5.10)). To make the power of all signals equal first the average power of each signal is determined. The average power of the dynamic part of the signals is equal to the variance of the signals. An estimate for the variance of a signal is given by [Kreyszig, 1970]:

$$s^2 = \frac{1}{I} \sum_{j=0}^{I} (x_j - \bar{x})^2 \qquad (6.27)$$

with: s^2 - estimate for the variance of signal x

$\bar{x}$ - average value of the signal x over all samples

To make the average power of each signal equal to one, each sample is divided by its standard deviation, i.e. the square root of the estimated variance eq. (6.27). As a consequence all outputs will be equally important for the identification algorithms and the relative accuracy of the various transfers will no longer depend on the signal amplitudes.

6.8 An example

To show the effects of the various signal treatments discussed in this chapter on identification results, a special data set is generated by a simulated, second order, two input, two output MIMO process with output disturbances consisting of white noise, spikes and trends. The simulated process data include most of the effects discussed. The characteristics of the simulated process (system 5) and the process data are given by:

$$x_{k+1} = F \cdot x_k + G \cdot u_k \qquad (6.28a)$$

$$y_k = H \cdot x_k + D \cdot u_k + y_{os} + y_{tr_k} + n_k + n_{sp_k} \qquad (6.28b)$$

with:

$$F = \begin{bmatrix} 0.87 & 0 \\ 0 & 0.93 \end{bmatrix} \qquad G = \begin{bmatrix} 5.0 & 0.5 \\ 0.75 & 0.5 \end{bmatrix}$$

$$H = \begin{bmatrix} 1.0 & 0.0 \\ 0.0 & 1.0 \end{bmatrix} \qquad D = \begin{bmatrix} 0.0 & 0.0 \\ 0.0 & 0.0 \end{bmatrix}$$

$u_k = \tilde{u}_k + u_{os}$; exogeneous input

$u_{os}^t = [40 \quad 150]$; input offset

$$y_{os}^t = [1000 \quad 50] \qquad ; \text{ output offset}$$

$$y_{tr_k}^t = [25 \cdot \sin(2 \cdot \pi \cdot k/7500) \quad 10 \cdot \cos(2 \cdot \pi \cdot k/3500)] \qquad ; \text{ output trend}$$

$$n_k^t = [\ 0.5 \cdot N_1(0,1) \quad 0.1 \cdot N_2(0,1)\ ]_k \qquad ; \text{ output noise}$$

$$n_{sp_k} = \begin{bmatrix} 150 \cdot N_3(0,1) \cdot U(\ abs(\ N_3(0,1) - 2.5)) \\ 300 \cdot N_4(0,1) \cdot U(\ abs(\ N_4(0,1) - 2.2)) \end{bmatrix}_k \qquad ; \text{ spikes}$$

$N_\alpha(0,1)$ - zero mean, white Gaussian noise with $\sigma^2 = 1$

$N_\alpha(0,1)_k$ - the sample generated by noise generator $N_\alpha(0,1)$ at sample moment k

$$U(x) = \begin{cases} 0 & x \leq 0 \\ 1 & x > 0 \end{cases}$$

The input signal applied to this simulated process for generating a input/output data set is a PRBN sequence with a clock frequency equal to 1/5 of the sample frequency. This redundancy in the signals allows the various signal treatments discussed without loss of relevant process information. The generated data set consists of 5000 samples.
To show the influence of the signal treatments on the ultimate model obtained from the identification, two FIR models are estimated on the basis of the simulated process input/output data using EXACTMARK (cf. chapter 3, section 3.6). The signal treatments done to prepare the data for parameter estimation are summarized in table 6.1 for both estimations. A '+' sign indicates that this treatment has been done a '-' sign is used to indicate that the signal treatment has not been done.

	first estimation	second estimation
offset correction	+	+
trend correction	+	-
spike correction	+	-
decimation	+	+
scaling	+	-

Table 6.1 Signal treatments done to prepare the data of the simulated process (System 5) for parameter estimation

For both identifications the data sets have been corrected for offsets. If this is not done and if no offset parameter is estimated, almost never a good model can be obtained. This is due to the fact that the model has to describe the dynamic properties of the process in the vicinity of its working point and, in general, the static gain for small amplitude changes in this environment will not be equal to the output offsets divided by the input offsets.

The results of the various steps are shown in fig. 6.6 - 6.11.
Fig. 6.6a - 6.6d give an overview of the input/output data. Fig. 6.6c and fig. 6.6d clearly show the disturbances -trends and spikes- on the output signals.

The first step executed is the computation of a trend of the signals (cf. section 6.2). To compute a trend from the data a low pass filter has to be designed that passes the frequencies of the trend without influencing frequencies that have to be covered by the process model. For this purpose a second order low pass filter with a double real pole is used, because such a filter has a nice flat frequency response characteristic and it only introduces smooth phase shifts. The filter is designed so that the highest trend frequency (about 1.5 period over 5000 samples) is hardly damped by the filter. The filter has a double real pole at $z \approx 0.99$. The characteristics of the used trend filter are given by:

$$y_k = a_1 \cdot y_{k-1} + a_2 \cdot y_{k-2} + b_0 \cdot u_k + b_1 \cdot u_{k-1} + b_2 \cdot u_{k-2} \qquad (6.29)$$

with: $a_1 = 1.98009966749$

$a_2 = -0.98019867331$

$b_0 = 0$

$b_1 = 0.496679133402 \cdot 10^{-4}$

$b_2 = 0.493378950759 \cdot 10^{-4}$

To keep errors in the static gain of the filter negligibly small computations with the filter have to be carried out in double precision. The trend found by applying this filter into two directions to the data (forward and backward) is given in fig. 6.7a and 6.7b (cf. eq. (6.5) and (6.6)). In these figures also the true simulated trend is plotted. Fig. 6.7c and 6.7d show the output signals together with the computed trends. As can be seen from these plots, the computed trend is not shifted in phase with the original signals. The computed trend closely follows the true trend in the output signals.
Fig. 6.8a and 6.8b show the output signals after subtraction of the computed trends.

The next step in the signal treatment is the removal of the spikes present in the output signals. For this purpose the algorithm described in section 6.3 is used (cf. eq. (6.9) - (6.12)). Clip levels for both outputs are

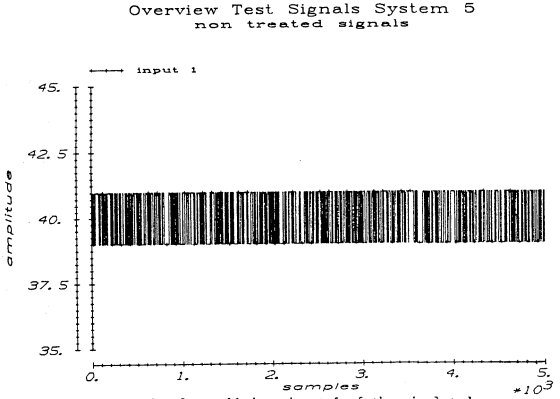

Fig. 6.6a Input signal applied to input 1 of the simulated process System 5

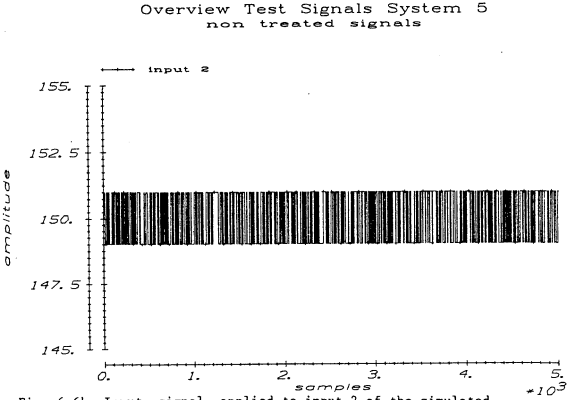

Fig. 6.6b Input signal applied to input 2 of the simulated process System 5

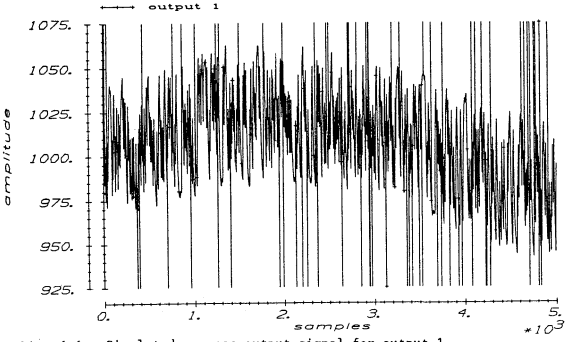

Fig. 6.6c Simulated process output signal for output 1

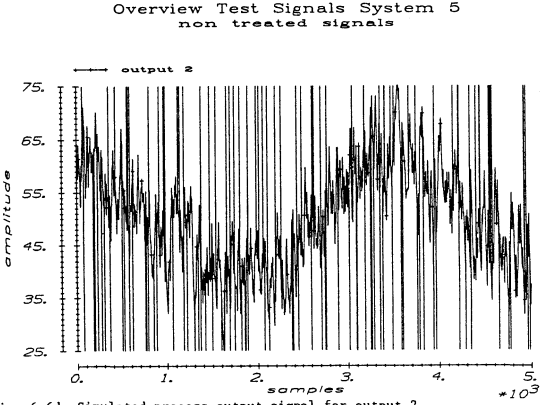

Fig. 6.6d Simulated process output signal for output 2

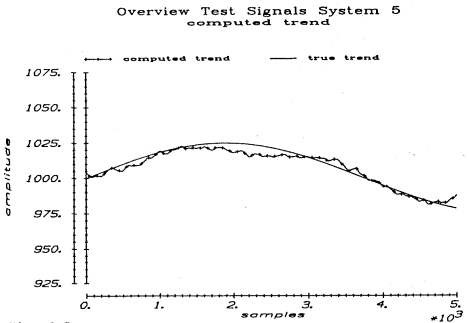

Fig. 6.7a Both the computed and the true trend signal of output 1

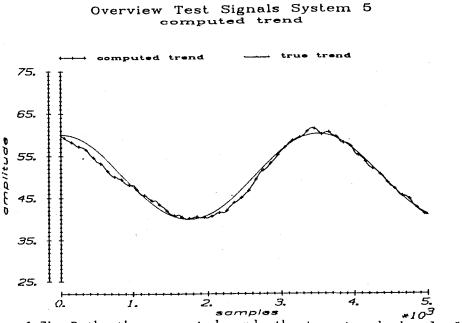

Fig. 6.7b Both the computed and the true trend signal of output 2

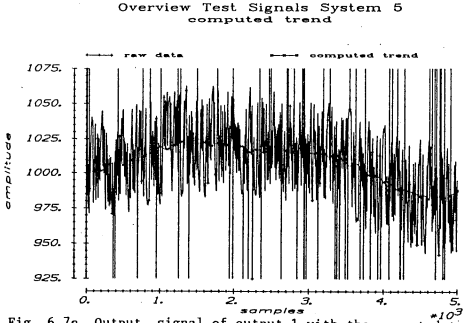

Fig. 6.7c Output signal of output 1 with the computed trend signal

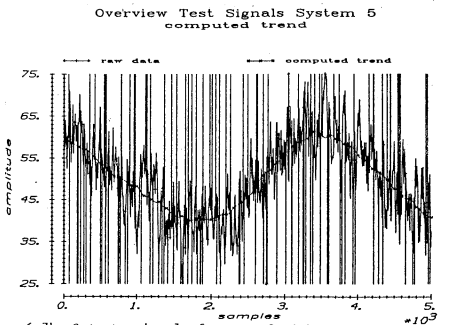

Fig. 6.7b Output signal of output 2 with the computed trend signal

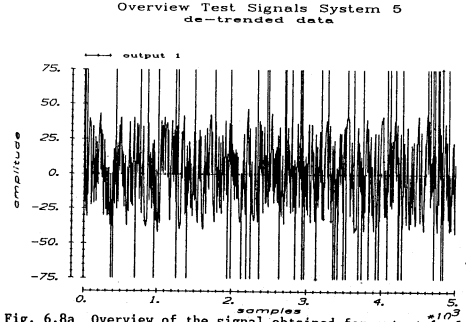

Fig. 6.8a Overview of the signal obtained for output 1 after trend correction

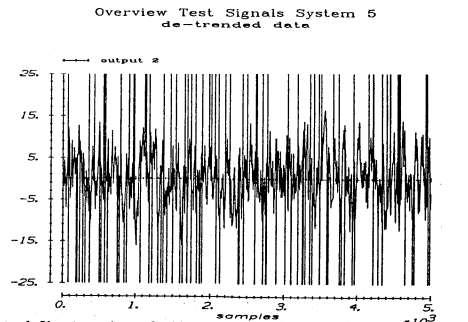

Fig. 6.8b Overview of the signal obtained for output 2 after trend correction

determined from the plots on the basis of the recorded process responses (cf. fig. 6.8a and 6.8b). The parameters used for the detection and removal of spikes are:

- amplitude levels used to clip the output signals at (cf. eq. (6.9)):
  output 1 +/- 75
  output 2 +/- 35
- for the determination of the signal trend in this case the same low pass filter is applied as for the computation of the trend (cf. eq. (6.29))
- width of the band used around the computed trend to detect spikes (cf. eq. (6.12)):
  output 1 +/- 55
  output 2 +/- 25

Fig. 6.9a and fig. 6.9b show the results obtained after peak shaving. As can be seen all spikes are removed from the signals.

As can be seen from fig. 6.9a and fig. 6.9b there is about a factor 5 difference in the amplitude levels of both output signals. The next step executed is the removal of the remaining average values of both the input and the output signals and to scale the resulting signals by dividing the signals by their computed standard deviation. Fig. 6.10a and 6.10b show the obtained output signals.

The last step executed before the signals are applied to the parameter estimation algorithm is decimation of input and output signals. In agreement with the ratio of the sample frequency and the clock frequency of the applied PRBN input signal sequences, of each 5 samples of each signal only one sample is retained in this step. Of the obtained data set consisting of 1000 input/output samples, the first and the last 50 samples are not used. This is done because these samples are contaminated by the influences of improper initial conditions of the filters during the various filtering actions applied to the signals to do the signal processing.

The signals obtained after these steps are used for the first estimation of a FIR model (cf. table 6.1).

To be able to compare the estimated models with the original system used for the simulation of the input/output data both the true system model and the model obtained from the estimation on the treated input/output data have to be transformed.
First the true system is transformed in accordance with the decimation of the signals. This transformation implies an oversampling with a factor 5.

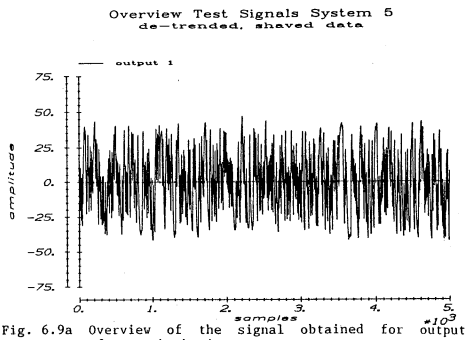

Fig. 6.9a Overview of the signal obtained for output 1 after peak shaving

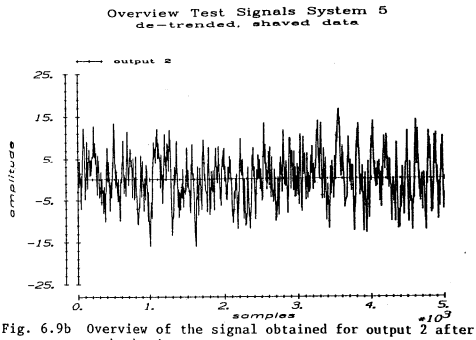

Fig. 6.9b Overview of the signal obtained for output 2 after peak shaving

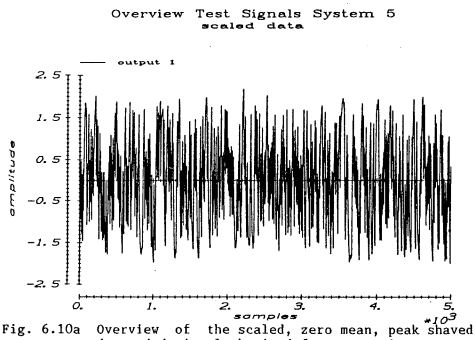

Fig. 6.10a Overview of the scaled, zero mean, peak shaved, detrended signal obtained for output 1

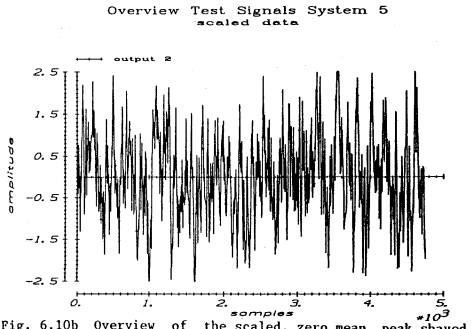

Fig. 6.10b Overview of the scaled, zero mean, peak shaved, detrended signal obtained for output 2

The model obtained after oversampling is given by:

$$x_{k+1} = F_1 \cdot x_k + G_1 \cdot u_k \qquad (6.30a)$$

$$y_k = H_1 \cdot x_k + D_1 \cdot u_k \qquad (6.30b)$$

with:

$$F_1 = \begin{bmatrix} 0.498 & 0.0 \\ 0.0 & 0.696 \end{bmatrix} \qquad G_1 = \begin{bmatrix} 19.2915 & 1.9292 \\ 3.2605 & 2.1737 \end{bmatrix}$$

$$H_1 = \begin{bmatrix} 1.0 & 0.0 \\ 0.0 & 1.0 \end{bmatrix} \qquad D_1 = \begin{bmatrix} 0.0 & 0.0 \\ 0.0 & 0.0 \end{bmatrix}$$

Next the model estimated on the basis of the treated input/output data has to be transformed in accordance with the scaling done on the signals. This implies that each entry of the estimated Markov parameters has to be multiplied with the product of input and output scaling factors belonging to that entry.

For the second FIR model parameter estimation data are used of which the average values for both input and output signals are subtracted. The signals also have been decimated the same way as the trend and spike corrected data (cf. table 6.1).

Fig 6.11a, 6.11b, 6.11c and 6.11d give an overview of the various impulse responses obtained. From these figures its clear that the impulse responses estimated on the basis of the data of which trends and spikes have not been removed, in general, do not resemble the true systems impulse responses. The only impulse response that still is not too bad is the impulse response that describes the transfer of input 1 to output 1. This is the transfer with the largest amplification factor. The impulse responses obtained from the treated data are quite good. All impulse responses of the 2 input 2 output system are estimated equally well.

6.9 Concluding remarks

In this chapter some methods have been discussed for the preparation of process data in order to improve estimation results that can be obtained on the basis of these process data. Most of the steps discussed are directed to gain a-priori information on the process behaviour and to use the obtained a-priori information for an improvement of the ratio of relevant and irrelevant data for the estimation of model parameters.

The signal treatment steps that have been discussed are:

- trend determination and correction
- spike detection and removal
- time delay estimation and correction of input/output data for estimated time delays
- linearity tests and steady-state linearization
- filtering and decimation of the data
- scaling of the signals and subtraction of average signal values

In an example it has been shown that, although the signals are contaminated with all kinds of disturbing effects, quite good estimation results can be obtained by applying the appropriate signal treatment (cf. section 6.8, fig. 6.11a - 6.11d). It has been demonstrated that incomplete treatment of the signals may lead to a useless model.

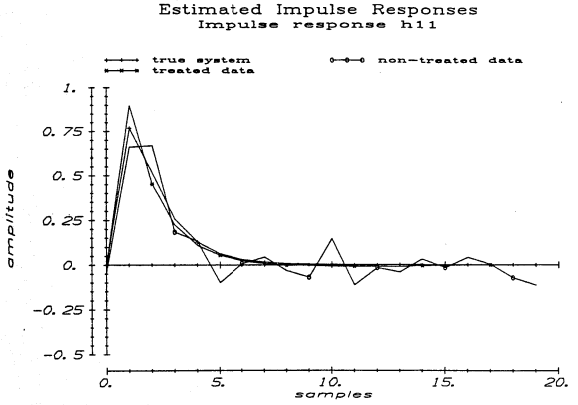

Fig. 6.11a Impulse responses h_{11} obtained for simulated process system 5

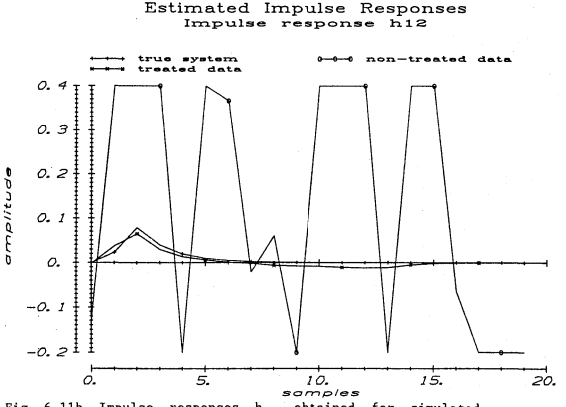

Fig. 6.11b Impulse responses h_{12} obtained for simulated process system 5

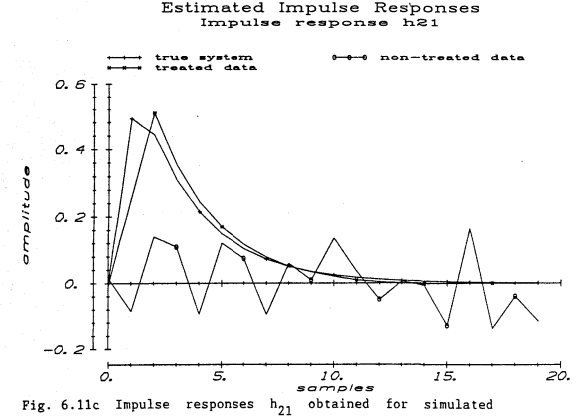

Fig. 6.11c Impulse responses h_{21} obtained for simulated process system 5

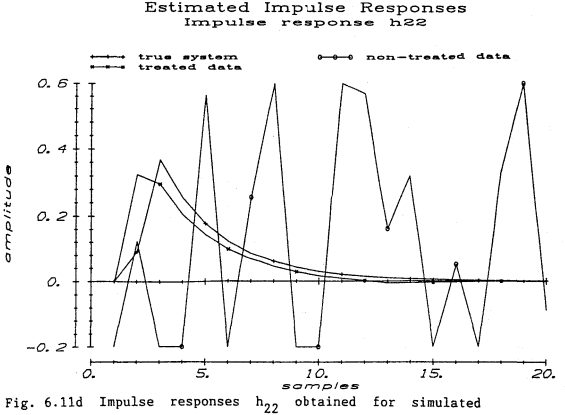

Fig. 6.11d Impulse responses h_{22} obtained for simulated process system 5

The most important conclusions with respect to the preparation of signals for parameter estimation are:

- In general it will not be possible to correct input/output data for all time delays because of a lack of degrees of freedom (cf. section 6.4) if the number of transfers p·q exceeds the sum of inputs and outputs
- In general not all steady-state non-linearities can be corrected completely due to a lack of degrees of freedom (cf. section 6.5)
- Scaling of input/output data to the same average signal power results in equal weighting during parameter estimation of all transfers from inputs to outputs under the condition that all measured output signals have the same signal to noise ratio
- Careful signal treatment higly improves estimation results (cf. section 6.8)

For most industrial data, collected for process identification, preparation of the signals as discussed in this chapter will be necessary to enable the acquisition of meaningful results.

7. APPLICATION OF THE DEVELOPED IDENTIFICATION METHOD TO GLASS PRODUCTION PROCESSES

7.1 Introduction

The identification method developed in the preceeding chapters has been applied for the modelling of the dynamic behaviour of several, different industrial processes. In this chapter the results of two applications will be discussed.
The first process of which the results are described is the shaping part of a Vello tube glass production process. Results similar to the results obtained for the Vello process have been obtained for the shaping part of a Danner tube glass production process (cf. [Wertz, 1987]). The second process of which the results are discussed is the conditioning part of a production installation for melting glass: a feeder.
In this chapter all executed steps to come from raw, measured process data to the validation of the obtained models will be discussed.

Section 7.2 gives a short description of the processes.
In section 7.3 the preparation of the signals for process identification and model validation is discussed (cf. chapter 6).
Section 7.4 describes the estimation of the FIR models with the EXACTMARK algorithm (cf. eq. (3.43)) on the basis of the prepared input/output data obtained in section 7.3.
Section 7.5 gives an overview of the order estimation and the fit of an initial MPSSM model to the estimated FIR models by application of the method of Gerth (cf. chapter 4, section 4.4).
Section 7.6 shows the results obtained with the Direct Estimation algorithm. The MPSSM model parameters obtained in section 7.5 are used as initial values for the direct estimation of the MPSSM model parameters on the basis of the prepared input/output data (cf. chapter 5, section 5.3).
Section 7.7 is devoted to the validation of the identified models. For the model validation input/output data are used that are different from the data used for the parameter estimation. However, the preparation of the data used for model validation has been done in accordance with the preparation of the data used for parameter estimation.
In section 7.8 some final conclusions will me given with respect to the results obtained from the identifications of the processes.

7.2 Process descriptions

The first process analysed is the shaping part of a tube glass production process.
Fig. 7.1 gives an outline of the most important part of the process. Shaping of the tube takes place at and just below the mandril. The shape of the tube is determined by two important parameters:

- average tube diameter
- average tube wall thickness

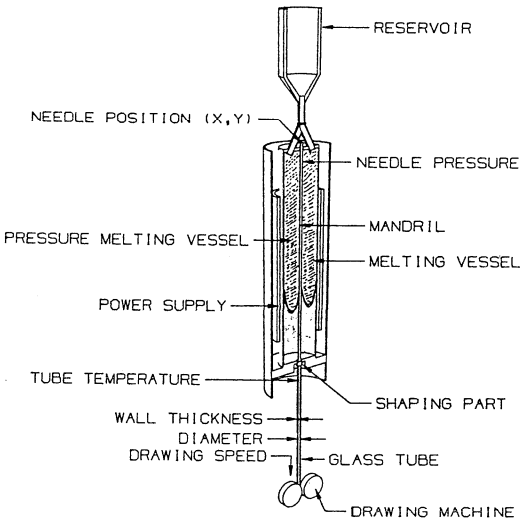

Fig. 7.1 Outline of the tube glass production process

Both dimensions (diameter and wall-thickness) are influenced by many process parameters. Process parameters that directly influence the shaping of the tube are:

- the mandril pressure
- the drawing speed
- the power applied to melt the glass
- the pressure in the melting vessel
- the composition of raw materials

The two process parameters that can be influenced most easilily and that affect the shaping of the tube most directly with the shortest delay times and over the largest frequency range, are the mandril pressure and the drawing speed.
With these two inputs it is possible to influence both diameter and wall-thickness independently.
The tube glass production process truly is a MIMO process:

- Increase of the mandril pressure results in an increase of the diameter and, simultaneously, in a decrease of the wall thickness of the tube

- Increase of the drawing speed results in a decrease of both diameter and wall thickness of the tube

The shaping part of the tube glass production process is a distributed parameter system. Shaping of the tube takes place in an area where the glass is weak. In the physical description of the shaping of the tube two partial differential equations play an important role:

- The first partial differential equation describes, as a function of mandril pressure and drawing speed for each position in the glass the flow of the glass from the mandril to form a tube with specific dimensions. In this partial differential equation the viscosity of the glass is an important parameter. The viscosity of the glass is a function of the temperature of the glass.
- The second partial differential equation describes the temperature distribution in the glass as a function of the energy input. The speed of the glass as a function of the position and as a function of time is an important parameter in this partial differential equation.

The model that is obtained from the physical description of the process describes the shaping of the tube entirely over the full range of all possible working points. However, the physical model has some parameters included that are not known for the various working points.
For control of the process only a model is required that describes the input/output behaviour of the process in the vicinity of its working points.
It is clear that the input/output transfer of this process can not exactly be described with a linear, lumped parameter model as used in the process identification method developed. However, we are going to try to find a model that properly describes the process dynamics in direct surroundings of a working point. For the modelling the developed identification tools will be used. The model finally obtained may be considered to be an approximation of the partial differential equations with a set of normal, linear differential equations in some point of application. The point of application is considered to be the point where the shaping of the tube mostly takes place. It is clear that the process surely does not belong to the model sets used for the identification.

The second process that is modelled with the developed identification tools is a feeder (cf. fig. 7.2). A feeder is the final part of a process installation that is used for melting glass. The feeder is the part of the production installation in which the glass is conditioned for further processing. The main task of a feeder is to realize a homogeneous temperature distribution of the glass at some absolute level that allows shaping of the glass. To realize a homogeneous temperature distribution of the glass that leaves the furnace, a feeder is divided into several sections in which energy can be supplied to the glass or extracted from the glass. To realize a homogeneous temperature distribution in the glass the transport of energy through the glass is important. Two mechanism take care of the

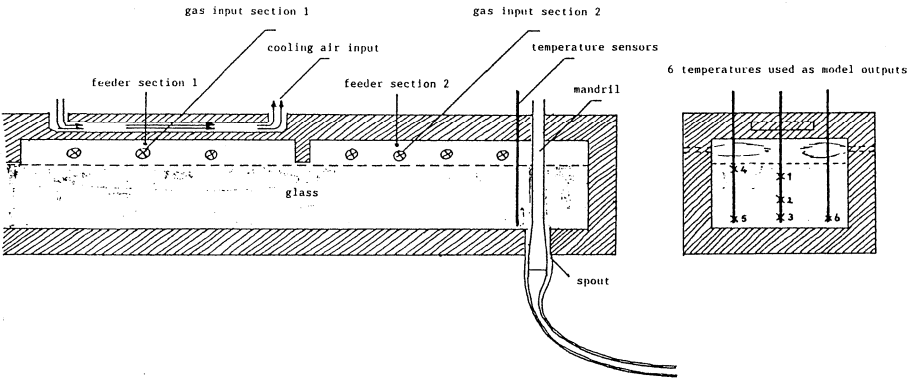

Fig. 7.2 Outline of a feeder

energy transport through the glass:

- radiation
- convection

The temperature distribution through the glass is a function of the speed of the glass, of the energy transport through the glass by radiation, of the energy exchange at the surfaces of the glass with its environment and of time. The velocity distribution of the glass in a cross section of the feeder is governed by the viscosity of the glass. The viscosity of the glass is a non-linear function of the temperature.
The model looked for has to describe the dynamic relations between the inputs of the feeder -burners and cooling air in the various sections- and some feeder temperatures close to the outlet (the "spout") of the feeder that have been selected as outputs. The selected temperatures are temperatures of the glass measured at some points in a cross section of the feeder just before the spout. The points are selected so that they give a good overview over the temperature distribution over a cross section of the feeder close to the spout.
Again, the process is a distributed parameter system that is modelled with a lumped parameter model. Also for this process will hold that the process certainly will not be contained in the model sets used for the process identification. The identified model has to describe the dynamic properties of the transfers of the process inputs to the various temperatures in direct surroundings of the working point in which the process has been operated during the measurements.

7.3 Signal preparation

Before the signals obtained from the processes can be used for the estimation of model parameters they have to be cleared up. All kinds of disturbances that entered the process signals during the experiments and that do not have a direct relation with the applied test signals have to be extracted from the signals. To enable treatment of the signals with the techniques described in chapter 6 without loss of information required for the estimation of model parameters, the sample frequencies of the experiments have been chosen higher than needed for the parameter estimations.
In section 7.3.1 the most important signal treatment steps will be described that have been carried out on the process signals obtained from the tube glass production process in preparation of the process identification.
Section 7.3.2 gives the results of the signal processing of the signals obtained from the feeder.

7.3.1 Preparation of the signals of the tube glass production process for parameter estimation

For the identification of the shaping part of the tube glass production process independent PRBN sequences have been applied simultaneously to both selected inputs of the process. The amplitude levels, sample time and clock frequency of the PRBN sequence have been determined on the basis of earlier obtained a-priori information on the dynamic behaviour of the process.

Fig. 7.3a - 7.3d give an overview of the applied test signals and the measured process responses that are to be used for the process identification. The data set consists of 12500 samples. The ratio between the sample time used and the clock frequency of the applied PRBN sequences is 5. The redundancy in the signals is required for the processing of the data in preparation of the parameter estimation (cf. chapter 6, section 6.6).
The amplitudes of the applied input signals are chosen so that both outputs have a ratio of the average noise power to the average signal power of a same order of magnitude.
Values for the noise to signal ratios have been computed from the ratio of the average power of measured responses of the wall thickness and diameter without excitation of mandril pressure and drawing speed and measured changes of the outputs with the PRBN signals aplied to the inputs. For the computation of the noise to signal ratios low frequency disturbances have been removed from the signals using the same trend correction as applied to the data used for the parameter estimation (cf. chapter 6, section 6.2).
Estimated values for the ratios of the average noise power and the average signal power (N/S) and for the values obtained for the standard deviations (s) are given in table 7.1. The values have been computed from 8 data sets of 2500 samples each.

	average N/S	s
output 1	0.1519	0.0671
output 2	0.0196	0.0066

Table 7.1 Values obtained for the average noise power to the average signal power ratios with their estimated standard deviations

As can be seen from fig. 7.3c and 7.3d both outputs have a trend. This trend is not caused by the applied process inputs, but by a drift of the glass temperature during the experiment.

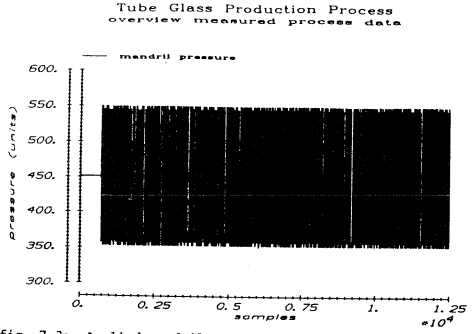

fig. 7.3a Applied mandril pressure (input 1)

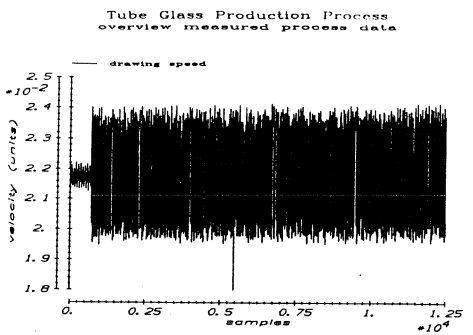

fig. 7.3b Applied drawing speed (input 2)

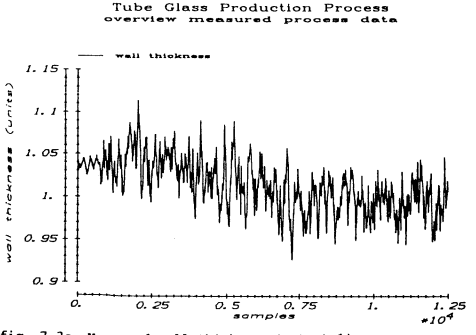

fig. 7.3c Measured wall thickness (output 1)

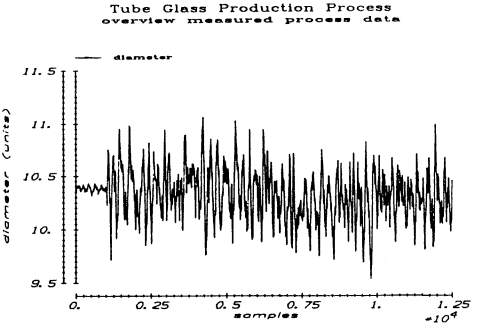

fig. 7.3d Measured diameter (output 2)

The trend is removed from the signals by making use of the method described in chapter 6, section 6.2. The low pass trend filter is designed so that the frequencies corresponding with the trend are passed without damping by the filter. The time constant of the second order filter with double real poles is about equal to 750 samples. The characteristics of the filter are (cf. eq. (6.29):

$- b_0 = 0.0$

$- b_1 = 0.88809916035104 \cdot 10^{-6}$

$- b_2 = 0.88731008962561 \cdot 10^{-6}$

$- a_1 = 1.9973351103213$

$- a_2 = -0.9973368857305$

Fig. 7.4 shows the detrended signals.

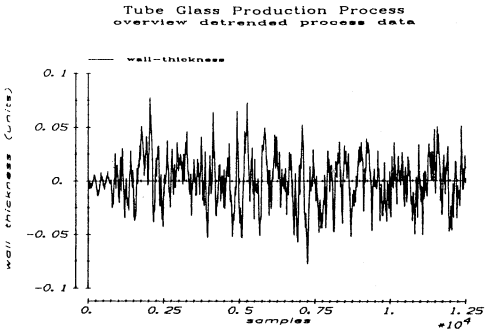

fig. 7.4a Wall thickness signal after removal of the trend

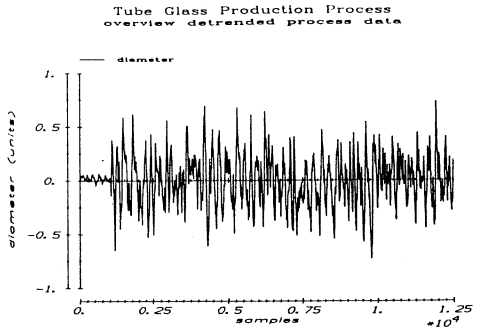

fig. 7.4b Diameter signal after removal of the trend

As can be seen from the plots no spikes are present on the data. The signals only have quite different amplitudes. The signal treatment still required therefore is subtraction of the average signal values and scaling of the signals to an average power one (cf. chapter 6, section 6.7). Fig. 7.5 shows the obtained detrended, zero mean, scaled data.

For the estimation of the delay times the cross correlations between inputs and outputs are computed (cf. chapter 6, section 6.4). For an estimation of the delay times present in the various transfers the data presented in fig. 7.3 is used. Fig. 7.6 gives an overview over the obtained cross correlation functions. As estimates for the delay time the last extremes before the rough estimates of the impulse responses in the obtained cross correlations are used.

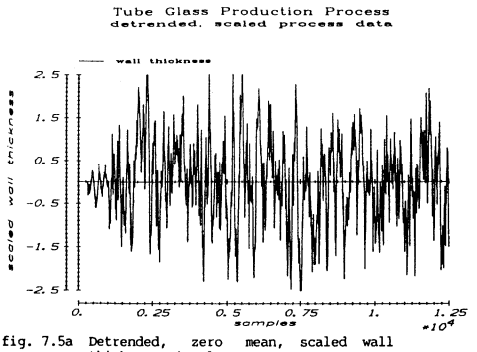

fig. 7.5a Detrended, zero mean, scaled wall thickness signal

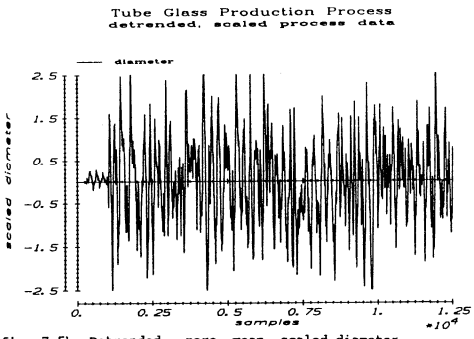

fig. 7.5b Detrended, zero mean, scaled diameter signal

From the computed cross correlations the following estimated time delays are found in the 4 transfers from inputs to outputs:

- Mandril pressure to wall thickness: 22 samples
- Mandril pressure to diameter: 287 samples
- Drawing speed to wall thickness: 39 samples
- Drawing speed to diameter: 294 samples

Especially the delay times from both inputs to the diameter are rather large. This is due to the fact that the distance between the place where the shaping of the tube occurs and the position of the diameter sensor compelled by necessity had to be large.
On the basis of the estimated delay times the process data are corrected. Only three delay times can be fully compensated for, because only three degrees of freedom are available for shifting data against each other. To compensate for the delay times three signals (i.e. mandril pressure, wall thickness and diameter) are shifted back. The number of samples used for shifting back the various signals are:

- mandril pressure: 7 samples
- wall thickness: 29 samples
- diameter: 294 samples

This implies that in the transfer from drawing speed to wall thickness 10 samples of delay time are not compensated and, consequently, still have to be estimated by the identification algorithms. The choice made with respect to the compensation of the signals for delay time compensation is arbitrarily. The remaining delay time in the transfer from the drawing speed input to the wall thicknes output expressed in samples after decimation will be 2.

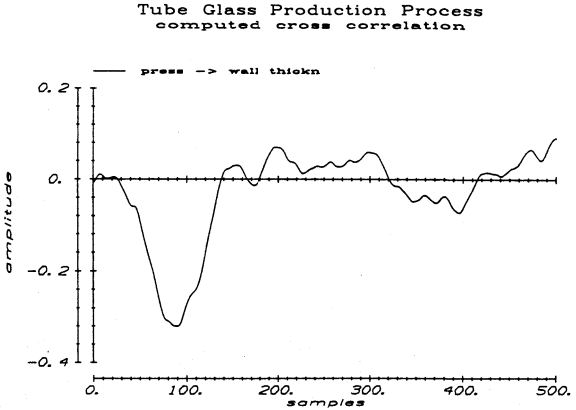

fig. 7.6a Computed cross correlation of the mandril pressure, excited with a PRBN signal, and the measured wall thickness response

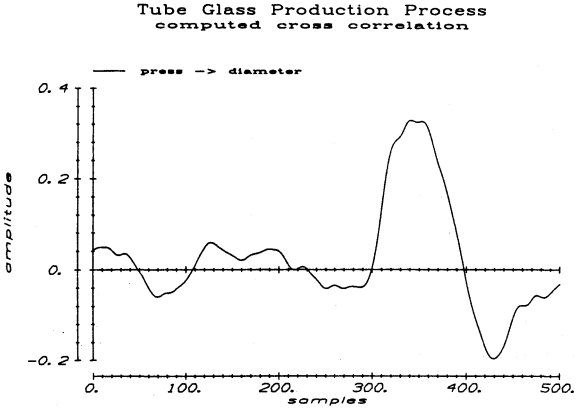

fig. 7.6b Computed cross correlation of the mandril pressure, excited with a PRBN signal, and the measured diameter response

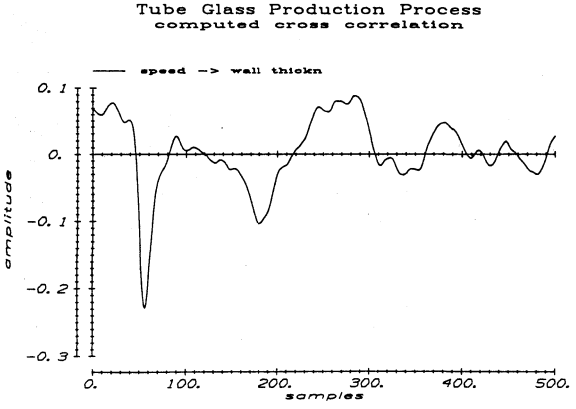

fig. 7.6c Computed cross correlation of the drawing speed, excited with a PRBN signal, and the measured wall thickness response

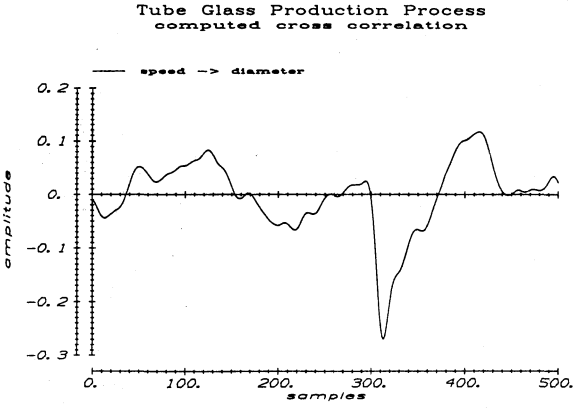

fig. 7.6d Computed cross correlation of the drawing speed, excited with a PRBN signal, and the measured diameter response

The final step in the preparation of the data for the estimation of model parameters is decimation to get rid of the redundancy in the signals that is no longer wanted. For decimation of the signals a data reduction factor 5 is used. This implies that of every 5 original samples only one sample is retained (cf. chapter 6, section 6.6). Fig. 7.7 gives an overview of the first 1250 samples of the signals finally obtained after all signal processing steps.

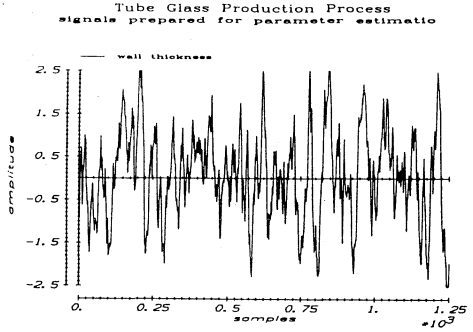

fig. 7.7a Wall thickness signal obtained after trend removal, subtraction of average value, scaling, correction for delay time and decimation

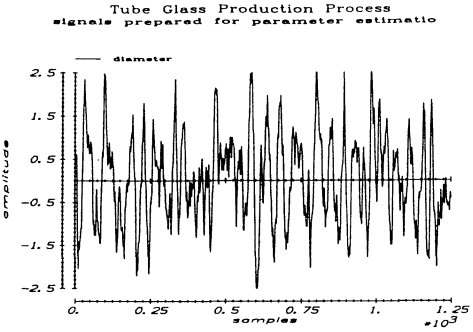

fig. 7.7b Diameter signal obtained after trend removal, subtraction of average value, scaling, correction for delay time and decimation

7.3.2 Preparation of the feeder signals for parameter estimation

For the identification of the feeder PRBN sequences have been applied simultaneously to the three process inputs (cf. fig. 7.2):

- input 1 gas input of the first feeder section
- input 2 cooling air input
- input 3 gas input of the second feeder section

As outputs of the process the glass temperatures at 6 points in a cross section of the feeder close to the spout have been measured. The glass temperatures in a cross section of the feeder close to the spout that have been selected as outputs are:

- output 1 temperature in the middle of the feeder close to the surface of the glass
- output 2 temperature in the centre of the cross section of the feeder
- output 3 temperature in the middle of the feeder close to the bottom
- output 4 temperature close to a side wall of the feeder and close to the surface of the glass
- output 5 temperature close to the side wall of the feeder and close to the bottom

- output 6 temperature close to the opposite side wall of the feeder and close to the bottom

The amplitudes of the applied input signals, the sampling time used for the experiments and the clock frequency of the PRBN sequence have been determined on the basis of a-priori knowledge obtained from earlier experiments and experiences with process. The ratio between sampling time and clock frequency of the PRBN input signals has been chosen equal to 10 for the feeder experiments.
The estimated values for the ratios of the average noise power to the average signal power for each output (N/S) and for their standard deviations (s) are given in table 7.2

	average N/S	s
output 1	0.0614	0.0394
output 2	0.0768	0.0341
output 3	0.0821	0.0353
output 4	0.0052	0.0022
output 5	0.0073	0.0040
output 6	0.0363	0.0097

Table 7.1 Values obtained for the average noise power to the average signal power ratios with their estimated standard deviations

Fig. 7.8 gives an overview over the various signals obtained from the experiment. The data set contains 12500 samples.
As can be seen from fig. 7.8 the measured output temperatures have a large trend. This trend is not caused by the applied process input energy changes, but by rather big changes in the environmental temperature of the feeder during the experiments and by changes measured in the temperature of the glass entering the feeder.

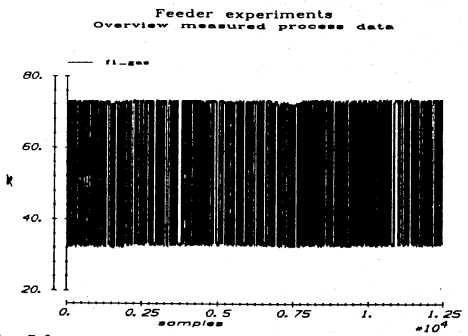

fig. 7.8a PRBN sequence applied to the gas input of section 2 of the feeder (input 1)

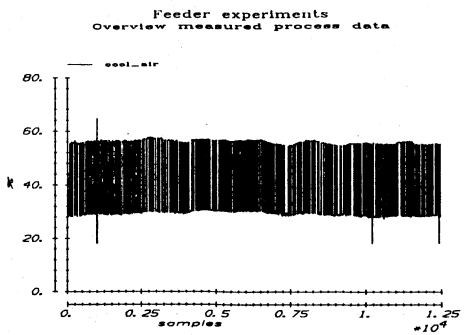

fig 7.8b PRBN sequence applied to the cooling input of the feeder (input 2)

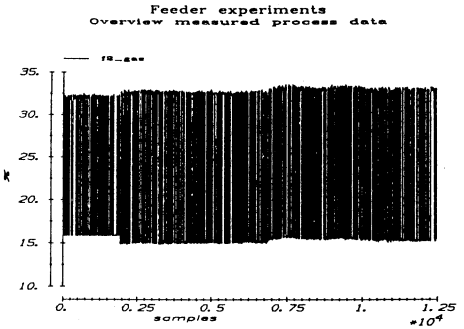

fig. 7.8c PRBN sequence applied to the gas input of section 2 of the feeder (input 3)

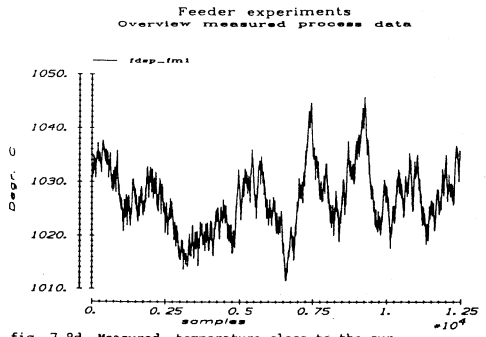

fig. 7.8d Measured temperature close to the surface of the glass in the middle of a cross section of the feeder just before the spout (output 1)

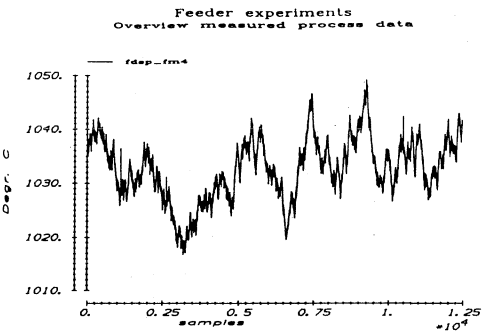

fig. 7.8e Measured temperature in the middle of a cross section of the feeder just before the spout (output 2)

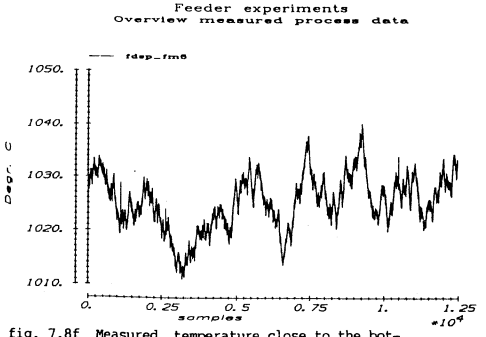

fig. 7.8f Measured temperature close to the bottom of the feeder in the middle of a cross section of the glass just before the spout (output 3)

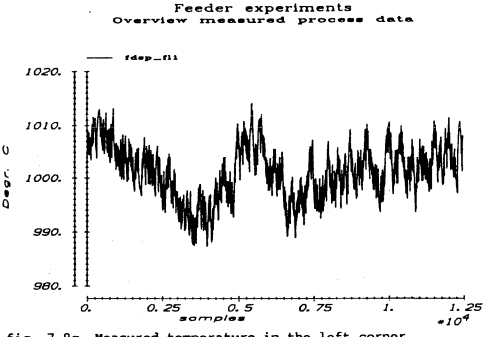

fig. 7.8g Measured temperature in the left corner of a cross section of the glass in the feeder just before the spout (output 4)

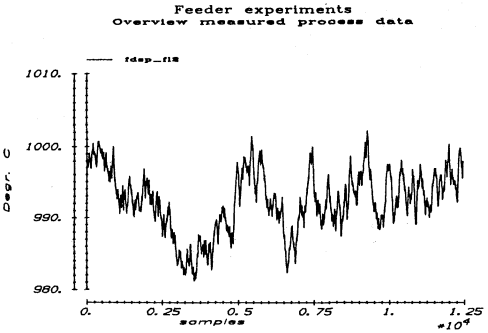

fig. 7.8h Measured temperature close to the left bottom corner of a cross section of the glass in the feeder just before the spout (output 5)

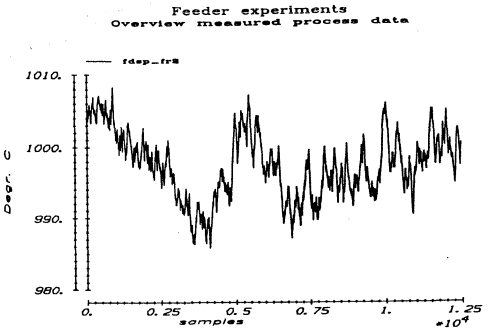

fig. 7.8i Measured temperature close to the left bottom corner of a cross section of the glass in the feeder just before the spout (output 6)

Fig. 7.9 shows the absolute values of the spectra computed from the experimental data applied to input 1 and from the first 5 outputs. The spectrum of output 6 is the same as the spectrum of output 5. Only one input signal spectrum is shown. All input signals have the same bandwidth. As required the bandwidths of the input signals applied to the process exceed the bandwidths of the temperature responses measured at the various points in the cross section at the end of the feeder.

To remove the trend from the signals the method described in chapter 6, section 6.2 is applied again. For the computation of the trend a second order low pass filter with a double real pole at $z \approx 0.986$ is applied. With this trend filter the rather big trends, mainly caused by environmental temperature changes during the experiments, can be reduced significantly (cf. fig. 7.8 and fig. 7.11). The coefficients of the filter applied for trend correction are (cf. eq. (6.29)):

- $b_0 = 0.0$
- $b_1 = 0.101074183418 \cdot 10^{-3}$
- $b_2 = 0.100116142754 \cdot 10^{-3}$
- $a_1 = 1.971631684705$
- $a_2 = -0.971832875033$

After the trends have been removed from the signals, also the average values have been subtracted. Finally, all signals have been scaled by dividing each signal by the square root of its computed variance (cf. chapter 6, section 6.7).

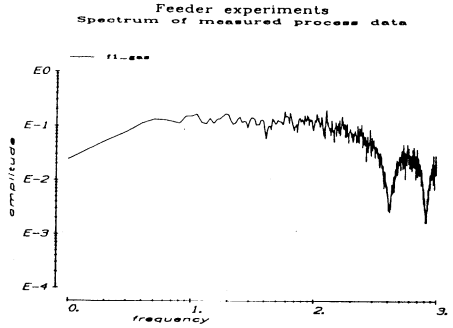

fig. 7.9a Absolute value of the FFT of the input signal applied to input 1 of the feeder

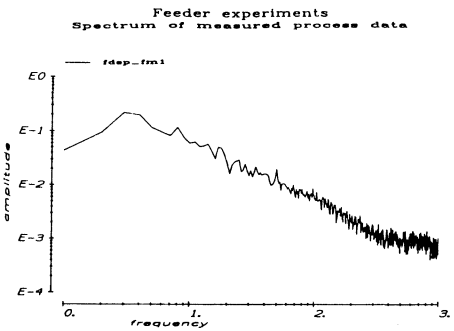

fig. 7.9b Absolute value of the FFT of the response of output 1 of the feeder to PRBN sequences on the inputs

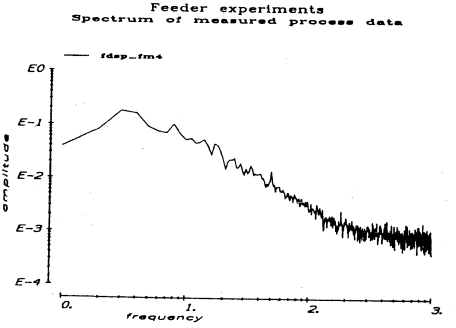

fig. 7.9c Absolute value of the FFT of the response of output 2 of the feeder to PRBN sequences on the inputs

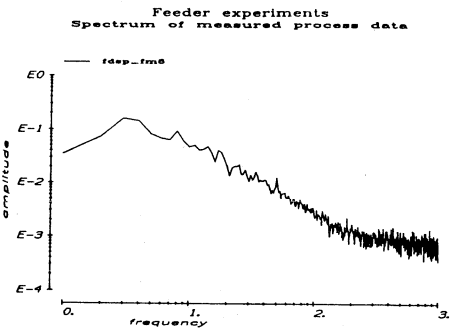

fig. 7.9d Absolute value of the FFT of the response of output 3 of the feeder to PRBN sequences on the inputs

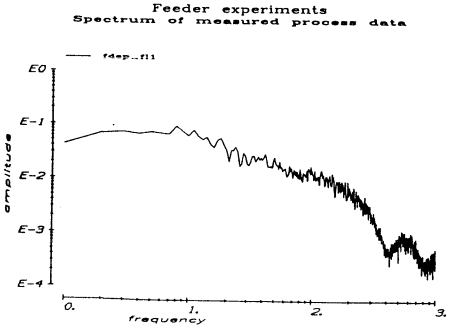

fig. 7.9e Absolute value of the FFT of the response of output 4 of the feeder to PRBN sequences on the inputs

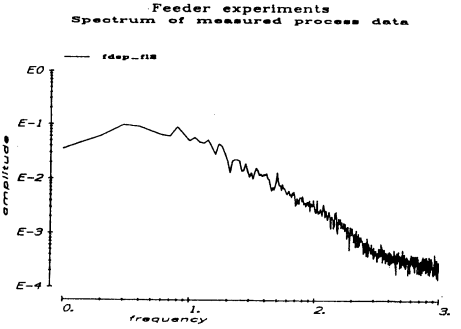

fig. 7.9f Absolute value of the FFT of the response of output 5 of the feeder to PRBN sequences on the inputs

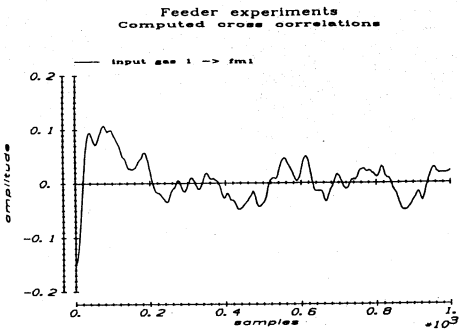

fig. 7.10a Computed cross correlation of input 1 of the feeder, excited with a PRBN signal, and the measured temperature response at output 1

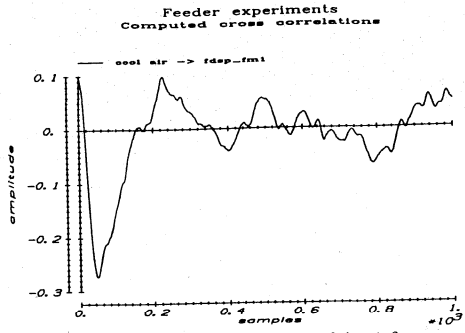

fig. 7.10b Computed cross correlation of input 2 of the feeder, excited with a PRBN signal, and the measured temperature response at output 1

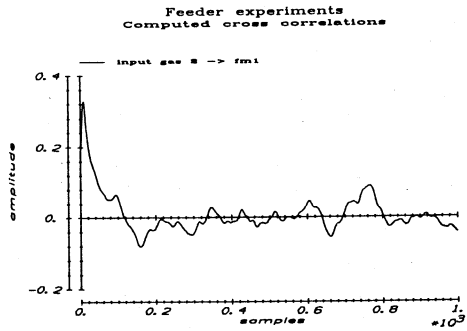

fig. 7.10c Computed cross correlation of input 3 of the feeder, excited with a PRBN signal, and the measured temperature response at output 1

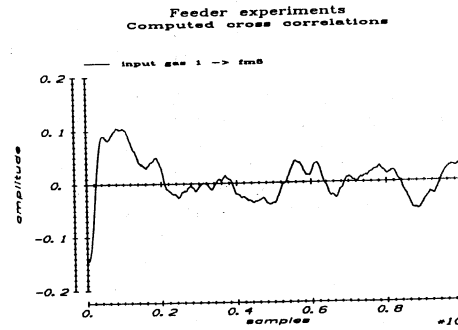

fig. 7.10d Computed cross correlation of input 1 of the feeder, excited with a PRBN signal, and the measured temperature response at output 3

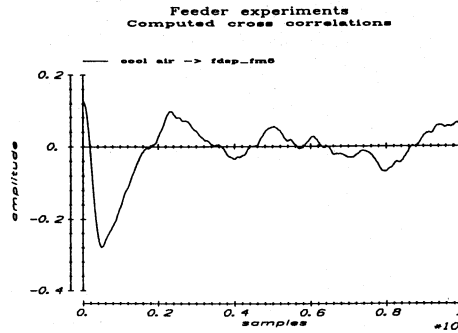

fig. 7.10e Computed cross correlation of input 2 of the feeder, excited with a PRBN signal, and the measured temperature response at output 3

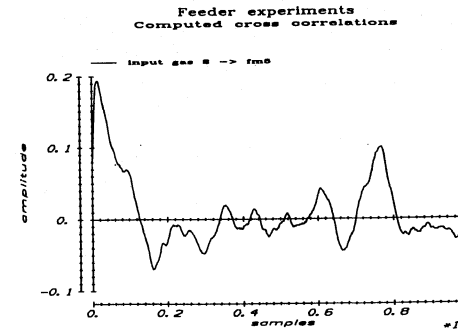

fig. 7.10f Computed cross correlation of input 3 of the feeder, excited with a PRBN signal, and the measured temperature response at output 3

For the feeder also estimates for the cross correlations between inputs (excited with PRBN sequences) and outputs have been computed to estimate time delay in the various transfers. However, the results obtained could not be used for the estimation of appropriate values for the time delays in the various transfers. Fig. 7.10a - 7.10f show the computed cross correlations from the three process inputs to output 1 and to output 3.
To find appropriate values for the time delays a FIR model has been estimated on the basis of the input/output data after decimation with a decimation factor 10, but without compensation for time delays. On the basis of the estimated impulse responses it has been decided to compensate for time delays in the transfers from inputs 1 and 2 to all outputs. The following signals are shifted back over the indicated number of samples to correct the data for the estimated time delays:

- gas input feeder section 2: 15 samples
- all measured temperatures: 15 samples

As a final step in the preparation of the signals for parameter estimation the data are decimated to remove the no longer desired redundancy from the signals. The decimation factor used in this case is 10. This is in agreement with the originally used ratio between sampling time and clock frequency of the PRBN sequences applied to the inputs. Fig. 7.11a - 7.11f give an overview of the signals after complete processing.

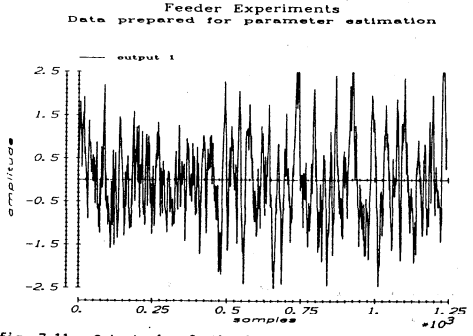

fig. 7.11a Output 1 of the feeder after signal processing

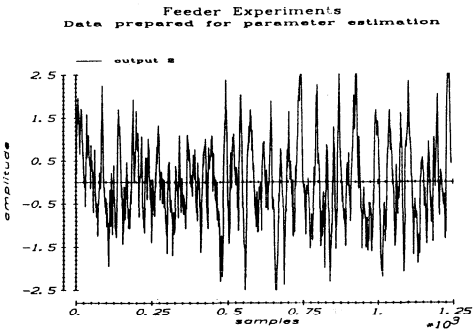

fig. 7.11b Output 2 of the feeder after signal processing

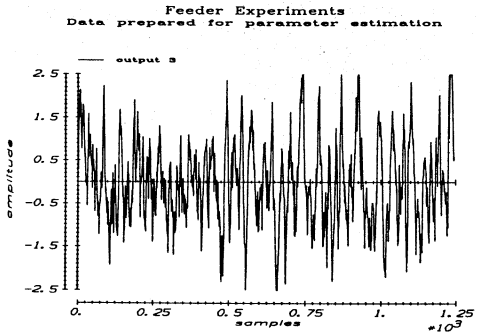

fig. 7.11c Output 3 of the feeder after signal processing

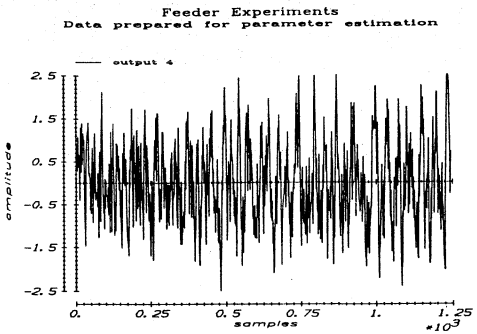

fig. 7.11d Output 4 of the feeder after signal processing

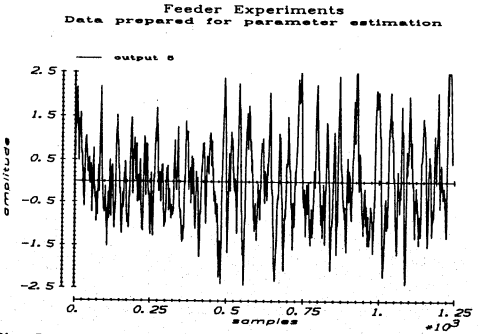

fig. 7.11e Output 5 of the feeder after signal processing

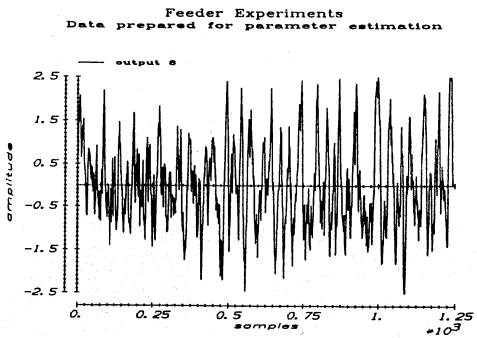

fig. 7.11f Output 6 of the feeder after signal processing

7.4 Finite impulse response estimation

To come to models that describe the process dynamics in surroundings of the working points used for both processes, in accordance with the identification strategy developed, FIR models are estimated in a first modelling step on the basis of the data obtained after the signal processing discussed in section 7.3. The only a-priori information required for the FIR model estimation is the number of samples of the impulse response that has to be estimated to assure that not too much energy is contained in the tail. This information is available for both processes from earlier recorded step responses.
For the estimation of the FIR models the algorithm based on eq. (3.31) and eq. (3.43) is used (cf. chapter 3, section 3.6, EXACTMARK).

To enable judgement of the quality of the fit of the outputs simulated by the models to the measured process responses, which have been obtained with the same input signals, the following measure is defined:

$$E = \frac{\sum_{i=1}^{l} (y_i - \hat{y}_i)^2}{\sum_{i=1}^{l} y_i^2} \qquad (7.1)$$

with: y_i - measured process output at sample interval i

$\hat{y}_i$ - output simulated by the model at sample interval i

This measure is the ratio of the average power of the output error and the average power of the measured process response.

A detailed description of the results obtained for the shaping part of the tube glass production process is given in section 7.4.1.
The results obtained from the FIR model estimation for the feeder are described in section 7.4.2.

7.4.1 FIR model estimation for the tube glass production process

The FIR model estimated for the shaping part of the tube glass production process consists of 50 samples which have been estimated on the first 1000 samples of the decimated, detrended, zero mean, scaled data obtained in section 7.3.1.
The number of samples of the FIR model (50) is chosen on the basis of several recorded step responses of the process. On the average the process appeared to reach a steady state after a time corresponding with 50 samples of the decimated signal.
The impulse responses obtained from the estimation are shown in fig. 7.12a - 7.12d.
As can be seen from the results the responses are in line with the expectations:

- The response of the wall thickness to an impulse shaped change of the mandril pressure is negative (cf. fig. 7.12a)
- The response of the diameter to an impulse shaped change of the mandril pressure is positive (cf. fig. 7.12b)
- The response of the wall thickness to an impulse shaped change of the drawing speed of the tube is negative (cf. fig. 7.12c)
- The response of the diameter to an impulse shaped change of the drawing speed is also negative (cf. fig. 7.12d)

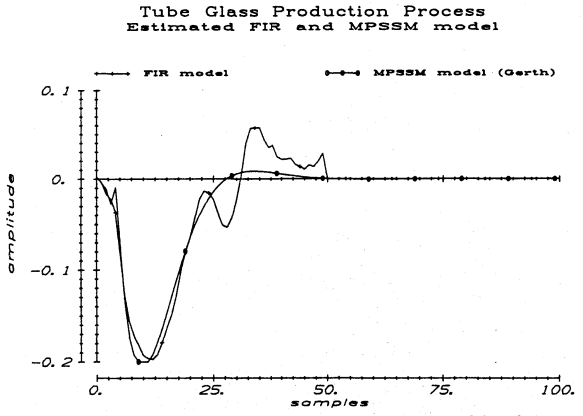

fig. 7.12a Impulse response h_{11} of the estimated FIR model and of the MPSSM model estimated with the method of Gerth

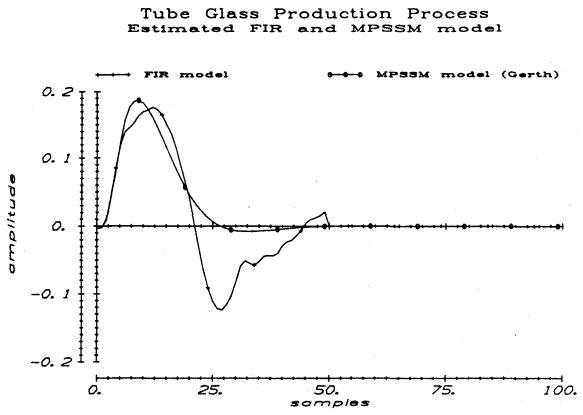

fig. 7.12b Impulse response h_{21} of the estimated FIR model and of the MPSSM model estimated with the method of Gerth

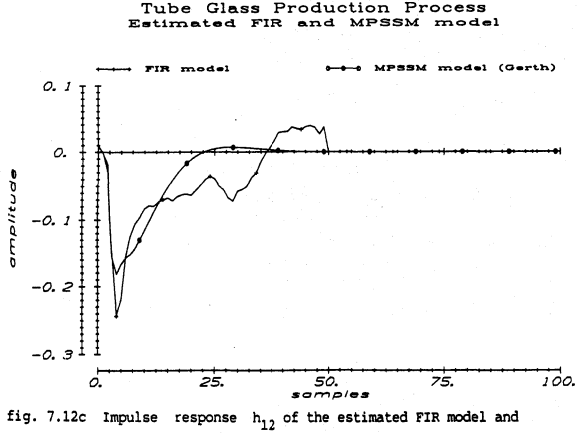

fig. 7.12c Impulse response h_{12} of the estimated FIR model and of the MPSSM model estimated with the method of Gerth

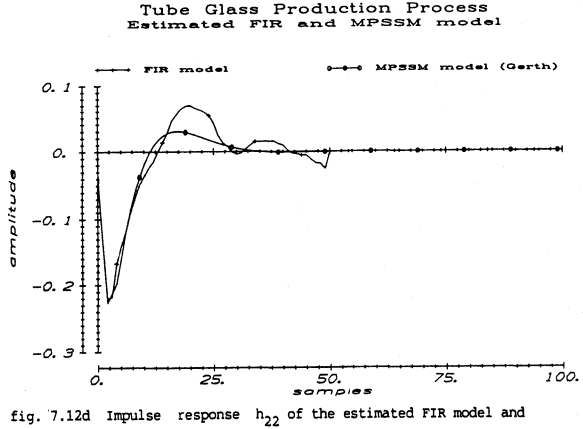

fig. 7.12d Impulse response h_{22} of the estimated FIR model and of the MPSSM model estimated with the method of Gerth

Especially the impulse responses that describe the behaviour of the diameter as a function of the process inputs indicate a rather large overshoot to occur when a step is applied to the process inputs. This corresponds to the results obtained in earlier experiments when steps were applied to the process inputs.
The impulse responses show that the responses of wall thickness and diameter to changes in drawing speed are faster than responses to changes in the mandril pressure.
To get an impression of the fit of the model to the data used for the estimation, the ratio E defined by eq. (7.1), has been computed for each output. The results obtained are presented in table 7.3.

	FIR
output 1	0.1523
output 2	0.0886

Table 7.3 Ratio of the average power of the output error and the average power of the measured process output of the tube glass production process computed on the samples 1 - 1000 of the data set used for the estimation of the model parameters.

The quality of the fit obtained is quite good. About 85% of the wall thickness power is explained by the model over the estimation interval. For the diameter even about 91% of the power is covered by the outputs simulated by the model. The results show that the fit of the simulated diameter to the measured diameter is better than the fit of the simulated wall thickness to the measured wall thickness. This difference in accuracy of the fit may be explained from the fact that the measurement of the wall thickness is not as accurate as the measurement of the diameter (cf. table 7.1). The difference in accuracy of the measurements is mostly caused by the fact that the wall thickness sensor is sensitive for movements of the tube, while the diameter sensor is not. Due to the cutting of the tube at the end of the line the tube is constantly moving. These tube movements result in inaccuracies of the wall thickness measurement.

7.4.2 FIR model estimation for the feeder

On the basis of the prepared data, discussed in section 7.3.2, a FIR model has been estimated that describes the transfer of the 3 process inputs (viz. gas input feeder section 1, cooling air input, gas inputs feeder section 2) to the 6 temperatures measured at a cross section of the feeder close to the spout.
For the estimation of the FIR model the first 1000 samples of the prepared data have been used. On the basis of earlier measured step responses of the process it was decided to estimate 75 Markov parameters. From earlier experiments (recorded step responses) it was observed that the process did not

yet reach a steady state in a time corresponding with 75 samples of the decimated signal, but most of the effets of an input change had passed within that time interval. Of the temperatures measured just below the surface of the glass about 70% of the response even elapsed within a time span equivalent to 20 sample intervals of the decimated signal. The resulting model therefore is expected to have rather fast and very slow time constants.
Also on physical grounds a difference in time constants is expected to occur in the process. Rather fast time constants, related to the direct transfer of energy from the process inputs to the glass, are to be expected. Also much slower time constants, related to the reaching of equilibrium states of the temperature distributions in the walls of the feeder, will be part of the process.

The finite impulse responses obtained from the parameter estimation with EXACTMARK (cf. chapter3, section 3.6) are shown in fig. 7.13a - 7.13r. The impulse responses obtained are well in agreement with what was expected on the basis of earlier experiences with the process. Impulses on the gas inputs result in positive temperature changes and an impulse on the cooling air input results in a negative change of the temperatures as expected.
The response of the gas input of feeder section 2 appears to be fast to all 6 temperatures measured. The responses from the gas input of feeder section 1 and of the cooling air input are much slower (about a factor 2).

The fit of the FIR model to the data appears to be good. The values obtained for the ratios of the average power of the output errors and the average power of the corresponding, treated output signals (cf. eq. (7.1)) are given in table 7.4.

	FIR
output 1	0.0937
output 2	0.0844
output 3	0.0862
output 4	0.0284
output 5	0.0310
output 6	0.0564

Table 7.4 Ratio of the average power of the output error and the average power of the measured process output of the feeder computed on the samples 1 - 1000 of the data set used for the estimation of the model parameters.

The results imply that for the temperatures in the middle of the feeder about 91% of the power corresponding to the temperature changes is covered by the estimated FIR model. Of the glass temperature close to the surface of the glass and close to the side walls of the feeder even about 97% of the

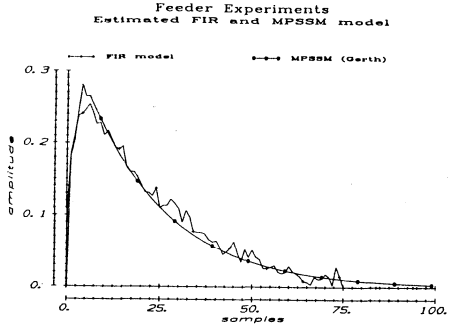

fig. 7.13a Impulse response h_{11} of the estimated FIR model and of the MPSSM model estimated with the method of Gerth

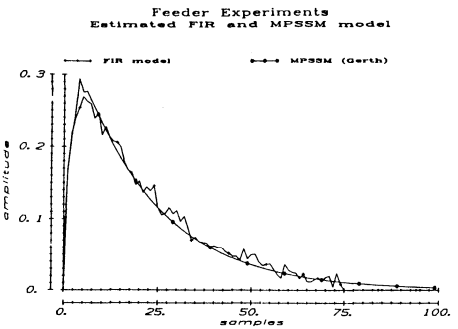

fig. 7.13b Impulse response h_{21} of the estimated FIR model and of the MPSSM model estimated with the method of Gerth

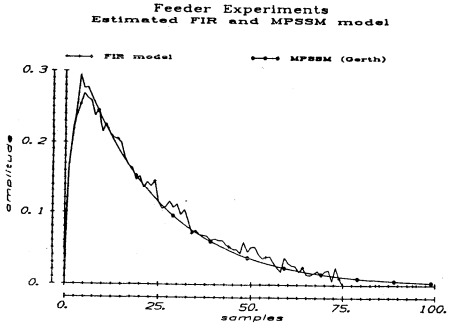

fig. 7.13c Impulse response h_{31} of the estimated FIR model and of the MPSSM model estimated with the method of Gerth

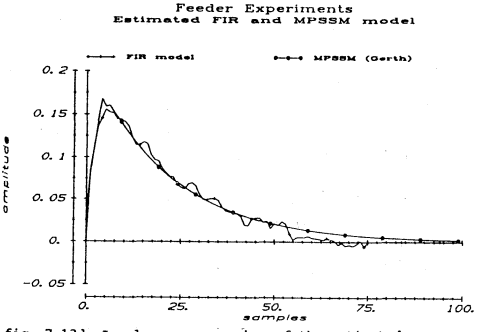

fig. 7.13d Impulse response h_{41} of the estimated FIR model and of the MPSSM model estimated with the method of Gerth

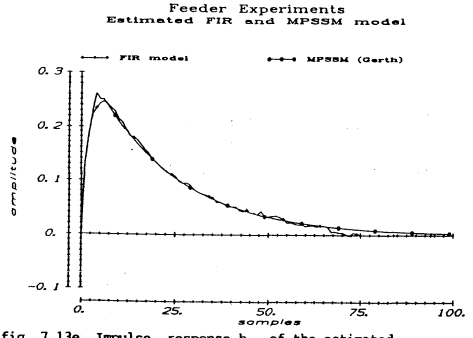

fig. 7.13e Impulse response h_{51} of the estimated FIR model and of the MPSSM model estimated with the method of Gerth

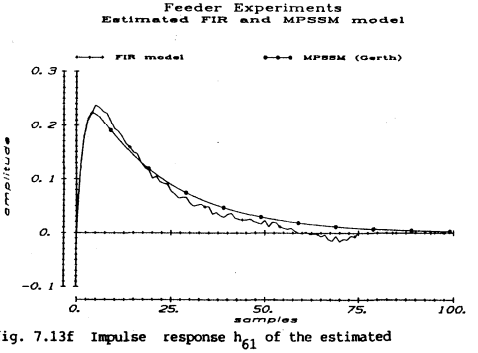

fig. 7.13f Impulse response h_{61} of the estimated FIR model and of the MPSSM model estimated with the method of Gerth

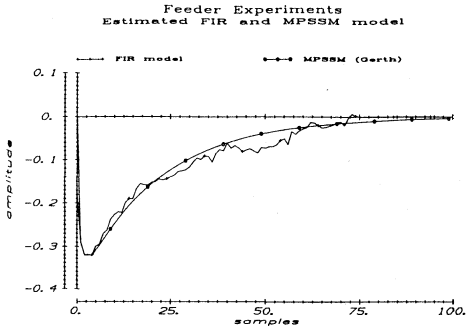

fig. 7.13g Impulse response h_{12} of the estimated FIR model and of the MPSSM model estimated with the method of Gerth

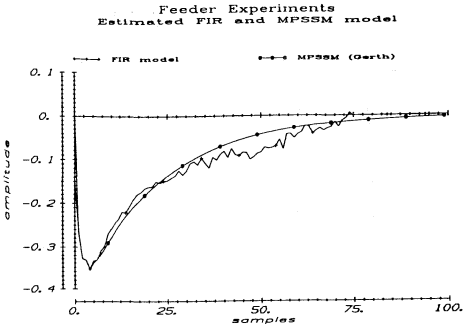

fig. 7.13h Impulse response h_{22} of the estimated FIR model and of the MPSSM model estimated with the method of Gerth

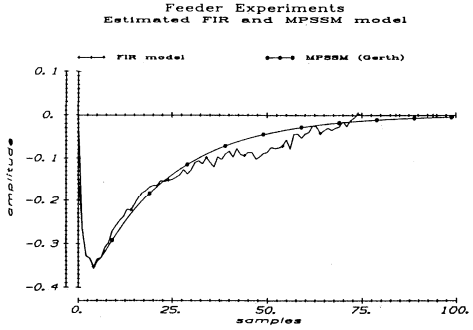

fig. 7.13i Impulse response h_{32} of the estimated FIR model and of the MPSSM model estimated with the method of Gerth

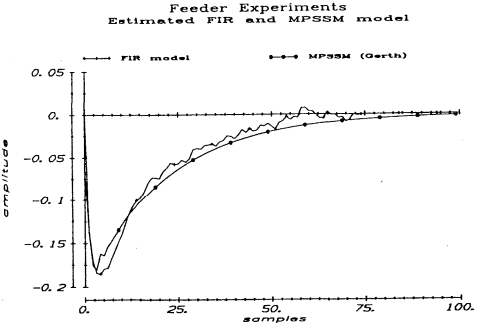

fig. 7.13j Impulse response h_{42} of the estimated FIR model and of the MPSSM model estimated with the method of Gerth

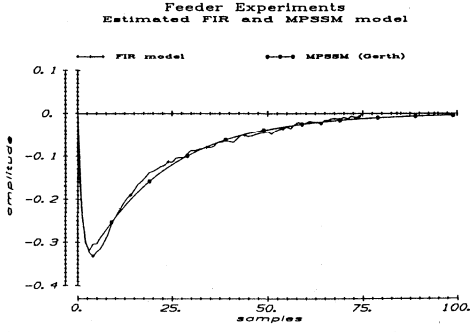

fig. 7.13k Impulse response h_{52} of the estimated FIR model and of the MPSSM model estimated with the method of Gerth

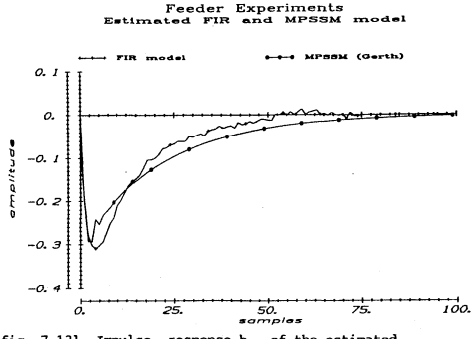

fig. 7.13l Impulse response h_{62} of the estimated FIR model and of the MPSSM model estimated with the method of Gerth

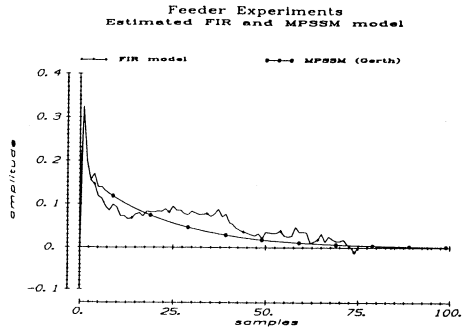

fig. 7.13m Impulse response h_{13} of the estimated FIR model and of the MPSSM model estimated with the method of Gerth

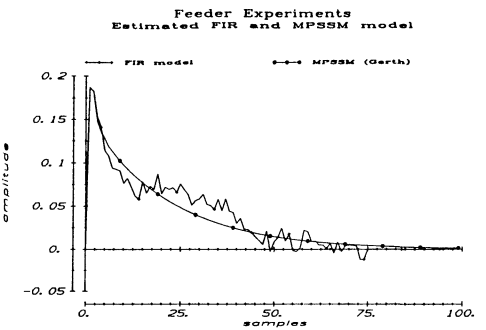

fig. 7.13n Impulse response h_{23} of the estimated FIR model and of the MPSSM model estimated with the method of Gerth

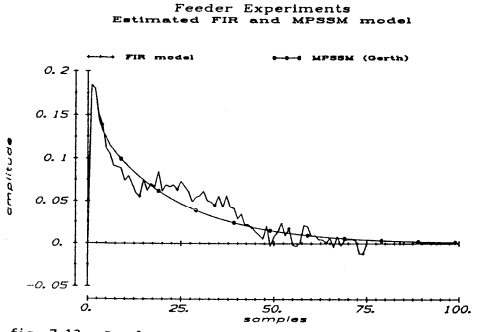

fig. 7.13o Impulse response h_{33} of the estimated FIR model and of the MPSSM model estimated with the method of Gerth

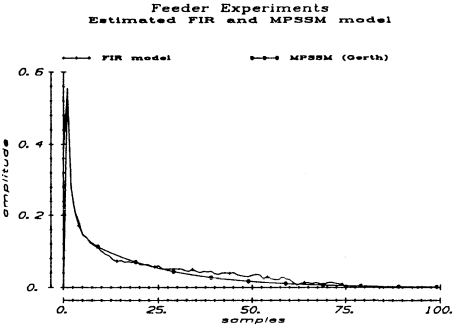

fig. 7.13p Impulse response h_{43} of the estimated FIR model and of the MPSSM model estimated with the method of Gerth

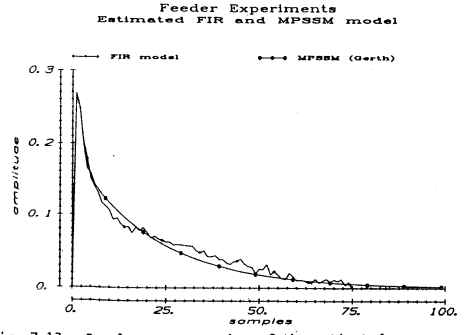

fig. 7.13q Impulse response h_{53} of the estimated FIR model and of the MPSSM model estimated with the method of Gerth

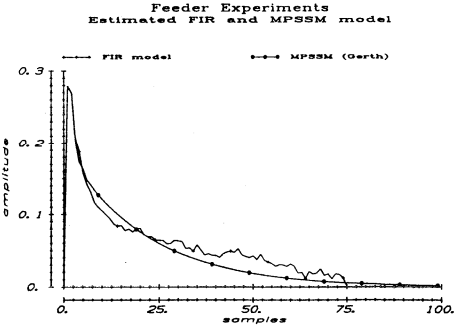

fig. 7.13r Impulse response h_{63} of the estimated FIR model and of the MPSSM model estimated with the method of Gerth

power of the signal changes is covered by the estimated FIR model. Of the bottom temperatures about respectively 97% and 94% of the power of the signal changes is covered by the model.
The values obtained are close to the estimated values for the ratios of the average noise power to the average signal power (cf. table 7.2).

7.5 Estimation of initial values for MPSSM model parameters

The FIR models obtained from the estimations described in section 7.4 are used as inputs for the second step in the identification of the processes. This second step is directed to getting a first estimate for the more compact MPSSM model on the basis of the FIR model that has been estimated for each of the two processes.
To be able to fit a MPSSM model to a FIR model first a suitable order for the minimal polynomial has to be determined. The estimated FIR models are used to determine the orders of the minimal polynomials. For the determination of the orders of the minimal polynomials the technique, based on the determination of the singular values of a finite block Hankel matrix filled with the estimated Markov parameters in vector form and the corresponding singular value ratios, is used (cf. chapter 4, section 4.3.2). Once appropriate values for the orders of the minimal polynomials are obtained, a first MPSSM model is determined for each process by means of the Gerth algorithm (cf. eq. (4.30) - (4.31)).

Section 7.5.1 describes the results obtained for the shaping part of the tube glass production process.
Section 7.5.2 gives an overview over the results obtained for the feeder.

7.5.1 Order determination and initial value estimation of MPSSM model parameters for the tube glass production process

Before a first MPSSM model is determined on the basis of the estimated FIR model, an appropriate value for the degree of the minimal polynomial is derived from the singular values of a finite block Hankel matrix constructed from the estimated Markov parameters in vector form (cf. eq. (4.25)).
For the construction of the block Hankel matrix all 50 estimated Markov parameters are used. The first block column and first row of the block Hankel matrix are built from all 50 Markov parameters. The rest of the block rows (columns) of the block Hankel matrix are at the end filled up with zeros.
Fig. 7.14a and 7.14b respectively show the singular values of the block Hankel matrix and the computed ratios of consecutive singular values. On the basis of the results obtained the selected degree for the minimal polynomial is r=6.

With the degree of the minimal polynomial equal to 6 a first estimate for the MPSSM model parameters is computed with the algorithm of Gerth (cf. eq. (4.30), (4.31)). The MPSSM model parameters are computed on the basis of the 50 estimated FIR model parameters. The result obtained from the estimation

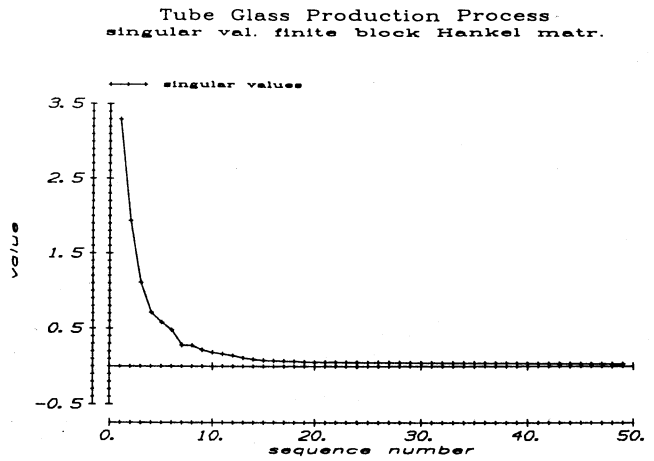

fig. 7.14a Singular values of the block Hankel matrix with 50 block rows and 50 columns of estimated Markov parameters in vector form

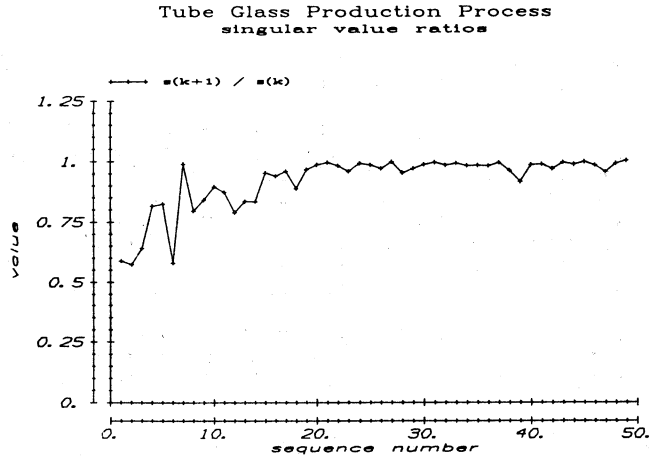

fig. 7.14b Ratios of successive singular values of the block Hankel matrix

with the Gerth method is shown in fig. 7.12a - 7.12d. The impulse responses of the MPSSM model are marked with O's.
The impulse responses computed with the obtained MPSSM model parameters fit very well to the estimated FIR model parameters in the first part of the impulse responses. However, a large difference between both sets of impulse responses is found in the tails.

To get a first impression of the quality of the obtained MPSSM model compared to the estimated FIR model, also for the MPSSM model the relative error defined by eq. (7.1) is computed for each output. For the computation of this ratio the same 1000 samples have been used that also have been used for the estimation of the FIR model parameters. The results obtained for both outputs are given in table 7.5. To ease comparison also the results obtained with the FIR model are repeated in table 7.5.

	FIR	MPSSM Gerth
output 1	0.1523	0.2156
output 2	0.0886	0.2327

Table 7.5 Ratio of the average power of the output error and the average power of the measured process output of the tube glass production process computed on the samples 1 - 1000 of the data set used for the estimation of the model parameters.

Compared to the results obtained with the estimated FIR model the fit to the data of this initial MPSSM model is not very good. Especially for the second output (diameter) the fit to the data has become much worse. On the basis of the difference between the pressure/diameter impulse responses of the MPSSM model and the FIR model (cf. fig. 7.12b) this deterioration of the diameter fit already was expected. Due to the fact that the MPSSM has been determined by a model to model fit on the basis of a first iteration only of the quadratic approximation of the impulse responses of the FIR model by the impulse responses of the initial MPSSM model it is not surprising that the fit to the estimation data becomes worse. Furthermore the last equations used for the computation of the minimal polynomial coefficients are rather noisy, while these equations involve the last of the 50 estimated FIR model parameters, which are noisy (cf. eq. (4.30) and fig. 7.12a - 7.12d).

7.5.2 Order determination and initial MPSSM model parameter estimation for the feeder

Also for the feeder an initial MPSSM model has been determined on the basis of the estimated FIR model.
To determine an appropriate order for the minimal polynomial the singular values and singular value ratios of a largest possible block Hankel matrix, built from all estimated Markov parameters in vector form, are computed (cf.

eq. (4.25)). The obtained singular values and singular value ratios are plotted in fig. 7.15a and 7.15b respectively. On the basis of the obtained singular values and of the singular value ratios a degree 4 is chosen for the minimal polynomial.

With the Gerth algorithm a 4-th order MPSSM model has been estimated on the basis of the 75 Markov parameters of the FIR model. The impulse responses computed from the estimated MPSSM model parameters are shown in fig. 7.13a - 7.13r. The impulse responses of the MPSSM model are marked with O's. The estimated FIR model parameters have been plotted in the same figures. The MPSSM model obtained for the feeder, in general, seems to have a good fit to the original FIR model. Especially in first part of the impulse responses the fit is good.

To enable a comparison between the FIR model and the MPSSM model the relative error defined by eq. (7.1) has been computed for all outputs. The result obtained for each output are given in table 7.6.

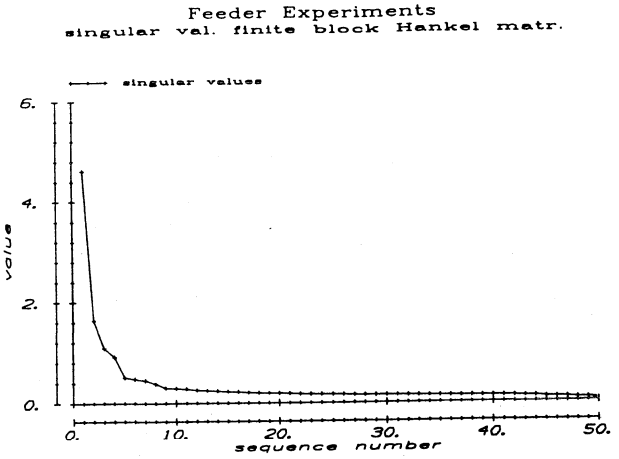

fig. 7.15a Singular values of the block Hankel matrix with 75 block rows and 75 columns of estimated Markov parameters in vector form

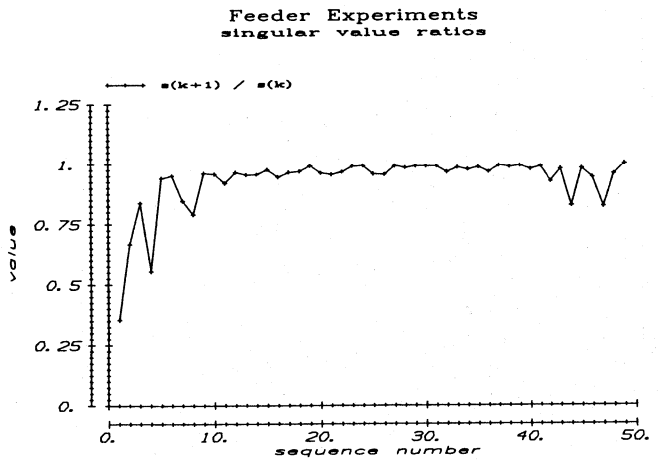

fig. 7.15b Ratios of successive singular values of the block Hankel matrix

	FIR	MPSSM Gerth
output 1	0.0937	0.1930
output 2	0.0844	0.1408
output 3	0.0862	0.1430
output 4	0.0284	0.2350
output 5	0.0310	0.0542
output 6	0.0564	0.1009

Table 7.6 Ratio of the average power of the output error and the average power of the measured process output of the feeder computed on the samples 1 - 1000 of the data set used for the estimation of the model parameters.

Remarkable in this result is the enormous increase of the error for the 4-th output. About 76% of the power of the temperature changes of output 4 are covered by the output signal simulated by the obtained MPSSM model.

7.6 Direct estimation results

The third step in the identification approach developed is the estimation of MPSSM models for both processes with the Direct Estimation algorithm (cf. chapter 5, section 5.4). On the basis of the available input/output data sets and with the initial MPSSM models of the previous sections as initial values for the parameters, new MPSSM models have been estimated. For the estimation of the MPSSM model parameters the same input/output data sets have been used as for the estimation of the FIR model parameters (cf. section 7.4.1 and section 7.4.2). For the estimation of the MPSSM model parameters samples 500 - 1000 of the data sets have been used. The first 500 samples have been used for reduction of the influence of the initial state of the model on the estimation results.

On the basis of the estimated MPSSM models also approximate realizations have been computed. The method of Zeiger and McEwen (cf. chapter 4, eq. (4.36) - (4.42)) has been applied to the MPSSM model of the shaping part of the tube glass production process. The method based on retaining the best observable and controllable parts of the balanced state space representation of the MPSSM model (cf. eq. (5.48), (5.49)) has been used for computation of an approximate realization of the MPSSM model of the feeder. The computation of the approximate realizations is done to remove inherently present irrelevant modes from the MPSSM models (cf. eq. (4.20); chapter 5, section 5.2.4).

The results obtained for the shaping part of the tube glass production process with the direct estimation algorithm are presented in section 7.6.1. Section 7.6.2 gives the results obtained for the feeder.

7.6.1 Direct estimation from input/output data of MPSSM model parameters for the tube glass production process

For the estimation of a MPSSM model directly from the available input/output data the MPSSM model parameters obtained with Gerth's method have been used as initial values (cf. section 7.5.1). For the direct estimation of the MPSSM model parameters the order of the minimal polynomial has been kept equal to 6.

To see what order has to be used for the computation of an approximate realization of the MPSSM model obtained from the Direct Estimation method, the Hankel singular values of the MPSSM model are computed (cf. eq. (3.50) - (3.59)). Small Hankel singular values indicate irrelevant modes which have to be removed from the model. The Hankel singular values of the 12-th order state space model obtained from a one to one MPSSM model to State Space model translation of the estimated MPSSM model (cf. eq. (5.56) - (5.57)) are given in fig. 7.16. On the basis of the Hankel singular values of the 12-th order state space model a 7-th order approximate realization of the MPSSM model is computed. The approximate realization has been computed from a finite block Hankel matrix with the method of Zeiger and McEwen (cf. eq.

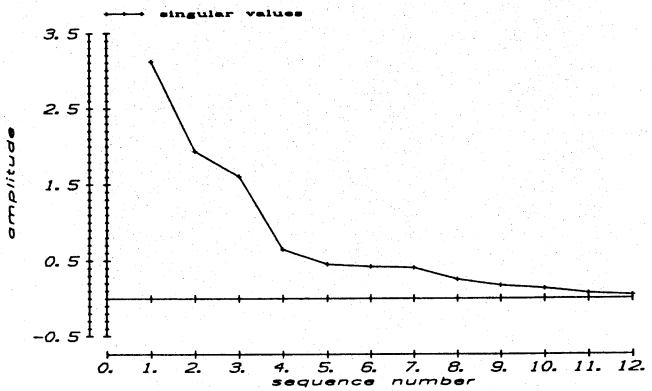

fig. 7.16 Hankel singular values of the MPSSM model obtained from parameter estimation on input/output data of the tube glass production process

(4.36) - (4.42)). For the computation of the approximate realization a Hankel matrix with 50 block rows and 50 block columns has been used.

The impulse responses generated with the estimated MPSSM model and the impulse responses belonging to the ultimately obtained 7-th order approximate realization are shown in fig. 7.17a - 7.17d. In these figures also the estimated FIR model parameters are plotted as dotted lines.
From the figures it is clear that the impulse responses obtained from the estimated MPSSM model parameters highly resemble the earlier estimated finite impulse responses. Also the impulse responses of the 7-th order approximate realization fit very well to the original FIR model.
According to the high degree of resemblance of the impulse responses also the fit to the data is expected to be good. To be able to compare the fit to the data of the MPSSM model and of the approximate realization with the fit of the FIR model to the data also for the MPSSM model and for the approximate realization the ratio of the average power of the output error and the average power of measured process responses (cf. eq. (7.1)) has been computed for each output. For the computations samples 1 - 1000 have been used. This implies that also the first interval of 500 samples, that has not been used for the estimation of the model parameters, has been included for the computation of the ratio of the average power of the error signals and the average power of the output signals of the data set.

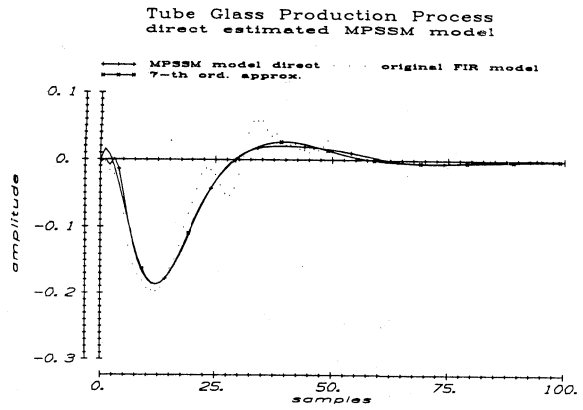

fig. 7.17a Impulse response h_{11} of the MPSSM model, obtained from parameter estimation on input/output data of the tube glass production process, and of its 7-th order approximate realization

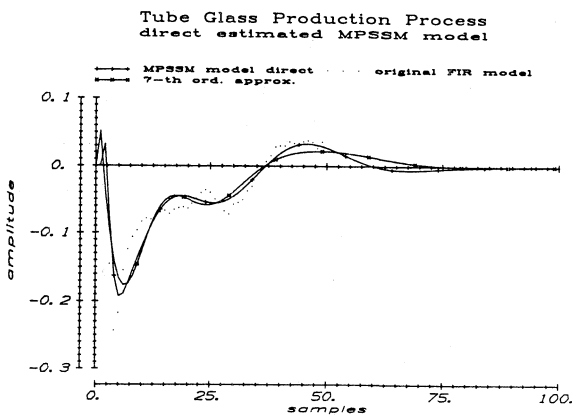

fig. 7.17c Impulse response h_{12} of the MPSSM model, obtained from parameter estimation on input/output data of the tube glass production process, and of its 7-th order approximate realization

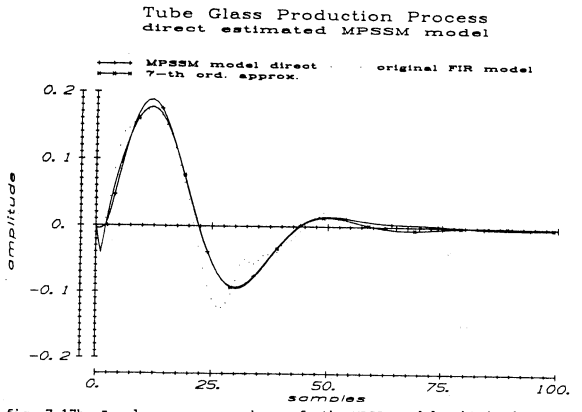

fig. 7.17b Impulse response h_{21} of the MPSSM model, obtained from parameter estimation on input/output data of the tube glass production process, and of its 7-th order approximate realization

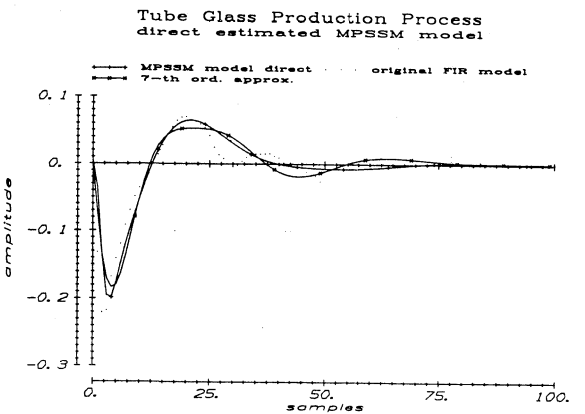

fig. 7.17d Impulse response h_{22} of the MPSSM model, obtained from parameter estimation on input/output data of the tube glass production process, and of its 7-th order approximate realization

Table 7.7 summarizes the results obtained with all models on the data set used for the estimation of the model parameters.

	FIR	MPSSM Gerth	MPSSM direct	7-th ord. appr
output 1	0.1523	0.2156	0.1257	0.1462
output 2	0.0886	0.2327	0.0621	0.0789

Table 7.7 Ratio of the average power of the output error and the average power of the measured process output of the tube glass production process computed on the samples 1 - 1000 of the data set used for the estimation of the model parameters.

The fit of both models to the data is remarkably good. Although the MPSSM model has less degrees of freedom than the FIR model and although the first 500 samples were not used for the estimation of the model parameters but nevertheless included in the sample interval used for the computation of the average power of the output error, for both models -the MPSSM model and the 7-th order approximate realization- the values obtained for the relative error E (cf. eq. (7.1)) are smaller than the values obtained with the FIR model. This effect may be caused by the limited length of the estimated finite impulse responses.
Comparison of the estimated values for the ratios of the average noise power to the average signal power for each output (cf. table 7.1) of the trend corrected outputs with the relative power of the output errors computed with the ultimately obtained MPSSM model shows a difference for the wall thickness of about -2.5% and a difference of about +4% for the diameter. This result implies that the model simulates the measured process responses with an accuracy that is close to the estimated noise level for the outputs.
It has to be noticed that for the computation of these results trends have been excluded.

7.6.2 Direct estimation from input/output data of a MPSSM model for the feeder

On the basis of the feeder input/output data a 4-th order, 3 input, 6 output MPSSM model has been estimated. For the estimation with the Direct Estimation algorithm the MPSSM model parameters obtained with the Gerth algorithm (cf. section 7.5.2) have been used as initial values for the MPSSM model parameters. For the estimation of the MPSSM model parameters from the prepared input/output data only the samples 500 - 1000 have been used.

To find an appropriate estimate for the order of the approximate realization of the obtained MPSSM model, the Hankel singular values of the model have

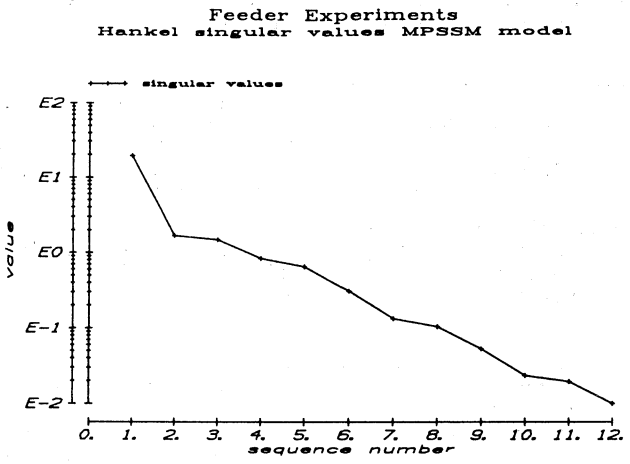

fig. 7.18 Hankel singular values of the MPSSM model obtained from parameter estimation on input/output data of the feeder

been computed. The Hankel singular values, obtained from the gramians of the 12-th order balanced state space representation of the MPSSM model are plotted in fig. 7.18. On the basis of the Hankel singular values it has been decided to compute a 6-th order approximate realization of the MPSSM model. For the computation of the approximate realization the method based on retaining the best observable and best controllable parts of the MPSSM model in balanced state space form has been used (cf. eq. (5.48) - (5.49)).

Fig. 7.19a - 7.19r show the impulse responses obtained from the estimated MPSSM model and from the 6-th order approximate realization. To facilitate comparison of the various estimated impulse responses also the earlier estimated FIR's have been plotted in the figures as dotted lines.
As can been seen from the figures the impulse responses of the MPSSM model and of its approximate realization highly resemble the estimated finite impulse responses in the first part. In the tails the differences between the estimated FIR and the impulse responses generated by the MPSSM model and by its approximate realization increase. This difference may be caused by the non-white input signal remaining after trend correction. Low signal frequencies have been attenuated by the trend correction in both the input and the output signals (cf. fig. 7.9a - 7.9f). The MPSSM model obtained from the direct estimation on input/output data contains low frequency dynamics the estimated FIR model does not have.
The eigenvalues of the MPSSM model that correspond with the low frequency dynamics indicate a low frequency time constant of the feeder of about 50

decimated samples. A slow drift of the temperatures in response to steps applied to the process inputs, corresponding with such a large time constant, has been observed during the initial step response experiments done with feeder. As a result the impulse responses of the MPSSM model are considered to be realistic.

To allow comparison of the fit of the various impulse responses to the data used for the estimations, the relative error E (cf. eq. 7.1)) has been computed both with the MPSSM model and with the 6-th order approximate realization for each output. For the computation of the signal power ratios samples 1 - 1000 have been used. So also the samples 1 - 500, which have not been used for the estimation of the MPSSM model parameters, have been included for the computation of the relative output error power. The results obtained for each output with the MPSSM model and with its 6-th order approximate realization are given in table 7.8. To make comparison of the results obtained with the various estimated models easy also the results obtained with the FIR model and the results obtained with the initial MPSSM model are repeated in table 7.8.

	FIR	MPSSM Gerth	MPSSM direct	6-th ord. appr
output 1	0.0937	0.1930	0.1163	0.1165
output 2	0.0844	0.1408	0.1025	0.1045
output 3	0.0862	0.1430	0.1041	0.1060
output 4	0.0284	0.2350	0.0324	0.0375
output 5	0.0310	0.0542	0.0357	0.0358
output 6	0.0564	0.1009	0.0665	0.0697

Table 7.8 Ratio of the average power of the output error and the average power of the measured process output of the feeder computed on the samples 1 - 1000 of the data set used for the estimation of the model parameters.

The fit of both models to the data is good. The difference between the fit of the estimated MPSSM model and the fit of its 6-th order approximate realization is negligibly small. Comparison of the results with the results obtained for the estimated FIR model shows only a small increase of the errors. The differences in the impulse responses with respect to the low frequency dynamics appear to have no influence on the computed output errors. This is probably caused by the relative low power of the low frequencies components in the input/output data (cf. fig. 7.9a - 7.9f).
Taken into account that the errors are computed over the samples 1 - 1000 and that the MPSSM model parameters are estimated on the samples 500 - 1000 only, this implies that the results obtained from the direct estimation method are quite good again.

Comparison of the values obtained for the relative output errors (cf. table 7.8) with the estimated values for the ratios of the average noise power to

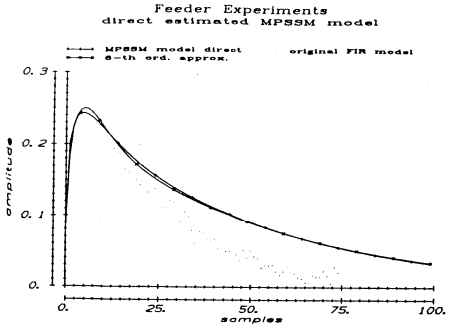

fig. 7.19a Impulse response h_{11} of the MPSSM model, obtained from parameter estimation on input/output data of the feeder, and of its 6-th order approximate realization

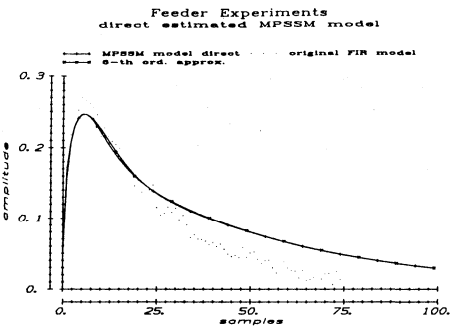

fig. 7.19b Impulse response h_{21} of the MPSSM model, obtained from parameter estimation on input/output data of the feeder, and of its 6-th order approximate realization

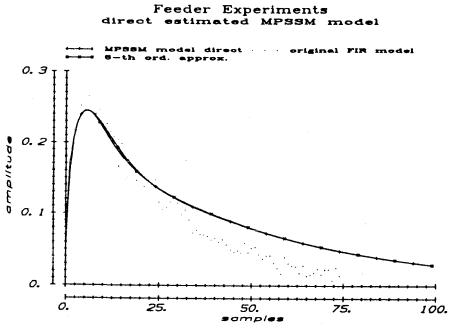

fig. 7.19c Impulse response h_{31} of the MPSSM model, obtained from parameter estimation on input/output data of the feeder, and of its 6-th order approximate realization

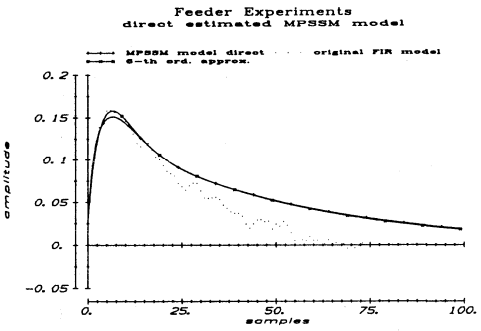

fig. 7.19d Impulse response h_{41} of the MPSSM model, obtained from parameter estimation on input/output data of the feeder, and of its 6-th order approximate realization

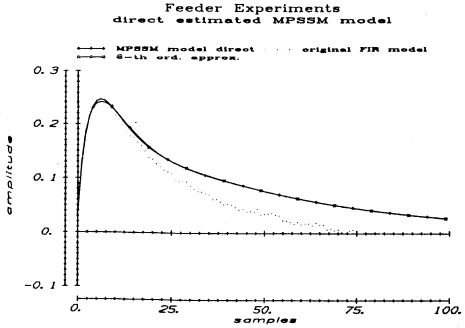

fig. 7.19e Impulse response h_{51} of the MPSSM model, obtained from parameter estimation on input/output data of the feeder, and of its 6-th order approximate realization

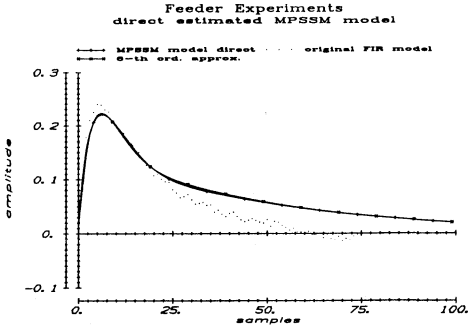

fig. 7.19f Impulse response h_{61} of the MPSSM model, obtained from parameter estimation on input/output data of the feeder, and of its 6-th order approximate realization

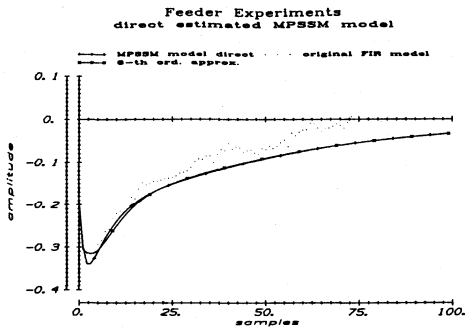

fig. 7.19g Impulse response h_{12} of the MPSSM model, obtained from parameter estimation on input/output data of the feeder, and of its 6-th order approximate realization

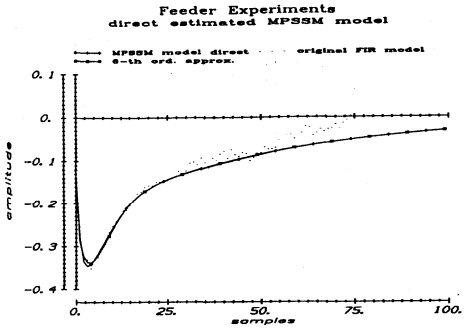

fig. 7.19h Impulse response h_{22} of the MPSSM model, obtained from parameter estimation on input/output data of the feeder, and of its 6-th order approximate realization

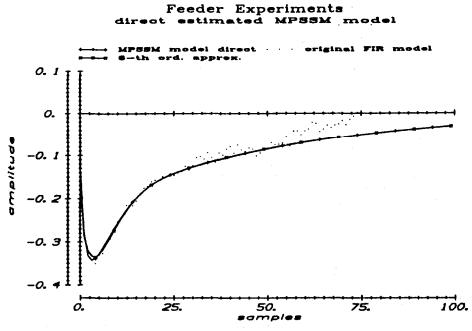

fig. 7.19i Impulse response h_{32} of the MPSSM model, obtained from parameter estimation on input/output data of the feeder, and of its 6-th order approximate realization

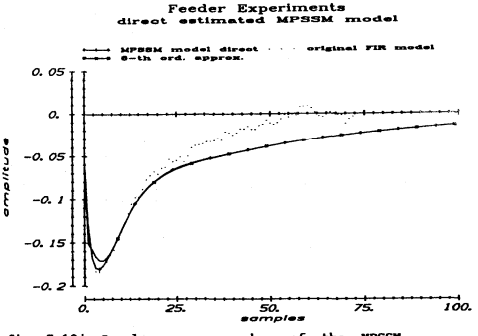

fig. 7.19j Impulse response h_{42} of the MPSSM model, obtained from parameter estimation on input/output data of the feeder, and of its 6-th order approximate realization

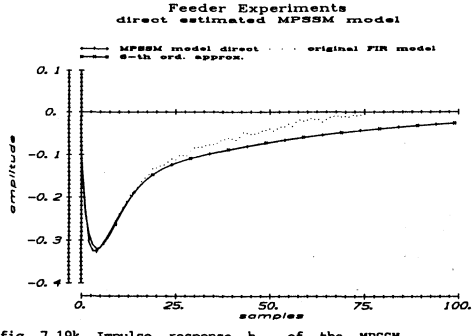

fig. 7.19k Impulse response h_{52} of the MPSSM model, obtained from parameter estimation on input/output data of the feeder, and of its 6-th order approximate realization

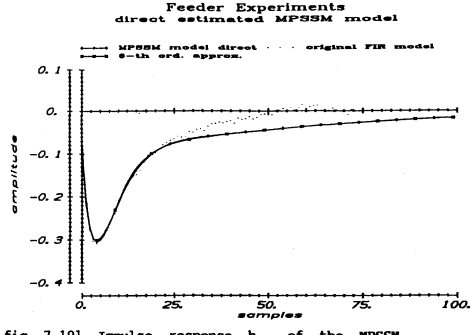

fig. 7.19l Impulse response h_{62} of the MPSSM model, obtained from parameter estimation on input/output data of the feeder, and of its 6-th order approximate realization

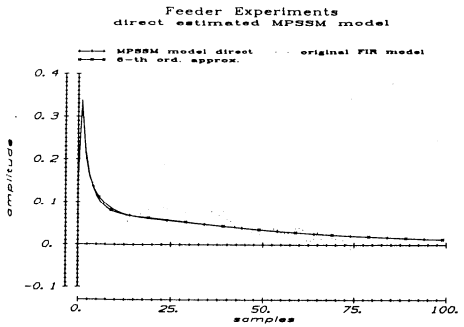

fig. 7.19m Impulse response h_{13} of the MPSSM model, obtained from parameter estimation on input/output data of the feeder, and of its 6-th order approximate realization

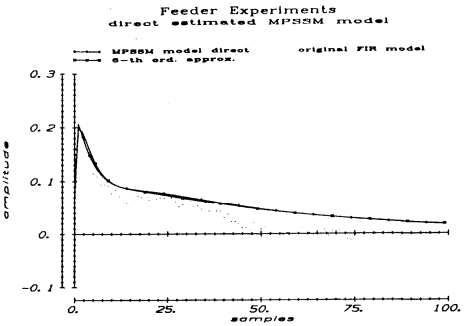

fig. 7.19n Impulse response h_{23} of the MPSSM model, obtained from parameter estimation on input/output data of the feeder, and of its 6-th order approximate realization

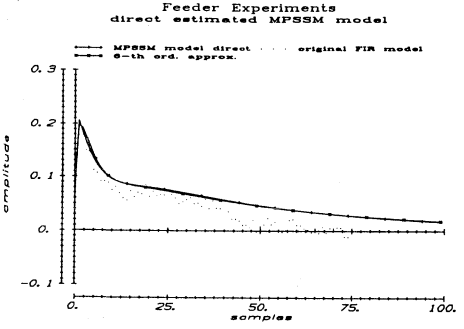

fig. 7.19o Impulse response h_{33} of the MPSSM model, obtained from parameter estimation on input/output data of the feeder, and of its 6-th order approximate realization

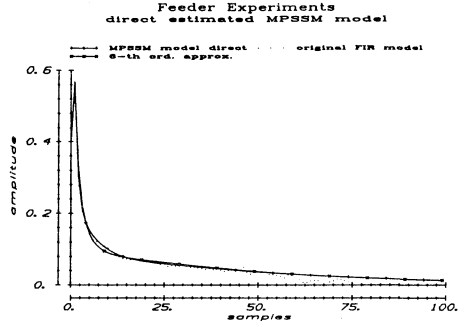

fig. 7.19p Impulse response h_{43} of the MPSSM model, obtained from parameter estimation on input/output data of the feeder, and of its 6-th order approximate realization

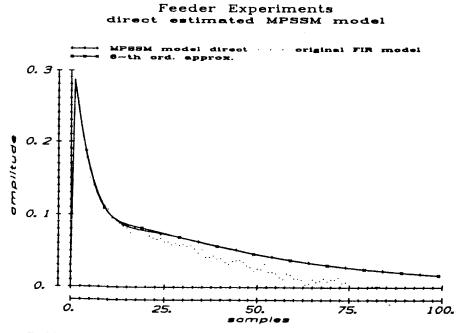

fig. 7.19q Impulse response h_{53} of the MPSSM model, obtained from parameter estimation on input/output data of the feeder, and of its 6-th order approximate realization

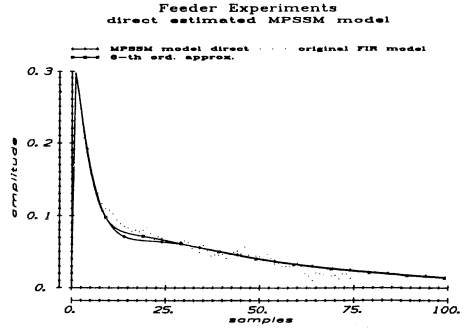

fig. 7.19r Impulse response h_{63} of the MPSSM model, obtained from parameter estimation on input/output data of the feeder, and of its 6-th order approximate realization

the average signal power (cf. table 7.2) again shows an accuracy of the simulated outputs that comes close the estimated average output noise power.

7.7 Model validation

An important step in the identification of a process is the validation of the model obtained from the estimations. The purpose of the model validation is to get an indication of the resemblance of the input/output behaviour of the model to the input/output behaviour of the process.
To validate a model test signals are applied both to the model and to the process that has been modelled. The responses of the process to the test signals are compared with the outputs simulated by the model. The ratio of the average power of the output error signal and the average power of the recorded process responses (cf. eq. (7.1)) is a measure for the simulation qualities of the model.

The validation results will of course highly depend on the characteristics of the test signals used for the validation. To allow comparison of the measured process responses with the output signals simulated by the model the validation signals have to be processed exactly the same way as the signals, used for the parameter estimations, have been processed.
To be able to judge the overall quality of the model, inter-channel independent, zero mean noise sequences are used as test signals for model validation. The bandwidth of the validation signals may be chosen in accordance with the bandwidth of the input signals usually applied to the process to get an impression of the quality of the model in practice.

For the validation of the models obtained for the shaping part of the tube glass production process two different test signals have been used:

- PRBN sequences with the same frequency spectrum properties as the signals used for the parameter estimations.
- PRBN sequences with spectral properties that correspond with the spectra of the input signals applied to the processes in daily practice.

For both validation sets the average power of the signals is almost equal to the average power of the signals used for the parameter estimations.

Section 7.7.1 describes the validation results obtained for the tube glass production process.

For the validation of the models obtained for the feeder a data set has been used consisting of PRBN input noise sequences with a clock frequency equal to 0.05 times the sample frequency used for the sampling of the process data. The data set used for the estimation of model parameters had a clock frequency of 0.1 times the sample frequency (cf. section 7.3.2). The average power of the signals used for model validation is about 35% of the average power of the signals used for the model parameter estimations.
The validation results obtained for the feeder are given in section 7.7.2.

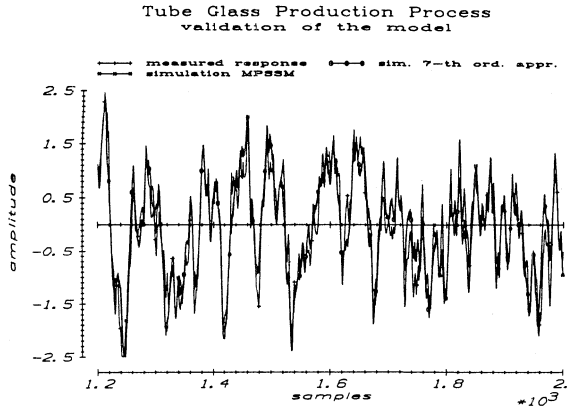

fig. 7.20a Validation results obtained for the wall thickness with the MPSSM model and with the 7-th order approximation of the MPSSM model of the tube glass production process on validation data set 1

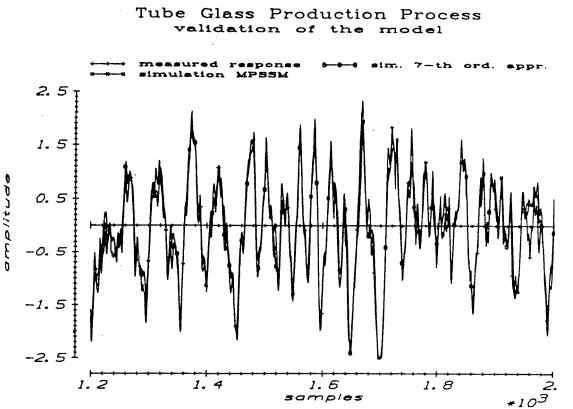

fig. 7.20b Validation results obtained for the diameter with the MPSSM model and with the 7-th order approximation of the MPSSM model of the tube glass production process on validation data set 1

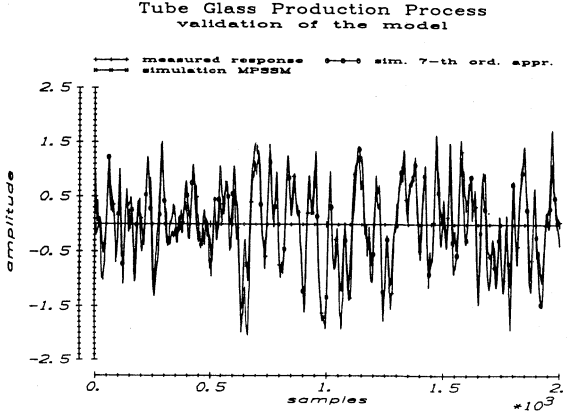

fig. 7.20c Validation results obtained for the wall thickness with the MPSSM model and with the 7-th order approximation of the MPSSM model of the tube glass production process on validation data set 2

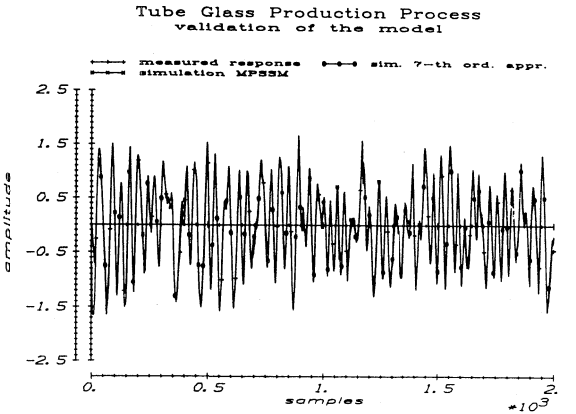

fig. 7.20d Validation results obtained for the diameter with the MPSSM model and with the 7-th order approximation of the MPSSM model of the tube glass production process on validation data set 2

7.7.1 Validation results for the shaping part of the tube glass production process

For the validation of the models estimated for the shaping part of the tube glass production process two data sets have been used that are different from the one used for the parameter estimation. The preparation of the data has been in accordance with the processing applied to the signals which have been used for parameter estimation.
The first data set applied for model validation consists of signals with the same properties as the signals used for the parameter estimations. The input signals are PRBN sequences with a clock frequency of 0.2 times the sample frequency. For the validation 800 samples have been used. Fig. 7.20a and 7.20b give an overview of the fit of the outputs simulated by the MPSSM model and of the outputs simulated by the 7-th order approximation of the MPSSM model to the measured process outputs. Table 7.9 summarizes the values of the ratios of the average powers of the output errors and of the measured output signals for the 4 estimated models (FIR, MPSSM-Gerth, MPSSM-direct, 7-th order approximate realization). To ease comparison also the results obtained on the estimation data are given in table 7.9.

	FIR	MPSSM Gerth	MPSSM direct	7-th ord. appr
		Validation results		
output 1	0.1731	0.2536	0.1437	0.1629
output 2	0.0996	0.2589	0.0879	0.0997
	Results obtained on data used for parameter estimation			
output 1	0.1523	0.2156	0.1257	0.1462
output 2	0.0886	0.2327	0.0621	0.0789

Table 7.9 Ratio of the average power of the output error and the average power of the measured process output of the shaping part of the tube glass production process computed with the 4 estimated models on the first data set used for model validation.

The second data set used for model validation consists of PRBN input signals with a clock frequency of 0.0133 times the sample frequency. The bandwidth of these input signals corresponds with the bandwidth of the input signals applied to the process during normal operation. Fig. 7.20c and 7.20d show the measured process responses together with the output signals simulated by the MPSSM model and its 7-th order approximation over an interval of 2000 samples.

Table 7.10 summarizes the ratios of the average powers of output errors and measured ouputs for the various outputs and for the 4 different estimated models. To ease comparison of the various results also in table 7.10 the

results obtained on the data used for the parameter estimations have been included.

	FIR	MPSSM Gerth	MPSSM direct	7-th ord. appr
		Validation data results		
output 1	0.2104	0.2967	0.1805	0.1835
output 2	0.1121	0.1937	0.0576	0.0581
		Results obtained on data used for parameter estimation		
output 1	0.1523	0.2156	0.1257	0.1462
output 2	0.0886	0.2327	0.0621	0.0789

Table 7.10 Ratio of the average power of the output error and the average power of the measured process output of the shaping part of the tube glass production process computed with the 4 estimated models on the second data set used for model validation.

Both validation results show that the input/output behaviour of the MPSSM model and of its 7-th order approximate realization very well resemble the input/output behaviour of the shaping part of the tube glass production process.
The average relative error for the first validation data set is for the wall thickness about 14% for the MPSSM model and about 16% for the 7-th order approximation. For the diameter the results are respectively about 9% for the MPSSM model and about 10% for its 7-th order approximation.
For the second validation data set the quality of the wall thickness simulation has slightly decreased to an average relative error of about 18%. For the diameter the results are slightly better. The average relative error in the diameter simulations has decreased to about 6%.
Especially for the diameter the validation results obtained with the models are good. Overall it can be stated that the accuracy of the simulations on the validation data is about the same as the accuracy of the fit reached during the estimation of the model parameters on the data used for model parameter estimation.

The results obtained with the MPSSM model estimated with the direct estimation method appear to be the best for both validation sets. The 7-th order approximate realization of the MPSSM model estimated with the direct method gives about the same results. The MPSSM model obtained by using Gerth's algorithm gives the worst validation results.

7.7.2 Validation results obtained with the feeder models

For the validation of the models obtained for the feeder a data set has been used with PRBN input sequences with clock frequency of 0.05 times the sample frequency. Also the nominal values and the amplitudes of the input signal changes of the validation data have been different from the values of the data of the experiment that has been used for the model parameter estimations. The validation data have been prepared similar to the preparation of the data used for parameter estimation. For the model validation 1250 samples have been used. Fig. 7.21a - 7.21f show the results obtained for the 6 outputs.
To get an impression of the quality of the fit of the simulated outputs to the measured process responses the ratio of the average power of the output error and the average power of the corresponding measured process response (cf. eq. (7.1)) has been computed for each output over the full validation interval. No data are used to decrease effects of wrong initial values of the models. Table 7.11 summarizes the results obtained with each of the 4 models (FIR, MPSSM-Gerth, MPSSM-direct and 6-th order approximate realization). Also the earlier obtained results on the data used for the estimation of the model parameters have been included in table 7.11 to make comparison of the various results easier.

	FIR	MPSSM Gerth	MPSSM direct	6-th ord. appr
		Validation data results		
output 1	0.2719	0.2719	0.2648	0.2633
output 2	0.3058	0.2874	0.3026	0.3028
output 3	0.3064	0.2918	0.3051	0.3048
output 4	0.0664	0.1057	0.0479	0.0504
output 5	0.0888	0.0584	0.0604	0.0602
output 6	0.1689	0.1173	0.0949	0.0984
		Results obtained on data used for parameter estimation		
output 1	0.0937	0.1930	0.1163	0.1165
output 2	0.0844	0.1408	0.1025	0.1045
output 3	0.0862	0.1430	0.1041	0.1060
output 4	0.0284	0.2350	0.0324	0.0375
output 5	0.0310	0.0542	0.0357	0.0358
output 6	0.0564	0.1009	0.0665	0.0697

Table 7.11 Ratio of the average power of the output error and the average power of the measured process output of the feeder computed with the 4 estimated models on the data set used for model validation.

The error on the validation data appears to be worst for the first three outputs. The error found for output 2 and output 3 is about 30% of the

average signal power of the measured process responses. This error may be caused by the differences between the characteristics (nominal values and amplitudes) of the testsignals used for the model validation and the signals used for the estimation of the model parameters. The average power of the validation signals has been about 1/3 of the average signal power of the signals used for the estimation of the model parameters.
Due to the character of the process the flow of the glass through the feeder and the temperature distribution in the glass will have been different for both excitations. As the temperatures are measured at fixed positions the observed transfers will also be slightly different.

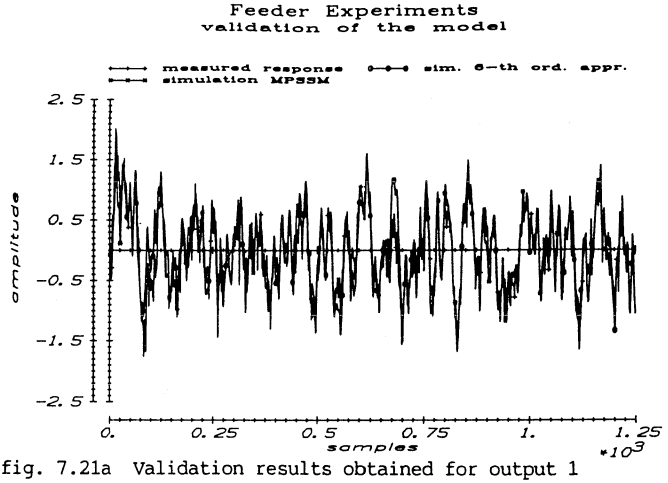

fig. 7.21a Validation results obtained for output 1

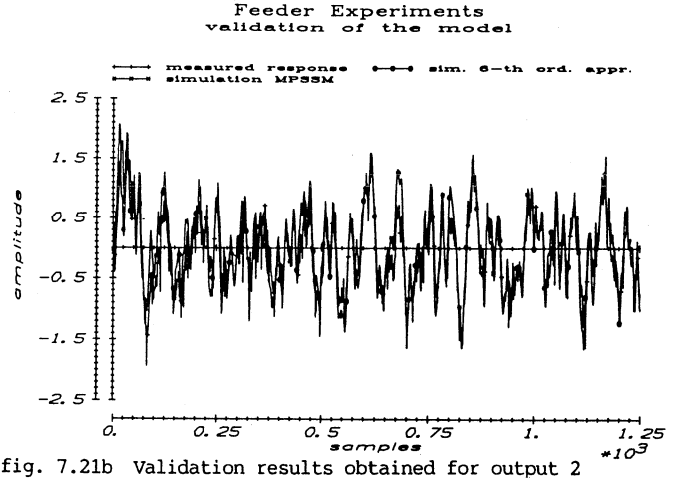

fig. 7.21b Validation results obtained for output 2

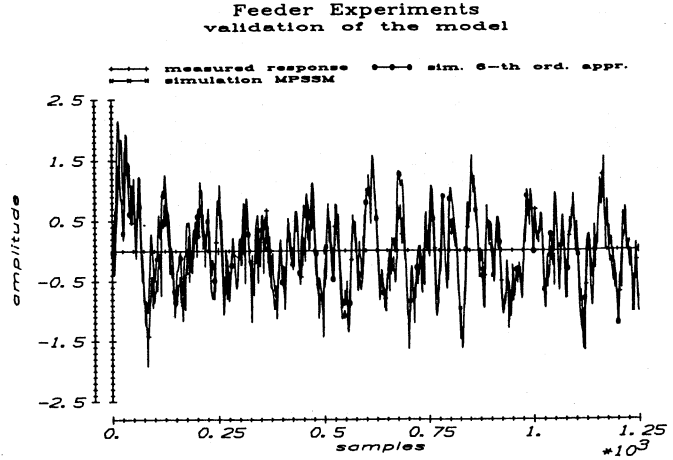

fig. 7.21c Validation results obtained for output 3

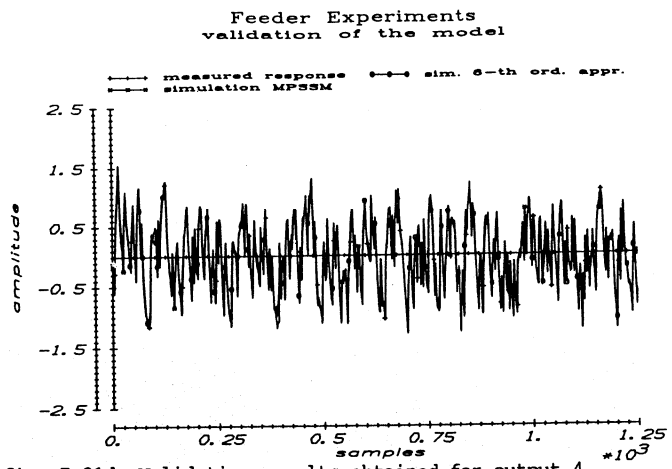

fig. 7.21d Validation results obtained for output 4

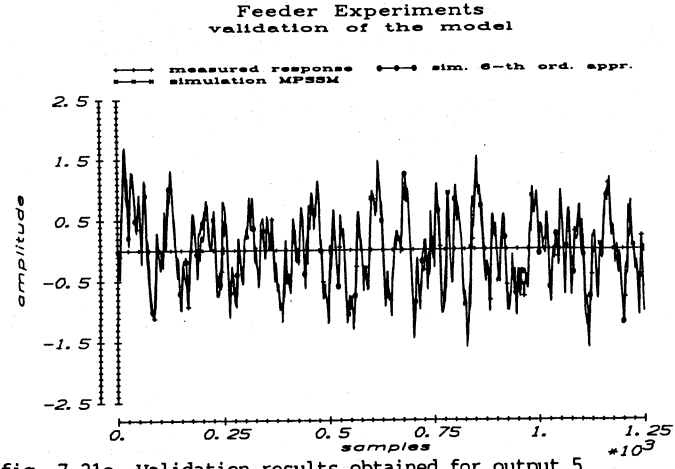

fig. 7.21e Validation results obtained for output 5

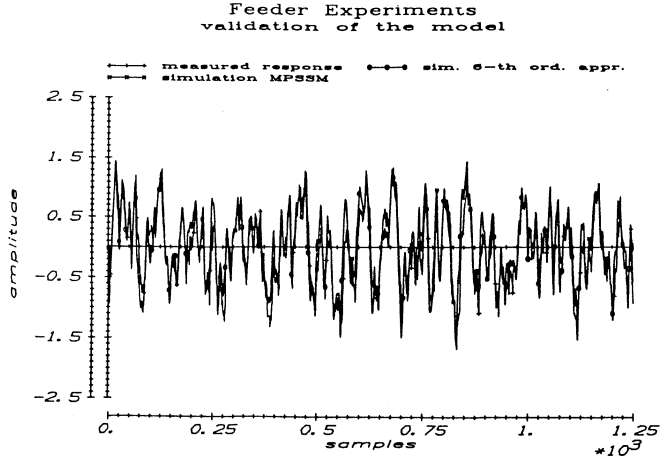

fig. 7.21f Validation results obtained for output 6

7.8 Concluding remarks

In this chapter the developed identification method has been applied to two different MIMO industrial processes. The first identified process is the shaping part of a tube glass production process. The second process is the feeder part of a glass melting installation.
Both investigated processes in fact are distributed parameter systems. The dynamic properties of both processes can therefore only approximately be described with the lumped parameter, linear, time invariant, discrete time type of models used for the identification. The processes certainly are not contained in the model sets used for the identification.

The initial experiments done with the processes and the first analyses of the processes to get insight in:

- the influences of all main process inputs on the measured outputs
- the bandwidth of the various transfers from inputs to outputs
- non-linearity of the processes in an environment of the working point
- the characteristics of disturbances measured at the outputs of the processes

have not been discussed. Knowledge obtained from the first experiments and analyses has been used to chose proper process inputs and sampling rates and to design the input signals applied for the modelling of the processes and for the validation of the models.

The signals measured from the processes have been prepared for parameter estimation and model validation with the techniques discussed in chapter 6.

All measured process outputs contained rather large trends caused by environmental disturbances. These trends have been removed from the signals because they are not caused by the applied process inputs. Furthermore these trends are expected not to be part of the process outputs any more as soon as an adequate control system, based on the obtained process model, is applied to the process.
The preparation of the signals for parameter estimation and model validation included (cf. section 7.3):

- removal of trends from the signals
- estimation of delay times and correction of the signals for the estimated delay times
- subtraction of average signal values and scaling of the signals to a standard deviation equal to one
- decimation of the signals used for parameter estimation to a clock frequency of the applied PRBN input sequences of one sample

The techniques applied for the analysis and the preparation of the signals worked well on the recorded process signals. No problems were encountered in the preparation of the signals.

The developed strategy for modelling of industrial processes approved to be successful.

The first step, the estimation of a FIR model (cf. section 7.4), only required little a-priori knowledge of the process. The knowledge required for the FIR model estimation is insight in the number of samples to be estimated of the impulse responses. This knowledge could be gained from measured step responses of the process and from computed cross correlation functions of applied PRBN input signals and the resulting process responses. The FIR model parameter estimation did not cause any problems and led to good results for both processes.

The second step in the modelling of the processes, the estimation of an appropriate degree for the minimal polynomial and the estimation of a MPSSM model with the Gerth algorithm (cf. section 7.5), also worked well for both processes. An appropriate degree for the minimal polynomial has been selected on the basis of the ratios of successive singular values of the finite block Hankel matrix in vector form (cf. fig. 7.14b, 7.14b, 7.15a and 7.15b).
The initial MPSSM models, obtained from the model to model estimation, appeared to have considerable worse simulation properties than the originally estimated FIR models.

The third step in the modelling of the processes, the estimation of MPSSM model parameters directly from the prepared input/output data, gave a large improvement of the MPSSM model for the tube glass production process with respect to the simulation of the process input/output behaviour. For the feeder the MPSSM model obtained from the direct estimation contained low frequency dynamics that were expected to be part of the model, but that did

not appear in the estimated FIR model. The MPSSM model parameters obtained in the second step have been used as initial values for the MPSSM model.

On the data used for the estimation of the model parameters the fit of the MPSSM models is as good as the fit of the FIR models for both processes. The direct estimated MPSSM models and their approximate realizations did not differ much with respect to the validation results obtained. Furthermore the simulation qualities of the direct estimated MPSSM models appeared to be better than or equal to the simulation qualities of the first estimated FIR models, while the number of degrees of freedom of the obtained MPSSM model and of its approximate realization are much lower than the number of degrees of freedom of the FIR model.

Validation of the models obtained for both processes showed a large improvement of the model during the last step of the identification for the shaping part of the tube glass production process. For the feeder only a minor improvement of the model was obtained with the direct estimation mehod. However, for the estimation of the MPSSM model parameters with the direct estimation method only 500 samples have been used. Regarding the length of the impulse responses generated by the estimated model this is a rather short data set.

From the results obtained for both processes it may be concluded that the developed identification method is a good method for the identification of stable industrial processes. The method is expected to give good results if the process satisfies the following conditions:

- almost linear or linearizable input/output behaviour in the environment of the working point in which the process is operated
- negligible time variance of the dynamic input/output behaviour of the process
- causal and stable transfers from inputs to outputs
- sufficiently accurate measurement of relevant process input and output signals possible
- possibility for simultaneous excitation of process inputs with noise sequences during at least about 5 - 10 times the response time of the process

Test of the method on both processes discussed showed that straightforward application of the method leads to good results.

8. USE OF THE ESTIMATED MODEL FOR CONTROL OF THE SHAPING PART OF THE TUBE GLASS PRODUCTION PROCESS

8.1 Introduction

An important application area for models obtained from process identification is the design of MIMO control systems. Many techniques for the design of control systems have been developed (cf. [Aström, 1984; Isermann, 1977; Kuo, 1980; Kwakernaak, 1972, 1985, 1986; Landau, 1979; MacFarlane, 1979; Owens, 1978; Rosenbrock, 1970; Vidyasagar, 1985, 1986; Zames, 1981, 1983; ...]). Many of the MIMO control system design techniques assume the availability of a model that exactly describes the input/output behaviour of the process. Sometimes the assumption of an exact process model is required to assure stabilility of the controlled process. Present research on the area of MIMO control systems is mainly concentrating on robust control systems for which stability of the controlled process is still guaranteed under the assumption of bounded modelling errors (cf. [Foias, 1986; Grimble, 1986; Kwakernaak, 1985, 1986; Nordström, 1984, 1985; O'Young, 1986; Vidyasagar, 1982, 1985, 1986; Zames, 1981, 1983, 1984; ...]).

The purpose of this chapter is to show, by means of an application, that, on the basis of the models obtained from the developed process identification method, well performing, industrially applicable MIMO control systems can be designed.

In this chapter the design will be discussed of a MIMO control system for the shaping part of the tube glass production process of which the identification has been discussed in the previous chapter. For the design of the control system the 7-th order approximate state space realization of the MPSSM model estimated with the direct estimation method (cf. section 7.6) has been used. For the control of the tube dimensions a model reference type of control system has been applied that does not require an exact process model to assure a good performance.
In section 8.2 the control system used for the control of the shaping part of the tube glass production process is introduced. Attention is paid to some properties of the control scheme used.
The actual design of the control system as it has been tested on the tube glass production process will be discussed in section 8.3.
Section 8.4 shows the results obtained with the control system in practice.
The chapter will be closed with some concluding remarks in section 8.5

8.2 Description of the applied control system

For control of the shaping part of the tube glass production process a model reference type of control system is applied. Fig. 8.1 shows the diagram of the MIMO control system. As in practice the process has two inputs and two outputs, in the analysis of the transfer properties of the controlled

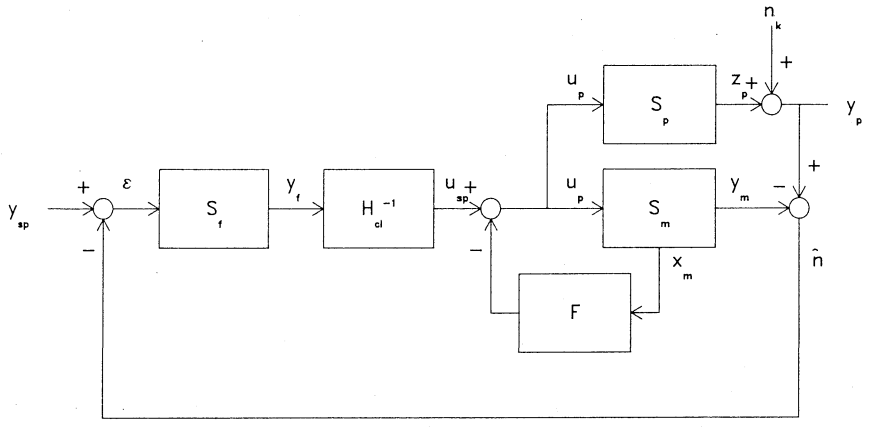

Fig. 8.1 Diagram of the MIMO control system

process the assumption is made that the process under control has an equal number of inputs and outputs.
The transfer of the process is assumed to be given by the following state space description (cf. eq. (2.3a) and (2.3b):

$$x_{p_{k+1}} = F_p \cdot x_{p_k} + G_p \cdot u_{p_k} \tag{8.1a}$$

$$z_{p_k} = H_p \cdot x_{p_k} + D_p \cdot u_{p_k} \tag{8.1b}$$

$$y_{p_k} = z_{p_k} + n_k \tag{8.1c}$$

with: u_{p_k} - input signal applied to the process
z_{p_k} - deterministic part of the process output signal
n_k - noise part of the process output signal

The state space model of the process, for example obtained from process identification, is given by the following equations:

$$x_{m_{k+1}} = F_m \cdot x_{m_k} + G_m \cdot u_{p_k} \tag{8.2a}$$

$$y_{m_k} = H_m \cdot x_{m_k} + D_m \cdot u_{p_k} \qquad (8.2b)$$

with: y_{m_k} - the output signal of the model

u_{p_k} - the input signal applied to the model which is the same as the input signal applied to the process

The dynamics of the model are modified with a state feedback controller F:

$$u_{p_k} = u_{sp_k} - F \cdot x_{m_k} \qquad (8.3)$$

with: F - the feedback matrix applied for state feedback control of the model

As the input signals u_p applied to the model are applied to the process as well (cf. fig. 8.1), also the dynamics of the process, considered between input u_{sp} and output y_p, will be modified accordingly if process and model have about the same input/output behaviour.

The difference of the measured process output signal and the output, simulated by the model, consists partly of the output noise of the process and partly of a residue of input signal u_{sp}, filtered by a transfer function, given by the differences in the dynamics of the process and the model. If the modelling errors are small over the frequency range of the actual signals, the difference between measured and simulated output signals may be considered to be an estimate for the process output noise n:

$$\hat{n}_k = y_{p_k} - y_{m_k} \qquad (8.4)$$

The estimated process output noise $\hat{n}_k$ is compared with the set point signal applied to the controlled process (cf. fig. 8.1). The resulting error signal ε is given by:

$$\varepsilon_k = y_{sp_k} - \hat{n}_k \qquad (8.5)$$

with: y_{sp_k} - set point signal applied to the controlled process

The error signal obtained, ε, is filtered by a filter with the following state space description:

$$x_{f_{k+1}} = F_f \cdot x_{f_k} + G_f \cdot \varepsilon_k \tag{8.6a}$$

$$y_{f_k} = H_f \cdot x_{f_k} \tag{8.6b}$$

with: y_{f_k} - the output signal of the filter

The output signal of the filter is multiplied with the inverse of the steady state transfer of the controlled process model:

$$u_{sp_k} = \{(H_m - D_m \cdot F) \cdot (I - F_m + G_m \cdot F)^{-1} \cdot G_m + D_m\}^{-1} \cdot y_{f_k} = H_{cl}^{-1} \cdot y_{f_k} \tag{8.7}$$

To enable analysis of the transfer characteristics of the controlled process a state space description is derived from eq. (8.1) - (8.3) that describes the transfer from u_{sp_k} to the outputs of the process and of the model:

$$\begin{bmatrix} x_p \\ x_m \end{bmatrix}_{k+1} = \begin{bmatrix} F_p & -G_p \cdot F \\ 0 & (F_m - G_m \cdot F) \end{bmatrix} \cdot \begin{bmatrix} x_p \\ x_m \end{bmatrix}_k + \begin{bmatrix} G_p \\ G_m \end{bmatrix} \cdot u_{sp_k} \tag{8.8a}$$

$$\begin{bmatrix} y_p \\ y_m \end{bmatrix}_k = \begin{bmatrix} H_p & -D_p \cdot F \\ 0 & (H_m - D_m \cdot F) \end{bmatrix} \cdot \begin{bmatrix} x_p \\ x_m \end{bmatrix}_k + \begin{bmatrix} D_p \\ D_m \end{bmatrix} \cdot u_{sp_k} + \begin{bmatrix} I \\ 0 \end{bmatrix} \cdot n_k \tag{8.8b}$$

An expression for the estimated output noise $\hat{n}_k$ as a function of the state of the process x_{p_k}, of the state of the model x_{m_k}, of the input u_{sp_k} and of

the output noise n_k is immediately obtained from eq. (8.8b):

$$\hat{n}_k = y_{p_k} - y_{m_k} = \begin{bmatrix} H_p & (-D_p \cdot F - H_m + D_m \cdot F) \end{bmatrix} \cdot \begin{bmatrix} x_p \\ x_m \end{bmatrix}_k +$$

$$(D_p - D_m) \cdot u_{sp_k} + n_k \qquad (8.9)$$

For convenience in notation the input/output transfer functions of the various parts of the controller will be used in the next part of the derivation. The transfer function of the process will be denoted by (cf. eq. (8.1a), (8.1b)):

$$S_p(z) = H_p \cdot (zI - F_p)^{-1} \cdot G_p + D_p \qquad (8.10)$$

The transfer function of the model will be denoted by (cf. eq. (8.2a), (8.2b)):

$$S_m(z) = H_m \cdot (zI - F_m)^{-1} \cdot G_m + D_m \qquad (8.11)$$

The transfer function of the filter is given by (cf. eq. (8.6a), (8.6b)):

$$S_f(z) = H_f \cdot (zI - F_f)^{-1} \cdot G_f \qquad (8.12)$$

To indicate the transfer function of the model controlled with state feedback controller F the following symbol will be used:

$$S_{mc}(z) = (H_m - D_m \cdot F) \cdot (zI - F_m + G_m \cdot F)^{-1} \cdot G_m + D_m \qquad (8.13)$$

Finally, the transfer function from input u_{sp_k} to process output z_{p_k}, the feedforward controlled process transfer, will be denoted by (cf. eq. (8.8a), (8.8b)):

$$S_{pc}(z) = \begin{bmatrix} H_p & -D_p \cdot F \end{bmatrix} \cdot \left(zI - \begin{bmatrix} F_p & -G_p \cdot F \\ 0 & (F_m - G_m \cdot F) \end{bmatrix} \right)^{-1} \cdot \begin{bmatrix} G_p \\ G_m \end{bmatrix} + D_p \qquad (8.14)$$

For notational convenience, in the sequel, the transfer functions will be denoted by S_p, S_m, S_f, S_{mc} and S_{pc} without explicit indication that they are functions of the advance operator z.
For the analysis of the transfer properties of the controlled process, y_p has to be expressed as a function of the setpoint y_{sp}. This expression is obtained as follows:

$$y_p = S_{pc} \cdot u_{sp} + n \tag{8.15}$$

$$y_m = S_{mc} \cdot u_{sp} \tag{8.16}$$

$$u_{sp} = H_{cl}^{-1} \cdot y_f = H_{cl}^{-1} \cdot S_f \cdot \varepsilon \tag{8.17}$$

$$\varepsilon = y_{sp} - y_p + y_m \tag{8.18}$$

Substitution of eq. (8.17) and (8.18) into eq. (8.15) and into eq. (8.16) respectively gives:

$$y_p = S_{pc} \cdot H_{cl}^{-1} \cdot S_f \cdot (y_{sp} - y_p + y_m) + n \tag{8.19}$$

$$y_m = S_{mc} \cdot H_{cl}^{-1} \cdot S_f \cdot (y_{sp} - y_p + y_m) \tag{8.20}$$

From eq. (8.20) follows:

$$(I - S_{mc} \cdot H_{cl}^{-1} \cdot S_f) \cdot y_m = S_{mc} \cdot H_{cl}^{-1} \cdot S_f \cdot (y_{sp} - y_p) \tag{8.21}$$

As a result of eq. (8.21) it is found that, in case the filter S_f is designed so that:

$$I - S_{mc} \cdot H_{cl}^{-1} \cdot S_f = 0 \tag{8.22}$$

the output of the process y_p necessarily has to be equal to y_{sp}. The controller has become a deadbeat control system. However, in general, S_f cannot be designed so that eq. (8.22) holds for all z. If S_f cannot be chosen so that eq. (8.22) holds for all frequencies it can be designed to hold for steady state. This implies that eq. (8.22) has to be satisfied for $z \to 1$. As a result the process response for steady state (i.e. z=1) has to be equal to the applied setpoint signal y_{sp} (cf. eq. 8.21):

$$y_p \Big|_{z=1} = y_{sp} \Big|_{z=1} \tag{8.23}$$

The condition:

$$I - S_{mc} \cdot H_{cl}^{-1} \cdot S_f \Big|_{z=1} = 0 \qquad (8.24)$$

implies, since (cf. eq. 8.7):

$$H_{cl} = S_{mc} \Big|_{z=1} \qquad (8.25)$$

that:

$$S_f \Big|_{z=1} = I \qquad (8.26)$$

As a consequence the controlled process will have a steady state error equal to zero if a filter with a steady state response equal to identity is applied.

From eq. (8.19) and (8.20) y_m may be eliminated. As a result the following expression is obtained:

$$(I + (S_{pc} - S_{mc}) \cdot H_{cl}^{-1} \cdot S_f) \cdot (I - S_{mc} \cdot H_{cl}^{-1} \cdot S_f) \cdot y_p =$$

$$S_{pc} \cdot H_{cl}^{-1} \cdot S_f \cdot (I - S_{mc} \cdot H_{cl}^{-1} \cdot S_f)^{-1} \cdot y_{sp} + n \qquad (8.27)$$

If $y_{sp} = 0$ then the contribution of the output noise to the output of the controlled process is found to be equal to:

$$y_p \Big|_{y_{sp}=0} = (I - S_{mc} \cdot H_{cl}^{-1} \cdot S_f) \cdot (I + (S_{pc} - S_{mc}) \cdot H_{cl}^{-1} \cdot S_f)^{-1} \cdot n \qquad (8.28)$$

If eq. (8.22) holds, optimal suppression of the noise is obtained. This implies, however, that the filter has to be equal to:

$$S_f = H_{cl} \cdot S_{mc}^{-1} \qquad (8.29)$$

In general (i.e. also for non-minimum phase S_{mc}) it will not be possible to satisfy eq. (8.29) with a stable filter. To maintain a good suppression of the noise a stable filter has to be used that assures $(I - S_{mc} \cdot H_{cl}^{-1} \cdot S_f)$ to be small over the full bandwidth of the noise since S_{mc} is assumed to be almost equal to S_{pc} in eq. (8.28).

A final point of interest is the stability of the closed loop system. This stability is determined by the eigenvalues of the state matrix of the total closed loop system. To derive a state space description for the closed loop system first the open loop system from input ε to output $\hat{n}$ (cf. fig. 8.1) is described by making use of eq. (8.8), (8.9), (8.15), (8.16) and (8.17). The loop is closed by applying output feedback to the obtained open loop system (cf. eq. (8.18)):

$$\hat{n} = S_t \cdot H_{cl}^{-1} \cdot S_f \cdot \varepsilon + n \tag{8.30}$$

with: S_t - the transfer of u_{sp} to $\hat{n}_k$

Transfer function S_t corresponds with the state space description given by eq. (8.8a) and (8.9). The inverse of the steady state closed loop model transfer H_{cl}^{-1} is given by eq. (8.7). A state space description of the filter S_f is given by eq. (8.6a), (8.6b). By series connection of the three systems a state space description for the total open loop transfer is obtained:

$$\begin{bmatrix} x_p \\ x_m \\ x_f \end{bmatrix}_{k+1} = \begin{bmatrix} F_p & -G_p \cdot F & G_p \cdot H_{cl}^{-1} \cdot H_f \\ 0 & (F_m - G_m \cdot F) & G_m \cdot H_{cl}^{-1} \cdot H_f \\ 0 & 0 & F_f \end{bmatrix} \cdot \begin{bmatrix} x_p \\ x_m \\ x_f \end{bmatrix}_k + \begin{bmatrix} 0 \\ 0 \\ G_f \end{bmatrix} \cdot \varepsilon_k \tag{8.31a}$$

$$\hat{n}_k = \begin{bmatrix} H_p & (D_m \cdot F - D_p \cdot F - H_m) & (D_p - D_m) \cdot H_{cl}^{-1} \cdot H_f \end{bmatrix} \cdot \begin{bmatrix} x_p \\ x_m \\ x_f \end{bmatrix}_k + n_k \tag{8.31b}$$

Closing the loop by application of output feedback gives, using eq. (8.5),

(8.31a) and (8.31b):

$$\begin{bmatrix} x_p \\ x_m \\ x_f \end{bmatrix}_{k+1} = \begin{bmatrix} F_p & -G_p \cdot F & G_p \cdot H_{cl}^{-1} \cdot H_f \\ 0 & (F_m - G_m \cdot F) & G_m \cdot H_{cl}^{-1} \cdot H_f \\ -G_f \cdot H_p & G_f \cdot (D_p \cdot F - D_m \cdot F + H_m) & F_f - G_f \cdot (D_p - D_m) \cdot H_{cl}^{-1} \cdot H_f \end{bmatrix} \cdot$$

$$\begin{bmatrix} x_p \\ x_m \\ x_f \end{bmatrix}_k + \begin{bmatrix} 0 \\ 0 \\ G_f \end{bmatrix} \cdot (y_{sp_k} - n_k) \qquad (8.32)$$

The outputs of the closed loop system are described by eq. (8.31b). Internal stability of the closed loop control system is determined by the eigenvalues of the state matrix of eq. (8.32). If the model is assumed to be an exact representation of the process dynamics, eq. (8.32) goes over into:

$$\begin{bmatrix} x_p \\ x_m \\ x_f \end{bmatrix}_{k+1} = \begin{bmatrix} F_m & -G_m \cdot F & G_m \cdot H_{cl}^{-1} \cdot H_f \\ 0 & (F_m - G_m \cdot F) & G_m \cdot H_{cl}^{-1} \cdot H_f \\ -G_f \cdot H_m & G_f \cdot H_m & F_f \end{bmatrix} \cdot \begin{bmatrix} x_p \\ x_m \\ x_f \end{bmatrix}_k +$$

$$\begin{bmatrix} 0 \\ 0 \\ G_f \end{bmatrix} \cdot (y_{sp_k} - n_k) \qquad (8.33a)$$

In this case the controlled process (cf. fig. 8.1) reduces to the system depicted in fig. 8.2. The output $\hat{n}$ of the closed loop system in this case becomes (cf. eq. (8.31b)):

$$\hat{n}_k = \begin{bmatrix} H_m & -H_m & 0 \end{bmatrix} \cdot \begin{bmatrix} x_f \\ x_m \\ x_f \end{bmatrix}_k + n_k \qquad (8.33b)$$

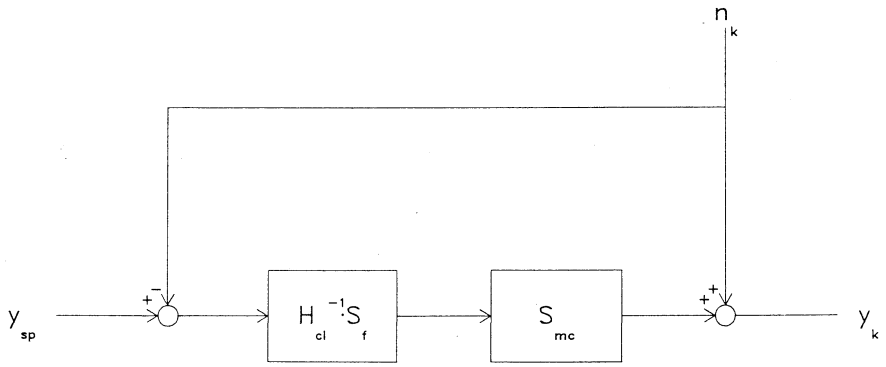

Fig. 8.2 Remaining control scheme in case the input/output behaviour of the model equals the input output behaviour of the process

To analyse the stability of the closed loop system a coordinate transformation is applied to the state of the closed loop system:

$$\begin{bmatrix} x_\alpha \\ x_\beta \\ x_f \end{bmatrix} = \begin{bmatrix} I & 0 & 0 \\ -I & I & 0 \\ 0 & 0 & I \end{bmatrix} \cdot \begin{bmatrix} x_p \\ x_m \\ x_f \end{bmatrix} = \begin{bmatrix} x_p \\ x_m - x_p \\ x_f \end{bmatrix} \tag{8.34}$$

After the coordinate transformation eq. (8.33a) and eq. (8.33b) go over into:

$$\begin{bmatrix} x_\alpha \\ x_\beta \\ x_f \end{bmatrix}_{k+1} = \begin{bmatrix} (F_m - G_m \cdot F) & -G_m \cdot F & G_m \cdot H_{cl}^{-1} \cdot H_f \\ 0 & F_m & 0 \\ 0 & G_f \cdot H_m & F_f \end{bmatrix} \cdot \begin{bmatrix} x_\alpha \\ x_\beta \\ x_f \end{bmatrix}_k +$$

$$\begin{bmatrix} 0 \\ 0 \\ G_f \end{bmatrix} \cdot (y_{sp_k} - n_k) \tag{8.35a}$$

$$\hat{n}_k = \begin{bmatrix} 0 & -H_m & 0 \end{bmatrix} \cdot \begin{bmatrix} x_f \\ x_m \\ x_f \end{bmatrix}_k + n_k \qquad (8.35b)$$

The output of the process y_p is equal to:

$$y_p = \begin{bmatrix} (H_m - D_m \cdot F) & -D_m \cdot F & G_m \cdot H_{cl}^{-1} \cdot H_f \end{bmatrix} \cdot \begin{bmatrix} x_\alpha \\ x_\beta \\ x_f \end{bmatrix}_k + n_k \qquad (8.35c)$$

In this representation the state x_β is no longer controllable. The eigenvalues of the closed loop system are determined by:

$$\det \left(\begin{bmatrix} \lambda I - F_m + G_m \cdot F & G_m \cdot F & -G_m \cdot H_{cl}^{-1} \cdot H_f \\ 0 & \lambda I - F_m & 0 \\ 0 & -G_m \cdot F & \lambda I - F_f \end{bmatrix} \right) =$$

$$\det (\lambda I - F_f) \cdot \det \left(\begin{bmatrix} \lambda I - F_m + G_m \cdot F & G_m \cdot F \\ 0 & \lambda I - F_m \end{bmatrix} + \begin{bmatrix} -G_m \cdot H_{cl}^{-1} \cdot H_f \\ 0 \end{bmatrix} \cdot (\lambda I - F_f)^{-1} \cdot \right.$$

$$\left. \begin{bmatrix} 0 & -G_m \cdot F \end{bmatrix} \right) =$$

$$\det(\lambda I - F_m + G_m \cdot F) \cdot \det(\lambda I - F_m) \cdot \det(\lambda I - F_f) \qquad (8.36)$$

As a result the eigenvalues of the closed loop system are found to be equal to the eigenvalues of the controlled model, the eigenvalues of the applied filter and the eigenvalues of the model. However, the modes of the model can not be excited from the setpoint input and will therefore only be observed at the process outputs as long as the states of the process and the states of the model differ.

As can be seen from eq. (8.36) the controlled process will always be stable if the process itself, the controlled model and the applied filter are stable and if the model is an exact representation of the process dynamics.

In this case the transfer from the controlled process input y_{sp} to the process output y_p will have eigenvalues determined by the applied filter and by the state feedback control applied to the model.

Of course modelling errors will influence the behaviour of the controlled process. In case of modelling errors the transfer of the controlled process input y_{sp} to the estimated noise $\hat{n}$ will no longer be equal to zero. As a consequence the stability of the controlled process will depend on the closed loop gain, which was not the case with modelling error equal to zero. However, by appropriate design of the filter S_f the controlled process will remain stable even when modelling errors occur.
The behaviour of the controlled process will depend on the differences in the input/output behaviour of the process and the input/output behaviour of the model. According to eq. (8.25) the output of the process will depend on the applied input y_{sp} as follows:

$$y_p = (I + (S_{pc} - S_{mc})\cdot H_{cl}^{-1}\cdot S_f)^{-1}\cdot S_{pc}\cdot H_{cl}^{-1}\cdot S_f\cdot y_{sp} +$$

$$(I + (S_{pc} - S_{mc})\cdot H_{cl}^{-1}\cdot S_f)^{-1}\cdot (I - S_{mc}\cdot H_{cl}^{-1}\cdot S_f)\cdot n$$

$$= (I + E_m)^{-1}\cdot S_{pc}\cdot H_{cl}^{-1}\cdot S_f\cdot y_{sp} + (I + E_m)^{-1}\cdot (I - S_{mc}\cdot H_{cl}^{-1}\cdot S_f)\cdot n \quad (8.37)$$

with: $E_m = (S_{pc} - S_{mc})\cdot H_{cl}^{-1}\cdot S_f$ the transfer related to the differences in the responses of process and model

The influence of the modelling errors on the behaviour of the controlled process compared to the behaviour with the modelling error being equal to zero is determined by the difference from zero of transfer function E_m. As long as the differences in the responses of the process and of the model are small for the applied input signals the behaviour will be close to the behaviour given by eq. (8.35a) - (8.35c).

Another nice property of the control scheme depicted in fig. 8.1 is that the results obtained so far remain valid, even if the process has time delays in the transfers from inputs to outputs. However, to allow comparison of measured process responses with the responses simulated by the model the model needs to have the same time delays included. In case of time delays the filter S_f has to be designed in such a way that disturbances with frequencies above $1/2\tau_d$ (τ_d is the time delay in a transfer) are sufficiently suppressed in each of the transfers to prohibit increase of the power of the noise for frequencies above $1/2\tau_d$ at the outputs of the controlled process.

8.3 Control system design

The control scheme discussed in the previous section has been applied for control of the shaping part of the Vello tube glass production process modelled in chapter 7. For the design of the control system the model obtained from the process identification has been used.
The process has delay times in the transfer from both inputs -mandril pressure and drawing speed- to the measured wall thickness and diameter responses (cf. section 7.3.1). For the experiments with the control system the diameter sensor has been positioned just below the wall thickness sensor. This implies that the delay time of the transfers to the diameter output have been almost equal to the delay times found for the transfers to the wall thickness output during the experiments.

Reduction of disturbances on the tube diameter and wall thickness with period times less than twice the delay time can not be realized. The design of the control system is therefore directed to the reduction of disturbances with frequencies less than $1/2\tau_d$ (τ_d: delay time from process inputs to a process output).

The design of the control system includes two steps:

- design of the state feedback controller F for the model
- design of the filter S_f

With the state feedback controller the dynamic behaviour of the process can be modified. For the design of the model state feedback controller two criteria have been used:

- the oscillatory behaviour of the responses, especially of the diameter response, had to be reduced
- the response time of the controlled process had to be reduced as much as possible without leading to too large input signal changes.

Limiting factors in the reduction of the response time of the process are the maximally allowed amplitudes of the input signals. For the design of the state feedback controller the implicit model-following technique has been used (cf. [Kreindler, 1976; Tyler, 1964]). With this technique its is possible to design a state feedback gain matrix F so that the controlled process has dynamic properties that highly resemble the properties of a reference system used for the design. The design starts with the definition of a desired dynamic behaviour of the controlled system:

$$y_{w_k} = A_1 \cdot y_{w_{k-1}} \tag{8.38}$$

with: A_1 - an AR parameter matrix that gives the desired system dynamics.

In a next step the behaviour of the system to be controlled is compared with the response characteristics defined by eq. (8.38):

$$z_k = y_{m_k} - y_{w_k} \simeq (H_m \cdot F_m - A_1 \cdot H_m) \cdot x_{k-1} \tag{8.39}$$

For the computation of the state feedback gain matrix F a linear quadratic criterium is used:

$$J = \frac{1}{2} \cdot \sum_{i=0}^{\infty} (z^t \; u^t)_i \cdot \begin{bmatrix} Q & 0 \\ 0 & R \end{bmatrix} \cdot \begin{bmatrix} z \\ u \end{bmatrix}_i \tag{8.40}$$

Minimization of the criterion as a function of the applied state feedback F results in a behaviour of the controlled system that closely follows the desired system behaviour if the weighting matrix Q is chosen much larger than weighting matrix R (e.g. $Q = 10^{10} \cdot I$ and $R = I$).

For the design of the state feedback gain F for the control of the shaping part of the tube glass production process the wanted process dynamics are given by:

$$y_{w_k} = \begin{bmatrix} 0.7 & 0.0 \\ 0.0 & 0.7 \end{bmatrix} \cdot y_{w_{k-1}} \tag{8.41}$$

	eigenvalues	transmission zeros
model without state feedback	0.8525 ± j0.2411 0.9212 ± j0.1590 0.9411 ± j0.0864 0.9656	5.8173 0.8679 ± 0.1462 0.9841 1.9369
model with state feedback	0.1719 0.5163 0.7000 0.7000 0.8679 ± j0.1462 0.9841	5.8173 1.9369 0.8679 ± j0.1462 0.9841

Table 8.1 Location of poles and transmission zeros without and with state feedback control of the model.

With the implicit model following design method a state feedback gain matrix F has been designed. Table 8.1 shows the eigenvalues and the transmission zeros of the model with and without state feedback control. As can be seen from table 8.1 the state feedback results in a system with the desired dynamics and an all pass characteristic. Transmission zeros outside the unit disk are compensated with poles at $1/z_i$ (z_i: transmission zero).

Transmission zeros inside the unit disk are compensated with poles positioned on top of the transmission zeros.

Fig. 8.3a and 8.3b show the step responses of the model premultiplied with the inverse steady state response.

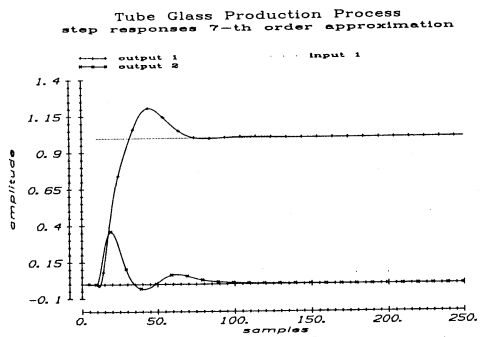

Fig. 8.3a Step responses of the model outputs to a step applied at input 1

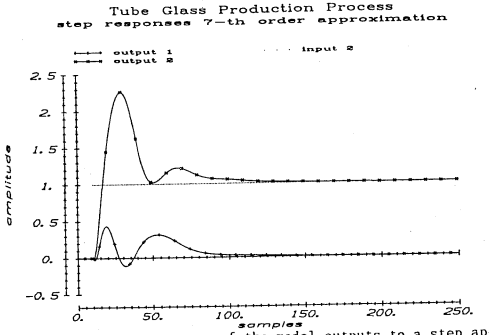

Fig. 8.3b Step responses of the model outputs to a step applied at input 2

Fig. 8.4a and 8.4b show the responses of the controlled model premultiplied with the inverse of its steady state response.

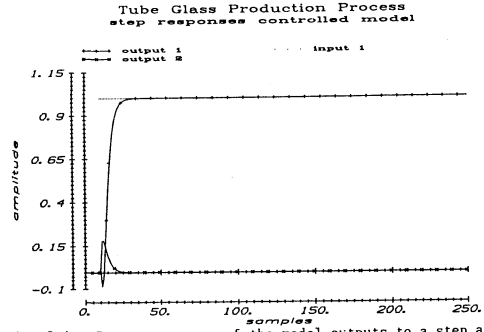

Fig. 8.4a Step responses of the model outputs to a step applied at input 1 after control of the model dynamics with state feedback

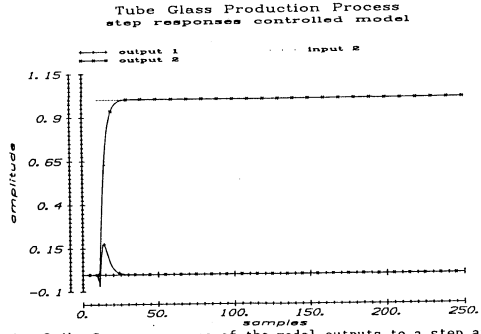

Fig. 8.4b Step responses of the model outputs to a step applied at input 2 after control of the model dynamics with state feedback

As can be seen from the responses the controlled model behaves much better than the uncontrolled model. The large overshoot disappeared completely and the process reaches its steady state in 25 sample intervals.

For the filter a first order low-pass filter with steady state gain equal to one has been used. As the controlled model, premultiplied with the inverse of its steady state response, has a nice, almost decoupled, response that reaches a steady state after 25 sample intervals, separate SISO filters have been applied for each input. The filters have been designed to suppress disturbances with frequencies higher than $1/2 \cdot \tau_d$. With τ_d equal to ≈10 (decimated) samples the poles of the first order filters have been chosen equal to z=0.95.

8.4 Results obtained with the control system

The control system has been applied for control of the shaping part of the tube glass production process. Experiments have been done alternately with the standard control system, consisting of a static decoupler and two SISO PID controllers, and the MIMO control system discussed in the previous sections.
While the standard control system showed a lot overshoot in the responses and needed about 750 sample intervals to reach a steady state, the MIMO control smoothly reached a steady state in about 60 sample intervals without overshoot. Fig. 8.5a and 8.5b show characteristic responses of the process with the standard control system recorded over 10000 sample intervals. Fig. 8.6a and 8.6b show the recorded process responses over 10000 sample intervals with the MIMO control system.
As can be seen from the recorded process responses the behaviour of the process has drastically improved during application of the MIMO control system. Fig. 8.7a - 8.7d finally show the computed frequency distributions of the tube wall thicknesses and diameters with the standard control system and with the MIMO control system. For the computation of the frequency distributions two other series of 10000 samples have been used.

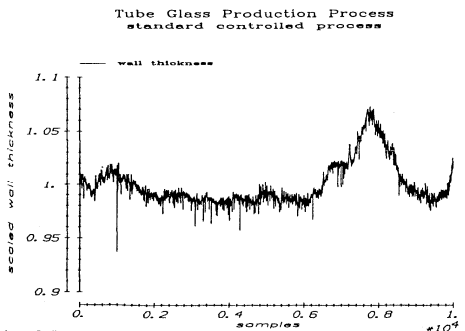

Fig. 8.5a Scaled wall thickness of the tube recorded during a time interval of 10000 samples with the standard control system applied

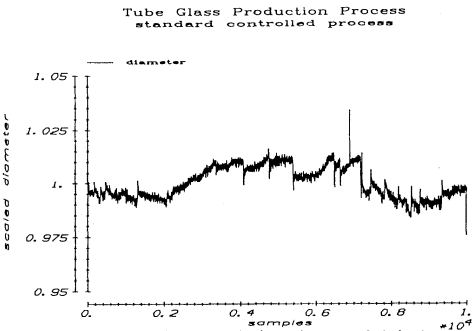

Fig. 8.5b Scaled diameter of the tube recorded during a time interval of 10000 samples with the standard control system applied

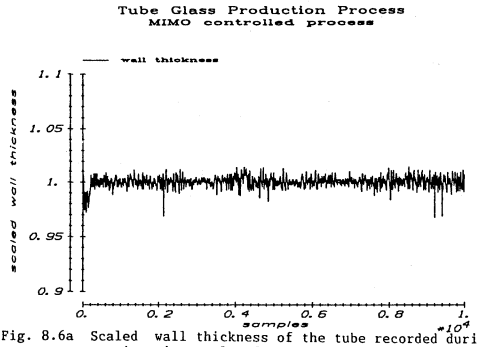

Fig. 8.6a Scaled wall thickness of the tube recorded during a time interval of 10000 samples with the MIMO control system applied

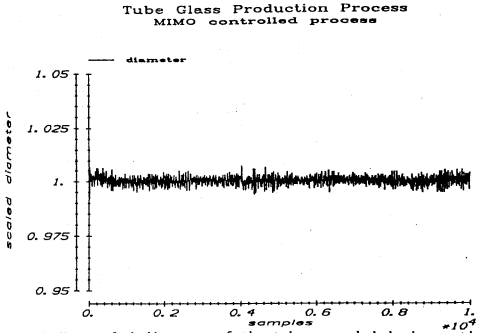

Fig. 8.6b Scaled diameter of the tube recorded during a time interval of 10000 samples with the MIMO control system applied

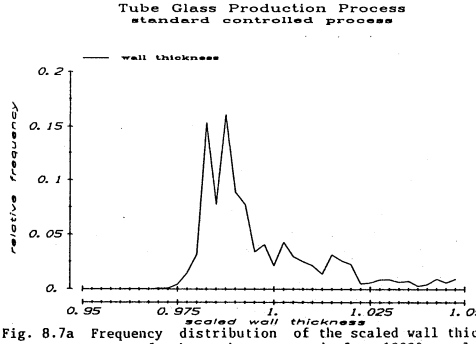

Fig. 8.7a Frequency distribution of the scaled wall thickness of the tube computed from 10000 samples. During the recording the process has been operated with the standard control system.

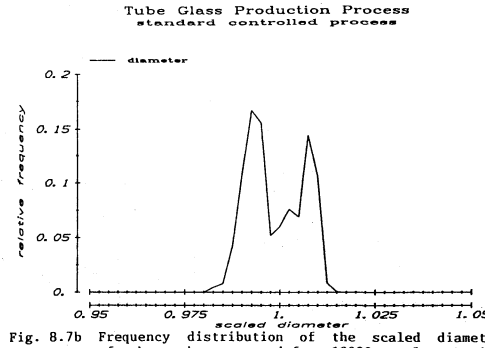

Fig. 8.7b Frequency distribution of the scaled diameter of the tube computed from 10000 samples. During the recording the process has been operated with the standard control system.

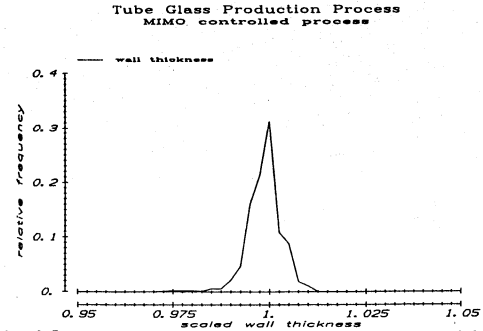

Fig. 8.7c Frequency distribution of the scaled wall thickness of the tube computed from 10000 samples. During the recording the process has been operated with the MIMO control system.

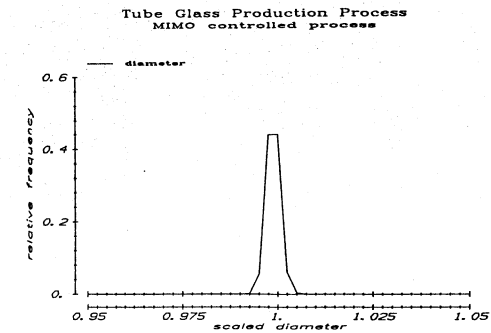

Fig. 8.7d Frequency distribution of the scaled diameter of the tube computed from 10000 samples. During the recording the process has been operated with the MIMO control system.

8.5 Concluding remarks

In this chapter the MIMO control system designed for the control of the shaping part of the tube glass production process has been discussed. For the design of the control system the model has been used that has been obtained from a process identification with the techniques developed in this thesis (cf. chapter 7).
For the control of the process a model reference type control system has been applied (cf. fig. 8.1). The type of control system used has the following characteristics:

- the process input signals are generated by the controlled model that acts as a feedforward controller for the process
- the process dynamics can be changed by appropriate design of a state feedback controller applied to the model
- application in the controller of a filter with a steady state response equal to the identity matrix guarantees a steady state error of the controlled process equal to zero
- if the modelling errors are negligibly small the eigenvalues of the controlled process are equal to the eigenvalues of the applied filter, the eigenvalues of the controlled model and the eigenvalues of the model
- the eigenvalues of the model only correspond to observable, not to controllable modes
- noise suppression of the closed loop system is determined by the characteristics of the applied filter. Appropriate design of the filter assures a good noise reduction.
- if modelling errors are not small the properties of the controlled process resemble those of a classic control system. In this case the applied filter acts as a controller and the performance of the closed loop system and the closed loop stability is fully determined by the applied filter
- delay times in the process input/output transfers can be handled easily during the design of the control system
- if modelling errors are small suppression of the noise is not restricted for frequencies exceeding $1/2\tau_d$ (τ_d: delay time) by required limitation of the loop gains

With the model obtained from the process identification the dynamic properties of the process could be modified. The responses of the process without the MIMO controller showed quite a lot of interaction and a lot of overshoot (cf. fig. 8.3a and 8.3b). The responses of the process, feedforward controlled by the model, turned into smooth and fast reacting first order responses (cf. fig. 8.4a and 8.4b). Furthermore the control system based on a compensation of the deterministic part of the measured process responses by the outputs predicted by the model enabled a good suppression of the noise components with frequencies lower than $1/2\tau_d$.

The control system has been tested in practice on the tube glass production process. The results obtained were good. With the MIMO control system based on the 7-th order state space model, obtained from the process identification, a large reduction could be reached in the time required to reach a steady state for both diameter and wall thickness after a change of the set-points of the MIMO control system compared to the time required with standard control system. The reduction in required time on the average during the experiments was better than a factor 10.
With the MIMO control system the overshoot in the process responses could be completely eliminated.
Finally, the standard deviation of both diameter and wall thickness responses of the process could be reduced to about 1/3 of the standard deviations obtained with the standard control.

The results obtained permit the conclusion that the technique developed for the modelling of industrial processes can be successfully applied to the design of MIMO process control systems.
Application of the models in combination with the type of control system discussed in this chapter is expected to enable both a good noise suppression and a fast and smooth response of the controlled process to setpoint changes.

9. CONCLUDING REMARKS

9.1 General conclusions

In this thesis a method for the identification of industrial processes has been developed, tested in simulation and applied to the modelling of the dynamic behaviour of two different industrial production processes.
Linear, causal, time invariant, discrete time models are used for the description of the process dynamics. Basically, the developed method consists of three separate identification steps:

1. Estimation of a FIR (Finite Impulse Response) model on the basis of measured process input/output data (cf. chapter 3)
2. Estimation of an MPSSM (Minimal Polynomial Start Sequence Markov parameter) model on the basis of the FIR model obtained from the first step (cf. chapter 4)
3. Estimation of an MPSSM model on the basis of measured process input/output data. The MPSSM model parameters obtained from the second identification step are used as initial parameter values for the iterative process in the Direct Estimation method. To remove inherently present, irrelevant modes (cf. section 4.2) from the estimated MPSSM model, an approximate state space realization of the MPSSM model is determined (cf. chapter 5)

Each of the three identification steps results in a useful model. The subsequent steps improve the models, either with respect to the computational effort required to simulate process input/output behaviour with the model (step 2), or with respect to the resemblance of the input/output behaviour simulated by the model to the measured input/output behaviour of the process (step 3).

The main advantages of the developed method are summarized by the following conclusions:

- Only limited a priori information is required for each identification step. The information that is needed for each subsequent step can be obtained from the results of previous steps:
  - .the estimation of the FIR model parameters only requires a priori information with respect to the number of Markov parameters to be estimated. The number of parameters to be estimated can be obtained from observed step responses of the process and from computed cross correlations between measured process inputs, excited with zero mean, white noise, and corresponding process outputs (cf. section 2.2, section 3.2, section 6.4 and 6.5).
  - .the estimation of the MPSSM model parameters in the second step only requires a value for the degree of the minimal polynomial

as a priori information. An estimate for the degree of the minimal polynomial can be obtained from the FIR model parameters estimated in the first step (cf. section 4.3, 4.3.1 and 4.3.2).

.the estimation of the MPSSM model parameters in the third step requires a value for the degree of the minimal polynomial and initial values for the model parameters (cf. section 5.2.1). The required a priori information is obtained from the results of the second identification step.

.the computation of an approximate realization of the MPSSM model obtained from the third step requires an appropriate value for the order of the approximate model. The Hankel singular values of the MPSSM model give an indication for the order to be used (cf. section 3.6 and section 5.4.2).

- No structural identification is required:

  .the determination of an appropriate structure for the model (cf. section 2.3.1), as required for the estimation of model parameters of a (pseudo) canonical model, is implicitly done during the computation of an approximate realization of the MPSSM model. The usually cumbersome estimation of an appropriate structure of the model, which structure often has no relation with the true process structure, is not needed.

- Even if the true process impulse responses do not belong to the model set used for the parameter estimation, the impulse responses of the obtained FIR model and the MPSSM model are expected to be as close as possible to the true process impulse responses in Frobenius norm under the following conditions (cf. sections 5.2, 5.2.1 and 5.2.2):

  .Input signals used for the estimation of the models parameters are stationary, zero mean, inter channel-independent, white noise sequences.

  .Applied input signals are not correlated with process output noise.

  .Number of input/output samples used for the parameter estimation is sufficiently large (cf. section 5.2.1 approximation of eq. (5.30) by eq. (5.32)).

  The first condition is sufficient, but not stricly necessary. In general, it will be sufficient to have input signals with a flat frequency spectrum and that are persistently exciting.

- The estimation of the MPSSM model parameters directly from input/output data involves minimization of a function of the minimal polynomial coefficients only (cf. section 5.3):

  .Cost function $V(\underline{a},\underline{M})$ is a quadratic function of the start sequence of Markov parameters. As a consequence the values of the start sequence of Markov parameters that minimize V can be found by solving a set of linear equations. An analytic solution has been derived for the computation of the start sequence of Markov parameters that minimize V. In the expression obtained the start sequence of Markov parameters is given as a

function of the minimal polynomial coefficients (cf. eq. (5.66)).

.Numerical minimization of the cost function implies minimization of a function of r (the degree of the minimal polynomial) independent variables, while minimization of a similar cost function for the estimation of corresponding parameters of a (pseudo) canonical model involves the determination of $n \cdot \min(p,q)$ (n: order of the model, p: number of inputs, q: number of outputs) independent variables with a numerical minimization method. The values of n and r used in the expressions satisfy the following inequality: $r \leq n$.

- In each of the identification steps compared to model sets related to (pseudo) canonical forms (cf. [Guidorzi, 1975, 1982]) relatively large sub sets of the set of linear, causal, time invariant, discrete time models are used:

  .As a consequence of the size of the model sets used during each of the identification steps and as a consequence of the availability of appropriate a priori information for each of the parameter estimations, the model resulting from a process identification is expected to be a good reflection of the process input/output behaviour. Applications of the identification method have confirmed this expectation (cf. chapter 7).

- For the estimation of the model parameters in the first and the third identification step cost functions based on output errors are minimized:

  .Model parameters are estimated by minimizing, as a function of the model parameters, the differences between measured process outputs and outputs simulated by the model on the basis of applied input signals only. The model is tuned to simulate output signals on the basis of input signals only. As a result the model only requires input signals to simulate outputs that will be close to the measured process outputs.
  The models obtained from the identification, in general, are expected to be well suited for the simulation of process input/output behaviour on the basis of applied input signals. This expectation has been confirmed by the validation results obtained with the identified models for both processes (cf. sections 7.7, 7.7.1 and 7.7.2).

The main disadvantages of the developed method are summarized by the following conclusions:

- In each of the three identification steps relatively large model sets are used:

  .The number of model parameters to be estimated, in general, is larger than the number of parameters of a (pseudo) canonical

model that could be used for modelling the same process. The number of parameters of the FIR model is equal to $(m+1)\cdot p\cdot q$. The number of parameters of the MPSSM model equals $(r+1)\cdot p\cdot q+r$ while the number of parameters of the pseudo canonical model is equal to $n\cdot(p+q)+p\cdot q$ where n (the order of the system) and r (the degree of the minimal polynomial) will be chosen so that $r \leq n$. As a consequence the accuracy of the estimated model parameters is expected to be worse for the FIR model and for the MPSSM model than for a (pseudo) canonical model if the true process fits in the set of models used for the parameter estimation.

- The MPSSM model has distinct multiple eigenvalues of a degree $r\cdot\min(p,q)$ (cf. section 4.2):

  .In general, not all modes of the MPSSM model resulting from a parameter estimation will give a significant contribution to the input/output behaviour of the model. To get rid of the inherently present, irrelevant part of the MPSSM model a reduced order approximate realization of the MPSSM model has to be computed (cf. section 5.2.4).

  .Processes almost never have multiple eigenvalues. As a consequence processes, in general, will not belong to the model set used for the estimation of the model parameters unless rather high degrees are used for the minimal polynomial.

- Due to the fact that, for the estimation of the MPSSM model parameters on the basis of input/output data, an output error criterion is minimized, a numerical method has to be used for the computation of the model parameters. The computational effort required for minimization of the cost function is large because of the complexity of the cost function that has to be minimized (cf. section 5.4).

- The estimation of MPSSM model parameters on the basis of input/output data requires good initial values for the model parameters (cf. section 5.2.1):

  .As the cost function, used for the estimation of the MPSSM model parameters, itself is a high order polynomial of the minimal polynomial coefficients, it will have many minima. In general, the numerical minimization method used for searching for the minimum only converges to a local minimum. As a consequence the model obtained from the parameter estimation will depend on the initial values used for the model parameters.
  Tests with initial values equal to zero and initial values obtained from earlier estimated MPSSM models led to different results and confirmed the expectation that a proper initialization of the model parameters is important. However, tests with initial parameter values obtained with the Gerth method (cf. section 4.4) and with initial parameter values obtained via approximate realizations of the FIR models (cf. section 4.5)

resulted in exactly the same MPSSM models for all of the 80 tests done (cf. section 5.5). This last result indicates that the parameter estimation is not very sensitive to small changes in initial parameter values.

So far the developed method has been applied for the modelling of several different industrial processes. The results obtained for two of the investigated processes have been discussed (cf. chapter 7).
The results obtained for each of the investigated processes showed on validation data sets that the models simulate the process outputs with accuracies that are close to the maximum obtainable accuracies determined by the output noise. The conditions, that have to be fulfilled to obtain a model that approximates "the impulse responses" of the process as closely as possible in Frobenius norm, can almost always easily be satisfied in industrial practice. Wether the conditions are satisfied can be tested on the basis of the available process input/output data.

Extrapolation of the results obtained with the various applications indicates that the developed method probably can be successfully applied for the identification of all (stable) processes, which are operated in a limited set of working points and which have the property that the dynamic behaviour in the vicinity of the working points can be linearized with the accuracy demanded by the application of the model.

9.2 Use of the method in practice

For successful identification of industrial processes with the developed method, an appropriate selection of process inputs and outputs, the use of test signals tuned to the process and a proper preparation of the measured process signals are crucial (cf. section 2.2, sections 5.2, 5.2.1, 5.2.2, chapter 6, chapter 7). In general the following guidelines can be used:

- The selected process inputs and outputs have to satisfy the following conditions:
  - .Excitation of the inputs and measurement of the outputs has to be possible.
  - .Independent excitation of the process outputs above the process output noise level has to be possible.
  - .Excitation of the process inputs with the maximally permitted input signals has to result in process responses that exceed, both with respect to amplitude and with respect to rate of change, the values needed during subsequent applications of the model.
  - .The bandwidth of the various transfers between the inputs and outputs has to be in correspondance with the requirements imposed by the application of the model.
  - .Linearization of the process input/output behaviour has to be allowable for the ranges used for the applied input and output signals.

- The sample frequency, the input signal amplitudes, the bandwidth of the applied testsignals and the length of the experiments have to satisfy the following conditions:
  - .The sample frequency has to be chosen high enough to allow processing of the recorded signals without loss of information that is relevant for the identification (cf. section 6.6).
  - .Input signal amplitudes have to be chosen in correspondence with the maximum amplitudes applied to the process during normal operation.
  - .The bandwidth of the input signals applied for process identification has to exceed the bandwidth of the process transfers that have to be modelled. All frequencies present in the input/output transfer of the process have to be equally excited.
  - .PRBN (Pseudo Random Binary Noise) sequences are preferred as input signals as they are, with respect to generation, deterministic signals that can easily be manipulated and, with respect to the application as input test signals, signals with the required stochastic properties: stationary, zero mean, white.
  - .The length of experiments used for the estimation of model parameters and for the validation of models obtained has to be chosen so that several periods of the lowest frequency that has to be accurately modelled during the parameter estimation, are included in the recorded process data.

- Preparation of recorded process signals for parameter estimation and model validation has, in general, to include the following steps (cf. chapter 6):
  - .Removal of trends from the recorded signals (cf. section 6.2, sections 7.3.1, 7.3.2).
  - .Removal of spikes from recorded process signals (cf. section 6.3)
  - .Estimation of delay times and compensation of recorded signals for estimated time delays (cf. section 6.4, sections 7.3.1, 7.3.2).
  - .Testing for linearity of the process input/output transfers that have to be modelled and linearization of the recorded process behaviour (cf. section 6.5).
  - .Decimation of the processed signals in order to remove no longer needed redundancies from the signals (cf. section 6.6).
  - .Scaling of the signals and subtraction of average signal values to allow a balanced estimation of the various input output transfers (cf. section 6.7).

In general, the conditions, that have to be satisfied to obtain models with impulse responses, which are as closely as possible to the true systems impulse responses, are easy to fulfil in practice. The conditions concentrate

on the input signals applied for the parameter estimation (cf. chapter 5, eq. (5.12) - (5.16)) and on the length of the experiments.
The length of experiments has to be chosen so that, within the finite interval used for the parameter estimation, approximation of the various signal product matrices by their limits is allowed (cf. chapter 5, eq. (5.12) - (5.16), (5.19) - (5.31)).

As a consequence of the assumptions a convergence problem can be expected if the identification method is applied to the modelling of a process in closed loop. In this case the condition that input signal and output noise may not be correlated, in general, will not be satisfied.

Finally, in all derivations made, unstable systems have been excluded as most industrial processes are stable if primary process control functions (cf. section 1.2) are considered to be part of the process that has to be modelled. The MPSSM model can also be used to describe unstable processes. If unstable processes have to be modelled too with the identification method described, instead of a FIR model an ARMA model has to be estimated initially and the estimation of the MPSSM model parameters has to be extended with an estimation of initial conditions.

The applications described in chapter 7 indicate that straightforward application of the developed method gives good results which can effectively be used in control schemes as has been explained in chapter 8. As simple, straightforward application of the method led to good results, even for such a complex process as the feeder, the method is expected to be suited for many industrial applications.

APPENDIX A

Derivation of the partial derivatives of cost function V with respect to the FIR process model and AR noise model parameters

Define cost function V by:

$$V = \mathrm{tr}\{(Y - \hat{\Theta}\cdot\Omega)\cdot(Y - \hat{\Theta}\cdot\Omega)^t\} \qquad (A.1)$$

with: $\hat{\Theta} = [\hat{M}_m \; ; \; \hat{A}_n]$ the model parameters that have to be estimated

$\hat{M}_m = [\tilde{M}_0 \; ; \; \tilde{M}_1 \; ; \; \tilde{M}_2 \; ; \; \ldots \; ; \; \tilde{M}_m]$ the Markov parameters

$\hat{A}_n = [\tilde{A}_1 \; ; \; \tilde{A}_2 \; ; \; \ldots \; ; \; \tilde{A}_n]$ the AR noise parameters

$\Omega = [\Omega_m^t \; ; \; \tilde{H}_n^t]^t$

$$\Omega_m = \begin{bmatrix} u_k & u_{k+1} & \cdots & u_{k+l} \\ u_{k-1} & u_k & \cdots & u_{k+l-1} \\ \cdot & \cdot & & \cdot \\ \cdot & \cdot & & \cdot \\ u_{k-m} & u_{k+1-m} & \cdots & u_{k+l-m} \end{bmatrix}$$

$$\hat{H}_n = \begin{bmatrix} \tilde{e}_{k-1} & \tilde{e}_k & \cdots & \tilde{e}_{k+l-1} \\ \tilde{e}_{k-2} & \tilde{e}_{k-1} & \cdots & \tilde{e}_{k+l-2} \\ \cdot & \cdot & & \cdot \\ \cdot & \cdot & & \cdot \\ \tilde{e}_{k-n} & \tilde{e}_{k+1-n} & \cdots & \tilde{e}_{k+l-n} \end{bmatrix}$$

$$\tilde{e}_k = y_k - \hat{y}_k = y_k - \hat{M}_m\cdot[u_k^t \;\; u_{k-1}^t \;\; \ldots \;\; u_{k-m}^t]^t$$

$$\tilde{e}_k = A_1\cdot\tilde{e}_{k-1} + A_2\cdot\tilde{e}_{k-2} + \; \ldots \; + A_n\cdot\tilde{e}_{k-n} + \xi_k$$

Working out eq. (A.1) gives:

$$V = \mathrm{tr}\,\{Y\cdot Y^t - 2\cdot\hat{\Theta}\cdot\Omega + \hat{\Theta}\cdot\Omega\cdot\Omega^t\cdot\hat{\Theta}^t\} =$$

$$= \mathrm{tr}\left\{Y\cdot Y^t - 2\cdot\left[\hat{M}_m\ ;\ \hat{A}_n\right]\cdot\begin{bmatrix}\Omega_m\\ \hat{H}_n\end{bmatrix}\cdot Y^t + \left[\hat{M}_m\ ;\ \hat{A}_n\right]\cdot\begin{bmatrix}\Omega_m\\ \hat{H}_n\end{bmatrix}\cdot \left[\Omega_m^t\ ;\ \hat{H}_n^t\right]\cdot\begin{bmatrix}\hat{M}_m^t\\ \hat{A}_n^t\end{bmatrix}\right\} =$$

$$= \mathrm{tr}\{Y\cdot Y^t - 2\cdot\hat{M}_m\cdot\Omega_m\cdot Y^t - 2\cdot\hat{A}_n\cdot(Y_m^* - \hat{M}_m^*\cdot\Omega_m^*)\cdot Y^t + \hat{M}_m\cdot\Omega_m\cdot\Omega_m^t\cdot M_m^t +$$

$$2\cdot\hat{A}_n\cdot(Y_m^* - M_m^*\cdot\Omega_m^*)\cdot\Omega_m^t\cdot\hat{M}_m + \hat{A}_n\cdot(Y_m^* - M_m^*\cdot\Omega_m^*)\cdot(Y_m^{*t} - \Omega_m^{*t}\cdot M_m^{*t})\cdot\hat{A}_n^t\} \qquad (A.2)$$

with: $Y_m^* = [Y_{-1}^t\ ;\ Y_{-2}^t\ ;\ \ldots\ ;\ Y_{-n}^t]^t$

$$Y_{-i} = [y_{k-i}\ ;\ y_{k-i+1}\ ;\ \ldots\ ;\ y_{k-i+l}]$$

$$M_m^* = \mathrm{diag}(\hat{M}_m) = \begin{bmatrix}\hat{M}_m & 0 & \ldots & 0\\ 0 & \hat{M}_m & \ldots & 0\\ \cdot & \cdot & & \cdot\\ \cdot & \cdot & & \cdot\\ 0 & 0 & \ldots & \hat{M}_m\end{bmatrix}$$

$$\Omega_m^* = \left[\Omega_{m_{-1}}^t\ ;\ \Omega_{m_{-2}}^t\ ;\ \ldots\ ;\ \Omega_{m_{-n}}^t\right]^t$$

$$\Omega_{m_{-i}} = \begin{bmatrix}u_{k-i} & u_{k-i+1} & \cdots & u_{k-i+l}\\ u_{k-i-1} & u_{k-i} & \cdots & u_{k-i+l-1}\\ \cdot & \cdot & & \cdot\\ \cdot & \cdot & & \cdot\\ u_{k-i-m} & u_{k-i+1-m} & \cdots & u_{k-i+l-m}\end{bmatrix}$$

The derivative of V with respect to the AR noise model parameters immediately follows from eq. (A.2):

$$\frac{\partial V}{\partial \hat{A}_n} = -2\cdot Y\cdot(Y_m^{*t} - \Omega_m^{*t}\cdot M_m^{*t}) + 2\cdot\hat{M}_m\cdot\Omega_m\cdot(Y_m^{*t} - \Omega_m^{*t}\cdot M_m^{*t}) +$$

$$2\cdot\hat{A}_n\cdot(Y_m^{*} - M_m^{*}\cdot\Omega_m^{*})\cdot(Y_m^{*t} - \Omega_m^{*t}\cdot M_m^{*t}) \qquad (A.3)$$

The derivatives of each of the terms of eq. (A.2) with respect to $\hat{M}_m$ are respectively:

$$\frac{\partial\, tr\{\hat{M}_m\cdot\Omega_m\cdot Y^t\}}{\partial \hat{M}_m} = Y\cdot\Omega_m^t \qquad (A.4)$$

$$\frac{\partial\, tr\{\hat{A}_n\cdot(Y_m^{*} - M_m^{*}\cdot\Omega_m^{*})\cdot Y^t\}}{\partial \hat{M}_m} =$$

$$- \frac{\partial\, tr\{\hat{A}_n\cdot\left[\Omega_{m-1}^t\cdot M_m^t\ ;\ \Omega_{m-2}^t\cdot M_m^t\ ;\ \ldots\ ;\Omega_{m-n}^t\cdot M_m^t\right]^t\cdot Y^t\}}{\partial \hat{M}_m} =$$

$$- \frac{\partial\, tr\{\sum_{i=1}^{n}\tilde{A}_i\cdot\hat{M}_m\cdot\Omega_{m-i}\cdot Y^t\}}{\partial \hat{M}_m} =$$

$$- \sum_{i=1}^{n}\tilde{A}_i^t\cdot Y\cdot\Omega_{m-i}^t \qquad (A.5)$$

$$\frac{\partial\, tr\{\hat{M}_m\cdot\Omega_m\cdot\Omega_m^t\cdot\hat{M}_m^t\}}{\partial \hat{M}_m} = 2\cdot\hat{M}_m\cdot\Omega_m\cdot\Omega_m^t \qquad (A.6)$$

$$\frac{\partial\, tr\{\hat{A}_n\cdot(Y_m^{*} - M_m^{*}\cdot\Omega_m^{*})\cdot\Omega_m^t\cdot\hat{M}_m^t\}}{\partial \hat{M}_m} =$$

$$\frac{\partial\, \mathrm{tr}\{ \sum_{i=1}^{n} \left(\tilde{A}_i \cdot Y_{-i} \cdot \Omega_m^t \cdot \hat{M}_m^t - \tilde{A}_i \cdot \hat{M}_m \cdot \Omega_{m_{-i}} \cdot \Omega_m^t \cdot \hat{M}_m^t \right) \}}{\partial\, \hat{M}_m} =$$

$$\sum_{i=1}^{n} \left(\tilde{A}_i \cdot Y_{-i} \cdot \Omega_m^t - \tilde{A}_i^t \cdot \hat{M}_m \cdot \Omega_m \cdot \Omega_{m_{-i}}^t - \tilde{A}_i \cdot \hat{M}_m \cdot \Omega_{m_{-i}} \cdot \Omega_m^t \right) \qquad \text{(A.7)}$$

$$\frac{\partial\, \mathrm{tr}\{\hat{A}_n \cdot (Y_m^* - M_m^* \cdot \Omega_m^*) \cdot (Y_m^{*t} - \Omega_m^{*t} \cdot M_m^{*t}) \cdot \hat{A}_n^t\}}{\partial\, \hat{M}_m} =$$

$$\frac{\partial\, \mathrm{tr}\{ \sum_{i=1}^{n} \sum_{j=1}^{n} \left(-2 \cdot \tilde{A}_i \cdot Y_{-i} \cdot \Omega_{m_{-j}}^t \cdot \hat{M}_m^t \cdot \tilde{A}_j^t + \tilde{A}_i \cdot \hat{M}_m \cdot \Omega_{m_{-i}} \cdot \Omega_{m_{-j}}^t \cdot \hat{M}_m^t \cdot \tilde{A}_j^t \right) \}}{\partial\, \hat{M}_m} =$$

$$\sum_{i=1}^{n} \sum_{j=1}^{n} \left(-2 \cdot \tilde{A}_j^t \cdot \tilde{A}_i \cdot Y_{-i} \cdot \Omega_{m_{-i}}^t + \tilde{A}_i^t \cdot \tilde{A}_j \cdot \hat{M}_m \cdot \Omega_{m_{-j}} \cdot \Omega_{m_{-i}}^t + \right.$$

$$\left. \tilde{A}_j^t \cdot \tilde{A}_i \cdot \hat{M}_m \cdot \Omega_{m_{-i}} \cdot \Omega_{m_{-j}}^t \right) \qquad \text{(A.8)}$$

With eq. (A.4) - (A.8) the derivative of V with respect to $\hat{M}_m$ is found to be equal to:

$$\frac{\partial\, V}{\partial\, \hat{M}_m} = -2 \cdot Y \cdot \Omega_m^t + 2 \cdot \sum_{i=1}^{n} \tilde{A}_i^t \cdot Y \cdot \Omega_{m_{-i}}^t + 2 \cdot \hat{M}_m \cdot \Omega_m \cdot \Omega_m^t +$$

$$2 \cdot \sum_{i=1}^{n} \left(\tilde{A}_i \cdot Y_{-i} \cdot \Omega_m^t - \tilde{A}_i^t \cdot \hat{M}_m \cdot \Omega_m \cdot \Omega_{m_{-i}}^t - \tilde{A}_i \cdot \hat{M}_m \cdot \Omega_{m_{-i}} \cdot \Omega_m^t \right) +$$

$$\sum_{i=1}^{n} \left(-2 \cdot \tilde{A}_j^t \cdot \tilde{A}_i \cdot Y_{-i} \cdot \Omega_{m_{-i}}^t + \tilde{A}_i^t \cdot \tilde{A}_j \cdot \hat{M}_m \cdot \Omega_{m_{-j}} \cdot \Omega_{m_{-i}}^t + \tilde{A}_j^t \cdot \tilde{A}_i \cdot \hat{M}_m \cdot \Omega_{m_{-i}} \cdot \Omega_{m_{-j}}^t \right)$$

(A.9)

Rewriting of eq. (A.3) gives:

$$\frac{\partial V}{\partial A_n} = 2\cdot(-Y + \hat{M}_m\cdot\Omega_m + \hat{A}_n\cdot(Y_m^* - M_m^*\cdot\Omega_m^*))\cdot(Y_m^{*t} - \Omega_m^{*t}\cdot M_m^{*t}) =$$

$$2\cdot A_n^*\cdot(Y_m^{**} - M_m^{**}\cdot\Omega_m^{**})\cdot(Y_m^{*t} - \Omega_m^{*t}\cdot M_m^{*t}) = 2\cdot X\cdot\hat{H}_n^t \qquad (A.10)$$

with: $A_n^* = [-I\ ;\ \hat{A}_1\ ;\ \hat{A}_2\ ;\ \ldots\ ;\ \hat{A}_n]$

$$Y_m^{**} = [Y^t\ ;\ Y_{-1}^t\ ;\ \ldots\ ;\ Y_{-n}^t]^t$$

$$M_m^{**} = \mathrm{diag}(\hat{M}_m)$$

$$\Omega_m^{**} = [\Omega_m^t\ ;\ \Omega_{m_{-1}}^t\ ;\ \ldots\ ;\ \Omega_{m_{-n}}^t]^t$$

$$X = A_n^*\cdot(Y_m^{**} - M_m^{**}\cdot\Omega_m^{**})$$

Similarly eq. (A.9) can be rewritten into:

$$\frac{\partial V}{\partial M_m} = 2\cdot(-Y\cdot\Omega_m^t + \hat{M}_m\cdot\Omega_m\cdot\Omega_m^t + \sum_{i=1}^{n}\tilde{A}_i\cdot Y_{-i}\cdot\Omega_m^t - \sum_{i=1}^{n}\tilde{A}_i\cdot\hat{M}_m\cdot\Omega_{m_{-i}}\cdot\Omega_m^t) +$$

$$2\cdot(\sum_{i=1}^{n}\tilde{A}_i^t\cdot Y\cdot\Omega_{m_{-i}}^t - \sum_{i=1}^{n}\tilde{A}_i^t\cdot\hat{M}_m\cdot\Omega_m\cdot\Omega_{m_{-i}}^t - \sum_{i=1}^{n}\sum_{j=1}^{n}\tilde{A}_j^t\cdot\tilde{A}_i\cdot Y_{-i}\cdot\Omega_{m_{-i}}^t +$$

$$\sum_{i=1}^{n}\sum_{j=1}^{n}\tilde{A}_j^t\cdot\tilde{A}_i\cdot\hat{M}_m\cdot\Omega_{m_{-i}}\cdot\Omega_{m_{-j}}^t) =$$

$$2\cdot A_n^*\cdot(Y_m^{**} - M_m^{**}\cdot\Omega_m^{**})\cdot\Omega_m^t - 2\cdot\sum_{i=1}^{n}\tilde{A}_i^t\cdot A_n^*\cdot(Y_m^{**} - M_m^{**}\cdot\Omega_m^{**})\cdot\Omega_{m_{-i}}^t =$$

$$2\cdot[\ I\cdot X\ ;\ -\tilde{A}_1^t\cdot X\ ;\ \ \ldots\ \ ;\ -\tilde{A}_n^t\cdot X\ ]\cdot\begin{bmatrix} \Omega_m^t \\ \Omega_{m-1}^t \\ \cdot \\ \cdot \\ \Omega_{m-n}^t \end{bmatrix} \qquad \text{(A.11)}$$

with: $X = A_n^*\cdot(Y_m^{**} - M_m^{**}\cdot\Omega_m^{**})$

From eq. (A.10) and (A.11) the derivative of V with respect to the model parameters follows to be:

$$\frac{\partial V}{\partial \Theta} = \frac{\partial V}{\partial [M_m\ A_n]} = 2\cdot[\ X\ ;\ -A_1^t\cdot X\ ;\ \ \ldots\ \ ;\ -A_n^t\cdot X\ ]\cdot\begin{bmatrix} \Omega_m^t & \hat{H}_n^t \\ \Omega_{m-1}^t & 0 \\ \cdot & \cdot \\ \cdot & \cdot \\ \Omega_{m-n}^t & 0 \end{bmatrix} =$$

$$2\cdot[I\ ;\ -\hat{A}_1^t\ ;\ \ \ldots\ \ ;\ -\hat{A}_n^t]\cdot$$

$$\text{diag}\left(\ [-I\ ;\ \hat{A}_1\ ;\ \ \ldots\ \ ;\ \hat{A}_n]\cdot\begin{bmatrix} (Y - \hat{M}_m\cdot\Omega_m) \\ (Y_{-1} - \hat{M}_m\cdot\Omega_{m-1}) \\ \cdot \\ \cdot \\ (Y_{-n} - \hat{M}_m\cdot\Omega_{m-n}) \end{bmatrix}\right)\cdot\begin{bmatrix} \Omega_m^t & \hat{H}_m^t \\ \Omega_{m-1}^t & 0 \\ \cdot & \cdot \\ \cdot & \cdot \\ \Omega_{m-n}^t & 0 \end{bmatrix}$$

(A.12)

Appendix B

Conversion between continuous and discrete time domain using bilinear transformations

Define:

$$s = \frac{z-1}{z+1} \qquad z,s\epsilon C \tag{B.1}$$

This corresponds with:

$$z = \frac{1+s}{1-s} \tag{B.2}$$

It is clear that:

$$|z|<1 \Leftrightarrow \mathrm{Re}(s)<0 \quad \text{and} \quad |z|=1 \Leftrightarrow \mathrm{Re}(s)=0 \tag{B.3}$$

Define a discrete time state space system:

$$\begin{cases} x_{k+1} = F\cdot x_k + G\cdot u_k & \text{(B.4a)} \\ y_k = H\cdot x_k + D_d\cdot u_k & \text{(B.4b)} \end{cases}$$

The z-domain transfer function of this system is:

$$F(z) = H\cdot(zI - F)^{-1}\cdot G + D_d \tag{B.5}$$

Next define the s-domain transfer function by:

$$G(s) = F\left(\frac{1+s}{1-s}\right) \tag{B.6}$$

Working out eq. (B.6) together with eq. (B.5) gives for the s-domain transfer function:

$$G(s) = H\cdot\left(\frac{1+s}{1-s}I - F\right)^{-1}\cdot G + D_d \tag{B.7}$$

$$= H\cdot[(1-s)\{(1+s)I - (1-s)F\}^{-1}]\cdot G + D_d$$

$$= H\cdot[(1-s)\{s(I+F) - (F-I)\}^{-1}]\cdot G + D_d$$

$$= H\cdot[(I+F)^{-1}\cdot\{(I+F) - s(I+F)\}\{s(I+F) - (F-I)\}^{-1}]\cdot G + D_d$$

$$= H\cdot[(I+F)^{-1}\cdot\{2I + (F-I) - s(I+F)\}\{s(I+F) - (F-I)\}^{-1}]\cdot G + D_d$$

$$= H\cdot[(I+F)^{-1}\cdot 2\{s(I+F) - (F-I)\}^{-1}]\cdot G + D_d - H\cdot(I+F)^{-1}\cdot G$$

$$= H\cdot[(I+F)^{-1}\cdot 2\{(I+F)\cdot(sI - (I+F)^{-1}\cdot(F-I))\}^{-1}]\cdot G + D_d - H\cdot(I+F)^{-1}\cdot G$$

$$= H\cdot[(I+F)^{-1}\cdot 2\{sI - (I+F)^{-1}\cdot(F-I)\}^{-1}\cdot(I+F)^{-1}]\cdot G + D_d - H\cdot(I+F)^{-1}\cdot G$$

$$= \sqrt{2}H\cdot(I+F)^{-1}\cdot\{sI - (I+F)^{-1}\cdot(F-I)\}^{-1}\cdot\sqrt{2}(I+F)^{-1}\cdot G + D_d - H\cdot(I+F)^{-1}\cdot G$$

$$= \tilde{C}\cdot(sI - \tilde{A})^{-1}\cdot\tilde{B} + \tilde{D}_c \qquad \text{(B.8)}$$

with: $\tilde{C} = \sqrt{2}H\cdot(I+F)^{-1}$ (B.9a)

$\tilde{B} = \sqrt{2}(I+F)^{-1}\cdot G$ (B.9b)

$\tilde{A} = (I+F)^{-1}\cdot(F-I)$ (B.9c)

$\tilde{D}_c = D_d - H\cdot(I+F)^{-1}\cdot G$ (B.9d)

Eq. (B.8) clearly is the s-domain transfer function of the continuous time state space system:

$$\begin{cases} \dot{x} = \tilde{A}\cdot x + \tilde{B}\cdot u & \text{(B.10a)} \\ y = \tilde{C}\cdot x + \tilde{D}_c\cdot u & \text{(B.10b)} \end{cases}$$

For a given s-domain transfer function G(s) the corresponding z-domain transfer function F(z) can be computed using eq. (B.1).

$$G(s) = C\cdot(sI - A)^{-1}\cdot B + D_c \qquad \text{(B.11)}$$

Define:

$$F(z) = G\left(\frac{z-1}{z+1}\right) \qquad \text{(B.12)}$$

Working out eq. (B.12) using (B.11) gives:

$$F(z) = C\cdot[(z+1)\{(z-1)I - (z+1)A\}^{-1}]\cdot B + D_c$$

$$= C\cdot[(I-A)^{-1}\cdot\{z(I-A) + (I-A)\}\cdot\{z(I-A) - (I+A)\}^{-1}]\cdot B + D_c$$

$$= C\cdot[(I-A)^{-1}\cdot 2\{z(I-A) - (I+A)\}^{-1}]\cdot B + D_c + C\cdot(I-A)^{-1}\cdot B$$

$$= \sqrt{2}C\cdot(I-A)^{-1}\cdot\{zI - (I-A)^{-1}\cdot(I+A)\}^{-1}\cdot\sqrt{2}(I-A)^{-1}\cdot B + D_c + C\cdot(I-A)^{-1}\cdot B$$

$$= \tilde{H}\cdot(zI - \tilde{F})^{-1}\cdot\tilde{G} + \tilde{D}_d \qquad \text{(B.13)}$$

with: $\tilde{H} = \sqrt{2}C\cdot(I-A)^{-1}$ (B.14a)

$\tilde{G} = \sqrt{2}(I-A)^{-1}\cdot B$ (B.14b)

$\tilde{F} = (I-A)^{-1}\cdot(I+A)$ (B.14c)

$\tilde{D}_d = D_c + C\cdot(I-A)^{-1}\cdot B$ (B.14d)

Eq. (B.13) clearly corresponds to the transfer function of a discrete time system as defined by eq. (B.4a,b).

For a discrete time system the controllability and observability gramians are defined by:

$$P_d = \sum_{k=0}^{\infty} F^k\cdot G\cdot G^*\cdot F^{*k} \qquad \text{(B.15)}$$

$$Q_d = \sum_{k=0}^{\infty} F^{*k}\cdot H^*\cdot H\cdot F^k \qquad \text{(B.16)}$$

These matrices satisfy the following Lyapunov equations if the system is strictly proper ($|\lambda_i(F)|<1$ for all $i\in I$):

$$P_d - F\cdot P_d\cdot F^* = G\cdot G^* \qquad \text{(B.17)}$$

$$Q_d - F^*\cdot Q_d\cdot F = H^*\cdot H \qquad \text{(B.18)}$$

The Hankel singular values of the strictly proper discrete time system are defined as:

$$\sigma_i(F(z)) = \{\lambda_i(P_d \cdot Q_d)\}^{1/2} \tag{B.19}$$

For a continuous time system, defined by eq. (B.10a,b), similar definitions can be formulated. The controllability and observability gramians of the continuous time system are defined by:

$$P_c = \int_0^\infty \exp(At) \cdot B \cdot B^* \cdot \exp(A^* t)\, dt \tag{B.20}$$

$$Q_c = \int_0^\infty \exp(A^* t) \cdot C^* \cdot C \cdot \exp(At)\, dt \tag{B.21}$$

These matrices P_c and Q_c satisfy the following Lyapunov equations:

$$A \cdot P_c + P_c \cdot A^* + B \cdot B^* = 0 \tag{B.22}$$

$$A^* \cdot Q_c + Q_c \cdot A + C^* \cdot C = 0 \tag{B.23}$$

For a strictly proper continuous time system the Hankel singular values are defined as:

$$\sigma_i(G(s)) = \{\lambda_i(P_c \cdot Q_c)\}^{1/2} \tag{B.24}$$

If the matrices $(\tilde{A}, \tilde{B})$, found from the bilinear transformation of the z-domain transfer function (eq. (B.9c,b), are substituted in the first Lyapunov equation (eq. (B.22)) for the continuous time system, the following result is obtained:

$$\begin{aligned}
&(I + F) \cdot \{\tilde{A} \cdot P_d + P_d \cdot \tilde{A}^* + \tilde{B} \cdot \tilde{B}^*\} \cdot (I + F^*) \\
&= (F - I) \cdot P_d \cdot (I + F^*) + (I + F) \cdot P_d (F^* - I) + 2G \cdot G^* \\
&= -2\{P_d - F \cdot P_d \cdot F^* - G \cdot G^*\} = 0
\end{aligned} \tag{B.25}$$

Clearly the controllability gramian of the continuous time system, corresponding with the discrete time system via the bilinear transformation, is the same as the one found for the discrete time system.

Similarly, by substituting the expressions for $(\tilde{A}, \tilde{C})$ given by eq. (B.9c,a) in the second Lyapunov equation for the continuous time system (B.23) gives:

$$(I + F^*)\cdot\{\tilde{A}^*\cdot Q_d + Q_d\cdot\tilde{A} + C^*\cdot C\}\cdot(I + F)$$

$$= (I+F^*)\cdot[(F^*-I)\cdot(I+F^*)^{-1}\cdot Q_d + Q_d\cdot(I+F)^{-1}\cdot(F-I) +$$
$$2(I+F^*)^{-1}\cdot H^*\cdot H\cdot(I+F)^{-1}]\cdot(I+F)$$

$$= (F^*-I)\cdot Q_d(I+F) + (I+F^*)\cdot Q_d\cdot(F-I) + 2H^*\cdot H$$

$$= 2F^*\cdot Q_d\cdot F - 2Q_d + 2H^*\cdot H$$

$$= -2\{Q_d - F^*\cdot Q_d\cdot F - H^*\cdot H\} = 0 \qquad \text{(B.26)}$$

Also the observability gramian of the continuous time system, corresponding with the discrete time system via the bilinear transformation, is the same as the one found for the discrete time system.
From eq. (B.25), (B.26), (B.19) and (B.24) it is easily seen that the Hankel singular values of the corresponding discrete and continuous time systems will be identical. Eq. (B.8) and (B.14) show that for strictly proper systems the McMillan degrees of corresponding s-domain and z-domain transfer functions are the same. The frequency responses of both systems also are the same for not too high frequencies as can be seen from:

$$F(\exp(j\theta)) = G\left(\frac{\exp(j\theta) - 1}{\exp(j\theta) + 1}\right) = G\left(j \tan\left(\frac{1}{2}\theta\right)\right) \qquad \text{(B.27)}$$

Appendix C

Matrix Calculus

The trace of a square matrix A of dimensions n × n is defined by:

$$tr\{A\} = \sum_{i=1}^{n} a_{ii} \qquad (C.1)$$

with:

$$A = \begin{bmatrix} a_{11} & a_{12} & \cdots & a_{1n} \\ a_{21} & a_{22} & \cdots & a_{2n} \\ \cdot & \cdot & & \cdot \\ \cdot & \cdot & & \cdot \\ a_{n1} & a_{n2} & \cdots & a_{nn} \end{bmatrix}$$

Some useful properties of the trace operator are:

$$tr\{\alpha \cdot A\} = \alpha \cdot tr\{A\} \qquad (C.2)$$

with: α - a scalar multiplication factor

$$tr\{A \cdot B\} = tr\{B \cdot A\} \qquad (C.3)$$

$$tr\{A + B\} = tr\{A\} + tr\{B\} \qquad (C.4)$$

$$tr\{A^t\} = tr\{A\} \qquad (C.5)$$

Property (C.2) immediately follows from the definition of the trace function and the definition of matrix multiplication with a scalar.
Property (C.3) can be proven as follows:

$$tr\{A \cdot B\} = \sum_{i=1}^{n} A_{i\cdot} \cdot B_{\cdot i} = \sum_{i=1}^{n} \sum_{j=1}^{n} a_{ij} \cdot b_{ji} = \sum_{i=1}^{n} \sum_{j=1}^{n} b_{ij} \cdot a_{ji} =$$

$$\sum_{i=1}^{n} B_{i\cdot} \cdot A_{\cdot i} = tr\{B \cdot A\} \; .$$

with: $A_{i\cdot} = [a_{i1} \; ; \; a_{i2} \; ; \; \cdots \; ; \; a_{in}]$

$$B_{\cdot j} = [b_{1j} \; ; \; b_{2j} \; ; \; \cdots \; ; \; b_{nj}]^t$$

As can be seen from this result matrices A and B not necessarily need to be square. A may have dimensions n × m and B may have dimensions m × n. Property (C.4) and (C.5) immediately follow from the definition of the trace and the definitions of matrix addition and matrix transpose.

The Vec operator applied to a matrix A with dimensions n × m is defined by:

$$\text{vec}\{A\} = \begin{bmatrix} A_{\cdot 1} \\ A_{\cdot 2} \\ \cdot \\ \cdot \\ A_{\cdot m} \end{bmatrix} \qquad \text{(C.6)}$$

With the vec operator a matrix is tranformed into a vector. Application of the vec operator to the matrices A and B of eq. (C.3) gives:

$$\text{tr}\{A \cdot B\} = \sum_{i=1}^{n} (A_{\cdot i}^{t})^{t} \cdot B_{\cdot i} = (\text{vec}\{A^{t}\})^{t} \cdot \text{vec}\{B\} \qquad \text{(C.7)}$$

The Kronecker product of two matrices A (dim: n × m) and B (dim: r × s) is defined as:

$$A \otimes B = \begin{bmatrix} a_{11} \cdot B & a_{12} \cdot B & \cdots & a_{1m} \cdot B \\ a_{21} \cdot B & a_{22} \cdot B & \cdots & a_{2m} \cdot B \\ \cdot & \cdot & & \cdot \\ \cdot & \cdot & & \cdot \\ a_{n1} \cdot B & a_{n2} \cdot B & \cdots & a_{nm} \cdot B \end{bmatrix} \qquad \text{(C.8)}$$

In the following equations matrices A and B respectively are assumed to have the following dimensions unless otherwise specified:

dim[A]: n × m
dim[B]: r × s

Some interesting properties of the Kronecker product are (proof: cf. [Graham, 1981]):

$$A \otimes \alpha B = \alpha(A \otimes B) \qquad \text{(C.9)}$$

with: α – a scalar multiplication factor

$$(A + B) \otimes C = A \otimes C + B \otimes C \qquad \text{(C.10)}$$

$$A \otimes (B + C) = A \otimes B + A \otimes C \tag{C.11}$$

$$A \otimes (B \otimes C) = (A \otimes B) \otimes C \tag{C.12}$$

$$(A \otimes B)^t = A^t \otimes B^t \tag{C.13}$$

$$(A \otimes B)\cdot(C \otimes D) = A\cdot C \otimes B\cdot D \tag{C.14}$$

$$(A \otimes B)^{-1} = A^{-1} \otimes B^{-1} \tag{C.15}$$

with: A and B square, non-singular matrices

$$\mathrm{vec}(A\cdot X\cdot B) = (B^t \otimes A)\cdot \mathrm{vec}\{X\} \tag{C.16}$$

with: dim[X]: m × r

$$\mathrm{tr}\{A \otimes B\} = \mathrm{tr}\{A\}\cdot \mathrm{tr}\{B\} \tag{C.17}$$

The derivative of a scalar function of a matrix X (dim[X]: n × m)with respect to a matrix is defined as:

$$\frac{\partial f(X)}{\partial X} = \begin{bmatrix} \frac{\partial f(X)}{\partial x_{11}} & \frac{\partial f(X)}{\partial x_{12}} & \cdots & \frac{\partial f(X)}{\partial x_{1m}} \\ \frac{\partial f(X)}{\partial x_{21}} & \frac{\partial f(X)}{\partial x_{22}} & \cdots & \frac{\partial f(X)}{\partial x_{2m}} \\ \vdots & \vdots & & \vdots \\ \frac{\partial f(X)}{\partial x_{n1}} & \frac{\partial f(X)}{\partial x_{n2}} & \cdots & \frac{\partial f(X)}{\partial x_{nm}} \end{bmatrix} \tag{C.18}$$

With the following properties general expressions can be obtained for the derivatives of scalar functions of matrices with respect to matrices (cf. [Graham, 1981]):

$$Y = A\cdot X\cdot B \quad \rightarrow \quad \frac{\partial y_{ij}}{\partial X} = A^t\cdot E_{ij}\cdot B^t \tag{C.19a}$$

$$\rightarrow \quad \frac{\partial Y}{\partial x_{rs}} = A\cdot E_{rs}\cdot B^t \tag{C.19b}$$

with: E_{rs} - the elementary matrix, a matrix with element r,s equal to one and all other elements equal to zero

$$E_{rs} = \begin{bmatrix} 0 & 0 & \dots & 0 & \dots & 0 \\ \cdot & \cdot & & \cdot & & \cdot \\ 0 & 0 & \dots & 1 & \dots & 0 \\ \cdot & \cdot & & \cdot & & \cdot \\ 0 & 0 & \dots & 0 & \dots & 0 \end{bmatrix} \leftarrow r$$

$$\uparrow$$
$$s$$

Derivative of a product of matrices:

$$Z = U(X)\cdot Y(X) \quad \rightarrow \quad \frac{\partial Z}{\partial x_{rs}} = \frac{\partial U}{\partial x_{rs}}\cdot V + U\cdot\frac{\partial V}{\partial x_{rs}} \tag{C.20a}$$

$$\rightarrow \quad \frac{\partial z_{ij}}{\partial X} = \sum_{\mu=1}^{q} \frac{\partial u_{i\mu}}{\partial X}\cdot v_{\mu j} + \sum_{\mu=1}^{q} u_{i\mu}\cdot\frac{\partial v_{\mu j}}{\partial X} \tag{C.20b}$$

with: dim[U]: $p \times q$
dim[V]: $q \times r$

Derivatives of the powers of a matrix:

$$Y = X^n \quad \rightarrow \quad \frac{\partial Y}{\partial x_{rs}} = \sum_{k=0}^{n-1} X^k\cdot E_{rs}\cdot X^{n-k-1} \tag{C.21a}$$

$$\rightarrow \quad \frac{\partial y_{ij}}{\partial X} = \sum_{k=1}^{n-1} (X^t)^k\cdot E_{ij}\cdot (X^t)^{n-k-1} \tag{C.21b}$$

Derivative of the trace of a function of a matrix:

$$V = tr\{Y(X)\} \qquad \dim[Y]: n \times n \tag{C.22}$$

With definitions (C.1) and (C.18) the trace of the derivative of matrix function Y of matrix X with respect to one entry x_{rs} of X is found to be equal to:

$$tr\left\{\frac{\partial Y}{\partial x_{rs}}\right\} = \sum_{k=1}^{n} \frac{\partial y_{kk}}{\partial x_{rs}} = \frac{\partial (y_{11} + y_{22} + \dots + y_{nn})}{\partial x_{rs}} =$$

$$\frac{\partial (tr\{Y\})}{\partial x_{rs}} \tag{C.23}$$

Using these results the derivatives of the following functions are easily obtained:

$$Y = A \cdot X \cdot B \quad \rightarrow \quad \frac{\partial\, tr\{Y\}}{\partial\, X} = A^t \cdot B^t \tag{C.24}$$

with: dim[A]: n × m
dim[X]: m × q
dim[B]: q × n

proof: Successive application of (C.23), (C.20), (C.19), (C.3), (C.5) and (C.7) gives:

$$\frac{\partial\, tr\{A \cdot X \cdot B\}}{\partial\, x_{rs}} = tr\left\{ \frac{\partial\, A \cdot X \cdot B}{\partial\, x_{rs}} \right\} = tr\{A \cdot E_{rs} \cdot B\} = tr\{E_{rs} \cdot B \cdot A\} =$$

$$tr\{A^t \cdot B^t \cdot E_{rs}^t\} = tr\{E_{rs}^t \cdot A^t \cdot B^t\} =$$

$$vec\{E_{rs}\}^t \cdot vec\{A^t \cdot B^t\}$$

With definition (C.18) result (C.24) is found:

$$\frac{\partial\, tr\{A \cdot X \cdot B\}}{\partial\, X} = A^t \cdot B^t \ .$$

$$Y = tr\{A \cdot X^t \cdot B \cdot X \cdot C\} \quad \rightarrow \quad \frac{\partial\, Y}{\partial\, X} = B \cdot X \cdot C \cdot A + B^t \cdot X \cdot A^t \cdot C^t \tag{C.25}$$

with: dim[A]: n × m
dim[X]: q × m
dim[B]: q × q
dim[C]: m × n

proof: Successive application of eq. (C.23), (C.20), (C.19), (C.3), (C.5), (C.4) and (C.7) gives:

$$\frac{\partial\, Y}{\partial\, x_{rs}} = tr\left\{ \frac{\partial\, A \cdot X^t \cdot B \cdot X \cdot C}{\partial\, x_{rs}} \right\} =$$

$$tr\{\ A \cdot E_{rs}^t \cdot B \cdot X \cdot C + A \cdot X^t \cdot B \cdot E_{rs} \cdot C\ \} =$$

$$tr\{\ E_{rs}^t \cdot B \cdot X \cdot C \cdot A + E_{rs}^t \cdot B^t \cdot X \cdot A^t \cdot C^t\ \} =$$

$$(\mathrm{vec}(\ E_{rs}))^t \cdot \mathrm{vec}(\ B\cdot X\cdot C\cdot A + B^t\cdot X\cdot A^t\cdot C^t)$$

With definition (C.18) result (C.25) is obtained:

$$\frac{\partial\ Y}{\partial\ X} = B\cdot X\cdot C\cdot A + B^t\cdot X\cdot A^t\cdot C^t\ .$$

$Z = \det\{Y(X)\} \quad \rightarrow$

$$\frac{\partial\ Z}{\partial\ X} = \begin{bmatrix} \mathrm{tr}\left\{ \frac{\partial\ Y^t}{\partial\ x_{11}}\cdot W \right\} & \mathrm{tr}\left\{ \frac{\partial\ Y^t}{\partial\ x_{12}}\cdot W \right\} & \cdots & \mathrm{tr}\left\{ \frac{\partial\ Y^t}{\partial\ x_{1m}}\cdot W \right\} \\ \mathrm{tr}\left\{ \frac{\partial\ Y^t}{\partial\ x_{21}}\cdot W \right\} & \mathrm{tr}\left\{ \frac{\partial\ Y^t}{\partial\ x_{22}}\cdot W \right\} & \cdots & \mathrm{tr}\left\{ \frac{\partial\ Y^t}{\partial\ x_{2m}}\cdot W \right\} \\ \vdots & \vdots & & \vdots \\ \mathrm{tr}\left\{ \frac{\partial\ Y^t}{\partial\ x_{n1}}\cdot W \right\} & \mathrm{tr}\left\{ \frac{\partial\ Y^t}{\partial\ x_{n2}}\cdot W \right\} & \cdots & \mathrm{tr}\left\{ \frac{\partial\ Y^t}{\partial\ x_{nm}}\cdot W \right\} \end{bmatrix} \qquad (C.26)$$

with: $\dim[X]: n \times m$
$\dim[Y]: k \times k$

$$W = \begin{bmatrix} Y_{11} & Y_{12} & \cdots & Y_{1k} \\ Y_{21} & Y_{22} & \cdots & Y_{2k} \\ \vdots & \vdots & & \vdots \\ Y_{k1} & Y_{k2} & \cdots & Y_{kk} \end{bmatrix}$$

Y_{ij} - cofactor of element y_{ij}

proof: Using the chain rule the following can be written for the derivative of $\det(Y)$ with respect to element x_{rs} of X:

$$\frac{\partial\ \det(Y)}{\partial\ x_{rs}} = \sum_{i=1}^{k}\ \sum_{j=1}^{k} \frac{\partial\ \det(Y)}{\partial\ y_{ij}} \cdot \frac{\partial\ y_{ij}}{\partial\ x_{rs}}$$

Under the assumption that the cofactors are independent of y_{ij} the first term equals:

$$\det(Y) = \sum_{j=1}^{k} y_{ij} \cdot Y_{ij} \quad \rightarrow \quad \frac{\partial \det(Y)}{\partial y_{ij}} = Y_{ij}$$

Substitution of this result in the previously obtained expression for the derivative of det(Y) with respect to x_{rs} gives:

$$\frac{\partial \det(Y)}{\partial x_{rs}} = \sum_{i=1}^{k} \sum_{j=1}^{k} Y_{ij} \cdot \frac{\partial y_{ij}}{\partial x_{rs}}$$

Using definition (C.1) and eq. (C.3) this expression can be rewritten into:

$$\frac{\partial \det(Y)}{\partial x_{rs}} = \sum_{i=1}^{k} Y_{i\cdot} \cdot \left[\frac{\partial y_{i\cdot}}{\partial x_{rs}} \right]^{t} =$$

$$\mathrm{tr}\left\{ W \cdot \frac{\partial Y^{t}}{\partial x_{rs}} \right\} = \mathrm{tr}\left\{ \frac{\partial Y^{t}}{\partial x_{rs}} \cdot W \right\}$$

With definition (C.18) result (C.26) is obtained.

Appendix D

D.1 Convergence of estimated FIR model parameters if no AR noise parameters are estimated simultaneously

Assume the true process input/output behaviour to be described by (cf. eq. (3.1)):

$$Y = M_{mp} \cdot \Omega_m + M_{tail} \cdot \Omega_{tail} + N \qquad (D.1)$$

with: Y - the output signal matrix $\quad \dim[Y]: \quad q \times (l+1)$

Ω_m - the input signal matrix $\quad \dim[\Omega]: \quad p\cdot(m+1) \times (l+1)$

M_{mp} - the main Markov parameter matrix $\quad \dim[M_{mp}]: \quad q \times p\cdot(m+1)$

M_{tail} - the tail Markov parameter matrix $\quad \dim[M_{tail}]: \quad q \times p\cdot(\kappa-m-1)$

N - the additive output noise signal matrix $\quad \dim[N]: \quad q \times (l+1)$

κ - length of the impulse responses of the process expressed in number of samples (In general for physical systems $\kappa \to \infty$)

$$Y = [y_k \;\; y_{k+1} \;\; y_{k+2} \;\; \cdots \;\; y_{k+l}]$$

$$M_{mp} = [M_0, M_1, M_2, \ldots, M_m]$$

$$M_{tail} = [M_{m+1}, M_{m+2}, M_{m+3}, \ldots, M_\kappa]$$

$$\Omega_m = \begin{bmatrix} u_k & u_{k+1} & u_{k+2} & \cdots & u_{k+l} \\ u_{k-1} & u_k & u_{k+1} & \cdots & u_{k+l-1} \\ \cdot & \cdot & \cdot & & \cdot \\ \cdot & \cdot & \cdot & & \cdot \\ u_{k-m} & u_{k-m+1} & u_{k-m+2} & \cdots & u_{k-m+l} \end{bmatrix}$$

$$\Omega_{tail} = \begin{bmatrix} u_{k-m-1} & u_{k-m} & u_{k-m+1} & \cdots & u_{k-m+l-1} \\ u_{k-m-2} & u_{k-m-1} & u_{k-m} & \cdots & u_{k-m+l-2} \\ \cdot & \cdot & \cdot & & \cdot \\ \cdot & \cdot & \cdot & & \cdot \\ u_{k-\kappa} & u_{k-\kappa+1} & u_{k-\kappa+2} & \cdots & u_{k-\kappa+l} \end{bmatrix}$$

$$N = [n_k \quad n_{k+1} \quad n_{k+2} \quad \cdots \quad n_{k+l}]$$

The FIR model is given by (cf. eq. (3.3)):

$$\hat{Y} = \hat{M}_{mp} \cdot \Omega_m \tag{D.2}$$

with: $\hat{M}_{mp} = [\hat{M}_0, \hat{M}_1, \hat{M}_2, \ldots, \hat{M}_m]$

To be able to do the convergence analysis first some assumptions have to be made on the characteristics of the signals. The input signal of the process is assumed to be stationary, white, inter channel independent, zero mean, Gaussian noise with covariance matrix R:

$$E\{u \cdot u^t\} = R = \sigma^2 \cdot I_p \qquad \dim[R]: p \times p \tag{D.3}$$

$$E\{u\} = 0 \tag{D.4}$$

$$E\{u_i \cdot u_j^t\} = 0_{p,p} \qquad i,j \in I,\ i \neq j,\ I=0,1,2,\ \ldots \tag{D.5}$$

The additive output noise is assumed not to be correlated with the input noise applied to the process:

$$E\{u_i \cdot n_j^t\} = 0_{p,q} \qquad \text{for all } i,j \in I,\ I=0,1,2,\ \ldots \tag{D.6}$$

Furthermore the additive output noise is assumed to be zero mean:

$$E\{n\} = 0 \tag{D.7}$$

Using eq. (D.1), (D.2) and the trace of the square of the output error matrix, the Least Squares estimates for the model parameters can be written as (cf. eq. (3.10), (3.12)):

$$\begin{aligned} \hat{M}_{mp} &= (Y \cdot \Omega_m^t) \cdot (\Omega_m \cdot \Omega_m^t)^{-1} \\ &= (M_{mp} \cdot \Omega_m \cdot \Omega_m^t) \cdot (\Omega_m \cdot \Omega_m^t)^{-1} + (M_{tail} \cdot \Omega_{tail} \cdot \Omega_m^t) \cdot (\Omega_m \cdot \Omega_m^t)^{-1} \\ &\quad + (N \cdot \Omega_m^t) \cdot (\Omega_m \cdot \Omega_m^t)^{-1} \end{aligned} \tag{D.8}$$

With eq. (D.8) the expectation for the estimated parameters is given by:

$$E\{\hat{M}_{mp}\} = M_{mp} + E\{(M_{tail} \cdot \Omega_{tail} \cdot \Omega_m^t) \cdot (\Omega_m \cdot \Omega_m^t)^{-1}\} +$$

$$+ E\{(N\cdot\Omega_m^t)\cdot(\Omega_m\cdot\Omega_m^t)^{-1}\} \qquad (D.9)$$

An interesting aspect of eq. (D.8) and (D.9) is given by the following observation on the products:

$$M_{tail}\cdot\Omega_{tail}\cdot\Omega_m^t = [n_{tail_k}\ ,\ \cdots\ ,\ n_{tail_{k+l}}]\cdot$$

$$\begin{bmatrix} u_k^t & u_{k-1}^t & \cdots & u_{k-m}^t \\ \cdot & \cdot & & \cdot \\ \cdot & \cdot & & \cdot \\ u_{k+l}^t & u_{k+l-1}^t & \cdots & u_{k+l-m}^t \end{bmatrix}$$

$$[\sum_{i=0}^{l} n_{tail_{k+i}}\cdot u_{k+i}^t\ ,\ \cdots\ ,\ \sum_{i=0}^{l} n_{tail_{k+i}}\cdot u_{k-m+i}^t] \qquad (D.10)$$

and

$$N\cdot\Omega_m^t = [n_k\ ,\ n_{k+1}\ ,\ \cdots\ ,\ n_{k+l}]\cdot$$

$$\begin{bmatrix} u_k^t & u_{k-1}^t & \cdots & u_{k-m}^t \\ \cdot & \cdot & & \cdot \\ \cdot & \cdot & & \cdot \\ u_{k+l}^t & u_{k+l-1}^t & \cdots & u_{k+l-m}^t \end{bmatrix}$$

$$[\sum_{i=0}^{l} n_{k+i}\cdot u_{k+i}^t\ ,\ \cdots\ ,\ \sum_{i=0}^{l} n_{k+i}\cdot u_{k-m+i}^t] \qquad (D.11)$$

In both expressions the rows of the matrices consisting of samples of the (possibly coloured) output noise and of the "tail noise" are multiplied with columns of the input signal matrix Ω_m^t. Because the input signal matrix is filled with white noise samples that are independent of the noise signals (cf. eq. (D.3) - (D.6)), as a result of these multiplication the columns of the resulting matrix will be a "randomized" matrix. Possible dependencies in succeeding columns of the noise matrices will be disrupted.

To get an impression of the qualities of the estimate $\hat{M}_{mp}$, the asymptotic behaviour of eq. (D.9) is investigated. First the influence of the tail effects is going to be analyzed. Using Slutsky's theorem (cf. [Goldberger, 1964]) the following can be written for the noise due to the tail effects:

$$\operatorname*{plim}_{l\to\infty} \{(M_{tail}\cdot\Omega_{tail}\cdot\Omega_m^t)\cdot(\Omega_m\cdot\Omega_m^t)^{-1}\} =$$

$$= (\operatorname*{plim}_{l\to\infty} \{\frac{1}{l+1}\cdot M_{tail}\cdot\Omega_{tail}\cdot\Omega_m^t\})\cdot(\operatorname*{plim}_{l\to\infty} \{\frac{1}{l+1}\cdot\Omega_m\cdot\Omega_m^t\})^{-1} \qquad (D.12)$$

Working out eq. (D.12) by making use of eq. (D.3) and (D.5) gives:

$$\operatorname*{plim}_{l\to\infty} \{(M_{tail}\cdot\Omega_{tail}\cdot\Omega_m^t)\cdot(\Omega_m\cdot\Omega_m^t)^{-1}\} = 0_{q,(m+1)\cdot p} \qquad (D.13)$$

The influence of the additive output noise on the estimated parameters can be analyzed similarly:

$$\operatorname*{plim}_{l\to\infty} \{(N\cdot\Omega_m^t)\cdot(\Omega_m\cdot\Omega_m^t)^{-1}\} = \operatorname*{plim}_{l\to\infty} \{\frac{1}{l+1}\cdot N\cdot\Omega_m^t\}\cdot(\operatorname*{plim}_{l\to\infty} \{\frac{1}{l+1}\cdot\Omega_m\cdot\Omega_m^t\})^{-1} \qquad (D.14)$$

With eq. (D.3) and (D.6) this gives:

$$\operatorname*{plim}_{l\to\infty}\{ (N\cdot\Omega_m^t)\cdot(\Omega_m\cdot\Omega_m^t)^{-1}\} = 0_{q,(m+1)\cdot p} \qquad (D.15)$$

For a sufficient large number of samples and signals that satisfy eq. (D.3) - (D.7), with eq. (D.13) and (D.15) the expectation of the estimated parameters, eq. (D.9), becomes:

$$\lim_{l\to\infty} E\{\hat{M}_{mp}\} = \operatorname*{plim}_{l\to\infty} \{\hat{M}_{mp}\} = M_{mp} \qquad (D.16)$$

This implies that the parameters will converge to the true parameters if:

- the process input/output behaviour can be described by eq. (D.1)
- the input signal used for the identification of the process is white, inter channel independent, zero mean noise.
- the output noise is zero mean and independent of the input signal used.

If the input signal is coloured, the estimated parameters will be biased due to the truncation of the impulse responses. The bias will depend on the energy in the tail parameters of the impulse responses, because these parameters act as weighting factors. The estimated parameters will also be biased if the output noise is correlated with the input signal. Both of these conditions can be controlled by selecting appropriate input signals to identify the process.

The first condition is the condition that in practice will be the most difficult one. However, in case the process dynamics can not be described exactly by an Impulse Response model, the impulse response model found will be the model that simulates outputs on the basis of the applied process input signals that are closest to the actual measured process outputs (cf. eq. (5.27)).

D.2 Convergence of estimated FIR model parameters in case also AR noise parameters are estimated simultaneously

Again the process is assumed to be described by eq. (D.1). The equation that describes the model now becomes (cf. eq. (3.7)):

$$\hat{Y} = \hat{M}_{mp} \cdot \Omega_m + \hat{A}_n \cdot \hat{H}_n \qquad (D.17)$$

with: $\hat{A}_n = [\hat{A}_1, \hat{A}_2, \ldots, \hat{A}_n]$

$$\hat{H}_n = \begin{bmatrix} \hat{e}_{k-1} & \hat{e}_k & \cdots & \hat{e}_{k+l-1} \\ \hat{e}_{k-2} & \hat{e}_{k-1} & \cdots & \hat{e}_{k+l-2} \\ \cdot & \cdot & & \cdot \\ \cdot & \cdot & & \cdot \\ \hat{e}_{k-n} & \hat{e}_{k-n+1} & \cdots & \hat{e}_{k+l-n} \end{bmatrix}$$

$$\hat{e}_{k+i} = y_{k+i} - \hat{y}_{k+i} = y_{k+i} - \hat{M}_{mp} \cdot \begin{bmatrix} u_{k+i} \\ u_{k+i-1} \\ \cdot \\ \cdot \\ u_{k+i-m} \end{bmatrix}$$

Using eq. (D.1), (D17) and a cost function defined by the trace of the square of the output error matrix the Least Squares estimates for the model parameters can be written as (cf. eq. (3.10) and (3.12)):

$$[\hat{M}_{mp}, \hat{A}_n] = (Y \cdot [\Omega_m^t, \hat{H}_n^t]) \cdot \left(\begin{bmatrix} \Omega_m \\ H_n \end{bmatrix} \cdot [\Omega_m^t, \hat{H}_n^t] \right)^{-1}$$

$$= \left[(M_{mp} \cdot \Omega_m \cdot \Omega_m^t + M_{tail} \cdot \Omega_{tail} \cdot \Omega_m^t + N \cdot \Omega_m^t), (M_{mp} \cdot \Omega_m \cdot \hat{H}_n^t + \right.$$

$$M_{tail} \cdot \Omega_{tail} \cdot \hat{H}_n^t + N \cdot \hat{H}_n^t) \Big] \cdot \begin{pmatrix} (\Omega_m \cdot \Omega_m^t) & (\Omega_m \cdot \hat{H}_n^t) \\ (\hat{H}_n \cdot \Omega_m^t) & (\hat{H}_n^t \cdot \hat{H}_n^t) \end{pmatrix}^{-1} \qquad \text{(D.18)}$$

During the estimation of the model parameters the impulse responses are truncated. Only the first m+1 Markov parameters are used for the reconstruction of the outputs of the process. The rest of the parameters are considered to be tail parameters and their contribution to the output signal is treated as output noise.
To analyse the convergence of the estimated Markov parameters the properties of the product of the input signal matrix with the estimated output error signal matrix has to be considered first. The output error signal matrix $\hat{H}_n$ is assumed to be generated using previously estimated Markov parameters that are expected to be converged to the true process parameters (cf. appendix D.1):

$$\operatorname*{plim}_{l\to\infty} \left[\frac{1}{l+1} \cdot \hat{H}_n \cdot \Omega_m^t\right] =$$

$$\operatorname*{plim}_{l\to\infty} \begin{bmatrix} \frac{1}{l+1} \sum_{i=0}^{l} \hat{e}_{k+i-1} \cdot u_{k+i}^t & \cdots & \frac{1}{l+1} \sum_{i=0}^{l} \hat{e}_{k+i-1} \cdot u_{k-m+i}^t \\ \frac{1}{l+1} \sum_{i=0}^{l} \hat{e}_{k+i-2} \cdot u_{k+i}^t & \cdots & \frac{1}{l+1} \sum_{i=0}^{l} \hat{e}_{k+i-2} \cdot u_{k-m+i}^t \\ \vdots & & \vdots \\ \frac{1}{l+1} \sum_{i=0}^{l} \hat{e}_{k+i-n} \cdot u_{k+i}^t & \cdots & \frac{1}{l+1} \sum_{i=0}^{l} \hat{e}_{k+i-n} \cdot u_{k-m+i}^t \end{bmatrix} \qquad \text{(D.19)}$$

In eq. (D.19) the probability limit of each of the elements of the matrix can be written as:

$$\operatorname*{plim}_{l\to\infty} \left\{\frac{1}{l+1} \cdot \sum_{i=0}^{l} \hat{e}_{k-j+i} \cdot u_{k-s+i}^t \right\} =$$

$$\operatorname*{plim}_{l\to\infty} \left\{\frac{1}{l+1} \cdot \sum_{i=0}^{l} \left(y_{k-j+i} - \hat{M}_{mp} \cdot \begin{bmatrix} u_{k-j+i} \\ u_{k-j+i-1} \\ \vdots \\ u_{k-j+i-m} \end{bmatrix}\right) \cdot u_{k-s+i}^t \right\} =$$

$$\underset{l\to\infty}{\text{plim}}\ \{\frac{1}{l+1}\cdot\sum_{i=0}^{l}\Big((M_{mp}-\hat{M}_{mp})\cdot\begin{bmatrix}u_{k-j+i}\\ \cdot\\ \cdot\\ u_{k-j+i-m}\end{bmatrix}\cdot u_{k-s+i}^{t}+$$

$$M_{tail}\cdot\begin{bmatrix}u_{k-j+i-m-1}\\ \cdot\\ \cdot\\ u_{k-j+i-\kappa}\end{bmatrix}\cdot u_{k-s+i}^{t}+n_{k-j+i}\cdot u_{k-s+i}^{t}\Big)\qquad(D.20)$$

If in eq. (D.20) $j>s$ each of the products will be zero due to the properties of the input signal and the output noise (cf. eq. (D.5) and (D.6)). If, however, in eq. (D.20) $j\leq s$ by making use of properties (D.3), (D.5) and (D.6) the probability limit is found to be:

$$\underset{l\to\infty}{\text{plim}}\ \{\frac{1}{l+1}\cdot\sum_{i=0}^{l}\Big((M_{mp}-\hat{M}_{mp})\cdot\begin{bmatrix}u_{k-j+i}\\ \cdot\\ \cdot\\ u_{k-j+i-m}\end{bmatrix}\cdot u_{k-s+i}^{t}\Big)=$$

$$(M_{mp}-\hat{M}_{mp})\cdot\begin{bmatrix}0\\ \cdot\\ \sigma^{2}\cdot I_{p}\\ \cdot\\ 0\end{bmatrix}=\quad\leftarrow\text{block row } s-j+1$$

$$\sigma^{2}\cdot(M_{s-j+1}-\hat{M}_{s-j+1})\qquad(D.21)$$

Substitution of eq. (D.21) into eq. (D.19) gives as a result for the probability limit of the term $\frac{1}{l+1}\cdot\hat{H}_{n}\cdot\Omega_{m}^{t}$:

$$\underset{l\to\infty}{\text{plim}}\ \{\frac{1}{l+1}\cdot\hat{H}_{n}\cdot\Omega_{m}^{t}\}=$$

$$\sigma^2 \cdot \begin{bmatrix} (M_0 - \hat{M}_0) & (M_1 - \hat{M}_1) & \dots & (M_m - \hat{M}_m) \\ 0 & (M_0 - \hat{M}_0) & \dots & (M_{m-1} - \hat{M}_{m-1}) \\ \cdot & \cdot & & \cdot \\ \cdot & \cdot & & \cdot \\ 0 & 0 & \dots & (M_{m-n+1} - \hat{M}_{m-n+1}) \end{bmatrix} \qquad \text{(D.22)}$$

Application of Slutsky's theorem to the first part of eq. (D.18) gives as a result for the probability limit of the estimated Markov parameters, if the difference between the true Markov parameters and the Markov parameters used for the computation of the estimated output errors is assumed to be negligibly small:

$$\operatorname*{plim}_{l\to\infty} \{\hat{M}_{mp}\} = \operatorname*{plim}_{l\to\infty} \Bigg\{ \Big(\frac{1}{l+1} \cdot (M_{mp} \cdot \mathcal{Q}_m \cdot \mathcal{Q}_m^t + M_{tail} \cdot \mathcal{Q}_{tail} \cdot \mathcal{Q}_m^t + N \cdot \mathcal{Q}_m^t),$$

$$\frac{1}{l+1} \cdot (M_{mp} \cdot \mathcal{Q}_m \cdot \hat{H}_n^t + M_{tail} \cdot \mathcal{Q}_{tail} \cdot \hat{H}_n^t + N \cdot \hat{H}_n^t) \Big) \cdot$$

$$\begin{pmatrix} \frac{1}{l+1} \cdot \mathcal{Q}_m \cdot \mathcal{Q}_m^t & \frac{1}{l+1} \cdot \mathcal{Q}_m \cdot \hat{H}_m^t \\ \frac{1}{l+1} \cdot \hat{H}_n \cdot \mathcal{Q}_m^t & \frac{1}{l+1} \cdot \hat{H}_n \cdot \hat{H}_n^t \end{pmatrix}^{-1} \cdot \begin{bmatrix} I_{(m+1)\cdot p} \\ 0_{n\cdot q,(m+1)\cdot p} \end{bmatrix} \Bigg\} =$$

$$\operatorname*{plim}_{l\to\infty} \Big\{ \frac{1}{l+1} \cdot (M_{mp} \cdot \mathcal{Q}_m \cdot \mathcal{Q}_m^t + M_{tail} \cdot \mathcal{Q}_{tail} \cdot \mathcal{Q}_m^t + N \cdot \mathcal{Q}_m^t) \ ,$$

$$\frac{1}{l+1} \cdot (M_{mp} \cdot \mathcal{Q}_m \cdot \hat{H}_n^t + M_{tail} \cdot \mathcal{Q}_{tail} \cdot \hat{H}_n^t + N \cdot \hat{H}_n^t) \Big) \cdot$$

$$\left\{ \operatorname*{plim}_{l\to\infty} \begin{pmatrix} \frac{1}{l+1} \cdot \mathcal{Q}_m \cdot \mathcal{Q}_m^t & \frac{1}{l+1} \cdot \mathcal{Q}_m \cdot \hat{H}_m^t \\ \frac{1}{l+1} \cdot \hat{H}_n \cdot \mathcal{Q}_m^t & \frac{1}{l+1} \cdot \hat{H}_n \cdot \hat{H}_n^t \end{pmatrix} \right\}^{-1} \cdot \begin{bmatrix} I_{(m+1)\cdot p} \\ 0_{n\cdot q,(m+1)\cdot p} \end{bmatrix} \approx$$

$$\Big\{ (M_{mp} \cdot \sigma^2 \cdot I_{(m+1)\cdot p} + 0_{q,(m+1)\cdot p} + 0_{q,(m+1)\cdot p}) \ ,$$

$$\operatorname*{plim}_{l\to\infty} \frac{1}{l+1} \cdot (M_{mp} \cdot \mathcal{Q}_m \cdot \hat{H}_n^t + M_{tail} \cdot \mathcal{Q}_{tail} \cdot \hat{H}_n^t + N \cdot \hat{H}_n^t) \Big) \cdot$$

$$\begin{bmatrix} \sigma^2 \cdot I_{(m+1)\cdot p} & 0 \\ 0 & R_{e,e} \end{bmatrix}^{-1} \cdot \begin{bmatrix} I_{(m+1)\cdot p} \\ 0_{n\cdot q,(m+1)\cdot p} \end{bmatrix} =$$

$$\sigma^2 \cdot M_{mp} \cdot I_{(m+1)\cdot p} \cdot (\sigma^2 \cdot I_{(m+1)\cdot p})^{-1} = M_{mp} \qquad \text{(D.23)}$$

So, in case the previously estimated Markov parameters used for the generation of output error matrix H_n are close to the true Markov parameters of the system, the estimated Markov parameters with this approach are expected to converge to the true Markov parameters again.

Appendix E

Derivation of the partial derivatives of cost function V with respect to the D-matrix, the start sequence Markov parameters and the minimal polynomial coefficients of the MPSSM model

First the partial derivative of $V(a_i, M_i \mid i \in I)$, I=1,2, ... ,r, with respect to the D-matrix and with respect to the start sequence Markov parameters is computed:

$$\frac{\partial V}{\partial \underset{\sim}{M}_i} = \frac{\partial\, tr\{(\underset{\sim}{Y} - \underset{\sim}{\hat{Y}})\cdot(\underset{\sim}{Y}^t - \underset{\sim}{\hat{Y}}^t)\}}{\partial \underset{\sim}{M}_i} =$$

$$= \begin{bmatrix} \frac{\partial\, tr\{(\underset{\sim}{Y}-\underset{\sim}{\hat{Y}})\cdot(\underset{\sim}{Y}-\underset{\sim}{\hat{Y}})^t\}}{\partial \underset{\sim}{M}_{11,i}} & \cdots & \frac{\partial\, tr\{(\underset{\sim}{Y}-\underset{\sim}{\hat{Y}})\cdot(\underset{\sim}{Y}-\underset{\sim}{\hat{Y}})^t\}}{\partial \underset{\sim}{M}_{1p,i}} \\ \vdots & & \vdots \\ \frac{\partial\, tr\{(\underset{\sim}{Y}-\underset{\sim}{\hat{Y}})\cdot(\underset{\sim}{Y}-\underset{\sim}{\hat{Y}})^t\}}{\partial \underset{\sim}{M}_{q1,i}} & \cdots & \frac{\partial\, tr\{(\underset{\sim}{Y}-\underset{\sim}{\hat{Y}})\cdot(\underset{\sim}{Y}-\underset{\sim}{\hat{Y}})^t\}}{\partial \underset{\sim}{M}_{qp,i}} \end{bmatrix} \qquad (E.1)$$

For the computation of this partial derivative a property of the derivative of a trace function is used (cf. Appendix C, eq. (C.23)):

$$\frac{\partial\, tr\{(\underset{\sim}{Y} - \underset{\sim}{\hat{Y}})\cdot(\underset{\sim}{Y}^t - \underset{\sim}{\hat{Y}}^t)\}}{\partial \underset{\sim}{M}_{\alpha\beta,i}} = tr\{ \frac{\partial\, [(\underset{\sim}{Y} - \underset{\sim}{\hat{Y}})\cdot(\underset{\sim}{Y}^t - \underset{\sim}{\hat{Y}}^t)]}{\partial \underset{\sim}{M}_{\alpha\beta,i}} \} \quad 1 \le i \le r \qquad (E.2)$$

With eq. (C.4), (C.5) and (C.20) eq. (E.2) equals:

$$\frac{\partial V}{\partial \underset{\sim}{M}_{\alpha\beta,i}} = 2\, tr\{ \frac{\partial \underset{\sim}{\hat{Y}}}{\partial \underset{\sim}{M}_{\alpha\beta,i}} \cdot(\underset{\sim}{\hat{Y}}^t - \underset{\sim}{Y}^t) \} \qquad (E.3)$$

In the sequal the number of outputs of the system q is assumed to be smaller than or equal to the number of inputs p. A similar derivation can be made for p>q by using the canonical controllability form for the state space representation of the MPSSM model.
Using the minimal state space representation in canonical observability form

of the MPSSM model the partial derivative of $\hat{Y}$ with respect to the Markov parameter entries becomes (cf. eq. (5.56), (5.57) and (5.58)):

$$\frac{\partial \hat{Y}}{\partial \hat{M}_{\alpha\beta,i}} = \frac{\partial \left[D \quad H\cdot G \quad H\cdot F\cdot G \quad \ldots \quad H\cdot F^{m-1}\cdot G \right]\cdot \Omega_m}{\partial \hat{M}_{\alpha\beta,i}} \tag{E.4}$$

While the matrices D and G only are functions of the start sequence Markov parameters $(M_i \mid 1 \leq i \leq r)$ and the direct transfer (M_0), with (C.20a) this expression can be rewritten to:

$$\frac{\partial \hat{Y}}{\partial \hat{M}_{\alpha\beta,i}} = \left[\frac{\partial D}{\partial \hat{M}_{\alpha\beta,i}} \quad H\cdot\frac{\partial G}{\partial \hat{M}_{\alpha\beta,i}} \quad \ldots \quad H\cdot F^{m-1}\cdot\frac{\partial G}{\partial \hat{M}_{\alpha\beta,i}} \right]\cdot \Omega_m \tag{E.5}$$

The derivative with respect to the direct transfer parameter $\hat{M}_0$ is:

$$\frac{\partial \hat{Y}}{\partial \hat{M}_{\alpha\beta,0}} = \left[E_{\alpha\beta} \quad 0 \quad 0 \quad \ldots \quad 0 \right]\cdot \Omega_m \tag{E.6}$$

The derivatives of $\hat{Y}$ with respect to the entries of the start sequence Markov parameters can be computed using eq. (5.57c):

$$\frac{\partial \hat{Y}}{\partial \hat{M}_{\alpha\beta,i}} =$$

$$\left[0 \quad H\cdot E_{(\alpha-1)r+i,\beta} \quad H\cdot F\cdot E_{(\alpha-1)r+i,\beta} \quad \cdots \quad H\cdot F^{m-1}\cdot E_{(\alpha-1)r+i,\beta} \right]\cdot \Omega_m \tag{E.7}$$

with: $E_{(\alpha-1)r+i,\beta} = \begin{bmatrix} 0 & \ldots & 0 & \ldots & 0 \\ \cdot & & \cdot & & \cdot \\ 0 & \ldots & 1 & \ldots & 0 \\ \cdot & & \cdot & & \cdot \\ 0 & \ldots & 0 & \ldots & 0 \end{bmatrix} \leftarrow (\alpha-1)r+i$

$\uparrow$
β

To find an expression for the derivatives of V with respect to the entries of the Markov parameters also the term $(\hat{Y} - Y)^t$ has to be worked out:

$$(\hat{Y} - Y)^t = \Omega_m^t \cdot F^t(\hat{\underline{a}}, \hat{\underline{M}}) - Y^t =$$

$$\Omega_m^t \cdot \begin{bmatrix} D^t \\ \begin{bmatrix} G_1^t \cdot e_1 & G_2^t \cdot e_1 & \cdots & G_q^t \cdot e_1 \end{bmatrix} \\ \begin{bmatrix} G_1^t \cdot \tilde{F}^t \cdot e_1 & G_2^t \cdot \tilde{F}^t \cdot e_1 & \cdots & G_q^t \cdot \tilde{F}^t \cdot e_1 \end{bmatrix} \\ \vdots \\ \begin{bmatrix} G_1^t \cdot \tilde{F}^{m-1^t} \cdot e_1 & G_2^t \cdot \tilde{F}^{m-1^t} \cdot e_1 & \cdots & G_q^t \cdot \tilde{F}^{m-1^t} \cdot e_1 \end{bmatrix} \end{bmatrix} - Y^t \qquad \text{(E.8)}$$

with: $G = \begin{bmatrix} G_1 \\ G_2 \\ \cdot \\ \cdot \\ G_q \end{bmatrix}$ $\qquad G_i = \begin{bmatrix} M_{i1,1} & M_{i2,1} & \cdots & M_{ip,1} \\ M_{i1,2} & M_{i2,2} & \cdots & M_{ip,2} \\ \cdot & \cdot & & \cdot \\ \cdot & \cdot & & \cdot \\ M_{i1,r} & M_{i2,r} & \cdots & M_{ip,r} \end{bmatrix}$

$$e_1 = [1\ 0\ 0\ \ldots\ 0]^t$$

$$\tilde{F} = \begin{bmatrix} 0 & & \\ \vdots & I_{r-1} & \\ a_r & a_{r-1} \cdots & a_1 \end{bmatrix}$$

As a result the following expression is obtained:

$$(\hat{Y} - Y)^t =$$

$$\begin{bmatrix} u_k^t \cdot D^t + \sum_{i=1}^{m} u_{k-i}^t \cdot \left[G_1^t \cdot \tilde{F}^{i-1^t} \cdot e_1 \; G_2^t \cdot \tilde{F}^{i-1^t} \cdot e_1 \; \ldots \; G_q^t \cdot \tilde{F}^{i-1^t} \cdot e_1 \right] - y_k^t \\ u_{k+1}^t D^t + \sum_{i=1}^{m} u_{k+1-i}^t \left[G_1^t \cdot \tilde{F}^{i-1^t} \cdot e_1 \; G_2^t \cdot \tilde{F}^{i-1^t} \cdot e_1 \; \ldots \; G_q^t \cdot \tilde{F}^{i-1^t} \cdot e_1 \right] - y_{k+1}^t \\ \vdots \\ u_{k+l}^t D^t + \sum_{i=1}^{m} u_{k+l-i}^t \left[G_1^t \cdot \tilde{F}^{i-1^t} \cdot e_1 \; G_2^t \cdot \tilde{F}^{i-1^t} \cdot e_1 \; \ldots \; G_q^t \cdot \tilde{F}^{i-1^t} \cdot e_1 \right] - y_{k+l}^t \end{bmatrix} \tag{E.9}$$

Substitution of eq. (E.6) and (E.9) into eq. (E.3) and application of (C.4) and (C.5) (cf. Appendix C) gives:

$$\frac{\partial V}{\partial M_{\alpha\beta,0}} = 2 \, tr\{ \left[E_{\alpha\beta} \; 0 \; \ldots \; 0 \right] \cdot \Omega_m \cdot$$

$$\left. \begin{bmatrix} u_k^t \cdot D^t + \sum_{i=1}^{m} u_{k-i}^t \cdot \left[G_1^t \cdot \tilde{F}^{i-1^t} \cdot e_1 \; G_2^t \cdot \tilde{F}^{i-1^t} \cdot e_1 \; \ldots \; G_q^t \cdot \tilde{F}^{i-1^t} \cdot e_1 \right] - y_k^t \\ \vdots \\ u_{k+l}^t D^t + \sum_{i=1}^{m} u_{k+l-i}^t \left[G_1^t \cdot \tilde{F}^{i-1^t} \cdot e_1 \; G_2^t \cdot \tilde{F}^{i-1^t} \cdot e_1 \; \ldots \; G_q^t \cdot \tilde{F}^{i-1^t} \cdot e_1 \right] - y_{k+l}^t \end{bmatrix} \right\}$$

$$= 2 \sum_{j=0}^{l} e_\beta^t \cdot u_{k+j} \cdot \left[e_\alpha^t \cdot D \cdot u_{k+j} + \sum_{i=1}^{m} e_1^t \cdot \tilde{F}^{i-1} \cdot G_\alpha \cdot u_{k+j-i} - e_\alpha^t \cdot y_{k+j} \right] \tag{E.10}$$

Using the vec operator (cf. Appendix C, eq. (C.6) and (C.16)) eq. (E.10) can be rewritten into:

$$\frac{\partial V}{\partial \hat{M}_{\alpha\beta,0}} = 2 \sum_{j=0}^{l} e_\beta^t \cdot u_{k+j} \cdot \left[\left(u_{k+j}^t \otimes e_\alpha^t \right) \cdot \mathrm{vec}(D) + \left(\sum_{i=1}^{m} u_{k+j-i}^t \otimes e_1^t \cdot \tilde{F}^{i-1} \right) \cdot \mathrm{vec}(G_\alpha) - e_\alpha^t \cdot y_{k+j} \right] \qquad \text{(E.11)}$$

Similarly an expression can be derived for the partial derivatives of V with respect to the entries of the start sequence Markov parameters. Substitution of eq. (E.7) and (E.9) into eq. (E.3) gives:

$$\frac{\partial V}{\partial \hat{M}_{\alpha\beta,i}} = 2 \, \mathrm{tr}\left\{ \left[0 \quad H \cdot E_{(\alpha-1)r+i,\beta} \quad \cdots \quad H \cdot F^{m-1} \cdot E_{(\alpha-1)r+i,\beta} \right] \cdot \Omega_m \cdot \begin{bmatrix} u_k^t \cdot D^t + \sum_{s=1}^{m} u_{k-s}^t \cdot \left[G_1^t \cdot \tilde{F}^{s-1^t} \cdot e_1 \; G_2^t \cdot \tilde{F}^{s-1^t} \cdot e_1 \; \cdots \; G_q^t \cdot \tilde{F}^{s-1^t} \cdot e_1 \right] - y_k^t \\ \vdots \\ u_{k+l}^t \cdot D^t + \sum_{s=1}^{m} u_{k+l-s}^t \cdot \left[G_1^t \cdot \tilde{F}^{s-1^t} \cdot e_1 \; G_2^t \cdot \tilde{F}^{s-1^t} \cdot e_1 \; \cdots \; G_q^t \cdot \tilde{F}^{s-1^t} \cdot e_1 \right] - y_{k+l}^t \end{bmatrix} \right\} \qquad \text{(E.12)}$$

Writing out this equation gives:

$$\frac{\partial V}{\partial \hat{M}_{\alpha\beta,i}} = 2 \, \mathrm{tr}\left\{ \left(\sum_{j=1}^{m} H \cdot F^{j-1} \cdot E_{(\alpha-1)r+i,\beta} \cdot \left[u_{k-j} \; u_{k+1-j} \; \cdots \; u_{k+l-j} \right] \cdot \begin{bmatrix} u_k^t \cdot D^t + \sum_{s=1}^{m} u_{k-s}^t \cdot \left[G_1^t \cdot \tilde{F}^{s-1^t} \cdot e_1 \; G_2^t \cdot \tilde{F}^{s-1^t} \cdot e_1 \; \cdots \; G_q^t \cdot \tilde{F}^{s-1^t} \cdot e_1 \right] - y_k^t \\ \vdots \\ u_{k+l}^t \cdot D^t + \sum_{s=1}^{m} u_{k+l-s}^t \cdot \left[G_1^t \cdot \tilde{F}^{s-1^t} \cdot e_1 \; G_2^t \cdot \tilde{F}^{s-1^t} \cdot e_1 \; \cdots \; G_q^t \cdot \tilde{F}^{s-1^t} \cdot e_1 \right] - y_{k+l}^t \end{bmatrix} \right) \right\}$$

$$= 2\ \mathrm{tr}\Bigg\{ \begin{bmatrix} 0 & \cdots & 0 \\ \vdots & & \vdots \\ \sum_{j=1}^{m} e_1^t \cdot \tilde{F}^{j-1} \cdot E_{i\beta} \cdot u_{k-j} & \cdots & \sum_{j=1}^{m} e_1^t \cdot \tilde{F}^{j-1} \cdot E_{i\beta} \cdot u_{k+l-j} \\ \vdots & & \vdots \\ 0 & \cdots & 0 \end{bmatrix} \cdot \leftarrow \alpha$$

$$\begin{bmatrix} u_k^t \cdot D^t + \sum_{s=1}^{m} u_{k-s}^t \cdot \left[G_1^t \cdot \tilde{F}^{s-1^t} \cdot e_1 \ G_2^t \cdot \tilde{F}^{s-1^t} \cdot e_1 \ \cdots \ G_q^t \cdot \tilde{F}^{s-1^t} \cdot e_1 \right] - y_k^t \\ \vdots \\ u_{k+l}^t \cdot D^t + \sum_{s=1}^{m} u_{k+l-s}^t \cdot \left[G_1^t \cdot \tilde{F}^{s-1^t} \cdot e_1 \ G_2^t \cdot \tilde{F}^{s-1^t} \cdot e_1 \ \cdots \ G_q^t \cdot \tilde{F}^{s-1^t} \cdot e_1 \right] - y_{k+l}^t \end{bmatrix} \Bigg\}$$

$$= 2 \left[\sum_{j=1}^{m} e_1^t \cdot \tilde{F}^{j-1} \cdot E_{i\beta} \cdot u_{k-j} \ \cdots \ \sum_{j=1}^{m} e_1^t \cdot \tilde{F}^{j-1} \cdot E_{i\beta} \cdot u_{k+l-j} \right] \cdot$$

$$\begin{bmatrix} e_\alpha^t \cdot D \cdot u_k + \sum_{s=1}^{m} e_1^t \cdot \tilde{F}^{s-1} \cdot G_\alpha \cdot u_{k-s} - e_\alpha^t \cdot y_k \\ \vdots \\ e_\alpha^t \cdot D \cdot u_{k+l} + \sum_{s=1}^{m} e_1^t \cdot \tilde{F}^{s-1} \cdot G_\alpha \cdot u_{k+l-s} - e_\alpha^t \cdot y_{k+l} \end{bmatrix}$$

$$= 2 \sum_{t=0}^{l} \left(\sum_{j=1}^{m} e_1^t \cdot \tilde{F}^{j-1} \cdot E_{i\beta} \cdot u_{k+t-j} \right) \cdot \left(e_\alpha^t \cdot D \cdot u_{k+t} + \right.$$

$$\left. + \sum_{s=1}^{m} e_1^t \cdot \tilde{F}^{s-1} \cdot G_\alpha \cdot u_{k+t-s} - e_\alpha^t \cdot y_{k+t} \right) \qquad \text{(E.13)}$$

By making use of the vec operator (cf. Appendix C, eq. (C.6) and (C.16))

eq. (E.13) becomes:

$$\frac{\partial V}{\partial \hat{M}_{\alpha\beta,i}} = 2 \sum_{t=0}^{l} \left(\sum_{j=1}^{m} e_1^t \cdot \tilde{F}^{j-1} \cdot E_{i\beta} \cdot u_{k+t-j} \right) \cdot \left(\left(u_{k+t}^t \otimes e_\alpha^t \right) \cdot \mathrm{vec}(D) + \left\{ \sum_{s=1}^{m} \left(u_{k+t-s}^t \otimes \left(e_1^t \cdot \tilde{F}^{s-1} \right) \right) \right\} \cdot \mathrm{vec}(G_\alpha) - e_\alpha^t \cdot y_{k+t} \right) \qquad \text{(E.14)}$$

The partial derivatives of V with respect to the minimal polynomial coefficients can be obtained in a similar way:

$$\frac{\partial V}{\partial a_i} = \frac{\partial\, \mathrm{tr}\{(Y - \hat{Y}) \cdot (Y - \hat{Y})^t\}}{\partial a_i} = 2\, \mathrm{tr}\left\{ \frac{\partial \hat{Y}}{\partial a_i} \cdot (\hat{Y}^t - Y^t) \right\} \qquad \text{(E.15)}$$

Using eq. (5.56), (5.57) and (5.58) the partial derivative of the simulated outputs $\hat{Y}$ with respect to minimal polynomial coefficient a_i becomes:

$$\frac{\partial \hat{Y}}{\partial a_i} = \frac{\partial\, [D \;\; H \cdot G \;\; H \cdot F \cdot G \;\; \ldots \;\; H \cdot F^{m-1} \cdot G] \cdot \Omega_m}{\partial a_i} \qquad \text{(E.16)}$$

In this expression only matrix F is a function of minimal polynomial coefficients a_i. Eq. (E.16) can therefore be written as:

$$\frac{\partial \hat{Y}}{\partial a_i} = [0_{qp} \;\; 0_{qp} \;\; H \cdot \frac{\partial F}{\partial a_i} \cdot G \;\; \ldots \;\; H \cdot \frac{\partial F^{m-1}}{\partial a_i} \cdot G] \cdot \Omega_m \qquad \text{(E.17)}$$

With eq. (C.21a) (cf. Appendix C) the partial derivative of F^j to minimal polynomial coefficient a_i becomes:

$$\frac{\partial F^j}{\partial a_i} = \sum_{s=0}^{j-1} F^s \cdot \frac{\partial F}{\partial a_i} \cdot F^{j-s-1} = - \sum_{s=0}^{j-1} F^s \cdot S_{r,r-i+1} \cdot F^{j-s-1} \qquad \text{(E.18)}$$

with: $S_{r,r-i+1} = \mathrm{diag}(E_{r,r-i+1})$

$$E_{r,r-i+1} = \begin{bmatrix} 0 & .. & 0 & .. & 0 \\ \cdot & & \cdot & & \cdot \\ \cdot & & \cdot & & \cdot \\ 0 & .. & 1 & .. & 0 \end{bmatrix}$$

$$\uparrow$$
$$r-i+1$$

Substitution of eq. (E.18) into eq. (E.17) gives:

$$\frac{\partial \hat{Y}}{\partial a_i} = \left[0_{qp} \; 0_{qp} \; -H \cdot S_{r,r-i+1} \cdot G \; \ldots \; -H \cdot \sum_{s=0}^{m-2} F^s \cdot S_{r,r-i+1} \cdot F^{m-s-2} \cdot G \right] \cdot \Omega_m \tag{E.19}$$

Substitution of eq. (E.19) and (E.9) into eq. (E.15) results in the following expression for the partial derivative of V with respect to a_i:

$$\frac{\partial V}{\partial a_i} =$$

$$2 \; tr\Bigg\{ \left[0 \;\; 0 \;\; -H \cdot S_{r,r-i+1} \cdot G \;\; \ldots \;\; -H \cdot \sum_{s=0}^{m-2} F^s \cdot S_{r,r-i+1} \cdot F^{m-s-2} \cdot G \right] \cdot \Omega_m \cdot$$

$$\begin{bmatrix} u_k^t \cdot D^t + \sum_{s=1}^{m} u_{k-s}^t \cdot \left[G_1^t \cdot \tilde{F}^{s-1^t} \cdot e_1 \; G_2^t \cdot \tilde{F}^{s-1^t} \cdot e_1 \; \ldots \; G_q^t \cdot \tilde{F}^{s-1^t} \cdot e_1 \right] - y_k^t \\ \\ \cdot \\ \cdot \\ u_{k+1}^t D^t + \sum_{s=1}^{m} u_{k+1-s}^t \cdot \left[G_1^t \cdot \tilde{F}^{s-1^t} \cdot e_1 \; G_2^t \cdot \tilde{F}^{s-1^t} \cdot e_1 \; \ldots \; G_q^t \cdot \tilde{F}^{s-1^t} \cdot e_1 \right] - y_{k+1}^t \end{bmatrix} \Bigg\} \tag{E.20}$$

Working out eq. (E.20) results in the expression for the partial derivative

of cost function $V(\underline{a},\underline{M})$ with respect to minimal polynomial coefficient a_i:

$$\frac{\partial V}{\partial a_i} = 2\,\mathrm{tr}\left\{ \begin{pmatrix} \sum_{j=2}^{m} e_1^t \cdot \sum_{s=0}^{j-2} -\tilde{F}^s \cdot E_{r,r-i+1} \cdot \tilde{F}^{j-s-2} \cdot G_1 \cdot \begin{bmatrix} u_{k-j} & \cdots & u_{k-j+l} \end{bmatrix} \\ \vdots \\ \sum_{j=2}^{m} e_1^t \cdot \sum_{s=0}^{j-2} -\tilde{F}^s \cdot E_{r,r-i+1} \cdot \tilde{F}^{j-s-2} \cdot G_q \cdot \begin{bmatrix} u_{k-j} & \cdots & u_{k-j+l} \end{bmatrix} \end{pmatrix} \cdot \right.$$

$$\left. \begin{bmatrix} u_k^t \cdot D^t + \sum_{s=1}^{m} u_{k-s}^t \cdot \begin{bmatrix} G_1^t \cdot \tilde{F}^{s-1^t} \cdot e_1 & G_2^t \cdot \tilde{F}^{s-1^t} \cdot e_1 & \cdots & G_q^t \cdot \tilde{F}^{s-1^t} \cdot e_1 \end{bmatrix} - y_k^t \\ \vdots \\ u_{k+l}^t D^t + \sum_{s=1}^{m} u_{k+l-s}^t \cdot \begin{bmatrix} G_1^t \cdot \tilde{F}^{s-1^t} \cdot e_1 & G_2^t \cdot \tilde{F}^{s-1^t} \cdot e_1 & \cdots & G_q^t \cdot \tilde{F}^{s-1^t} \cdot e_1 \end{bmatrix} - y_{k+l}^t \end{bmatrix} \right\}$$

$$= 2 \sum_{\alpha=1}^{q} \sum_{t=0}^{l} \left(\sum_{j=2}^{m} \sum_{s=0}^{j-2} -e_1^t \cdot \tilde{F}^s \cdot E_{r,r-i+1} \cdot \tilde{F}^{j-s-2} \cdot G_\alpha \cdot u_{k-j+t} \right) \cdot$$

$$\left(e_\alpha^t \cdot D \cdot u_{k+t} + \sum_{s=1}^{m} e_1^t \cdot \tilde{F}^{s-1} \cdot G_\alpha \cdot u_{k-s+t} - e_\alpha^t \cdot y_{k+t} \right) \qquad \text{(E.21)}$$

literature

Adamjan, V.M., D.Z. Arov and M.G. Krein (1978)
Analytic properties of Schmidt pairs for a Hankel operator and the generalized Schur/Takaji problem. Translation: Math. USSR Sbornik, vol. 15, no 10 pp. 31-73, 1978. Original: Iz. Akad. Nauk Armjan. SSR. Ser. Mat. 6 pp.87 (1971)

Aström, K.J. (1980)
Maximum-likelihood and prediction error methods.
Automatica, vol 16, pp. 551-574, 1980

Aström, K.J. (1985)
Process control - past, present and future.
IEEE Control Systems Magazine, pp 3-10, August 1985

Aström, K.J. and T. Häglund (1984)
Automatic tuning of simple regulars with specifications on phase and amplitude margins.
Automatica, vol. 20, no.5, pp. 645-651, 1984

Aström, K.J. and B. Wittenmark (1984)
Computer controlled systems: theory and design.
Prentice-Hall international editions

Backx, A. (1985)
Development of robust tools for process identification.
Internal report, PICOS-R-045, Philips PICOS glass

Backx, A. and P. van den Hof (1987)
Output error methods in multivariable process identification.
Internal report, PICOS-R-077, Philips PICOS Glass

Bartels, R.H. and G.W. Stewart (1972)
Solution of the matrix equation AX + XB = C
Communications of the ACM, vol 15, no. 9, 1972, pp. 820-826

Van den Boom, A.W. (1982)
System Identification. On the variety and coherence in parameter- and order estimation methods.
PhD Thesis, Eindhoven University of Technology.

Berben, P. (1985)
Order estimation methods.
Internal report PICOS-R-051, Philips PICOS glass.

Cramér, H. (1961)
Mathematical methods of statistics.
Princeton University Press, Princeton, N.J.

Damen A.A.H., P. Eykhoff (1982)
Maximum-likelihood estimation.
Journal A, vol 23, no 4, 1982

Damen, A.A.H. , P.M.J. van den Hof and A.K. Hajdasinski (1982)
The page matrix: An excellent tool for Noise filtering of Markov parameters, order testing and realization.
Eindhoven Univerity of Technology, TH report 82-E-127.

Damen, A.A.H. and A.K. Hajdasinski (1982)
Practical tests with different approximate realizations based on the singular value decomposition of the Hankel matrix.
Proc. 6th IFAC Symposium on Identification and System Parameter Estimation, Washington.

Van Dooren, P. (1982)
Algorithm 590: DSUBSP and EXCHQZ, Fortran subroutines for computing deflating subspaces with specified spectrum.
ACM TOMS, Vol. 4, 1982, pp. 376-382

Eykhoff,P. (1974)
System Identification: Parameter and State Estimation.
London Wiley and Sons

Eykhoff, P. (1981)
Trends and Progress in System Identification.
Pergamon Press. IFAC series for Graduates, researchers & practising Engineers, vol. 1, 1981.

Fletcher, R. (1981)
Practical Methods of Optimization. Vol. 1: Unconstrained Optimization.
John Wiley and Sons. Chichester

Fletcher, R. (1980)
Practical Methods of Optimization. Vol. 2: Constrained Optimization.
John Wiley and Sons. Chichester

Foias, G., A. Tannenbaum and G. Zames (1986)
Weighted sensitivity minimization for delay systems.
IEEE Trans. A.C., Vol AC-31, no. 8, 1986, pp. 763-766

Francis, B.A., J.W. Helton and G. Zames (1984)
H^{∞}-optimal feedback controllers for linear multivariable systems
IEEE Trans. A.C., Vol. AC-29, No. 10, 1984, pp 888-900

Gantmacher, F.R. (1959)
The Theory of Matrices.
Chelsea Publishing Company.

Genin, Y. (1981)
An introduction to the model reduction problem with Hankel norm criterium.
Proc. Europ. Conf. on Circuit Theory and Design. The Hague 1981, pp.205-212

Gevers, M.R. (1986)
ARMA Models, their Kronecker indices and their Mc Millan degree.
Int. J.Control, vol. 43, no.6, 1986, pp. 1745-1761.

Gershwin, B.G. , R.R. Hildebrant, R. Suri and S.K. Mitler (1986)
A control perspective on recent trends in manufacturing systems.
Control Systems Magazine, vol. 6, no. 2, 1986

Gerth, W. (1972)
Zur Minimalrealisierung von Mehrgrossenübertragungssystemen durch Markovparameter.
PhD Thesis, Fakultät für Maschinenwesen der Technischen Universität Hannover.

Glover, K. (1984)
All optimal Hankel-norm approximations of linear multivariable systems and their L^{∞}-error bounds.
Int.J. Control 1984, vol. 39, no.6, 1984, pp 1115-1193
Goldberger, A.S. (1964)
Econometric Theory.
Wiley, New York
Golub, G.H., S. Nash and C. Van Loan (1979)
A Hessenberg-Schur method for the problem A·X + X·B = C
IEEE Trans. A.C., Vol. AC-24, 1979, pp. 909-913
Golub G.H. and C.F. van Loan (1980)
An analysis of the Total Least Squares Problem.
SIAM J. Numer. Anal., Vol. 17, no. 6, 1980, pp. 883-893.
Graham, A. (1981)
Kronecker Products and Matrix Calculus With Applications
Ellis Horwood Ltd, Halsted Press, John Wiley & Sons
Grimble, M.J. (1986)
Optimal H^{∞} robustness and the relationship to LQG design problems
Int. J. Control, Vol. 43, no. 2, 1986, pp 351-372
Guidorzi, R.P. (1975)
Canonical structures in the identification of multivariable systems.
Automatica. vol.11, pp. 361-374. 1975
Guidorzi, R.P. and S. Beghelli (1982)
Input output multistructural models in multivariable system identification.
Received via personal communication
Hajdasinski, A.K. (1976)
A Markov parameter approach to identification of multivariable dynamical systems.
Technical Report, Group Measurement and Control, Electrical Engineering Department, Eindhoven University of Technology, November 1976
Hajdasinski,A.K. (1978)
The Gauss-Markov approximated scheme for identification of multivariable dynamical systems via the realization theory. An explicit approach.
Electrical Engineering Department, Eindhoven University of Technology, TH report 78-E-88
Hajdasinski, A.K. and A.A.H. Damen (1979)
Realization of the Markov parameter sequences using the singular value decomposition of the Hankel matrix.
Eindhoven University of Technology, TH-report 79-E-95.
Hajdasinski, A.K. (1980)
Linear multivariable systems: Preliminary problems in mathematical description. Modelling and Identification.
Eindhoven University of technology, Report TH 80-E-106
Hajdasinski, A.K., P. Eykhoff, A.A.H. Damen and A.J.W. van den Boom (1982)
The choice and use of different model sets for system identification.
Invited contribution, 6th IFAC symposium on Identification and System Parameter Estimation, Washington D.C.

Hautus, M.L.T. (1969)
Controllability and Observability conditions of Linear Autonomous Systems.
Ned. Akad. Wetenschappen, Proc. ser. A, vol. 72, pag. 443-448.
Ho, B.L., R.E. Kalman (1966)
Effective construction of linear state-variable models from input/output functions.
Regelungstechnik, no. 14, 1966
Van den Hof, P.M.J. and P.H.M. Janssen (1985)
Some asymptotic properties of multivariable models identified by equation error techniques.
Eindhoven University of Technology. Report 85-E-153.
Van Huffel, S. and J. Vandewalle(1985)
The use and applicability of the total least squares technique in linear regression analysis.
Catholic University of Leuven. Departement Electrotechnic, afd. ESAT.
Van Huffel, S., J. Vandewalle and A. Haeyemans (March 1980)
An efficient and reliable algorithm for computing the singular subspace of a matrix associated with its smallest singular values.
Received via personal communication.
Van Huffel, S., J. Vandewalle and J. Staar (1984)
The total linear least squares problem: properties, applications and generalization.
Received via personal communication.
Van Huffel, S. (1987)
Analysis of the total least squares problem and its use in parameter estimation
PhD Thesis, Catholic University Leuven, Dept. ESAT
IEEE Standard dictionary of electrical and electronics terms (1984)
The Institute of Electrical and Electronics Engineers, Inc.
Isermann, R. (1974)
Prozess Identifikation. Identifikation und Parameterschätzung dynamischer Prozesse mit diskreten Signalen.
Springer Verlag.
Isermann, R. (1977)
Digitale Regelsysteme
Springer Verlag.
Janssen, P.H.M. (1986)
The choice of model sets for identification part (1): general considerations on model representations and parametrizations.
Eindhoven University of Technology, Internal report ER 86/03
Kailath, T (1980)
Linear Systems.
Prentice Hall, Englewood Cliffs.
Kalman, R.E. (1960)
On the general theory of control systems.
Proc. of the 1st IFAC World Congress, pp 481-492, Moscow, 1960.
Kreindler, E. and D. Rothchild (1976)
Model following in a linear quadratic optimization
AIAA Journal, july, 1976

Kreyszig, E. (1970)
Introductory Mathematical Statistics. Principles and methods.
John Wiley and Sons.
Kung, S. and D.W. Lin (1981)
Optimal Hankel-norm model reductions: Multivariable systems.
IEEE trans. A.C., vol. AC-26, no. 4, 1981, pp. 832-852.
Kung, S. and D.W. Lin (1981)
A state space formulation for optimal Hankel-norm approximations.
IEEE trans. A.C., vol. AC 26, no. 4, 1981, pp. 942-946.
Kuo, B.C. (1980)
Digital Control Systems.
Holt, Rinehart and Winston, Inc. HRW series in electrical and computer engineering.
Kwakernaak, H and R. Sivan (1972)
Linear optimal control systems
Wiley-Interscience, Wiley and Sons
Kwakernaak, H. (1985)
Minimax frequency domain performance and robustness of linear feedback systems
IEEE Trans. A.C., Vol. AC-30, No. 10, 1985
Kwakernaak, H. (1986)
A polynomial approach to minimax frequency domain optimizationof multivariable feedback systems.
Int. J. Control, Vol. 44, No. 1, 1986, pp 117-156
Landau, I.D. (1979)
Adaptive Control. The Model Reference Approach.
Dekker, New York.
Van der Linden, W.P.M. (1985)
Gebalanceerde realisaties en optimale Hankel-norm modelreductie.
M.Sc. Thesis, Mathematics Department, Eindhoven University of Technology.
Ljung, L. (1971)
Characterization of the concept of 'persistently exciting' in the frequency domain.
Report 7129, Lund institute of Technology, Lund, Sweden.
Ljung, L. (1979)
Convergence of recursive estimators.
Survey paper, 5th IFAC Symposium on Identification and System Parameter Estimation, Darmstadt
Ljung, L. and T. Söderström (1983)
Theory and Practice of Recursive Identification.
The MIT press.
Ljung, L. (1987)
On the estimation of transfer functions.
Proceedings of the 10th IFAC World Congress, Munich, 1987
Laub, A.J. (1980)
Computation of balancing transformations.
Proc. Joint Automatic Control Conference, Vol. 1, paper FA8-E
MacFarlane, A.G.J. (Edit.) (1979)
Frequency Response Methods in Control Systems.
IEEE Press

Moore, B.C. (1981)
Principal component analysis in linear systems: Controllability, observability and model reduction.
IEEE Trans. A.C., Vol. AC-26, 1981, pp 17-32
Niederlinski, A., A.K. Hajdasinski (1979)
Multivariable system identification. A survey.
5-th IFAC Symposium on Identification and System Parameter Estimation.
Nordström, K. (1984)
Robustness improvement of LQG controllers
Report LiTH-ISY-I-0715, Lund institute of Technology, Lund, Sweden
Nordström, K. (1985)
On the trade-off between noise sensitivity and robustness for LQG regulators
Report LiTH-ISY-I-0745, Lund institute of Technology, Lund, Sweden
Oudbier, R. (1986)
A different approach to the minimal polynomial and start sequence of Markov parameters estimation problem.
M.Sc.Thesis, Group Measurement and Control, Electrical Engineering Department, Eindhoven University of Technology.
Oudbier, R. (1986)
Documentation of estimation program DIRECTO.
Internal report, Philips PICOS Glass, PICOS-R-071.
Owens, D.H. (1978)
Feedback and Multivariable Systems.
IEEE Control Engineering Series 7, Peter Peregrinus Press, London, England
O'Young, S.D. and B.A. Francis (1986)
Optimal performance and robust stabilization
Automatica, Vol. 22, No. 2, 1986, pp 171-183
Papoulis (1967)
Probability, Random Variables and Stochastic Processes.
Mc Graw Hill International Book Company.
Papoulis, A. (1977)
Signal Analysis.
Mc Graw Hill International Book Company.
Pernebo, L. and L.M. Silverman (1982)
Model reduction via balanced state space representations.
IEEE Trans A.C., Vol. AC-27, no. 2, 1982, pp 382 - 387
Rademaker, O. (1984)
Produktie automatisering: Systematische bedrijfsdoorlichting
De Servobode, nummer 30, juni 1984
Richalet, J. et al (1978)
Model predictive heuristic control: applications to industrial process.
Automatica 1978, vol. 14, 1978, pp. 413-428.
Rosenbrock, H.M. (1970)
State Space and Multivariable Theory.
J. Wiley & Sons, New York.
Senning, M.F. (1982)
Process parameters identification: A total least squares approach
IFAC Software for Computer Control, Algorithms for digital computer control, 1982, pp. 301-306.

Sidar, M. (1976)
Recursive identification and tracking of parameters for linear and non-linear multivariable systems.
Int. J. Control, vol 24, no 3, 1976
Silverman, L.M. and M. Bettayeb (1980)
Optimal approximation of linear systems.
Proc. 1980, Joint Automat. Control. Conf. San Francisco, paper FA8-A.
Smith, O.J.M. (1957)
Closer control of loops with deadtime.
Chem. Eng. Progr., vol. 53, 1957, pp. 217-219.
Staar, J. et al (1981)
Realization of truncated impulse response sequences with prescribed uncertainty.
Control Sciences and Technology for the progress of society.
Proc. 8-th Triennial World Congress of IFAC. Kyoto
Staar, J. and J. Vandewalle (1982)
Singular value decomposition: a reliable tool in the algorithmic analysis of linear systems.
Journal A., vol. 23, no. 2, 1982, pp. 69-74.
Staar, J. (1982)
Concepts for reliable modelling of linear systems with application to on-line identification of multivariable state space descriptions
PhD thesis, Catholic University Leuven, Dept. ESAT
Stewart, G. (1976)
Algorithm 506: HQR3 and EXCHNG, Fortran subroutines for calculating and ordering the eigenvalues of a real upper Hessenberg matrix.
ACM TOMS, Vol. 2, 1976, pp. 275-280
Stoer, J. and R. Bulirsch (1980)
Introduction to Numerical Analysis.
Springer Verlag (translation from: Einfuhrung in die Numerische Mathematik I, II, Springer Verlag 1972)
Swaanenburg, H.A.C. (1985)
Practical aspects of industrial multivariable process identification.
Proceedings 7-th IFAC Symposium on Identification and System Parameter Estimation. York.
Swaanenburg, H.A.C. (1983)
A two stage identification method for multivariable systems by means of least squares estimation and approximate realization.
M.Sc.Thesis, Delft University of Technology, laboratory for measurement and control.
Tyler, J.S. (1964)
The characteristics of model-following systems as synthesized by optimal control
IEEE Trans. A.C., Vol. AC-9, 1964, pp 485-498
Tether A.J. (1970)
Construction of minimal linear state variable models from finite input-output data
IEEE Trans. A.C., Vol AC-15, no. 4, 1970, pp. 427-436
Vaessen, J. (1983)
Least squares and maximum likelihood estimation of Markov parameters
M.Sc. Thesis, Group Measurement and Control, Electrical Engineering Department, Eindhoven University of Technology.

Vaessen, J. (1983)
Documentation of simulation program syssimul.
Internal report, Philips PICOS-Glas, PICOS-R-012
Vaessen, J. (1983)
Documentation of estimation programs.
Internal report, Philips PICOS-Glas, PICOS-R-013
Vidyasagar, M., H. Schneider and B.A. Francis (1982)
Algebraic and topological aspects of feedback stabilization
IEEE Trans. A.C., Vol. AC-27, no. 4, 1982, pp. 880-894
Vidyasagar, M. (1985)
Control System Synthesis. A Factorization Approach
The MIT press
Vidyasagar, M. and H. Kimura (1986)
Robust controllers for uncertain linear multivariable systems
Automatica, Vol. 22, no. 1, 1986, pp 85-94
Watanabe, K., I. Masami (1981)
A process model control for linear systems with delay.
IEEE Trans. A.C., Vol AC-26, no. 6, 1981, pp. 1261-1269
Wertz, V., G. Bastin and M. Haest (1987)
Identification of a glass tube drawing bench.
Proceedings of the 10th IFAC World Congress, Munich
Van der Weijden, J.L.J.M. (1984)
The estimation of minimal polynomial coefficient and a start sequense of Markov parameters.
M.Sc. Thesis, Group Measurement and Control, Electrical Engineering Department, Eindhoven University of Technology.
Van der Weijden, J.L.J.M. (1984)
Documentation of the direct method.
Internal report, Philips PICOS Glas, PICOS-R-025.
Zames, G. (1981)
Feedback and optimal sensitivity: model reference transformations, multiplicative seminorms, and approximate inverses.
IEEE Trans A.C., vol. AC-26, no. 2, 1981, pp. 301-320
Zames, G. and B.A. Francis (1983)
Feedback, minimax sensitivity and optimal robustness.
IEEE Trans A.C., vol. AC-28, no. 5, 1983, pp. 585-601
Zeiger,H.P., A.J. McEwen (1974)
Approximate linear realizations of given dimension via Ho's algorithm.
IEEE Trans A.C., vol. AC-19, 1974, pp. 153 ev.
Ziegler, J.G. and N.B. Nichols (1942)
Optimum settings for automatic controllers.
Trans ASME 64, pp. 759-768

NOTATIONS, SYMBOLS AND ABBREVIATIONS

On the notation

Throughout the thesis matrices are indicated with capitals; vectors and scalars are indicated with small letters. With respect to the notation no further distinction is made between scalars and vectors. If the type of a variable is not clear from the context it is explicitly indicated with a dimension description.

Mathematical notations used:

A^t	Transpose of matrix A
A^+	Moore Penrose pseudo inverse of matrix A
A^*	Complex conjugate, transpose of matrix A
A^{-1}	Inverse of square, full rank matrix A
A^k	k-th power of matrix A
$A_{i.}$	i-th column of matrix A
$A_{.i}$	i-th row of matrix A
a_{ij}	i-th element of the j-th column of matrix A
$\sigma_i(A)$	i-th singular value of the ranged singular values of matrix A
$\lambda_i(A)$	i-th eigenvalue of matrix A. The eigenvalues of the matrix are assumed to be ranged to their absolute values
dim[A]	Size of matrix A: $\dim[A] = m \times n$ denotes that matrix A has m rows and n columns

$||A||_k$ — L^k norm of matrix A (dim[A] = m × n) defined by:

$$||A||_k = \left(\sum_{i=1}^{m} \sum_{j=1}^{n} |a_{ij}|^k \right)^{1/k}$$

$||A||_F$ — Frobenius norm of matrix A (dim[A] = m × n) defined by:

$$||A||_F = \left(\sum_{i=1}^{\min(m,n)} \sigma_i^2 \right)^{1/2}$$

$||A||_H$ — Hankel norm of matrix H defined by:

$$||A||_H = \sigma_1(A)$$

diag(A) — Block diagonal matrix defined by:

$$\text{diag}(A) = \begin{bmatrix} A & 0 & 0 & \dots & 0 \\ 0 & A & 0 & \dots & 0 \\ 0 & 0 & A & \dots & 0 \\ \cdot & \cdot & \cdot & & \cdot \\ \cdot & \cdot & \cdot & & \cdot \\ 0 & 0 & 0 & \dots & A \end{bmatrix}$$

$\text{diag}(A_1, \dots, A_m)$ — Block diagonal matrix defined by:

$$\text{diag}(A_1, A_2, \dots, A_m) = \begin{bmatrix} A_1 & 0 & 0 & \dots & 0 \\ 0 & A_2 & 0 & \dots & 0 \\ 0 & 0 & A_3 & \dots & 0 \\ \cdot & \cdot & \cdot & & \cdot \\ \cdot & \cdot & \cdot & & \cdot \\ 0 & 0 & 0 & \dots & A_m \end{bmatrix}$$

$\frac{\partial A}{\partial x}$ — Partial derivative of matrix A with respect to scalar variable x (cf. Appendix C)

$\frac{\partial f(X)}{\partial X}$ — Partial derivative of scalar function f of matrix X with respect to matrix X (cf. Appendix C)

$\hat{X}$	Estimated value for matrix variable X
$\tilde{X}$	Estimated value for matrix X used to indicate an estimated matrix different from $\hat{X}$
$E\{\xi\}$	Mathematical expectation of the random variable ξ
$P(\xi)$	Probability density function of the random variable ξ
$\underset{k\to\infty}{\text{plim}}\ \{\xi\}$	Probability limit of the random variable ξ
I	Identity matrix
$I_{q,p}$	Identity matrix with q rows and p columns; elements on main diagonal are equal to one, all other elements are equal to zero
H_+^∞	Hardy space of functions that is bounded and analytic in the right half plane and defined by: Let $G(s)$: $\mathbb{C} \to \mathbb{C}^{q\times p}$ then $G(s)\in H_+^\infty$ if and only if $G(s)$ is analytic in the open right half plane and bounded in the closed right half plane
H_-^∞	Hardy space of functions that is bounded and analytic in the left half plane and defined by: Let $G(s)$: $\mathbb{C} \to \mathbb{C}^{q\times p}$ then $G(s)\in H_-^\infty$ if and only if $G(s)$ is analytic in the open left half plane and bounded in the closed left half plane
tr(A)	Trace of matrix A defined as the sum of the diagonal elements of A (cf. Appendix C)
vec(A)	Transformation of matrix A into vector form (cf. Appendix C)
det(A)	Determinant of matrix A

symbols used:

F: system matrix of a discrete time state space system (cf. chapter 2, eq. (2.3a))

G: input matrix of a discrete time state space system (cf. chapter 2, eq. (2.3a))

H: output matrix of a discrete time state space system (cf. chapter 2, eq. (2.3b))

D: matrix that describes the direct transfer from inputs to outputs of the state space system (cf. chapter 2, eq. (2.3b))

$\underline{a}$: minimal polynomial coefficients $(a_1, a_2, \ldots, a_r)$ of an MPSSM model

$\underline{M}$: start sequence Markov parameters of a MPSSM model including the M_0 (direct transfer) matrix $(M_0, M_1, M_2, \ldots, M_r)$

M_i: i-th Markov parameter

a_i: i-th coefficient of the minimal polynomial

F_i: i-th Markov parameter of the MPSSM model

r: degree of the minimal polynomial (cf. chapter 2, eq. (2.2))

n: order of a minimal state space realization of the system (cf. chapter 2, section 2.3.1)

p: number of inputs of the system

q: number of outputs of the system

l: number of input and output samples in a data set

m: number of Markov parameters of the FIR model

$H_{i,j}$: block Hankel matrix with i block rows and j block columns:

$$H_{i,j} = \begin{bmatrix} M_1 & M_2 & \cdots & M_j \\ M_2 & M_3 & \cdots & M_{j+1} \\ \vdots & \vdots & & \vdots \\ M_i & M_{i+1} & \cdots & M_{i+j-1} \end{bmatrix}$$

H_i: block Hankel matrix with i block rows and i block columns

$M_{\alpha\beta,i}$: element $m_{\alpha\beta}$ of Markov parameter M_i

u_k: input signal vector at sample moment k

y_k: output signal vector at sample moment k

n_k: process output noise vector at sample moment k

e_k: output error vector at sample moment k

Ω: input signal matrix defined by:

$$\Omega = \begin{bmatrix} u_k & u_{k+1} & \cdots & u_{k+l} \\ u_{k+1} & u_{k+2} & \cdots & u_{k+l+1} \\ \cdot & \cdot & & \cdot \\ \cdot & \cdot & & \cdot \\ u_{k+m} & u_{k+1+m} & \cdots & u_{k+l+m} \end{bmatrix}$$

Y: output signal matrix defined by:

$$Y = [y_k \; ; \; y_{k+1} \; ; \; y_{k+2} \; ; \; \cdots \; ; \; y_{k+l}]$$

E: output error matrix defined by:

$$E = Y - \hat{Y} = [e_k \; ; \; e_{k+1} \; ; \; \cdots \; ; \; e_{k+l}]$$

R(ξ): covariance matrix of random variable ξ: $R=E\{\xi \cdot \xi^t\}$

V: cost function: scalar function of the chosen error (cf. chapter 2, section 2.3.2) that has to be minimized by manipulation of the model parameters

Abbreviations used:

AR	Auto Regressive
ARMA	Auto Regressive Moving Average
det	Determinant
eq.	equation
EXACTMARK	Algorithm for the estimation of FIR process model parameters and AR noise model parameters (cf. chapter 3, eq. (3.43))
FIR	Finite Impulse Response
LS	Least Squares
MA	Moving Average
MARKEST	Algorithm for the estimation of FIR process model parameters and AR noise model parameters (cf. chapter 3, eq. (3.45))
MARKMIN	Algorithm for the estimation of FIR process model parameters and AR noise model parameters (cf. chapter 3, eq. (3.42), (3.11))
MARKMIND	Algorithm for the estimation of FIR process model parameters and AR noise model parameters (cf. chapter 3, eq. (3.46))
MPSSM	Minimal Polynomial Start Sequence of Markov parameters
PRBN	Pseudo Random Binary Noise
PSD	Power Spectral Density

RECMAK	Recursive algorithm for the estimation of FIR process model and AR noise model (cf. chapter 3, eq. (3.36), (3.37))
SS	State Space
SVD	Singular Value Decomposition
TLLS	Total Linear Least Squares
tr	Trace

IDENTIFICATIE VAN EEN INDUSTRIEEL PROCES: EEN AANPAK GEBASEERD OP MARKOV PARAMETER MODELLEN

Samenvatting

Het in het proefschrift beschreven onderzoek betreft het ontwikkelen van een binnen een industriële omgeving bruikbare methode voor het bepalen van mathematische modellen van processen, die het dynamisch gedrag van de processen in een omgeving van een werkpunt beschrijven.

De achtergrond van het onderzoek is de groeiende behoefte binnen de industrie om op basis van een gedegen kennis van het gedrag van processen de processen beter te beheersen teneinde de flexibiliteit en de kwaliteit te verhogen.
Het probleem met betrekking tot de identificatie van industriële processen is vooral, dat de processen niet exact kunnen worden beschreven met de modellen, die voor de identificatie van de processen worden gebruikt en dat geen algemeen toepasbare technieken beschikbaar zijn om modelsets zo te kiezen dat daarbinnen altijd een model te vinden is, dat het gedrag van het proces goed benadert.
Met de ontwikkelde methode kunnen mathematische modellen worden gemaakt van processen, die het dynamisch gedrag van de processen in omgevingen van werkpunten voldoende nauwkeurig beschrijven om het dynamisch gedrag te simuleren en om multivariabele proces regelsystemen te ontwerpen.

In het beschreven onderzoek is een zogenaamde "black box" identificatie methode ontwikkeld, die in essentie uit drie stappen bestaat, waarbij elke stap een model oplevert, dat het gedrag van het proces compacter of nauwkeuriger beschrijft, ook als het proces niet exact door de gebruikte modellen kan worden beschreven:

- In de eerste stap wordt een model bepaald uit de set van de eindige impuls responsies. De set van de eindige impulsresponsies is de grootst mogelijke modelset voor stabiele systemen. Uit deze modelset wordt het model gekozen, dat het waargenomen gedrag van het proces op aangeboden testsignalen zo dicht mogelijk benadert. Het bepaalde model is kwalitatief goed, maar het bevat veel parameters en is daardoor niet goed bruikbaar voor simulatie en regelaarontwerp.

- In de tweede stap wordt, op basis van het uit de eerste stap verkregen eindige impulsresponsie model, een veel compacter model -het zogenaamde Minimal Polynomial Start Sequence Markov parameter (MPSSM) model- bepaald.
  De modelset waaruit dit MPSSM model wordt gekozen wordt vastgelegd aan de hand van het uit de eerste stap verkregen eindige impulsresponsie model. Het MPSSM model vereist alleen de bepaling van een orde voor het minimale polynoom. Er hoeft geen structuur te worden bepaald, hetgeen voor industriële processen, die vaak een volledig verweven structuur hebben, nauwelijks mogelijk is. Ook voor processen met een bekende structuur is het gebruik van het MPSSM model als tussenstap aantrekkelijk, omdat het model meer gebalanceerd

is ten aanzien van de beschrijving van de overdrachten van ingangen naar uitgangen dan modellen gebaseerd op (pseudo) canonieke vormen. Er worden geen overdrachten bevoor- of benadeeld.
Het met deze tweede stap verkregen model beschrijft het gedrag van het proces in het algemeen minder nauwkeurig dan het oorspronkelijke eindige impulsresponsie model. Doordat het MPSSM model echter veel compacter is dan het eindige impulsresponsie model en direct kan worden omgezet naar een toestandsruimte model is het goed bruikbaar voor simulatie van dynamisch procesgedrag en voor het ontwerp van multivariabele regelsystemen.

- De derde stap bestaat uit het, op basis ven het gemeten proces gedrag, bijstellen van het uit de tweede stap verkregen MPSSM model. Deze stap zal in het algemeen een model opleveren, dat het dynamisch gedrag van het proces in een direkte omgeving van het werkpunt beter beschrijft dan het uit de eerste stap verkregen eindige impulsresponsie model. Deze verbetering is mogelijk, omdat het MPSSM model een model is dat oneindig lange impulsresponsies kan beschrijven en omdat met de ontwikkelde directe schattingsmethode uit de geselecteerde set van MPSSM modellen het best op de proces data passende model wordt gekozen. Deze stap vereist een goede startwaarde voor de MPSSM modelparameters. De modelparameters verkregen uit de tweede stap voldoen aan deze eis.
Schatting van de parameters van een MPSSM model op basis van ingangs-/uitgangsdata en met een criterium functie, die is opgebouwd opgebouwd met te minimaliseren "output errors", heeft een belangrijk voordeel ten opzichte van het schatten van de parameters van een model in een canonieke vorm: Er hoeft slechts te worden geminimaliseerd met een numeriek algorithme naar r (de graad van het minimale polynoom) polynoom coefficienten voor een systeem dat generiek orde r·min(p,q) is (p: aantal ingangen, q: aantal uitgangen) in plaats van naar n·min(p,q) coefficienten (n: orde van het proces).

In het eerste deel van het onderzoek worden de drie stappen van de ontwikkelde identificatie procedure uitvoerig geanalyseerd. Uit de voor iedere stap onderzochte mogelijke alternatieven voor het schatten van de modelparameters en voor het bepalen van de te gebruiken modelset wordt steeds, op basis van uit simulaties verkregen resultaten, die methode gekozen, die ook voor processen met wat grotere omvang en complexiteit kwalitatief goede resultaten oplevert binnen een acceptabele rekentijd.

In het tweede deel van het onderzoek is de ontwikkelde identificatie methode toegepast op twee verschillende, industriële processen.
Het eerste onderzochte proces is een produktie proces waarmee kwarts glazen buizen worden geproduceerd. Van het vormgeef gedeelte van dit proces zijn modellen gemaakt, die het dynamisch gedrag van deze vormgeving beschrijven. De kwaliteit van de verkregen modellen is onderzocht aan de hand van uitgevoerde validatie experimenten. In deze validatie experimenten zijn willekeurige test signalen zowel aan het proces als aan de modellen aangeboden. De geregistreerde responsies van het proces zijn vergeleken met de door de modellen gesimuleerde responsies.

Het tweede onderzochte deel proces is een feeder. Een feeder is het gedeelte van een produktie installatie voor het smelten van glas, waar het glas moet worden geconditioneerd voor verdere verwerking tot produkten. Het conditioneren heeft vooral betrekking op het realiseren van een homogene temperatuur verdeling in het uit de feeder stromende glas, waarbij de absolute waarde van de temperatuur van het glas binnen nauwe, voorgeschreven grenzen constant moet worden gehouden. Van de feeder is een model gemaakt, dat de overdrachten beschrijft van drie energie inputs naar zes temperaturen op vast gekozen plaatsen (de meetpunten) in een dwarsdoorsnede dicht bij de uitstroom opening van de feeder. Ook met dit proces zijn validatie experimenten uitgevoerd.
Uit de resultaten verkregen met de validatie data blijkt dat de verkregen modellen het gedrag van de processen in een omgeving van de gekozen werkpunten nauwkeurig beschrijven.

Met het verkregen model voor het vormgeefgedeelte van het buisglas produktie proces is een multivariabel regelsysteem ontworpen voor het besturen van de buis dimensies. Met dit nieuwe regelsysteem blijkt het proces veel nauwkeuriger beheersbaar dan met het oorspronkelijk toegepaste regelsysteem. Tevens zijn omsteltijden aanzienlijk gereduceerd.

De verkregen resultaten laten de conclusie toe, dat met de ontwikkelde identificatie methode modellen van processen kunnen worden gemaakt, die een nauwkeurig inzicht geven in het dynamisch gedrag van de onderzochte processen en die gebruikt kunnen worden, in combinatie met binnen de systeem theorie ontwikkelde technieken, voor het ontwerp van robuuste, multivariabele regelsystemen voor deze processen.
Toepassing van de onderzochte technieken levert een basis voor een volledig geautomatiseerde proces besturing (zie: hoofdstuk 1 "Introduction"); nader onderzoek zal evenwel nodig zijn om deze volledig automatisch bestuurde processen daadwerkelijk te realizeren.

LEVENSBERICHT

19-04-1954	Geboren te Roosendaal
1966-1972	Gymnasium-β gevolgd aan het St. Norbertuslyceum te Roosendaal
1972-1977	Studie Elektrotechniek aan de Technische Universiteit Eindhoven
1977-1981	Wetenschappelijk medewerker Dr. Neher laboratorium PTT
1981-heden	In dienst van de Nederlandse Philips bedrijven B.V. te Eindhoven bij de HTG Glas

STELLINGEN

- I -

Het modelleren van industriële processen met behulp van identificatie-technieken vereist redundantie in de ten behoeve van de identificatie geregistreerde processignalen om voorbewerking van de signalen, op basis van verkregen kennis van het proces gedrag, mogelijk te maken zonder verlies van voor de parameterschatting belangrijke informatie.

P. Eykhoff (1974) System Identification. Parameter and State Estimation. J. Wiley and Sons
R. Isermann (1980) Practical Aspects of Process Identification Automatica, Vol. 16, pp 575-587

- II -

Procesbesturingssystemen dienen zodanig te worden ontworpen, dat zij processen over hun volledige bandbreedte kunnen exciteren. Als niet aan deze voorwaarde wordt voldaan, is het besturingssysteem een ongewenste, beperkende factor in de maximaal haalbare snelheid waarmee optredende procesverstoringen kunnen worden onderdrukt en waarmee procesverstellingen kunnen worden gedaan.

- III -

Een in de literatuur vaak ten onrechte gewekte suggestie is, dat het direkt gebruik van zo compact mogelijke modelsets voor de identificatie van een proces leidt tot modellen, die het waargenomen procesgedrag zo goed mogelijk representeren. In tegenstelling hiermee levert het initieel gebruik van een grote modelset voor het identificeren van industriële processen en in vervolg stappen reduceren van de grootte van de modelset een belangrijk voordeel: het stapsgewijs reduceren van de omvang van de modelset op basis van uit eerdere stappen verkregen kennis, vergroot de kans, dat uiteindelijk een compact model wordt gevonden, waarmee het waargenomen procesgedrag beter kan worden gerepresenteerd.

Ljung, L, T. Söderström (1983) Theory and Practice of Recursive Identification. The MIT Press
Guidorzi, R.P. (1981) Invariants and Canonical Forms for Systems Structural and Parametric Identification. Automatica, Vol. 17, pp 117-133

- IV -

In het algemeen worden industriële processen, met het oog op de beheersbaarheid door operators, zo ontworpen en zo bedreven, dat zij in direkte omgevingen van de gebruikte werkpunten goed zijn te beschrijven met lineaire, tijdinvariante, gewone differentiaalvergelijkingen.

- V -

Een in oneindig norm of in Hankel norm optimale benadering van een hoge orde procesmodel is veelal voldoende om garanties te kunnen geven ten aanzien van de stabiliteit van een op basis van het verkregen model geregeld proces. Voor het met behoud van de robuustheid minimaliseren van de variantie van geregelde procesvariabelen dient evenwel een benadering te worden gekozen, die is gebaseerd op een optimale Hankel norm approximatie en die resterende vrijheidsgraden benut om de Frobenius norm van de overblijvende verschillen tussen hoge orde model en benaderende realizatie te minimalizeren.

Glover, K. (1984) All optimal Hankel-norm approximations of linear multivariable systems and their L^{∞}-error bounds. Int. J. Control, Vol. 39, no. 6, pp 1115-1193

O'Young, S.D. and B.A. Francis (1986) Optimal Performance and Robust Stabilization. Automatica, Vol. 22, no. 2, pp 171-183

- VI -

Het ontwerpen van software louter aan de hand van een strakke ontwerpmethode leidt in het algemeen tot een goede structuur in de programmatuur, maar geeft geen garantie, dat het uiteindelijke systeem aan de gestelde eisen met betrekking tot gewenste prestaties zal voldoen.

Nettesheim, H. (1982) Programmentwurf und Programmdokumentation. Methoden und Techniken bei der Prozessdatenverarbeitung. VDI-Verlag GmbH, Düsseldorf

- VII -

Voor het ontwikkelen van betrouwbare en onderhoudbare software is een toets van het produkt aan vooraf vastgestelde normen door een onafhankelijke instantie vereist.

- VIII -

Creativiteit, hoewel vereist voor het initiëren van een nieuwe ontwikkeling, vormt een belemmering voor het snel afronden van die ontwikkeling.

- IX -

Gerichte geldelijke steun aan bedrijven mag niet alleen worden verstrekt met het oog op behoud van de bestaande werkgelegenheid, maar dient vooral te zijn gericht op verbetering van de rendementen en van de toekomstige concurrentiepositie van die bedrijven.

- X -

Beslissingen ten aanzien van uit te voeren ontwikkelingen en ten aanzien van de introductie van nieuwe technieken binnen een bedrijf mogen, in verband met de in het algemeen hoge mate van onzekerheid en onnauwkeurigheid van het gebruikte cijfermateriaal, niet uitsluitend gebaseerd zijn op rentabiliteitsbeschouwingen.

- XI -

Binnen een groot concern zijn informele kontakten van vitaal belang voor het op efficiente wijze realiseren van nieuwe ontwikkelingen, voor het soepel uitwisselen van informatie binnen het concern en voor het vermijden van dubbele ontwikkelingen.

Ton Backx,

3 november 1987